Sex differences in Cued Fear Discrimination: A Combined Behavioural, Computational and Electrophysiological Study

Harriet Laura Lavinia Day, BSc (Hons)

Thesis submitted to The University of Nottingham for the Degree of

Doctor of Philosophy, September 2017

The University of Nottingham · BBSRC bioscience for the future

Abstract

Women are up to twice as likely to suffer from post-traumatic stress disorder (PTSD) than men. Failure to discriminate between cues predicting threat and safety is associated with PTSD, yet sex differences in fear discrimination remain poorly understood. Here, we examined sex differences in auditory fear discrimination in rats using a combination of behavioural, computational and electrophysiological methods.

In the initial behavioural study, males and naturally cycling females underwent 1-3 days of discrimination training, consisting of pairings of one tone (CS+) with shock and presentations of another tone (CS-) alone. After one day of training, females, but not males, discriminated between the CS+ and CS-. With 2-3 days of training, however, males discriminated and females generalised between the CS+ and CS-. Further testing also revealed that males successfully encode the CS- as a safety signal, whereas females do not.

Using reduced computational models, we investigated how both 'discrimination' and 'generalisation' phenotypes can be generated *in silico*. We achieved this through a simulation of neural activity produced via 'fear' and 'safety' neural sub-populations of the basolateral amygdala (BLA) in response to CS+ and CS- cues. By using a model representation of extended fear discrimination training and retrieval, we found that generalisation between the CS+ and CS- could be produced from reduced inhibition, or increased excitation, of fear neurons.

Due to their involvement in regulating learned fear, we additionally aimed to investigate the roles of the prelimbic (PL) and infralimbic (IL) cortices of the

medial prefrontal cortex in fear discrimination. By concurrently recording activity from the PL, IL and BLA in awake behaving animals during retrieval of the CS+ and CS- after extended discrimination training, we examined the individual contributions and functional interactions of these regions during this learning paradigm. We found that, in males, the PL showed an increase in power at both theta (4-12 Hz) and gamma (30-120 Hz) frequencies during presentations of the CS- compared to the CS+, whereas this increase was largely absent in females.

Taken together, these results indicate that, while females show fear discrimination with limited training, they generalise with extended training. We hypothesised that this generalisation in females is likely due to impaired safety learning, which may result, in part, from sex differences in the neural circuitry underlying fear discrimination.

List of Definitions

AMPA = Alpha-amino-3-hydroxy-5-methyl-4-isoxazolepropionic acid

ANOVA = Analysis of variance

BLA = Basolateral amygdala

BNST = Bed nucleus of the stria terminalis

CS+ = Conditioned stimulus plus (i.e. associated with an unconditioned stimulus)

CS- = Conditioned stimulus minus (i.e. not associated with an unconditioned stimulus)

CEm/l = Medial/lateral central nucleus of the amygdala

CI = Conditioned inhibition

CR = Conditioned response

CS = Conditioned stimulus

dACC = Dorsal anterior cingulate cortex

EEG = Electroencephalography

E/I = Excitatory and Inhibitory neurons in the Wilson-Cowan model

EPSP = Excitatory postsynaptic potential

F+/F-/S+/S- = Excitatory (+) and inhibitory (-) fear (F) and safety (S) neural populations from Models 1-3 (Chapter 3)

fMRI = Functional magnetic resonance imaging

FPS = Fear-potentiated startle

GABA = Gamma-aminobutyric acid

GAD65 or 67 = Glutamic acid decarboxylase 65 or 67

ITC = Intercalated cells

IL = Infralimbic cortex

ITI = Inter-trial interval

LH/VH/DH = Lateral, Ventral or Dorsal Hippocampus

LA = Lateral amygdala

LFP = Local field potential

LI = Latent inhibition

LTP = Long-term potentiation

mPFC = Medial prefrontal cortex

NMDA = N-methyl-D-aspartate

PAG = Periaqueductal grey

PAC = Phase-amplitude coupling

PFA = Paraformaldehyde

PL = Prelimbic cortex

PTSD = Post-traumatic stress disorder

PVN = paraventricular nucleus

PVIN = Prefrontal parvalbumin interneurons

SNS = Sympathetic nervous system

UR = Unconditioned response

US = Unconditioned stimulus (i.e. footshock)

VGCC = Voltage-gated calcium channels

vmPFC = Ventromedial prefrontal cortex

wXY = Connection weight of X on Y, where X and Y can be any value or neural

population in Models 1-3 (Chapter 3)

Table of Contents

1. General Introduction

1.1 Overview

Defined as a sensation generated by the threat of pain, harm, or danger, fear is considered to be one of the universal emotions and an integral part of the human experience (Steimer, 2002). Although often associated with negative connotations, the feeling of fear and its resultant behaviours are critical to survival. In rapidly changing environments and situations, fear underlies the mechanisms which cause us to learn appropriate predictors of danger, allowing us to react accordingly to them when encountered again in the future. However, disruptions to the normal learning and retrieval of fear memories can lead to the pathological fear seen in numerous mental health conditions, such as anxiety and post-traumatic stress disorder (PTSD) (Quirk et al., 2010).

Lifetime prevalence for these chronic conditions is high, at 28.8% for anxiety and 8.3% for PTSD (Kessler et al., 2005; Kilpatrick et al., 2013). In addition, anxiety and PTSD are frequently comorbid with other anxiety disorders (e.g. panic disorder), depressive disorders, and substance abuse, causing a considerable impact on quality of life (Martin, 2003). Further, it is now evident that there are clear sex differences in the incidence rates of these mental health disorders; as highlighted by McLean et al., (2011) and Lebron-Milad & Milad, (2012), women are up to 60% more likely to suffer from an anxiety disorder than men, and are twice as likely to suffer from PTSD. Yet, studies involving both male and female cohorts have been noticeably absent in the field of fear and anxiety until relatively recently (Donner & Lowry, 2013). By

studying the interconnected brain circuitry of the fear network, this PhD aims to improve the understanding of the neurological features underlying anxiety-related mental health disorders, in addition to investigating differences in fear learning and memory observed between both males and females. The literature on the neurobiology of fear behaviour will be reviewed below, in addition to highlighting areas where research needs to be further developed. For example, although there is considerable information consolidating the underlying neurobiology of fear learning and memory in males, the corresponding literature on females is limited. To conclude, this chapter will summarise the objectives proposed to achieve the overall research aims of this PhD.

1.2 Natural Fear Behaviours

Fear learning and the demonstration of fear behaviours are apparent in all mammals, and have even been observed in crustaceans and molluscs (Burnovicz & Hermitte, 2010; Gelperin, 1975). Fear behaviours are typically described as the physiological representations that are assumed to be generated when fear is felt, or when the body is reacting to a fearful stimulus (Killcross et al, 1997). For example, the 'fight or flight' response felt when threat is perceived. Under these circumstances, the anticipation of a fearful stimulus can produce the same reaction as actually experiencing it, which can confer an advantage when faced with threat. These behaviours are generated automatically in response to sensory stimuli that are innately feared by the organism, such as the shadow or scent of a cat presented to a mouse. However, we can also study fear learning and its associated behaviours by

generating cues and contexts designed to elicit the fear response via highly specific conditioned fear learning paradigms in clinical and laboratory settings (Gross & Canteras, 2012). Under carefully controlled conditions, we can investigate the neurobiology of fear; from its beneficial function as an adaptive evolutionary response to threat, to the pathological underpinning of numerous and debilitating mental disorders, including generalised anxiety and PTSD.

1.2.1 Conditioned Fear Behaviours

Classical conditioning is an example of associative learning that has been examined extensively since it was first described by Pavlov (1927), (reviewed by Balkenius & Morén, (1999)). In Pavlov's seminal experiments, the biologically relevant stimulus of food (which produced salivation, the unconditioned response; UR) was paired with a previously neutral stimulus (the infamous sound of a bell). Over time, Pavlov's dogs learned to associate the sound of the bell with the appearance of food, and thus would salivate when they were presented with the bell during future presentations. Once the association between the sound of the bell and the appearance of food was learned, the sound of the bell had become a reliable predictor of future food presentation. Through this process, the sound of the bell had become a conditioned stimulus (CS), which would elicit the UR (salivation) even in the absence of food. Over the following nine decades, this influential behavioural paradigm has been exploited to study conditioned fear responses by training mainly rodents in a similar manner to Pavlov's dogs (LeDoux, 2014).

In this instance, fear conditioning is also an example of associative learning (Blair et al. 2001) wherein the neutral stimulus (e.g. a tone) is associated with a noxious US (e.g. footshock) instead of something rewarding, like food. With repeated pairings, the original neutral stimulus becomes a CS, meaning that subsequent exposure to the CS (in the absence of the unconditioned stimulus; US) will initially generate a fear response if the memory of the CS-US association is successfully retrieved. The CS is not restricted to discrete auditory stimuli; other cues may be used as the CS, such as lights and odours (Dielenberg et al., 2001; Cassaday et al., 2001; Laviolette et al. 2005). Further, specific spatial representations (e.g. the testing chamber) can also be associated with the US in the form of learned contextual fear, in addition to a discrete stimulus or on its own (Anagnostaras et al., 2001). A return to the training context after conditioning will then initially elicit the fear response experienced when the original association was made, even in the absence of the US (Garelick & Storm, 2005).

During the design of fear conditioning experiments, it is important that the CS and the parameters under which it is being used (e.g. tone frequency or amplitude), do not themselves generate fear; naïve subjects exposed to the CS should show little to no fear in comparison to conditioned subjects. It is also worth mentioning that the modality (i.e. type) of CS can potentially have an effect on behavioural outcomes. For example, a light cue may evoke subtly lower conditioned freezing levels in comparison to a tone (Sigmundi & Bolles, 1983). However, as tones were consistently used as CSs as examples in this chapter and throughout the thesis, this is unlikely to be relevant to data

presented in chapters 2 and 4. The timing of the CS-US pairings should also be considered. Delay conditioning, where the CS co-terminates with the US, is used in classical conditioning in order to generate fear behaviour only when the discrete stimulus is present (Burman & Gewirtz, 2004). Subjects are typically habituated to the CS before testing begins to control for behaviour generated from novel cue exposure alone. However, habituation must be brief to avoid latent inhibition (LI), the process by which many presentations of the CS prior to training retards the learning of CS-US associations using that same stimulus (Joseph et al., 2000).

Once the training paradigm has been established, factors including aspects like age, sex, genetics and life experience must be controlled for, not only because heterogeneity increases variance, but because these factors can all have an effect on the acquisition and expression of learned fear (Broadwater & Spear, 2013; Chauret et al., 2014; Orr et al., 2000). In human studies, including a properly controlled for and reasonable sample is hard to achieve, although recent efforts have been made to include more representative sample groups in psychological studies. Further, there must be effective methods in place to record the physiological response generated by the CS. Typically in humans, this is achieved by measuring skin conductance (Huff et al., 2011), eye-blink, flinching (Flaten & Powell, 1998) and respiratory changes (Ayers & Powell, 2002), which are all indirect methods of measuring sympathetic nervous system (SNS) responses. Self-reporting can also be used, but as self-reports are intrinsically subjective, it is often better to combine them with measured physiological changes.

In rodents, conditioned suppression of appetitive responding was, and still is, a common measure of fear responding. During appetitive conditioning a rat is initially trained to lever press, nose poke or lick for food (Bouton & Bolles, 1980; Bouton & Peck, 1989; Malkki et al., 2010). The amount of lever pressing, nose poking or licking for food is used as the baseline appetitive response for the animal. The same animal is subsequently conditioned with a CS (e.g. a light or tone) paired with an aversive US (e.g. footshock). The appetitive response is then measured again in the presence of the CS alone; conditioned suppression is said to have occurred if the appetitive response is reduced during presentations of the CS compared to baseline (Desiderato & Newman, 1971; Vanderschuren & Everitt, 2004). In addition to appetitive suppression, SNS responses (such as heart rate and blood pressure) were also used as physiological measures of fear (reviewed in Thompson et al., (2012)) but as these were found to largely correlate with specific behaviors (freezing and fear-potentiated startle (FPS)) these behaviours are now typically used to measure the fear response. A startle response is a reflexive reaction to an intense, unexpected stimulus, involving a whole body flinch to protect the back of the neck and facilitate escape (Daldrup et al., 2015). Although this reaction is innate and unlearned, it can be potentiated when the rat is experiencing fear. For example, rats exhibit a larger startle response to a loud noise when a shock-associated CS (e.g. a light) is present in comparison to when the CS is not present (Davis, 2001). FPS is also used as a measure in humans, which provides a useful basis for translational research in rodents using this method (Grillon, 2002). In addition to FPS, freezing is also used as a measure of

conditioned fear behaviour. During freezing, the rodent remains completely still, except for movement necessary for respiration. This is a biologically evolved response to a fearful stimulus, as the cessation of movement acts to protect the animal from being seen by predators in the wild. Under experimental conditions, this can be measured as a percentage of time spent freezing during presentations of a CS previously paired with a noxious stimulus. For example, a high percentage of freezing upon exposure to the CS post-conditioning is indicative that a CS-US association has been made, and then successfully retrieved by the subject. An outline of habituation, conditioning and retrieval is shown by Figure 1.1 below:
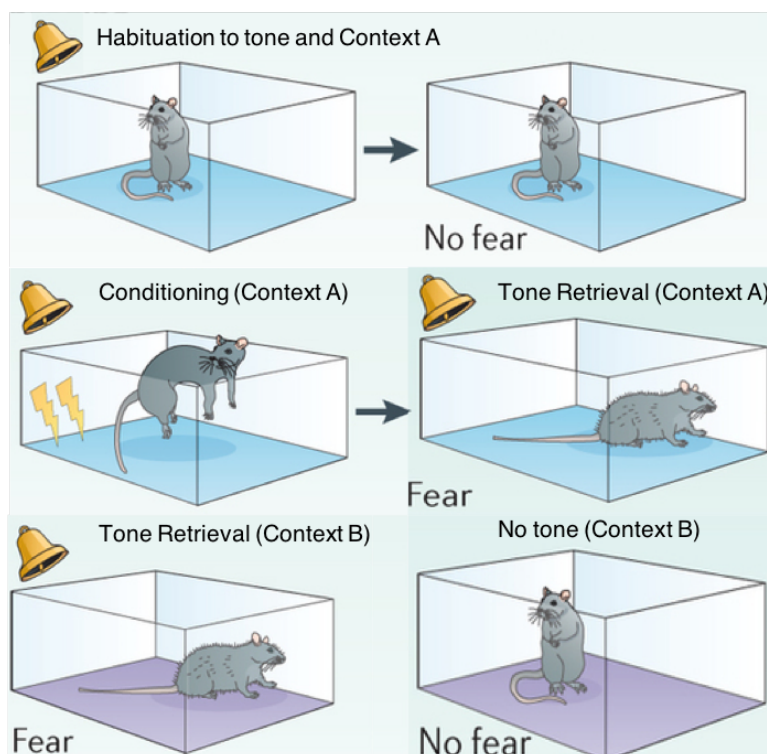
Figure 1.1 Habituation, fear conditioning and retrieval in rodents. In the top two panels, the rat is habituated to the discrete cue that will become the auditory CS (as shown by the yellow bell) and the context of the testing chamber (box with the blue floor). During habituation, there is no US, meaning that there is no fear response generated. In the middle left panel, the CS is paired with the US (foot-shock; yellow lightning bolts) during auditory fear conditioning. In the middle right panel, subsequent presentations of the CS initially cause a fear response (freezing). The bottom two panels show that the fear is both context and cue dependent; in the bottom left panel, presentations of the CS in a novel context (purple floor) still evoke a fear response, but the bottom right panel shows that the novel context alone does not evoke any fear response. Figure adapted from Maren et al. (2013).

1.3. The Neurobiology of Learned Fear to Discrete Cues

As described above, the behavioural responses of freezing, FPS and conditioned suppression have typically been used to measure fear in rodents during conditioning and retrieval. Nevertheless, these processes only address the physically apparent behavioural response when fear is experienced; the corresponding neurophysiological changes which occur within the brain must also be taken into consideration. Current literature states that there is no single 'emotion region' that can perceive, process and assess stimuli in order to produce the complex behaviours associated with fear (Lindquist et al., 2012).

Instead, the neurophysiological basis for these behaviours occurs within multiple parts of the brain including the amygdala, hypothalamus, periaqueductal grey (PAG), bed nucleus of the stria terminalis (BNST) hippocampus, prefrontal cortex, and thalamus (LeDoux, 2003). These brain areas are inter-connected, allowing them to communicate with one another to form functional neural circuits. Importantly, these neural circuits act to generate short and long-term memory representations of an individual's fear experiences, such as the CS-US associations described above, which can then have a profound influence on future behavior (Ehrlich et al., 2009). Despite numerous years of study on this topic, exactly how these regions are connected functionally, however, and how fear learning and memory is encoded by these regions, is still poorly understood. Before describing specific brain regions and circuits involved in the neurobiology of learned fear in further detail, the methods used to record neural activity in humans and experimental animals will be summarised below.

1.3.1 Methods for recording brain activity

In humans, functional magnetic resonance imaging (fMRI) scans can be used to investigate which brain regions are metabolically active during different stages of a fear conditioning and retrieval paradigm in a time-dependent manner (Liu et al., 2010 and Phelps et al., 2001). Even though the spatial and temporal resolution of fMRI has increased dramatically in recent years, there can still be issues regarding neuronal activity and image capture (Bandettini, 2009). The temporal resolution of fMRI is often in the order of seconds (Glover, 2011). Yet, in the brain, events can occur in the order of tens of milliseconds (Aghdaee et al., 2014), meaning that very rapid and/or transient activity changes in certain regions may be missed. Improved temporal resolution, albeit at the cost of spatial resolution, can be achieved during human brain activity recordings using electroencephalography (EEG); wherein electrodes are applied on different regions of the scalp and can record to within the millisecond range. In place of fMRI or EEG, a much more direct approach to recording changes in brain activity during fear conditioning and memory retrieval can be achieved by implementing surgically implanted electrodes in areas of interest.

Implanted electrodes are devices that can record neural signals from the brain to an output monitor, where they can be observed and saved for further analysis. In this instance, action potentials of neurons cause a difference in voltage between the inside and outside of the cell body, which can then be recorded by local electrodes (Pine, 1980). In addition, current can also be applied to certain parts of the brain using additional electrodes designed to stimulate brain activity (Jones, 2009). Applied current causes voltage-gated ion

channels on the membranes of target cells to open, resulting in an increased likelihood for action potentials to occur. Implanted electrodes serve as a neural interface between the brain and observable/controllable input and output meaning that they have both very high spatial and temporal resolution. However, implanted electrodes need additional filters to remove noise artefacts from signals (e.g. a low-pass filter to attenuate unwanted interference). Unambiguous identification of the recorded neuron using multi-electrode extracellular arrays can also cause issues. Despite these minor drawbacks, implanted electrodes are the method of choice to determine the function of neural circuits. It is now accepted that electrophysiological studies are instrumental to understand how neuronal circuits generate, store and transfer information both locally and in concert with other inter-connected brain areas (Scanziani & Häusser, 2009).

Although useful, implanted electrodes present obvious problems in humans; namely that surgically implanted electrodes are intrinsically invasive and can cause brain damage (Kozai et al., 2015), meaning that they are ethically impossible in most cases. Apart from under certain circumstances, such as utilising deep brain stimulation (DBS) as a treatment for the advanced stages of Parkinson's disease, implanted electrodes are typically not used in humans. In this instance, the use of animals (e.g. rodents) in studies involving implanted electrodes, can offer a convenient solution to the issues of spatial and temporal resolution and ethical concerns.

Using animals also enables better cohort composition design than can be accounted for in human studies, as it is much easier to control for inter- and

intra-group variation within subjects. Importantly, lesions and (reversible) drug treatments can be administered in rodents to inactivate certain brain regions, in addition to facilitating or blockading specific neurotransmitters, thus determining their involvement during fear conditioning (Holland et al., 2002, Balleine et al., 2003; Stevenson et al., 2007). Manipulations of individual brain areas and/or their connective circuitry can also be functionally mapped with the use of chronically implanted electrodes when combined with behavioural studies. Moreover, as it is now accepted that the basic fear circuits involved in fear learning and memory are largely conserved across all mammals (LeDoux, 2012), rodent experiments work to offer an excellent and appropriate complement to human research.

1.3.2 Neural Oscillations

Surgically implanted electrodes are able to record activity in the form of action potentials from individual neurons (single unit firing) and local field potentials (LFPs) resultant from large groups of neurons in multiple areas of interest in rat brains (Stevenson et al., 2007), offering better overall resolution than that available from human fMRI or EEG. When the action potentials resultant from a large group of neurons follow a pattern of synchronised firing, oscillations are generated (see Figure 1.2, below). Oscillatory activity is generated locally via interactions between excitatory and inhibitory neurons (Dupret et al., 2008). Inhibitory neurons are often referred to as 'Interneurons', wherein interneuron and inhibitory neuron are used interchangeably. However, this is not strictly accurate as although the vast majority of interneurons are inhibitory, a small

percentage are excitatory. For the purpose of this thesis, the term 'interneuron''
is used to refer to inhibitory neurons, only. Interneurons rhythmically modulate
the firing rate of excitatory neurons at certain frequencies, for example a neural
oscillation at 10 Hz would be generated from the neurons in that population
being inhibited and then all firing at roughly the same time, ten times per
second.
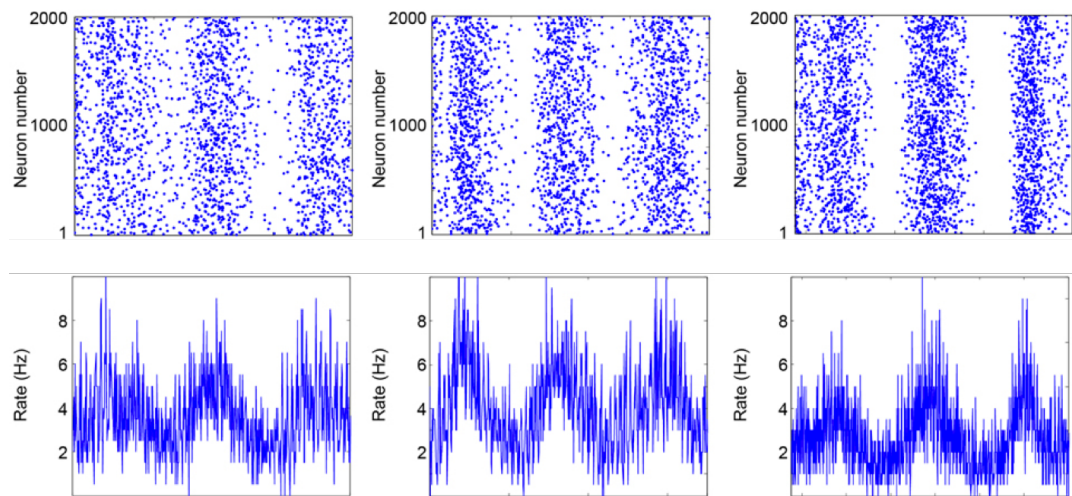
Figure 1.2. A simulation of synchronous spiking activity from a population of neurons generating neural oscillations at various frequencies. The upper panels depict the spiking of individual neurons, wherein each dot is representative of an individual action potential, and the lower panels show the LFP of their summed activity. Spiking of the neuronal population becomes more synchronous from left to right, with the top right panel showing an example of progressively more synchronous neuronal firing. Figure adapted from Goldental et al., (2015).

Neural oscillations have been linked to a multitude of cognitive functions such
as information transfer, perception, motor control and memory (Fell &
Axmacher, 2011; Schnitzler & Gross, 2005). Overall, oscillations allow the
integration and transfer of diverse neural information from various stimuli,
facilitating the understanding of, and flexible responses to, complex events
(Senkowski et al., 2008). Oscillations can be measured in terms of coherence;
a mathematical method that can be used to determine if two or more brain
regions have similar neuronal oscillatory activity with respect to each other

(Yeragani et al., 2006), where coherence is a measure of synchrony in the frequency domain specifically, compared to the temporal domain. In addition to coherence, oscillations are measured in terms of phase, i.e. where action potential firing can be locked to oscillation phase, and the start and end of an oscillation cycle is locked to a specific, rhythmic pattern. For example, neurons in a population may simultaneously spike at fixed points in time in response to the periodic input of a stimulus or other neurons; referred to as phase-locking (Lowet et al., 2016). Phase-locking assists in the transfer of information between oscillating neuronal groups (Silva, 2013).

Oscillation frequencies of interest include theta (between 4-12Hz), which is used by large groups of neurons to transfer information over comparatively long distances, both within and between multiple brain structures. Importantly, oscillations in the theta frequency range have been associated with facilitated communication between regions in response to aversive stimuli (Adhikari et al., 2011; Lesting et al., 2011; Paz et al., 2008; Popa et al., 2010; Seidenbecher at al., 2003). Moreover, following fear conditioning, coherent oscillations in the theta range between the prefrontal cortex and amygdala during sleep are positively correlated with fear memory consolidation. Similar to theta oscillations, activity in the high frequency gamma range (30-120 Hz) is also associated with long-range communication between brain areas. Additionally, gamma oscillations are also present in circuits which underlie sensory processing and higher cognitive functions, such as attention (Fries, 2009). Recently, gamma oscillations have also been implicated in fear memory

(Fenton et al., 2016). The dynamics of oscillatory activity and how it contributes to fear learning and memory will be discussed in more detail in Chapter 4.

1.3.3 The Neural Circuitry of Cued Fear

To better understand the activity and circuitry in the brain when fear is experienced, we must first address each process at a neurobiological level at points before, during and after fear conditioning. Initially, the subject must perceive stimuli (e.g. tones, lights, etc.) through the sensory organs to gain awareness of them. From here, this information travels to the lateral amygdala (LA) either via the somatosensory cortex or via the sensory thalamus (Rovó et al., 2012). Using the example of a tone CS, during habituation where no shock is paired with the tone (see Figure 1), there is no fear response generated by presentations of the CS. However, in the case of fear conditioning, if a foot-shock US is administered at the termination of the tone, the pain generated by the shock travels from the somatosensory thalamus and will also converge in the LA with the sound of the CS (Barot et al., 2009). This process is outlined by Figure 1.3. below:
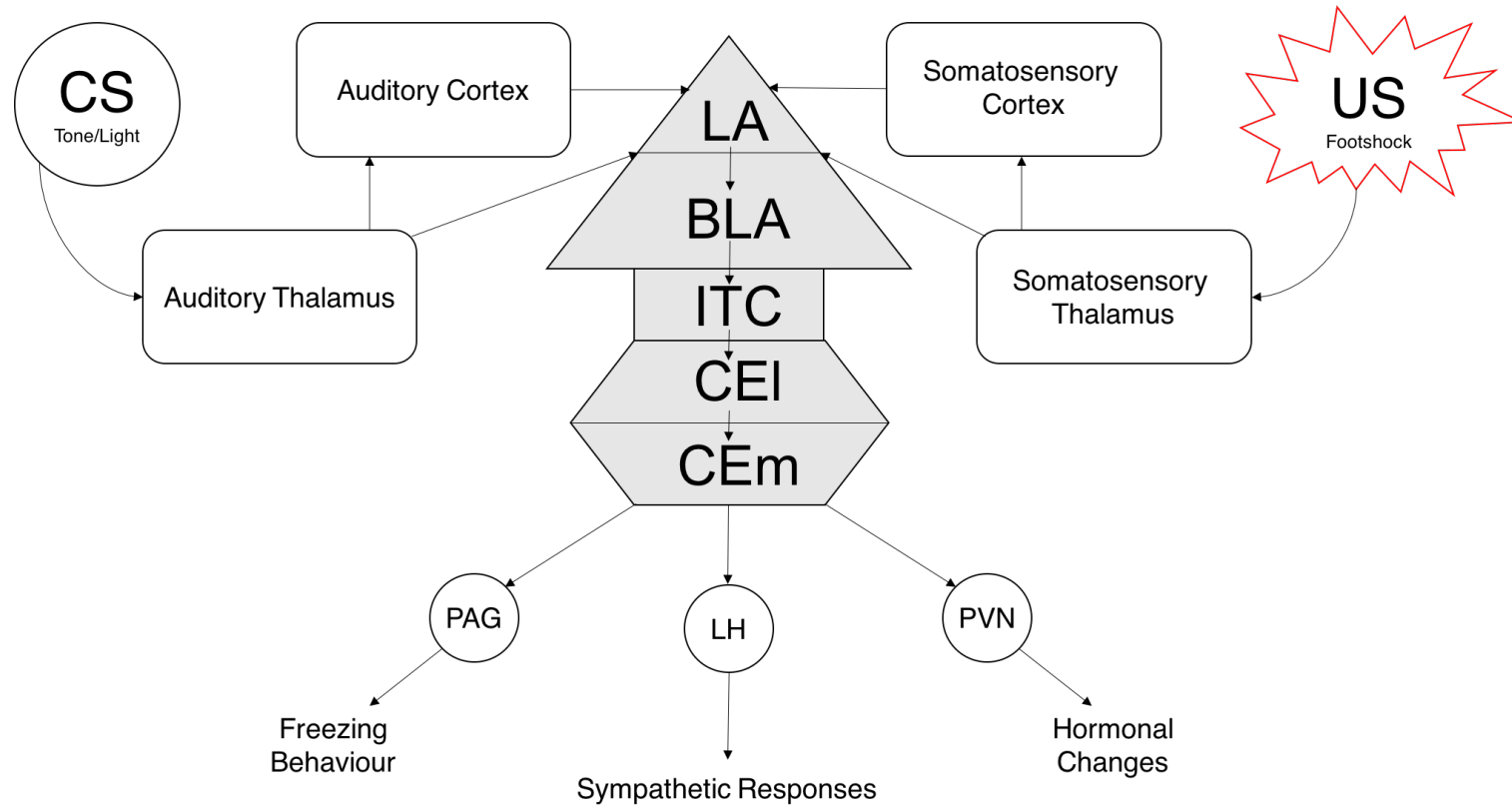
Figure 1.3. The convergence of information from the CS/US in the lateral nucleus of the amygdala (LA). All structures of the amygdala are featured with a grey background. When a stimulus or stimuli (i.e. the CS and/or the US) is perceived, cells within the LA then undergo synaptic plasticity, and information is transferred to the central nucleus of the amygdala (CEm/l) via the basolateral nuclei (BLA) and intercalated cells (ITC). Once this association has been learned and neural plasticity has been generated in the LA, future presentations of the CS alone will instigate various changes in behaviour and physiology. These changes are mediated by numerous downstream structures such as the periaqueductal grey (PAG) to cause freezing, the lateral hypothalamus (LH) to cause SNS responses (e.g. increased heart rate), and the paraventricular nucleus (PVN) to cause hormonal changes (e.g. corticosterone release). Figure adapted from Armony et al., (1997).

As shown by Figure 1.3, the LA is connected to the central nucleus of the amygdala (CE) which projects into the main somatomotor and autonomic centers involved in generating behavioural and physiological fear responses (Kim & Jung, 2006). Here, the LA to CE connection is indirect, and that CE mediation of responses is also indirect. Under normal circumstances these behaviours and physiological responses would only occur as a reaction to innately frightening or unpleasant stimuli (e.g. pain generated by foot-shock (US)). However, when the CS co-terminates with the US during conditioning, neurons in the LA that were originally stimulated only in response to the US are later also stimulated when the CS alone is present; for example, during memory retrieval of the CS post-conditioning (LeDoux, 2003). Prior to conditioning, the CS only weakly stimulates neurons in the LA, but this signal is then strengthened and perpetuated upon the co-occurrence of the US. This change in neuronal strength is a prime example of long term potentiation (LTP), and is a direct consequence of the temporal and spatial convergence of signals from the CS and US in the LA. LTP was initially discovered in the hippocampus, but has now been well established in multiple areas of the brain, including the amygdala (LeDoux, 2000 and Rogan et al., 1997). LTP is a form of synaptic plasticity, wherein the strength of signal transmission between two or more neurons is enhanced when they are simultaneously stimulated (Cooke & Bliss, 2006). This, in accordance to Hebbian theory, is used to explain the adaptation of neurons in the brain during learning (reviewed in Brown et al., 1990)). This process of is outlined in Figure 1.4. below:
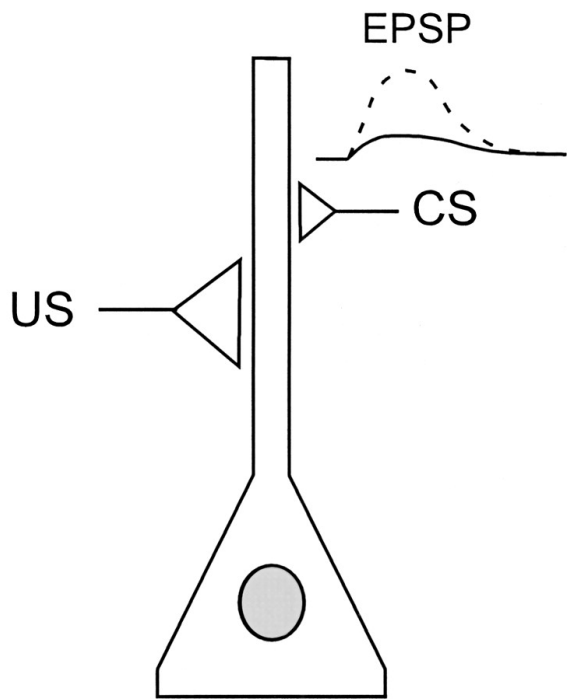
Figure 1.4. A diagram of a single neuron within the LA being weakly stimulated by the CS (smaller triangle) and strongly stimulated by the US (larger triangle). Prior to conditioning the CS will only generate a small excitatory postsynaptic potential (small EPSP, solid line) but after simultaneous activation with the US the neuron is strongly de-polarised, leading to a large EPSP (dotted line). In this instance, the neuron is demonstrating synaptic plasticity in response to the combined CS-US input. Because of the associative strengthening of CS inputs, the CS is then able to acquire the ability to activate amygdala-driven defensive responses, even in the absence of the US. Figure adapted from Blair et al. (2001).

This physiological change in neuron connectivity and firing strength underlies the initial formation of fear memory; known as a memory trace or engram (Fanselow & LeDoux, 1999). As previously described, plasticity of the neurons within the LA drives the behavioural and physiological change initially observed upon future presentations of the CS post-conditioning, such as freezing, FPS, cardiovascular changes and hormone release. These changes can then be measured to gauge the fear response to conditioned stimuli.

In summary, the generation of the fear memory trace is dependent upon changes in synaptic strength within the amygdala. The changes in synaptic strength of pre- and post-synaptic neurons are dependent on changes on a

molecular level. It is now well accepted that the consolidation of fear memory relies on increased intracellular calcium ions (Ca^{2+}) (Voglis & Tavernarakis, 2006), but Ca^{2+} release is dependent on a complex process. Activation of a pre-synaptic cell within the LA (similar to the one shown in Figure 1.4, above) causes glutamate to be released into the synaptic cleft. This pre-synaptic cell will at first be activated weakly via neurons transmitting information about a perceived CS prior to training (i.e. during habituation). During training, this pre-synaptic cell will be activated strongly by an increased number of neurons transmitting information regarding the perceived combination of CS and US. Post-conditioning, presentation of the CS alone will continue to strongly activate this pre-synaptic cell.

At rest, glutamate-responsive alpha-amino-3-hydroxy-5-methyl-4-isoxazolepropionic acid (AMPA) and N-methyl-D-aspartate (NMDA) receptors located in the membrane of the post-synaptic cell receptors are inactivated (not pictured). When the pre-synaptic cell is weakly activated (i.e. during habituation) the pre-synaptic cell will release glutamate from pre-synaptic vesicles into the synaptic cleft, where it binds to both NMDA and AMPA receptors. Although the AMPA receptors are activated, causing an influx of Na^+ ions into the post-synaptic cell and corresponding weak depolarisation, NMDA receptors have an additional Mg^{2+} block which is not removed by this weak activation. It is only upon strong activation of the pre-synaptic cell (i.e. by concurrent CS and US inputs) that there is enough depolarisation of the post-synaptic cell to remove the Mg^{2+} block from the NMDA receptors (Voglis & Tavernarakis, 2006). Once this block is removed, activated NMDA receptors

allow an influx of Ca^{2+}, which in turn activates a host of intracellular events; primarily second messenger cascades. Interestingly, Ca^{2+}-mediated post-synaptic signalling can recruit additional AMPA receptors into the post-synaptic membrane, facilitating further influx of Ca^{2+} and therefore increases post-synaptic excitation by a given pre-synaptic stimulus. Sustained depolarisation of the post-synaptic cell also allows additional influx of calcium ions via voltage-gated calcium channels (VGCC) (Kerr et al., 2000).

This increase of intracellular calcium activates certain proteins, e.g. cAMP-dependent protein kinase A (PKA) and the extracellular-regulated kinase/mitogen-activated protein kinase (ERK/MAPK) (Schafe & LeDoux, 2000). Once activated, these proteins translocate into the nucleus of the cell to modify gene transcription, ultimately resulting in gene induction and the synthesis of new proteins (Huang & Kandel, 1998; Blair et al,. 2001; LeDoux, 2000). It is these changes in gene transcription, along with epigenetic modifications (e.g. histone acetylation and methylation), that eventually lead to the consolidation of the original fear memory trace (Zovkic et al., 2013).

Within the amygdala, differing levels of excitatory (e.g. glutamate) and inhibitory (e.g. gamma-aminobutyric acid, GABA) neurotransmitters act in tandem to instigate or prevent the consolidation of fear memory and its resultant behaviours. For example, the dorsal and medial ITC of the amygdala (shown in Figure 1.2) receive excitatory glutamatergic input from the BLA, but the medial ITC additionally receives GABAergic inhibition from the dorsal ITC (Ehrlich et al., 2009; Geracitano et al., 2007; Paré et al., 2004; Royer et al., 1999). From this, the amygdala is an excellent example of the complex interplay

of excitation and inhibition within the brain, highlighting the importance in elucidating the intracellular signals that underlie fear memory.

1.4. Contextual Fear and Underlying Neurophysiology

In addition to cued fear conditioning described above (e.g. a tone CS), it is also important to consider contextual fear. Studies have shown that rats with lesions or inactivation of the BLA prior to cued fear conditioning display severe deficits in freezing during cued fear memory retrieval in comparison to control rats (Maren & Holt, 2000; Stevenson, 2011). Initially this result was thought of as unremarkable, due to the extensive involvement of the amygdala in the retrieval of fear memory and the production of fear behaviours via downstream projections (e.g. through the PAG). However, it was discovered that these freezing deficits could be overcome when the lesioned rats were subject to extensive overtraining (Maren & Holt, 2000). Over the course of this study, it was made apparent that the lesioned rats were responding to the context in which the CS was administered, in addition to just the discrete stimulus alone.

Contexts are complex and multimodal representations which are formed by unifying individual elements into a distinct representation (Maren et al., 2013). The learning of spatial contexts (e.g. places, configuration of objects within places, etc.), appears to be different from learning about a discrete stimulus (Fanselow, 2010). The individual elements within a context are perceived through the sensing organs, just like a discrete stimulus, but a context is categorically more than just the sum of its parts. Certain elements during training (e.g. smell of testing chamber, wall pattern, floor texture,

background noise, etc.) are bound together to form a representation of that context. The formation of this representation involves the hippocampus (Rudy et al., 2002); a brain region involved in spatial navigation and the consolidation of short and long-term memory (Good & Honey, 1991). The process of configuring individual context elements into a representation is known as context encoding, which is thought to depend on hippocampal LTP (Maren, 2001).

Context encoding is integral to contextual fear conditioning; a context cannot be associated with a US (and therefore feared) until it has been learned. This can be shown by the immediate shock deficit (ISD) phenomenon. Rats that are shocked immediately after being placed in a novel context, and then immediately removed, will fail to freeze later when returned to that context (Fanselow, 1990). This is because there has not been enough time for the encoding of the context as a cue and thus a context-US association has not been formed. Although context encoding takes more time than that of learning a discrete stimulus (Urcelay & Miller, 2014; Phillips & LeDoux, 1992), once learned, a context functions in a similar way to that of a CS during conditioning. For example, if enough time is given so that the subject can form a representation of the context prior to shock, the ISD is eliminated and freezing behavior during later retrieval is restored. As context encoding is hippocampal-dependent, freezing to contextual cues is significantly decreased in subjects with hippocampal lesions (Gewirtz et al., 2000; McNish et al., 1997). In addition, bilateral amygdala lesions have also been shown to almost completely eliminate contextual freezing (LaBar et al., 1995; Onishi & Xavier, 2010).

Specifically, it has been shown that the LA, CE and anterior basal nuclei of the amygdala are necessary for contextual fear conditioning (Goosens & Maren 2001). The hippocampus and the amygdala are linked via reciprocal projections (Maren & Fanselow, 1997; Kishi et al., 2006) which act to exchange information between the two structures, enabling the contextual representation to become associated with a US. The formation of a Context-US association is outlined in Figure 1.5, below:
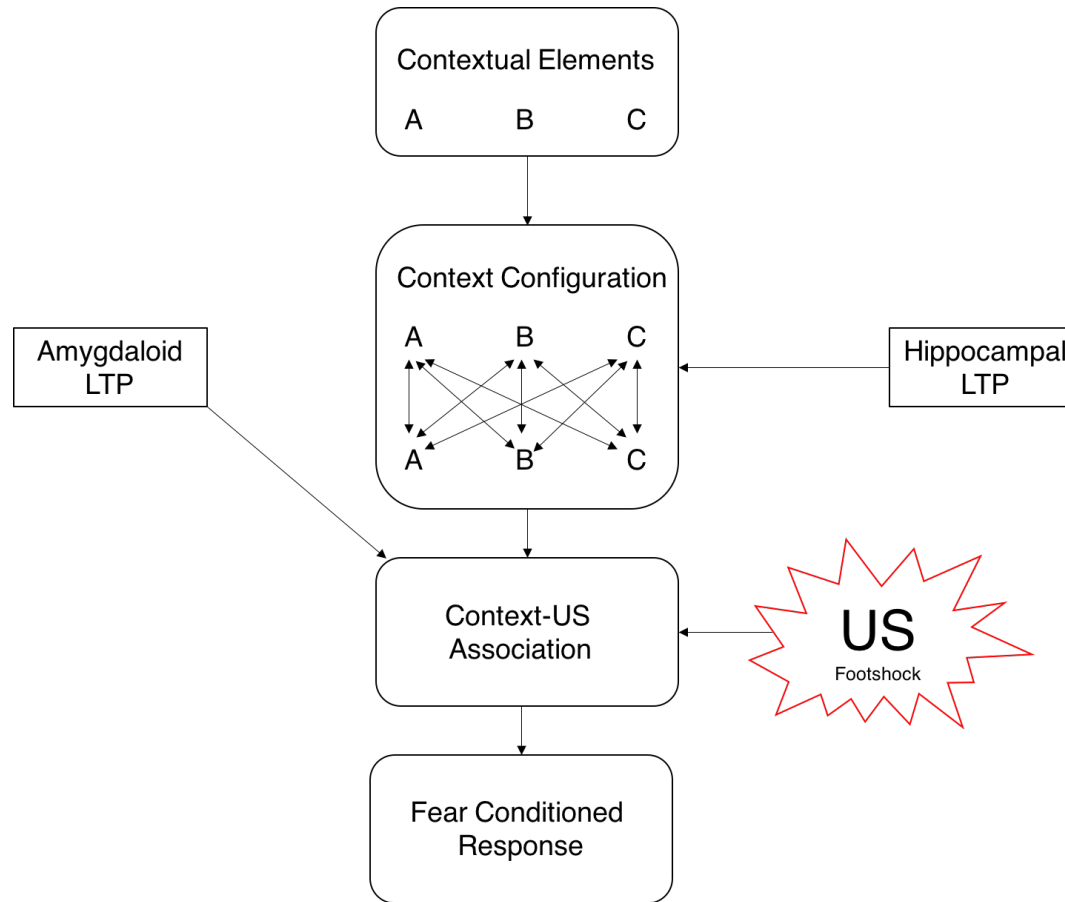
Figure 1.5. A flow diagram showing the process of contextual fear learning. Initially, the elements within a context (A, B and C) are consolidated into a single representation (context configuration); a process thought to depend on hippocampal LTP. Once encoded, this context can then be associated with a US and/or CS to form a contextual-US association. Context-US association probably involves LTP in the hippocampus-BLA projection specifically. Once an association has been made, future presentations of the context, even in the absence of a US, will evoke conditioned fear responses. Figure adapted from Maren (2001).

Initially, it was thought that once a contextual-US association memory was formed, the memory trace remained permanently within the hippocampus. However, this only appears to be true in the short term, i.e. for time periods of less than one month. Hippocampal lesions received 1 day after training produced severe contextual deficits in comparison to rats with lesions administered at 28 days post-training (Anagnostaras et al., 1999). Interestingly, after 28 days, memories of contextual fear can be disrupted by neurotoxic lesions of the medial prefrontal cortex (mPFC) (Quinn et al., 2008). Both the hippocampus and the mPFC are therefore involved in contextual retrieval, as well as the BLA. In addition to contextual memory storage, recent evidence has shown that the mPFC may also be involved in contextual retrieval.

The mPFC also has additional roles in fear learning and memory, which will be described in more detail in later sections. Contextual retrieval seems to occur in tasks where the context is very complex, or when the subject has to decide on a course of action which relates to a particular context; for example choosing an object versus choosing a location (Hyman, et al., 2012; Lee & Solivan, 2008). The mPFC, hippocampus, amygdala, sensory cortices and posterior insula also have additional roles in determining the appropriate response when the subject encounters a known CS in different contexts. For example, in one context (e.g. seen in the wild), a poisonous snake (the CS) might evoke fear, but in another context (e.g. behind glass in an enclosure) might evoke interest. This decision-making process is outlined in Figure 1.6, below:
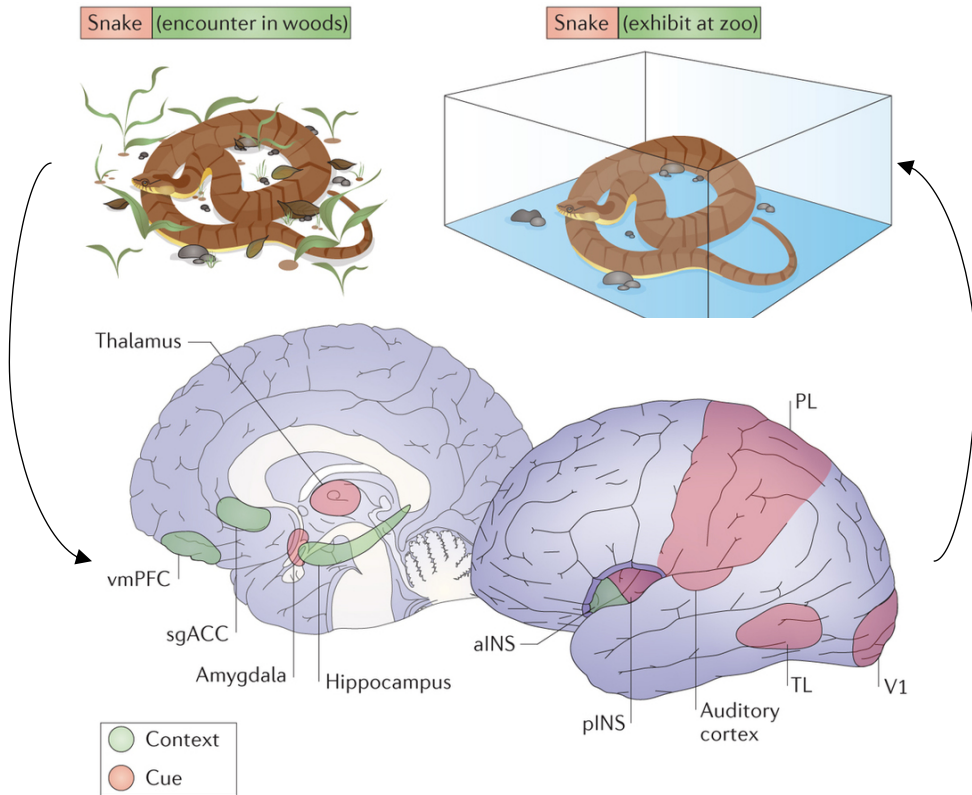
Figure 1.6. The brain areas involved in processing a cue (red) and a context (green). The cue processing system primarily includes the thalamus, amygdala, sensory cortices (the primary visual cortex (V1) and auditory cortex), posterior insula (pINS) and associated areas (in the parietal lobe (PL) and temporal lobe (TL)). The context processing systems primarily involve the ventromedial prefrontal cortex (vmPFC), hippocampus, anterior insula (aINS) and subgenual anterior cingulate cortex (sgACC). These areas work in parallel to determine the appropriate response to the combined context and cue (Orsini et al., 2013).

1.5. Inhibition of Learned Fear

The processes outlined by Figures 1.2, 1.4 and 1.5 allow us to understand and suitably respond to the cue in addition to the context in which it is perceived. As the fear response is only appropriate in certain circumstances, there must be additional systems in place to inhibit fear behaviours in situations where they are unnecessary, or even detrimental to survival. For example, being in a constant state of vigilance when it is unnecessary to do so can waste valuable resources, which can be an impedance to survival.

1.5.1 Fear Extinction

In addition to the learning and retrieval of associative fear, the ability to inhibit or extinguish fear responses is central to the dynamic mechanisms of fear behaviours. This inhibitory process is known as extinction, wherein the paired CS or context is dissociated from the US by presentations of the CS or context alone (without the US) in order to partially reduce or even completely eliminate the original fear response (Myers et al., 2006; Myers & Davis, 2007). In this instance, the CS or context is now no longer a reliable predictor of the US. Once enough cue-no-US pairings have been presented, fear behaviours (such as freezing) tend to reduce.

Originally, it was thought that extinction training erased or replaced the CS-US memory (Bouton, 2004), but the fact that this memory can be recalled to differing extents under certain circumstances after successful extinction undermines this point (Figure 1.7, below). If the CS-US memory was merely forgotten or erased during an extinction training paradigm, then the subject would show little to no fear to the CS regardless of the context, but this is not the case. It is now accepted that a new meaning is associated with the CS during extinction training. This new CS-no-US associative memory then competes with the original CS-US memory (Myers & Davis, 2007). When the CS-US memory is outcompeted by the new CS-no-US meaning, extinction is said to be successful, and vice versa.

As mentioned in Section 1.1, dysfunction in the fear network can lead to pathological anxiety and fear. For example, uncontrollable fear in response to certain stimuli (e.g. snakes, crowds) can lead to the development of panic

disorder and phobias. Extinction training forms the theoretical basis of a psychological treatment for these fear-based phobias, known as exposure therapy (ET). This practice is now one of the most common ways to treat phobias and anxiety disorders (reviewed in Sars & van Minnen, (2015)). During ET, the subject will be invited to discuss what they fear, before working up to images/videos and eventually live presentations, which are carried out in the absence of any danger (e.g. tame snakes behind glass). Initially, the stimulus presentation will evoke a strong fear response, but with repeated exposure the patient will learn that the stimulus no longer predicts threat or danger. Throughout this process, the original negative stimulus association is out-competed, leading to a reduced fear response (Myers & Davis, 2007). ET has been successful in reducing the symptoms of PTSD in combat veterans (Yoder et al., 2012), panic disorder, agoraphobia (Meuret et al., 2012) and obsessive compulsive disorder (OCD) (Foa, 2010).

Although successful in many cases, patients and therapists often find that the newly formed extinction memory does not generalise to circumstances where the stimulus is encountered outside of the extinction context. For example, a patient might have had their phobia of snakes reduced or even eliminated during ET, but still shows a heightened fear response when encountering a snake outside of therapy, even when the context is arguably safe (e.g. behind glass in an exhibit). This is because the process of extinction is highly context-dependent (Orsini et al., 2013). For example, in both rodent and human studies, repeated presentations of the CS alone initially appear to reduce fear responding to the CS, indicating successful fear extinction.

However, this fear has been shown to return to pre-extinction levels when exposed to the CS in any other context but the one in which extinction occurred. Interestingly, this response is graded after extinction training, with the highest fear response occurring in the conditioning context, lower fear responses in other contexts, and the lowest occurring in the extinction context (Hobin et al., 2003; Harris et al., 2000).

The original CS-US memory can not only return in the conditioning context, a process known as fear renewal, but it can also strengthen with the passage of time (Myers & Davis, 2007). This process is known as spontaneous recovery, wherein the longer the time interval from extinction training, the higher the level of spontaneously recovered fear. Interestingly, a subject is much more likely to forget the extinction training than the fear memory itself, as it has been shown that conditioned fear memories can last a lifetime in rats without further training (Poulos et al., 2009). From an evolutionary perspective, the comparatively enhanced strength of fear memory over extinction memory is highly advantageous. It is more adaptive to remain frightened and defensive in response to a cue that was once predictive of a potential threat, and thus react appropriately to it during future encounters were it to become dangerous again, than to assume that the cue or context will forever remain safe. In addition to renewal and spontaneous recovery, conditioned fear memories can be re-instated by further presentations of the US alone after extinction (Rescorla & Heth, 1975). The processes of extinction, spontaneous recovery, renewal and reinstatement are shown in Figure 1.7. below:
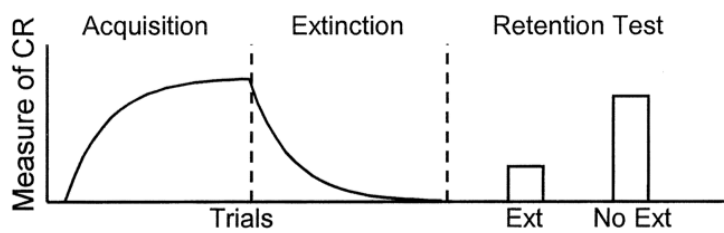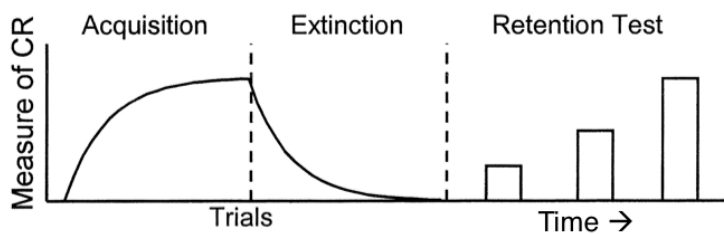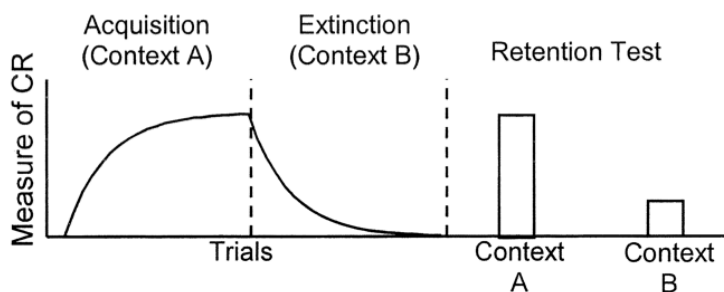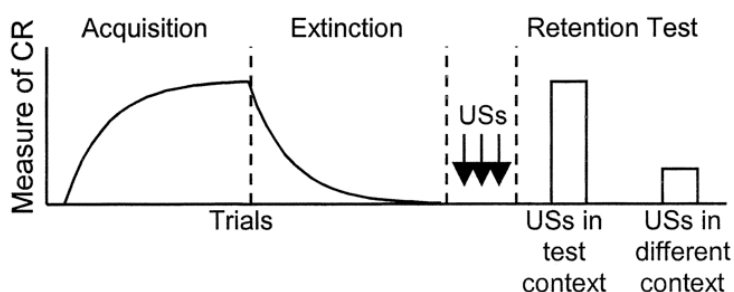
Figure 1.7. The processes of extinction, spontaneous recovery, renewal and reinstatement. A. Extinction –The acquired fear response (CR) is maintained over time even in the absence of further training but is significantly reduced after extinction. B. Spontaneous recovery – the longer the time interval between extinction training and a retention test, the higher the CR, due to a return of fear. C. Renewal – extinction is context specific; a lower CR will be observed in the extinction context (B) in comparison to the conditioning context (A). D. Reinstatement – fear can be reinstated if US-only presentations are made in the retrieval context after extinction training but before retrieval. Adapted from Myers & Davis, (2007).

1.5.2 Neural Circuitry Underlying Fear Extinction

Recently, it has been proposed that mental health disorders should be viewed as disorders of brain circuitry, biomarkers of which may be detected using current and emerging tools in clinical neuroscience (Graham & Milad, 2011). Perhaps unsurprisingly, given its role in fear acquisition and the retrieval of fear behaviours, the amygdala is also involved in the process of extinction (Moustafa et al. 2013). After acquisition, the BLA regulates the CEm/l to generate a behavioural fear response upon future presentations of the CS and/or context. During extinction, however, this fear response is reduced or even eliminated, suggesting that this pattern of activity within the amygdala has also changed.

In the early stages of extinction, repeated presentations of the CS alone act to reduce the firing rate of specific neurons in the BLA complex (Sotres-Bayon et al., 2007), but in the later stages of extinction other brain regions actively inhibit the amygdala. For example, the mPFC has an inhibitory or controlling effect on the amygdala. Specifically, the vmPFC has a major role in the control of emotion (Blair, 2008; Bechara et al., 2000). For example, projections from the vmPFC act to inhibit activity within the amygdala both during and after extinction training. This view is supported by studies showing that lesions of the mPFC impair extinction memory encoding and retrieval, and that stimulation of the mPFC (mimicking activation) reduces the number of repetitions of the unpaired CS needed to induce extinction (Sierra-Mercado et al. 2006). When the CS is presented after extinction training, the vmPFC has been shown to suppress activity in the amygdala via a combination of inhibiting

activity within the LA and increasing activity within the inhibitory ITC. This inhibitory manipulation of the amygdala by the mPFC results in reduced output of the CEl/m, leading to a rapid decrease in fear behaviours such as freezing (Sotres-Bayon et al., 2006). In addition, the hippocampus can further modulate extinction via projections to the vmPFC and the LA (Sotres-Bayon et al., 2004). It is thought that these combined interactions act to contribute to the context-dependent nature of fear extinction. An outline of the neural process of extinction is shown in Figure 1.8. below:
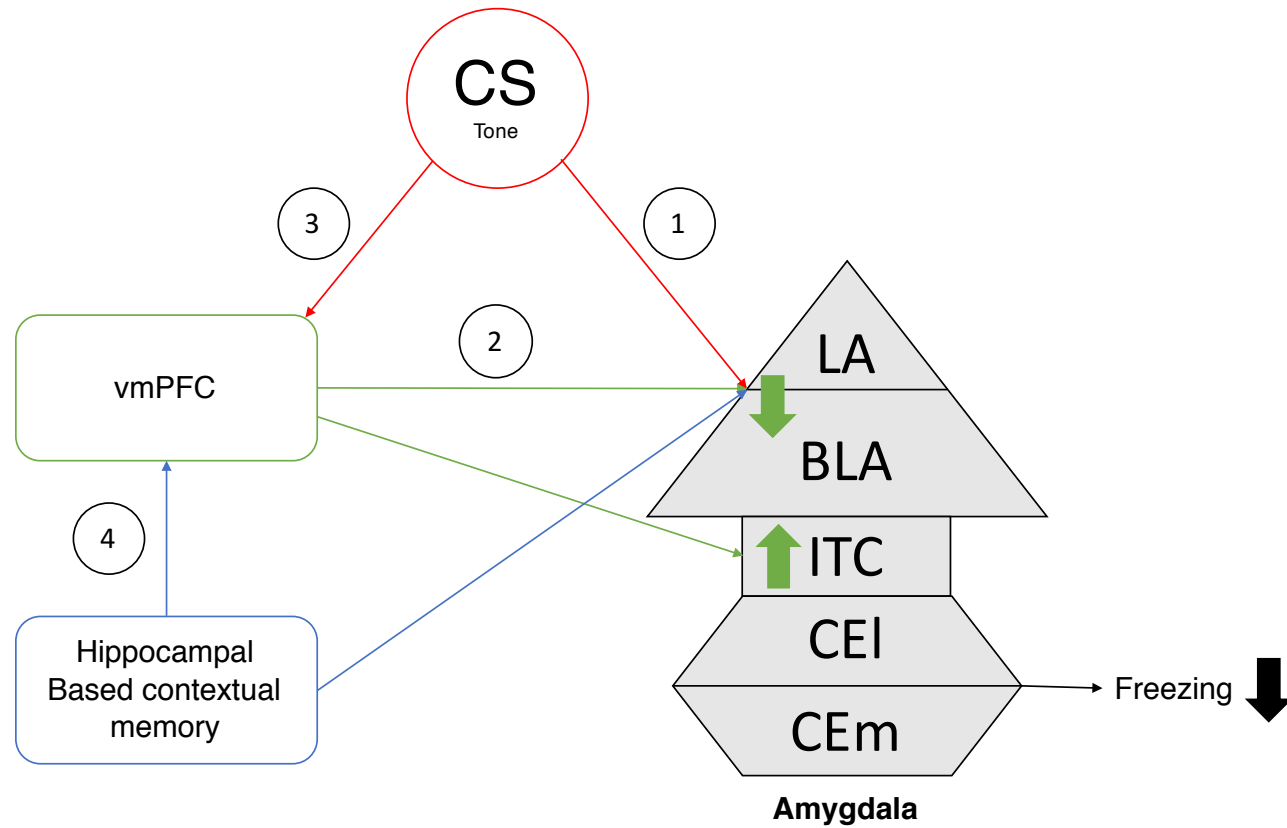
Figure 1.8. Neural circuitry underlying fear extinction. Repeated CS alone presentations (red circle) result in reduced freezing behavior over time. 1. Post-fear conditioning, repeated CS presentations cause some LA/BLA neurons to decrease their firing rate (red arrow 1). 2. During the consolidation of extinction, the inhibitory memory trace between the vmPFC and the LA and/or ITC is established, allowing mPFC-mediated amygdala inhibition (small green arrows from vmPFC to LA and ITC). 3. Upon future presentations of the CS post-extinction training, the vmPFC suppresses activity in the amygdala through inhibition of LA neurons and/or activation of the inhibitory ITC. These combine to cause a decrease in freezing via CE modulation (large green arrows, LA; suppression and ITC; activation). 4. Hippocampal-based contextual memory additionally modulates the neural activity of the vmPFC and/or LA during extinction expression to regulate the animal's behavioral response appropriately in accordance to the context. Adapted from Sotres-Bayon et al., (2006).

Following this, it is evident that the mPFC is critically involved in the process of fear extinction. Interestingly, more recent studies have highlighted that the mPFC is a heterogonous area composed of several sub-regions that are involved in dissociable ways in the modulation of fear memory, retrieval and inhibition. Although the mPFC can be catagorised into three sub-sections in rodents (the dorsal anterior cingulate (dACC), the pre-limbic cortex (PL) and the infra-limbic cortex (IL)) the PL and IL will be the focus here due to their seemingly opposing functional roles in fear memory modulation.

For example, the IL has been shown to play a key role in extinction; electrical stimulation of the IL induces comparably low levels of freezing in rats that had been conditioned but had no extinction training as those that had undergone extinction training (Milad & Quirk, 2002). Further, damage to the IL produces resistance to extinction (Vidal-Gonzalez et al., 2006). This may be because there is evidence to suggest that a previously extinguished CS can activate IL neurons that have glutamatergic (excitatory) projections to the inhibitory ITC masses (Li et al., 2011; Pare et al., 2004; Quirk et al., 2003).

These projections from IL axons are known to target the medial region of the ITC (Giustino & Maren, 2015), which additionally receives GABAergic inhibition from the dorsal ITC, meaning that there are both inhibitory connections between, as well as within, ITC cell clusters (Royer et al., 1999; Geracitano et al., 2007). With increased overall activation, the ITC reduces conditioned fear responding (e.g. freezing) via inhibiting the downstream CEl/m neurons (see Fig 1.7) (Paré et al., 2004). In addition, electrical stimulation of the IL was found to greatly reduce how responsive the CEl/m neurons were to

inputs from the BLA (Quirk et al., 2003). Moreover, post-conditioning training activation of IL using the GABA$_A$ receptor antagonist picrotoxin facilitates between-session extinction of cued and contextual fear, further supporting a role of IL in consolidation of fear extinction (Courtin et al., 2013). Overall, the IL is thought to inhibit the expression of fear behaviours through its projections to the amygdala.

In direct contrast to the IL, the PL of the mPFC has been shown to be involved in the promotion of fear behaviours. For example, increased single-unit firing rates in the PL correlate strongly with sustained fear and poor extinction during training (Fitzgerald et al., 2014a). Similarly, sustained LFP activity within the PL contributes to enhanced learned fear expression and a resistance to extinction (Fenton et al. 2014; 2016). Bilateral inactivation of the PL has also been shown to disrupt fear memory expression (Stevenson, 2011). Further, the PL has been hypothesised to promote fear expression through its activation of BLA neurons projecting to the CEl/m. Via these connections, the PL is thought to modulate and even promote the renewal of extinguished conditioned fear responses (Courtin et al., 2013).

In support of this, recent studies have shown that the overriding inputs to active neurons in the LA were from the IL during the retrieval of extinction memory, whereas the renewal of fear memory was instead associated with active neurons receiving inputs from the PL (Orsini et al., 2013; Knapska & Maren, 2009). In addition, stimulation of the PL has been shown to be associated with an increase in conditioned fear behaviours. Interestingly, the expression of fear behaviours also correlates with an increase in CS-evoked

activity in the PL (Burgos-Robles et al., 2009). For example, approximately 15% of all PL neurons have been shown to be specifically activated with presentations of the CS post conditioning, and upwards of 25% of PL neurons also showed sustained responses during fear behaviour expression (Milad & Quirk, 2002).

These rodent brain regions are homologous to brain regions within primates and humans, with the PL bearing functional resemblance to the dACC and the IL to the vmPFC (Milad & Quirk, 2012). In support of this, high-frequency stimulation of in the vmPFC facilitated extinction learning in monkeys. Similarly, suppressing the dACC/PL also had a positive effect on extinction learning in monkeys and rodents (Goode & Maren, 2014; Klavir et al., 2012). Similar to the IL in rodents, the vmPFC has been shown to modify the ITC of the amygdala (Phelps et al., 2004). Hippocampal input to the vmPFC has also been shown to be involved in contextual modulation of fear acquisition and extinction, with damage sustained or lesions administered to the vmPFC impairing extinction. Specifically, the vmPFC receives input from hippocampus during extinction recall (Mueller et al., 2014), and co-ordination of activity between the amygdala and the vmPFC is necessary for successful extinction learning (Morriss et al., 2015). In humans, the degree and rate of extinction learning is positively correlated with the cortical thickness of the right vmPFC (Milad & Quirk, 2002; Winkelmann et al., 2016).

The PL, IL, hippocampus and BLA are all reciprocally connected, allowing them to communicate with one another and form functional neural circuits. Importantly, these neural circuits act to generate short and long-term

memory representations of associative fear learning, which then influence behavior (Ehrlich et al., 2009). In further detail, excitatory glutamatergic neurons from the ventral hippocampus and the BLA project to prefrontal inhibitory interneurons (Tierney et al., 2004; Gabbott et al., 2006). Similarly, studies in anesthetised rats have shown that IL principal neurons can inhibit PL principal neurons via local PL interneurons (Ji & Neugebauer, 2012). Moreover, the PL and IL each receive distinct inputs from specific BLA neuronal circuits; the PL receives input from the BLA during high fear states whereas the IL receives input from the BLA during low fear states. These projections facilitate the development and maintenance of neuronal plasticity in the mPFC and contribute to the outcome of the amygdala output; whether the fear response is ultimately promoted or inhibited (Maroun and Richter-Levin, 2003; Herry et al., 2008).

Another key finding of this study highlighted the existence of so-called groups of 'fear' and 'extinction' neurons which are distributed in the BLA in a 'salt and pepper' like manner. This is due to the lack of laminar structure in the BLA, unlike the layers found in the mPFC and hippocampus. 'Fear neurons' were shown to exhibit a temporally selective increase in spike firing during presentations of the CS during and after fear conditioning. This increase in spike firing was entirely negated after subsequent extinction training, even being converted to CS-evoked inhibition in some cases. Conversely, another group of neurons did not show any increase in CS-evoked responses during or after fear conditioning, but instead showed subtle reductions in firing rate. Extinction training was then shown to induce a dramatic and selective increase

in firing rate in this group of neurons upon future presentations of the CS. Finally, changes in CS-evoked firing of 'fear' and 'extinction' neurons were inversely correlated with successful extinction retrieval, as measured by differing freezing levels.

Even though there is some literature detailing how the PL, IL and BLA are interconnected, exactly how these regions communicate with each other is generally still poorly understood. In addition to improving understanding of these mechanisms, research into the neural circuitry of fear memory has clinical potential concerning the treatment of anxiety disorders (Zlomuzica et al., 2014). Taking into consideration the mPFC for example, dysfunction of this region has been related to psychiatric disorders, such as PTSD (Pitman et al., 2012). For example, PTSD patients express abnormal or inadequate fear extinction learning, which may in part be modulated by the dACC (PL) and vmPFC (IL) regions of the mPFC (VanElzakker et al., 2014). In addition, it has been shown that sufferers of PTSD have a significantly smaller mPFC regions and hippocampi than those of control subjects (Gurvits et al., 1996), which may help to explain why they express fear in inappropriate contexts. PTSD patients who display impaired extinction also have reduced overall activation of the amygdala, the hippocampus, the vmPFC and the dACC when examined via fMRI (Shvil et al., 2014). There is also evidence to suggest that PTSD patients display a greater activation of the dACC during extinction recall (Giustino & Maren, 2015). Similarly, the vmPFC-amygdala pathway may be dysregulated in some patients suffering from PTSD, as patients with bilateral vmPFC damage present heightened amygdala activation to aversive images in

comparison to controls (Motzkin et al., 2015). Recently, PTSD patients have been shown to display a hypoactive vmPFC (Soler-Cedeño et al., 2016). Combined with the fact that reduced vmPFC activity is associated with decreased inhibition of the amygdala, and that hyper-activation of the amygdala is associated with increases in fearful behaviour, it is unsurprising that the influences of the dACC and the vmPFC play critical roles in the regulation of fear expression and inhibition. Additional studies have also shown that patients with PTSD display an impaired ability to extinguish fear during extinction in comparison to non-sufferers (Wessa & Flor, 2007; Jovanovic et al., 2012).

1.6. Fear Discrimination

It is important to note that an inability to extinguish fear is not the only issue affecting sufferers of anxiety or panic disorders; the inability to discriminate between fear-inducing and safe stimuli is also proving to be a major factor of these conditions. Fear conditioning, retrieval and extinction and have all been extensively used in laboratory and clinical settings to examine the neurobiology of fear and its underlying mechanisms. However, it is also important to consider the neural circuitry underpinning the switching between exploratory and defensive behaviour in response to safety and danger-predicting cues, respectively. Not only is it fundamental to survival, but dysfunction of this behaviour has been shown to have pathological consequences. We can study this process by examining fear discrimination, a conditioning paradigm that allows us to simultaneously study the behavioural and neurobiological changes

which occur during the learning and retrieval of stimuli associated with threat or safety.

Fear discrimination typically involves a subject having to distinguish between two stimuli. One stimulus is always predictive of a US (e.g. foot-shock) and is known as the CS+, whereas another stimulus predicts the *absence* of a US (e.g. is never paired with foot-stock) and is known as the CS- (Kurayama et al., 2012). The CS+ and CS- can be presented as discrete, auditory stimuli (e.g. high and low pitched tones, (Lissek et al., 2005)). The CS+ and CS- can also be different contexts instead of discrete cues (Christianson et al., 2012; Kim et al., 2013). Previous studies have used multiple sensory modalities as the CS+ and CS-, for example, different olfactory cues (Laviolette et al., 2005), a combination of tones and lights (Lee & Choi, 2012) and distinct auditory cues (Ito et al., 2009). In the case where the CS+ and CS- were two discrete tones, the CS+ would be interpreted as the 'fear' tone, and the CS- would be interpreted as the 'safety' tone. If fear discrimination training is successful, a subject will produce more of a fear response when exposed to the CS+, compared to the CS-, even in the absence of any US reinforcement. See Figure 1.9 below for an outline of a fear discrimination paradigm:
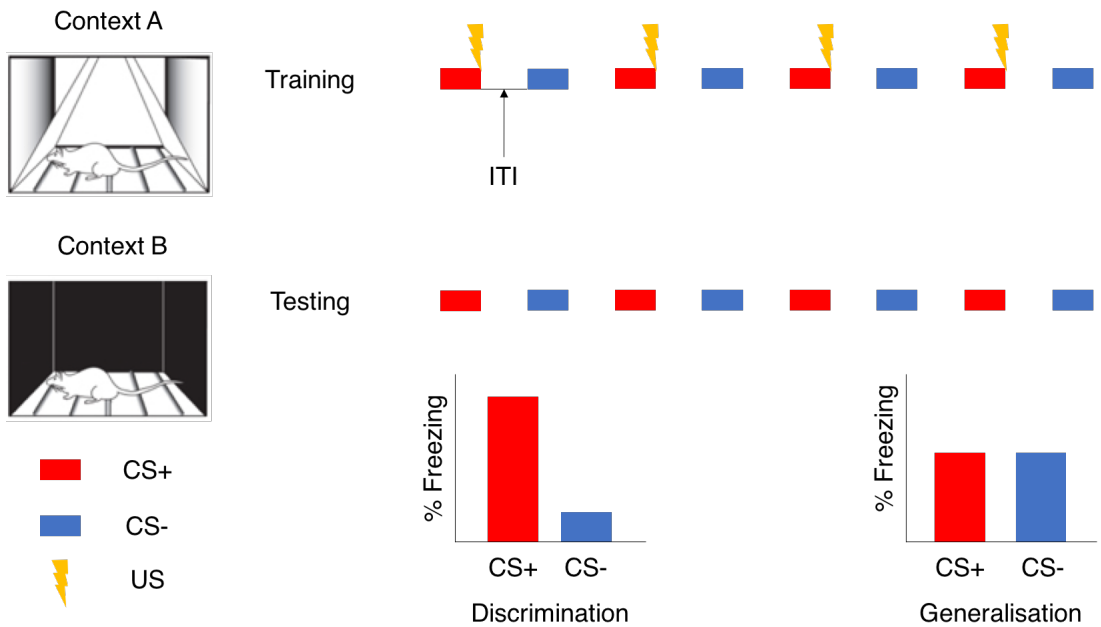
Figure 1.9. An outline of fear discrimination training using discrete cues with either discrimination or generalisation at retrieval. During training in context A, CS+ and CS- are presented to the subject. The CS+ (in red) is always paired with a footshock (US; yellow lightning bolt), and the CS- (in blue) is never paired with the US. During testing in context B, the CS+ and CS- are presented multiple times, but there is no US presentation. Training and testing take place in different contexts to prevent additional transfer of fear from the training context (with which the US could be associated, albeit to a lesser extent than the CS+) to the testing context (in which no US ever occurs, so should be treated as 'safe'). After testing, freezing responses to the CS+ and CS- are analysed – significantly higher levels of freezing to the CS+ in comparison to the CS- (as shown by the higher red bar compared to the blue bar; bottom left) depict successful discrimination, whereas equal levels of freezing to the CS+ and CS- depict fear generalisation (red and blue bars of equal height; bottom right).

It is evolutionarily advantageous to be able to discriminate between cues that signal safety and danger, as without discrimination, the subject is in an hyper-vigilant state of arousal, which wastes resources (Zhu et al., 2014). An inability to reliably discriminate between cues can also lead to fear generalisation, where fear behaviours originally evoked by the CS+ are transferred across to other cues (Dunsmoor et al., 2011).

When the subject has generalised between cues, an inappropriate fear response is generated in the presence of the CS-. There is evidence to support a link between fear generalisation and certain pathologies, such as generalised

anxiety disorder (GAD). In one experiment, patients with GAD expressed a fear response to a much wider selection of cues during a visual discrimination task in comparison to controls (Lissek et al., 2014). It is thought that the over-generalisation of fear to neutral or safe cues could be a major contributor to GAD, as it works to increase the overall number of fearful stimuli the subject perceives to encounter, thus increasing and maintaining worry and anxiety in sufferers. In mice, it has been shown that fear memory generalisation depends on training intensity, i.e. both the US intensity and the number of CS-US pairings applied; if the US intensity is stronger and there are larger numbers of CS-US pairings, generalisation is more likely to occur (Laxmi et al., 2003). In this instance, it is 'safer' to generalise the fear response to more cues, as the consequences of not doing so are arguably worse.

Perhaps unsurprisingly, some patients suffering from PTSD have been shown to generalise previously learned fear responses to safe stimuli and contexts (Christianson et al., 2012). In their past traumatic experiences, acting inappropriately and not treating potential threats as truly dangerous could have literally been the difference between life and death under certain circumstances (e.g. a war veteran who has been on a battlefield). Therefore, patients with PTSD are far more likely to generalise prior fear responses to cues and contexts reminiscent of prior trauma.

Although they share some similarities, failure to learn that the CS-predicts safety is arguably different to the process of conditioned inhibition, where the subject is initially presented with one stimulus (e.g. a tone) that is associated with a US (e.g. a foot-shock). This initial stimulus is known as A+

(e.g. a tone) and presentation of A+ alone is learned as a reliable predictor of shock. However, when A+ is paired with another stimulus B (e.g. a light), which is presented simultaneously with A+, then there is no US paired with these cues. This combination of stimuli is described as AB-. After training, the combination of the tone and light evokes less of a fear response than the tone alone. This is because in the AB- paradigm, the light (B) is acting as a conditioned inhibitor (CI) and acts to inhibit the fear evoked by the tone (A+). During fear discrimination on the other hand, the CS- is never presented concurrently with the CS+. Therefore, although the fear response is significantly lower during the CS- presentation than during the CS+ presentation after successful fear discrimination (Christianson et al., 2012), the CS- arguably does not directly reduce the fear generated by the learned CS+, making it subtly distinct from a true CI described above. Indeed, as the CS+ and CS- are presented as distinct entities during training and retrieval, and different properties are conferred to each of the two stimuli, this provides evidence for the CS- acting as a learned safety signal (Kong et al., 2014).

It is worth noting that there is some ongoing discussion as to the exact definition of a "safety signal" in the current literature. In some instances, "safety signals" have been described as a special kind of CI (Christianson et al., 2012), yet this is typically reserved for instances where the "safety signal" and the fear-conditioned stimulus are presented simultaneously. In the instance of fear discrimination described by Figure 1.9 above (and in subsequent chapters 2, 3 and 4), the CS- does not act merely as a CI of the fear generated by the CS+ as the two stimuli are never presented concurrently. Further to this, if prior CS-

presentations were in some way inhibiting the fear generated by the CS+ then the relative fear response at the beginning, compared to the end, of conditioning would decrease, which is not the case. For the purpose of this thesis, when the subject has opposing responses to the CS+ and CS-, and when the CS+ and CS- are not presented concurrently, it is more likely that the CS- is acting as a safety signal, not a true CI. Moreover, if the CS- during fear discrimination training and retrieval is an example of learned safety, it further highlights the wider importance of understanding the neurobiology of this process. Indeed, recent research has shown that impaired safety signal learning may be a biomarker of PTSD (Jovanovic et al., 2012). Therefore, research furthering our understanding of the process of fear discrimination is critical to our clinical approach in helping to treat such disorders.

Considering this, it is also important to note that during fear discrimination, the CS- acting as a safety signal is distinct from the process of fear extinction. The CS+ evokes the same level of fear throughout, as it remains a reliable predictor of the US. Further, it has been shown that there are increases in dACC activation during acquisition of fear conditioning in response to the CS+ compared to the CS- (Baeg et al., 2001). The CS- does not act as a direct inhibitor of the fear evoked by the CS+, nor is the latter extinguished. Further, conditioning discrimination-trained animals to the CS- after fear discrimination training results in slower fear acquisition than using the same stimulus in the training of naive animals (Kong et al., 2014). This reduction in the rate of conditioning to the CS- after discrimination training is known as

retardation, providing evidence that the CS- takes on properties of a safety signal.

1.6.1 The Neurobiology of Fear Discrimination

There is evidence to suggest that the CS- may employ different (but potentially overlapping) neurobiological mechanisms than those involved in either CI or extinction, meaning that fear discrimination has strong potential to contribute new information to the field of fear neurobiology. Although it has been shown that learned CS+ and CS- cues can evoke differential behaviours, there has been relatively little research investigating the contribution from various brain regions involved in mediating these behaviours, in comparison to fear conditioning and extinction.

So far, the mPFC and the amygdala have been implicated to have key roles in discrimination learning. For example, it has recently been shown that CS+ presentations evoke increases in BLA neuronal excitability during discrimination learning under anesthesia in rats, but that CS- presentations do not (Fenton et al., 2013). In this instance, the CS+ and CS- were in the form of tones, wherein the CS+ was paired with electrical stimulation of the hind-paw to mimic footshock used as the US in awake-behaving studies. Similarly, another study also showed that mPFC activity selectively increased during presentations of the CS+ in comparison to the CS- after discrimination learning (Fenton et al., 2014b). Prior to this, a discrimination task with odors in rats was reported by Laviolette et al., (2005). In this study, a subpopulation of neurons in the mPFC which received inputs from the BLA showed increased

spontaneous and bursting activity to odors paired previously with foot-shock (CS+), but not to odors that were not paired with foot-shock (CS-). Further research into discrimination in anaesthetised rats has shown that the LA also displays an enhanced post-synaptic potential (i.e. increased excitability) in response to a previously conditioned CS+ odour, but converesly displays a decrease in response to a CS- odour (Rosenkranz & Grace, 2002). The same group also found that stimulation of the mPFC suppressed LA neuronal activity that was previously evoked by both CS+ and CS- stimuli (Rosenkranz et al., 2003) . Although these studies have shown that that discrimination learning can occur at the neural level in the BLA and mPFC under anesthesia, there is still a considerable amount of research to be undertaken in recording from the brains of freely-moving rats undergoing similar discrimination training and retrieval tasks.

GABA is the main inhibitory neurotransmitter secreted in the brain, where it is mostly synthesised by interneurons. GABA transmission in the amygdala is known to be important for controlling levels of fear and anxiety (Bremner et al., 2000), with diminished central GABA and GABA receptor levels found in patients suffering from anxiety disorders and PTSD (Heldt et al., 2012). In addition to this, recent research has begun to highlight the role of GABA in fear discrimination. Most GABA synthesis is catalysed by the enzyme glutamic acid decarboxylase 67 (GAD67) and the isozyme GAD65 (Fenalti et al., 2007). Targeted ablation of the GAD65 gene in Gad65−/− mice results in context-independent generalisation of auditory fear memory during retrieval (Bergado-Acosta et al., 2008; Sangha et al., 2009). Further, GAD65 deficiency in mice

was found to reduce synaptic transmission and plasticity at cortical inputs to LA principal neurons, resulting in a generalisation phenotype (Lange et al., 2014)

In addition to the amygdala, the mPFC has also been shown to have a key role in fear discrimination in awake behaving animals. Initial results by (Lee & Choi 2012) showed that when muscimol, a $GABA_A$ receptor agonist, was administered into the mPFC after discrimination training but before retrieval testing, the level of freezing in rats during retrieval in response to the CS- was indiscriminate from the level of freezing in response to the CS+, i.e. generalisation. Lesions to the mPFC also produce a large impairment in contextual discrimination, as shown in the study by Antoniadis & McDonald, (2006). Further to their individual contributions, work has been emerging to describe the combined influences of the BLA and the mPFC on the process of fear discrimination.

The study by Likhtik et al., (2014) examined theta power and synchrony between the BLA and mPFC of male mice trained with an auditory fear discrimination paradigm. Here, it was shown that there was increased theta synchrony between the mPFC and BLA during the CS+, but that this increased synchrony was only present in mice that could successfully differentiate between the CS+ and CS-. In mice that had similar levels of freezing between the two tones (generalisers), theta power increased in the BLA and mPFC equally during the CS+ and CS-. Further they found that, in mice who discriminated, BLA firing became entrained to theta input from the mPFC during recognised safety across learned (i.e. during the CS-) and innate (i.e. when the mouse was in the darkened outer edge of an open field) fear protocols.

Another study from Stujenske et al. (2014) advanced the data generated by Likhtik & Gordon, (2014) by looking at both gamma and theta frequency activity in the BLA and mPFC during fear conditioning and extinction as well as during exposure to an open field. This group found that slow (40-70 Hz) and fast (70-120 Hz) gamma oscillations in the BLA were coupled to distinct phases of the local theta cycle in the BLA. In addition, this study showed that the coupling between BLA theta and BLA fast gamma was enhanced and that fast gamma power was suppressed during periods of fear, whilst relative periods of safety were correlated with enhanced fast gamma power in the BLA, strong coupling of BLA gamma to mPFC theta and mPFC-to-BLA directionality. This suggest that states of fear and safety could be mediated by changes in BLA gamma coupling to theta frequency inputs.

Taken together, these results suggest that the mPFC could be responsible for the safety signaling mechanism acting on the amygdala to diminish fear, in addition to the strong evidence for PL, IL and BLA involvement in fear discrimination learning, expression and extinction. Further, the interconnectivity of the mPFC and BLA has been shown to be central for these processes (Bukalo et al., 2014; Laviolette et al., 2005; Tejeda & O'Donnell, 2014). If the IL and PL have already been shown to have key roles in fear inhibition, it is also likely that they could be involved in safety learning specifically.

In addition to this, more studies are distinguishing between the functionally separate PL and IL to investigate their individual contributions to fear discrimination learning and retrieval. For example, it has been shown that

reducing PL GABA$_A$ transmission via the antagonist bicuculline before the acquisition or expression of fear discrimination eliminated the ability to discriminate between CS+ and CS- (Piantadosi & Floresco, 2014b). Further to this, a discriminative conditioning task that included presentations of a reward cue (paired with a reward pellet), a fear cue (paired with footshock), and a safety cue (no footshock) found that rats with IL inactivation showed no significant differences in freezing to any of the cues, meaning they no longer exhibited discrimination (Sangha et al. 2014). Recently, it has also been shown that unit firing and LFP power in the PL and, to a lesser extent the IL, increases in response to an auditory CS+, but not during CS- presentation or footshocks alone. This was shown in anaesthetised animals that had undergone discrimination training (Fenton et al. 2014a). These studies together show evidence for PL and IL involvement in discrimination learning.

1.7. Sex Differences

As previously discussed, women are more likely to suffer from an anxiety disorder and PTSD than men, yet the vast majority of work in animal models of fear and anxiety has been conducted in male rats (Shansky, 2015). However, there is evidence to support that fear learning, retrieval and inhibition differ between males and females, in rodents as well as in humans. For example, during an aversive learning task, females are faster to acquire eye-blink conditioning than males (Dalla & Shors, 2009), and are more likely than males to escape during inhibitory avoidance tasks (Dalla et al., 2008). Sexual dimorphism in the amygdala and mPFC has also been previously documented

in humans (Goldstein et al., 2001; Neufang et al., 2009) with males having larger amygdaloid volumes relative to cerebrum size. Interestingly, males also have elevated levels of oestrogen receptors in these areas (Lebron-Milad & Milad, 2012). In rodents, males show mPFC dendritic remodeling in neurons that do not project to the amygdala after chronic stress, but females fail to do so (Shansky et al., 2010). Taken together, these results highlight the need to consider the neurobiological reasons behind increased instances of anxiety disorders in women.

It has already been established that sex hormones such as oestrogens can affect neural processes such as latent inhibition (LI), fear learning and fear extinction in rodents (Farrell et al., 2015). For example, LI has been shown to be affected by the phase of oestrous in naturally cycling female rats (Quinlan et al. 2010). Recent evidence has also shown that estradiol can modulate mPFC and amygdala activity in both women and rats during fear extinction (Zeidan et al., 2011). Further work has shown that oestrogen may modulate the fear extinction network and fear inhibition in females (Lebron-Milad & Milad, 2012). For example, female rats in the proestrous (i.e. high oestrogen) phase of the oestrous cycle exhibited significantly less overall freezing during extinction learning compared to female rats at different points of the cycle and to male rats (reviewed in Gruene et al., 2015).

Further, oestrogen may interact with dopamine to influence fear inhibition. An injection of a dopamine agonist after conditioning, but before extinction learning, reversed the impaired extinction retrieval seen in proestrous females (Rey et al., 2014). Interestingly, administration of a dopamine agonist

additionally impaired extinction in low oestrogen phase females, suggesting that dopamine and oestrogen have optimum levels at which they interact to influence extinction. This study also illuminated structural connectivity differences between the IL and BLA which are influenced by oestrogen and dopamine; treatment with dopamine induced a positive correlation between freezing and IL-BLA circuit activation in low oestrogen females, but a negative correlation in high oestrogen females. In addition, a study by Toufexis et al., (2007) has illuminated the role of oestrogen in the disruption of conditioned fear inhibition in female rats, showing that gonadectomised female rats implanted with 17β-estradiol generalised their fear to a conditioned inhibitor compared to controls.

There is also data to support the influence of hormones on sex differences seen in contextual fear discrimination tasks. In one study, males were able to display contextual discrimination over the entire time-course of the experiment, whereas females exhibited generalisation five days after training (Lynch et al., 2013). Further, this study showed that ovariectomised females with no hormone replacement could discriminate just as well as males, whereas those receiving 17β-estradiol generalised their fear response to a neutral context. Testosterone, in addition to oestrogen, also has sex-specific effects on the physiology of neurons in various brain areas. In the hippocampus, gonadectomised male rats have a 50% reduction in density of spine synapses on pyramidal neurons in the CA1 area compared to intact males. Treatment with testosterone, but not oestrogen, returned spine synapse density back to pre-gonadectomy levels (Leranth et al., 2003). In addition, testosterone has

been shown to influence fear discrimination and generalisation. Gonadectomised male rats were implanted with a capsule containing either testosterone, estradiol, or left empty (Lynch et al., 2016). In this study, it was found that treatment with testosterone or estradiol maintained contextual discrimination. However, male rats treated with empty capsules generalised, showing enhanced freezing in the neutral context. As male rats aromatise testosterone into oestrogen (reviewed in Simpson & Davis, (2001)), and yet oestrogen appears to impair fear discrimination in females, these results suggest opposing effects of these two hormones in males and females with respect to fear discrimination and generalisation.

Outside of the influence of sex hormones, studies are beginning to elucidate basic neurobiological differences in how males and females process fear learning, retrieval and inhibition. For example, recent research has shown sex differences in PL oscillations in the theta range during fear extinction in awake behaving animals (Fenton et al. 2014a). During this study, females showed higher expression of learned fear during extinction training and displayed more spontaneous fear recovery in comparison to male subjects. This enhanced fear expression was associated with sustained theta activity in the PL and IL in females compared to males, highlighting that the sex differences seen in fear conditioning, retrieval and extinction may be region specific. Research has also shown sex differences in PL and IL activity in the lower gamma (30–45Hz) frequency band range during extinction. For example, Fenton et al. (2016) showed that females display both higher levels of freezing in addition to persistent PL gamma activation during extinction recall compared

to males. Further, the same females also show a lack of IL gamma activation during extinction recall in comparison to males.

From these data, it has been shown that there are marked differences in males and females in terms of contextual fear discrimination and fear inhibition tasks, potentially involving differing levels of oestrogens and/or differential activity in the PL and IL in females. However, neurobiological and behavioural sex differences during cued fear discrimination and recall are still largely unexplored. As previously discussed, Likhtik & Gordon, (2014) did investigate fear discrimination learning and memory retrieval, but this study involved only male mice. Further, the extent to which connections between the PL, IL and BLA might mediate discrimination between discrete threat and safety cues, and how biological sex influences the activity and connectivity of these brain areas, remains mostly unknown.

1.8. Computational modelling

In addition to observing neural oscillations *in vivo*, very recent research is starting to explore the dynamics of brain activity inside of a computational framework. Here, the brain is considered a dynamic system, where neural activity can be generated and then studied under differing conditions (Ashwin et al., 2015). Although computational models can never truly replace *in vivo* experiments, models make use of observations taken from such experiments and can invoke manipulations designed to expose how the system of interest functions (Brodland, 2015). Further, computational modelling provides numerous advantages compared to more traditional experiments.

For example, models can demonstrate hypothesis testing (e.g. determining whether a proposed mechanism is sufficient to produce an observed phenomenon, given known properties of the system components (Weinhardt & Vancouver, 2012)), run experiments over scale lengths which are impossible to measure in real time (e.g. speeding up a slow process or slowing down a fast process (Brodland, 2015)), provide novel sources of insight into behaviour (e.g. allowing seemingly contradictory hypotheses to be tested (Servedio et al., (2014)), be reversibly broken or interrupted at certain stages of processing (e.g. avoiding complications sometimes caused by lesion studies (Andino et al., 2011)), and generate data leading to novel predictions to be tested later (e.g. *in vivo* (Schellenberger et al., 2016)). In addition, the utilisation of computational models over *in vivo* experiments contributes to the replacement of using live animals in research (Kilkenny et al., 2010), which is supported by the Medical Research Council (Perel et al., 2007). Importantly, models allow for higher levels of control than a real system (e.g., the inclusion or omission of more variables, each of which can be manipulated more precisely). This means that elements of the system can be investigated individually to identify their specific role in the overall outcome.

In some variants of these models, differential equations are used to describe how a system (e.g., a neuron, brain region, network between regions etc.) changes and evolves over time (Brette et al., 2007). Differential equations offer a framework from which the initial conditions of a system can be used to generate a prediction of how that system will change over time (i.e. in the future) (Schmidt et al., 2015). The initial conditions and how these change over time

can be set to certain values or rules, depending on the research question at hand. For example, if we wanted to know if a simulation of 'neural activity' in a model of a brain area would increase, decrease or stay the same over time when another simulated input (i.e. from another brain area or outside stimulus) was applied, this could be achieved from a computational model using differential equations (Courbage et al., 2007).

In this case, the initial conditions, or parameters/variables, of the model would have to be provided, or set, before running the model. For example, the parameter of the neural activity prior to the outside influence is a condition that can be initially set as relatively high or low. In addition, the type and amount of input from the outside influence would be another parameter to be provided; e.g., the outside influence could be set as large or small (i.e. causing a major or minor perturbation to the neural activity), and positive or negative (i.e. causing increases or decreases to the neural activity). Further, thresholds which determine how likely it is that the activity level in the system changes can also be set; e.g. setting a very low threshold would mean the neural activity is easily perturbed by external input. This would be similar to reducing the membrane potential on a neuron, meaning that action potentials are more likely to occur more frequently. A diagram comparing *in vivo* to *in silico* neural activity is outlined in Figure 1.10. below:
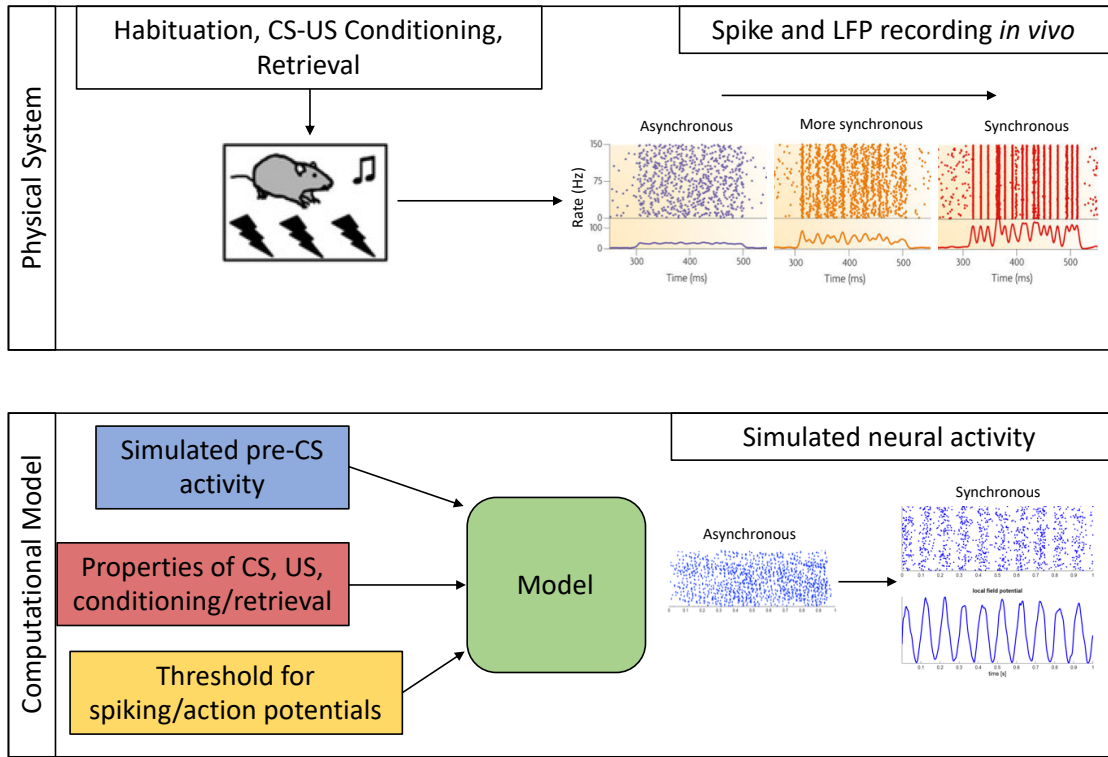
Figure 1.10. A comparison of a physical system (upper panel) and computational model (lower panel) of neural activity in the brain being changed by an outside input (stimulus). In the physical system, oscillations in the rodent brain are maintained by the synchronous firing of neurons within a population. Pre-conditioning, neural spike firing is asynchronous, but becomes more synchronous during and after CS-US fear conditioning (purple to orange to red examples of neural activity in the upper panel). Concurrent presentations of the CS and the US causes the pattern of activity to change (i.e. becoming more synchronous). In the computational model, the variables (i.e. simulated baseline neural activity, properties of the CS and US, firing threshold value, 'learning' rules of the neurons, etc.) are all set as initial inputs to the model to generate an approximation of the resultant neural activity post-stimulus. Here, the simulated neural activity is also shown as going from an asynchronous firing pattern to a more synchronous one. Electrophysiological data taken from Esfahani et al. (2016).

Once the initial parameters and the properties and interactions of the system have been set, the results which occur in this model system can be observed over different epochs of time (Roenneberg et al., 2008). We can see what happens to the variables initially, and how do the variables change if the system runs for longer, etc. As the control of variables is one of the main advantages of computational modelling, any of the conditions can be changed after the initial results have been observed. This means that the model is able to rapidly adapt to evolving hypotheses posed by the data (Fischer, 2008). Due to these

advantages, computational models complement studying complex processes typically investigated in neuroscience. There are multiple types of model which can be used for different areas of study (Chapter 3). Briefly, these models can be biologically realistic; for example, looking at the dynamics of ion channels and their influence on membrane current in a single neuron, describing processes such as spike-train irregularity (Softky & Koch, 1993; van Vreeswijk & Sompolinsky, 1996; Shadlen et al., 1998), and membrane-potential fluctuations (Destexhe & Paré, 1999). In contrast, these models can also be more abstract, such as found in rate-based models, originally described in the influential research developed by Wilson and Cowan (1972) (reviewed by Destexhe and Sejnowski (2009)).

Rate-based models offer a more tangible description of the overall activity of large-scale neuronal networks, for example examining the activity summated from hundreds or thousands of neurons. Of interest are Izhikevich neurons, which have been used to model dynamical properties like bursting and spike frequency (Izhikevich, 2004). Because of this, rate-based models are able to describe some of the more complex dynamics of neuronal network activity, such as oscillations (Roxin et al., 2005). This means that these models can be used to investigate multifaceted functions of the brain which are sometimes difficult to study *in vivo*, such as memory, sensory and motor processes, decision making and spatial navigation (reviewed in Coombes (2005), Schmidt et al., 2015; Fransén & Lansner, 1998). Biologically realistic models are extremely complex, meaning that they often require large amounts of computer memory to develop and run, which can lead to problems of time

and cost investment. In addition, as they are often developed to investigate only parts of single neurons (e.g. the dynamics of membrane ion channels); they cannot describe the more complex subtleties and processes revealed by the interplay of multiple neurons (Siettos & Starke, 2016). Certainly, biologically realistic models cannot describe the activity or functional connectivity of certain brain regions on a systems level. In contrast, rate-based models are relatively quick to design, computationally inexpensive to run, and can simulate large-scale activity dynamics within and between sizeable neural populations (Einevoll et al., 2013).

To summarise, rate models and similar simplified models aim to simulate the complex activity dynamics of large groups of neurons which have been described as characteristic of certain brain regions or neuronal types (e.g. excitatory vs inhibitory neurons). Moreover, the use of simplified models allows us to study these dynamics in a more abstract setting; often avoiding the over-fitting and extrapolation of concepts that can occur in highly complex biophysical models. In addition, it can be argued that simpler rate models are much more flexible, as it is easier to change both the rules of the system, relative timeframes for the system to run to, and the initial input conditions, compared to biophysical models (Standage et al., 2014). However, it must be noted that these models are unable to achieve the same level of detail as biologically realistic models, or grounded spiking neuron models which are able to simulate temporally accurate firing rates of action potentials.

Following this, modelling and computational neuroscience have started to bridge research carried out between the differing scales of biologically

realistic and rate-based models (Armony et al., 1997; Sompolinsky, 2014; Abbott et al., 2016). Importantly, modelling is now being used to answer pertinent questions about the neural circuit mechanisms of emotion (Reisenzein et al., 2013), specifically anxiety and fear (reviewed in Raymond et al., (2017)). Although Pavlovian conditioning has been explored computationally for several decades (e.g. neural dynamics of attention in conditioning, Grossberg & Schmajuk, (1987)), computational models of fear learning and memory have become progressively more advanced over time. For example, Grossberg et al. (2000) developed models of conditioned reinforcement as an example of antagonistic neural processes, such as fear and relief. Further, computational descriptions of the amygdala, sensory cortex and thalamus have been described by Balkenius & Morén, (2002). Expanding on this, Li et al., (2009) developed a model focused on acquisition and extinction of fear in LA neurons. Most recently, Nair et al., (2016a) developed a biologically based neural model to study fear learning and extinction which was discussed in relation to other computational models of the amygdala in acquisition and extinction of conditioned fear in a recent review by Li, (2017).

Of particular interest to fear discrimination, Vlachos et al. (2011) expanded on experimental work previously described by Herry et al. (2008) to develop a neural network model that reproduced the differential recruitment of two distinct subpopulations of basal amygdala neurons ('fear' and 'extinction') as reported in *in vivo* experiments. In summary, this model postulated how the two populations of 'fear' and 'extinction' neurons might encode the contextual specificity of fear and extinction memories. As studying such a complex

neurobiological process as fear discrimination via computational modelling has considerable challenges, there is a distinct lack of research in this area. However recently this has been improving; with advances in our understanding of appropriate computational modelling, in conjunction with *in vivo* experiments, allowing us to investigate how dysfunction in these circuits can lead to the maladaptive fear responses seen in mental disorders (Nair et al., 2016b).

1.9 Aims and Objectives

Our primary aim was to investigate the neural circuitry underpinning fear discrimination and retrieval in both males and females to discrete auditory stimuli. There has been little research conducted specifically looking at the sex differences in fear discrimination in relation to discrete cues. As current research is now exposing a link between the failure to discriminate and disorders such as PTSD, it is critical that we increase our understanding of the basic biology behind this process. Moreover, as these disorders are significantly more prevalent in women, it is imperative to study fear discrimination and retrieval in both male and female subjects.

Objective one

We aimed to develop a working fear discrimination protocol, to be tested on male and naturally cycling female rats to measure behavioral differences observed during presentations of discrete auditory CS+ and CS- stimuli.

Objective two

In addition to measuring fear behavior *in vivo*, we also developed a computational model to simulate the activity levels of differential groups of 'fear' and 'safety' neurons in the BLA during both discrimination training and retrieval of discrete CS+ and CS- cues. We aimed to use this model to make predictions on the neural mechanisms involved in fear discrimination and generalisation, in addition to providing a framework for further study to be tested in this rapidly evolving field.

Objective three

Using the same fear discrimination protocol described in objective one, we aimed to measure the corresponding neurophysiological activity in the PL, IL and BLA via surgically implanted electrodes in awake behaving animals undergoing fear discrimination retrieval. These areas were chosen as both the mPFC and BLA have been shown to be important in the process of fear discrimination (Stujenske et al., 2014). However, in that study, recordings from the mPFC were not described in relation to the PL and IL sub-regions. As the PL has been shown to display sustained activity in females which correlates with failed extinction learning (Fenton et al., 2016; Fenton et al., 2014b), and that the IL has been shown to be involved in fear inhibition during extinction, each region may in turn be differentially involved in safety learning and retrieval.

Chapter 2. Sex Differences in Fear Discrimination Behaviour

2.1 Introduction

It is now well established that there are marked sex differences present in stress- and fear-based disorders, such as anxiety and PTSD (Maeng and Milad 2015). As highlighted by McLean et al. (2011) and Lebron-Milad and Milad (2012), women are up to 60% more likely to suffer from an anxiety disorder than men, and are up to twice as likely to suffer from PTSD. Women are also more likely to report that they experience a greater severity and longer persistence of PTSD symptoms, such as flashbacks, panic attacks and disturbed sleep (Seedat et al., 2005). Moreover, these differences remain even when the exposure frequency to traumatic events is equal between males and females (Breslau et al., 1997). The reasons for this marked discrepancy remain unclear and are thought to be multi-factorial in nature, including hormonal status, stress, temperament, cognition, environmental effects and societal influences (Catuzzi and Beck 2014; McLean and Anderson 2009).

Understanding the neurobiological basis behind the increased likelihood of women to develop PTSD has been severely hindered by the lack of preclinical studies investigating fear learning and memory processing in female animals (Lebron-Milad and Milad 2012). It is imperative that females be included in such translational research to provide valuable insight into the contributing factors underlying sex differences in PTSD susceptibility, which in turn may lead to the development of more effective interventions or treatments.

A hallmark feature of PTSD is the impaired inhibition of fear, wherein patients will often re-experience negative emotions which can be triggered by elements associated with a prior trauma. Additionally, PTSD sufferers find suppressing these inappropriate fear responses difficult (VanElzakker et al., 2014). After the trauma, elements of the event (e.g. a gun), similarities in the spatial environment with the traumatic event, or feeling panicked can all act as cues to generate fear during subsequent exposure. These invasive and distressing fear responses are often managed with exposure therapy, a specialised form of extinction training where patients are repeatedly exposed to cues related to the trauma in a safe environment (Rothbaum et al., 2001).

Over time, patients extinguish previously triggering cues, reducing their potential to cause flashbacks, panic and fear. However, a growing body of evidence indicates that PTSD is associated with deficits in the extinction of learned fear (Graham & Milad, 2011; Jovanovic & Norrholm, 2011; Shvil et al., 2014a). Moreover, recent human studies have demonstrated that women show impaired extinction memory recall, which can be influenced by fluctuations in oestrogen levels. Multiple studies have identified that women using hormonal birth control or tested at the early follicular stage of their menstrual cycle, both factors resulting in a low oestrogen state, displayed typical fear conditioning but impaired extinction recall compared to high oestrogen levels in both women and men (Graham and Milad 2013; Milad et al. 2006; Milad et al. 2010; Seidan et al. 2011). Further to this, Glover et al. (2012) highlighted that prolonged periods of low oestrogen may be a vulnerability factor in the development of PTSD in women.

Individuals with impaired extinction memory recall may struggle to benefit from exposure therapy, which could partially account for the substantial proportion of patients who experience the return of fear and subsequent symptoms after treatment (Craske et al., 2014). However, there has been relatively little research on whether the sex of the patient plays an important role in the recovery rates and/or effects of exposure therapy in PTSD survivors (Blain et al., 2010; Galovski et al. 2013). Importantly, studies containing cohorts of PTSD sufferers usually focus on the trauma type of the treatment group (e.g. combat-related trauma, with primarily male candidates, or interpersonal/sex-related violence, with primarily female candidates). This is a natural reflection of the types of trauma experienced by people who go on to develop PTSD; for example, females are more often exposed to rape and sexual assault than males (Seedat et al., 2005). Therefore, it is hard to determine whether any potential sex differences seen in treatment response are truly due to underlying biological sex differences, or to the potential confounding effect of trauma type (Galovski et al., 2013). Without further research, this trauma exposure confound also makes it difficult to determine whether potential improvements seen with differential treatment types or pharmacological interventions involve sex, trauma type or a combination of both. In animal studies, we can control the trauma exposure type and the subjects' sex. More recently, animal studies have begun to examine the underlying neurobiological characteristics of impaired inhibition in the regulation of learned fear using relevant behavioural paradigms which compare both sexes.

Although there is little human evidence available so far to determine whether the spontaneous return of fear is more common in females in a clinical treatment setting after PTSD, there is supporting evidence from animal studies to show that females are more resistant to extinction than males. During extinction learning, repeated presentations of a discrete conditioned stimulus (CS) or prolonged exposure to a conditioned context in the absence of the unconditioned stimulus (US) will normally decrease fear responding to the original CS or context (Chapter 1). Multiple studies have shown that females typically require more extinction to prevent spontaneous fear recovery than their male counterparts (Fenton et al. 2014; Baker-Andresen et al. 2013; Matsuda et al. 2015). Additionally, Catuzzi and Beck (2014) also suggested that females are more likely to have a "behavioural inhibition temperament", wherein original stimulus–response associations are rapidly acquired but inflexible, and are therefore more resistant to extinction. Further to this, animal studies are beginning to elucidate the underpinning neural circuit, neurochemical, and endocrine mechanisms of this altered regulation of learned fear in females (Matsuda et al. 2015; Milad et al. 2009; Rey et al., 2014). For example, these sex differences in behaviour have been shown to involve the mPFC (Baran et al., 2010), which displays altered theta and gamma activity between males and females during extinction (Fenton et al. 2014; Fenton et al. 2016).

In addition to impaired fear inhibition, another characteristic of PTSD is the over-generalisation of fear to innocuous stimuli or contexts (Jovanovic & Norrholm, 2011). For example, panic attacks induced by flashbacks can be elicited when a cue reminiscent of prior trauma is encountered, even if the

surrounding environment or the cue trigger itself are considered neutral. The processes underpinning fear discrimination and generalisation can be investigated using comparable behavioural paradigms in humans and animals, where one cue (CS+) predicts threat through its association with the US and the other cue (CS-) signals safety by predicting that the US will not occur (Dunsmoor & Paz, 2015). Fear discrimination can be viewed as a form of learned fear inhibition by the safety cue, wherein fear is reduced during presentations of the CS-, compared to presentations of the CS+ alone. Emerging evidence has highlighted that the fear generalisation characteristic of PTSD results from a deficit in fear inhibition due to impaired safety signal learning (Christianson et al., 2012; Jovanovic and Norrholm 2011). Further, although a failure to discriminate between cues predicting threat and safety has been proposed as a biomarker of PTSD, little is known about sex differences in fear discrimination. Recent human and animal studies have demonstrated impaired contextual fear discrimination in females (Lonsdorf et al. 2015; Lynch et al. 2013; Reppucci et al., 2013), yet sex differences in fear discrimination involving discrete cues, and the role of altered safety signalling in mediating these differences, are poorly understood.

In the present study, we investigated sex differences in auditory fear discrimination in male and female rats by examining learned fear behaviour (i.e. freezing) in response to two distinct tones predictive of threat or safety. As previous studies have shown sex differences in the rates of learning using various aversive conditioning paradigms (Dalla & Shors, 2009), we examined the effects of both limited and extended discrimination training on later retrieval.

We also determined if any sex differences in freezing observed during discrimination retrieval were attributable to non-specific effects on anxiety-like behaviour, locomotor activity, and/or nociception. Finally, we investigated whether sex differences in fear discrimination with extended training involve altered safety signalling by using a retardation test to examine the inhibitory properties of the safety cue during subsequent fear conditioning (Christianson et al., 2012; Rescorla 1969; Sangha et al., 2013).

2.2 Materials and Methods

Experiments were performed on young adult male and naturally cycling female Lister hooded rats (Charles River, UK). Rats were group housed (4–5/cage) by sex in individually ventilated cages on a 12-h light/dark cycle (lights on at 8 AM) with access to food and water *ad libitum*. All experiments were conducted with internal ethical approval and in accordance with the Animals (Scientific Procedures) Act 1986, UK. All behavioural testing occurred during the rats' light cycle.

2.2.1 Experiment 1A: Auditory fear discrimination training and retrieval testing

Rats underwent auditory fear discrimination training and retrieval testing using two chambers that have been described previously (Stevenson et al., 2009). On the first day rats were habituated for 10 min each to contexts A and B, which had distinct visual (black and white stripes or spots on two walls), olfactory (40% ethanol or 40% methanol), and tactile (metal floor bars or white Perspex floor)

cues. During habituation, the rats were also presented with 2 and 9 kHz tones (two presentations of each; 30 s, 80 dB, 2 min inter-trial interval (ITI)) in both contexts. From the next day, separate cohorts of males and females underwent one, two, or three days of fear discrimination training in context A, resulting in six separate groups of rats undergoing behavioural testing. This consisted of five presentations of one tone (CS+; 30 s, 80 dB, 2 min ITI) paired with footshock (0.5 s, 0.5 mA, ending at tone offset) and five presentations of a different tone alone (CS-; 30 s, 80 dB, 2 min ITI). The CS+ and CS- tones used were either 2 or 9 kHz and fully counterbalanced between rats. One day after the last day of discrimination training rats received two presentations each of the CS+ and CS= in context B to test discrimination retrieval. Tone and footshock delivery were controlled automatically by a computer running MED-PC IV software (Med Associates, VT). Rats were tested at approximately the same time of day on each day and behaviour was recorded with a digital camera for later data analysis. The chambers were cleaned with 40% ethanol (context A) or 40% methanol (context B) between each testing session.

2.2.2 Experiment 1B: Open field testing

The rats that underwent two days of discrimination training in Experiment 1A were also tested in the open field to examine sex differences in anxiety-like behaviour and locomotor activity using an apparatus described previously (Heath et al., 2015). Open field testing occurred the week before fear discrimination testing. Rats were placed in the open field for 10 min and

behaviour was digitally recorded during testing for later data analysis. The floor of the open field was cleaned with 40% methanol between each session.

2.2.3 Experiment 2: Shock sensitivity testing

A separate cohort of rats was used to examine sex differences in shock sensitivity as described previously (Heath et al., 2015). Rats were placed in the chambers and after two min received 10 un-signalled footshocks (0.5 s, 1 min ITI) of increasing intensity (0.05–0.5 mA in 0.05 mA increments). Behaviour during the test was digitally recorded for later data analysis and the chambers were cleaned with 40% ethanol between each session.

2.2.4 Experiment 3: Auditory fear discrimination and retardation testing

A separate cohort of rats underwent auditory fear discrimination followed by retardation testing to examine sex differences in safety signalling by the CS-. Half of the rats were habituated to the two contexts and tones, underwent three days of discrimination training in context A, and were tested for discrimination retrieval in context B as in Experiment 1A above. The day after discrimination retrieval testing these rats were habituated for 10 min to context C, which had distinct visual (complete darkness) and olfactory (1% acetic acid) cues. The next day these rats were subjected to auditory fear conditioning in context C using the previous CS- as the conditioning cue. This consisted of five presentations of the tone (30 s, 2 min ITI; 2 or 9 kHz, fully counterbalanced) paired with footshock (0.5 s, 0.5 mA, ending at tone offset). The following day these rats received two presentations of the cue alone in context B to test fear

retrieval. The other half of the (Control) rats were subjected to these same procedures except that no shocks were presented during discrimination training, which served to pre-expose the controls to the same number of tones before auditory fear conditioning. In the retardation test, if fear discrimination results in the CS- acting as a safety signal then later fear conditioning to that CS- is impaired (or retarded) in relation to controls conditioned to the pre-exposed cue; this, in turn, results in reduced learned fear responding compared to the pre-exposed controls at fear retrieval test. Rats were tested at approximately the same time of day on each day and behaviour was digitally recorded for later data analysis. The chambers were cleaned with 40% ethanol (context A), 40% methanol (context B), or 1% acetic acid (context C) between each session.

2.2.4 Data analysis

In Experiment 1A, freezing (i.e. absence of movement except relating to respiration) in response to CS+ and CS- presentations during discrimination retrieval testing was quantified. Freezing was scored manually by 2–3 trained observers. The observers scored freezing blind to the CS type and one was blind to the sex of the rats. Freezing was determined at 3 s intervals during tone presentation. The cumulative duration of freezing was then calculated and expressed as a percentage of the 30s tone. The mean percentage of freezing during each of the two tones (CS+ and CS-) was calculated and used in the statistical analysis. Sex differences in freezing during CS+ and CS- presentation were analysed separately in the different groups of rats that

underwent one, two or three days of discrimination training using two-way analysis of variance (ANOVA), with sex and CS type as between- and within-subject factors, respectively. Direct comparisons between freezing during CS+ and CS- presentation in males and females that underwent one, two or three days of discrimination training were also conducted separately using independent paired t-tests (Keeley et al., 2015; Lynch et al., 2013). Contextual fear was inferred from freezing during the 2min period before tone presentations, which was scored as above. Sex differences in contextual fear were analysed separately in the different groups that underwent one, two or three days of discrimination training using independent paired t-tests.

In Experiment 1B, behaviour in the open field was analysed using Ethovision software (Noldus, Netherlands). The time spent in, latency to enter, and frequency of entries into the centre were quantified as indices of anxiety-like behaviour, while the horizontal distance moved throughout the whole open field during testing was quantified as an index of locomotor activity (Heath et al., 2015; Prut and Belzung 2003; Stevenson et al., 2009). Sex differences in the anxiety-like behavioural measures were analysed using two-way ANOVA, with sex and measure as between- and within-subject factors, respectively. Sex differences in locomotor activity were examined separately by analysing the horizontal distance moved using an unpaired t-test.

In Experiment 2, the threshold current needed to elicit 'flinch' responses and audible vocalisations during shock sensitivity testing were scored manually, as previously described in (Heath et al., 2015). Sex differences in

flinch and vocalisation responses were analysed using two-way ANOVA, with sex and response type as between- and within-subject factors, respectively.

In Experiment 3, freezing in response to CS+ and CS- presentations during discrimination retrieval testing was determined and sex differences were then analysed using two-way ANOVA as in Experiment 1A above. In the subsequent retardation test, freezing in response to cue presentations during fear retrieval testing was quantified and the mean percentage of freezing was calculated and used in the statistical analysis. Sex differences in freezing during cue presentation between rats subjected previously to fear discrimination training or cue pre-exposure were analysed using two-way ANOVA, with sex and cue history as between-subject factors. Direct comparisons between freezing in discrimination trained and cue pre-exposed controls in males and females were also conducted separately using independent unpaired t-tests. All data are presented as the mean plus the standard error of the mean. two-way ANOVA post-hoc comparisons were conducted using the Bonferroni multiple-comparisons test where indicated. The level of significance for all comparisons was set at $P < 0.05$.

2.3 Results

2.3.1 Experiment 1A: Sex differences in fear discrimination depend on the extent of training received

The fear discrimination paradigm used in Experiment 1A is outlined in Figure 2.1 (A). Freezing in response to CS+ and CS- presentation during fear

discrimination retrieval testing after one, two, or three days of fear discrimination training is shown in Figure 2.1 (B–D). In males (n = 9) and females (n = 9) subjected to one day of training (Figure 2.1 (B)), the two-way ANOVA revealed a significant main effect of CS type ($F_{(1,16)}$ = 10.86, P = 0.005) but no main effect of sex ($F_{(1,16)}$ = 2.71, P = 0.12) or sex × CS type interaction ($F_{(1,16)}$ = 0.16, P = 0.68). Despite the lack of significant interaction, we were interested in examining differences in freezing during CS+ and CS- presentation in males and females. Further comparisons were therefore conducted using independent unpaired *t*-tests. After one day of freezing, males showed a decrease in the mean freezing in response to the CS+ compared to the CS-, but this did not reach statistical significance ($t_{(8)}$ = 2.13, P = 0.066). However, females did show a significant increase in freezing during CS+ compared to CS- presentation ($t_{(8)}$ = 2.52, P = 0.036). In males (n = 8) and females (n = 8) subjected to two days of training (Figure 2.1 (C)), the two-way ANOVA again revealed a significant main effect of CS type ($F_{(1,14)}$ = 12.21, P = 0.004) but no main effect of sex ($F_{(1,14)}$ = 0.0, P > 0.99) or sex × CS type interaction ($F_{(1,14)}$ = 2.86, P = 0.11). Despite there being no significant interaction, direct comparisons were conducted to examine differences in freezing in response to the CS+ and CS- in each sex. Males again showed more freezing during CS+ compared to CS- presentation and this difference reached statistical significance ($t_{(7)}$ = 3.37, P = 0.01). In contrast, females showed no difference in freezing in response to the CS+ and CS− ($t_{(7)}$ = 1.41, P = 0.20).

In males (n = 10) and females (n = 9) subjected to three days of training (Figure 2.1 (D)), the two-way ANOVA revealed a significant main effect of CS type ($F_{(1,17)}$ = 24.66, P = 0.0003) and a significant sex × CS type interaction ($F_{(1,17)}$ = 5.55, P = 0.031) but no main effect of sex ($F_{(1,17)}$ = 1.47, P = 0.24). Post-hoc analysis (Bonferroni multiple-comparisons test) indicated that males showed significantly increased freezing during CS+ compared to CS- presentation (P < 0.001), while females showed no such difference (P > 0.05). This was also confirmed by the direct comparison analysis using t-tests, which showed that freezing was significantly increased in response to the CS+ compared to the CS- in males ($t_{(9)}$ = 4.31, P = 0.002) but not females ($t_{(8)}$ = 1.95, P = 0.087). Taken together, these results suggest that extended training resulted in fear discrimination in males, while females showed fear discrimination with limited training and fear generalisation with extended training. Contextual freezing before CS+ and CS- presentations during fear discrimination retrieval testing after one, two, or three days of fear discrimination training is shown in Figures 2.1 (E–G). Although males showed an increase in mean contextual freezing than females, this did not reach statistical significance in the rats that underwent one ($t_{(16)}$ = 1.01, P = 0.33; Figure 2.1 (E)), two ($t_{(14)}$ = 1.40, P = 0.18; Figure 2.1 (F)), or three ($t_{(17)}$ = 1.34, P = 0.20; Figure 2.1 (G)) days of discrimination training. This finding suggests that there were no sex differences in contextual fear before testing auditory fear discrimination retrieval.
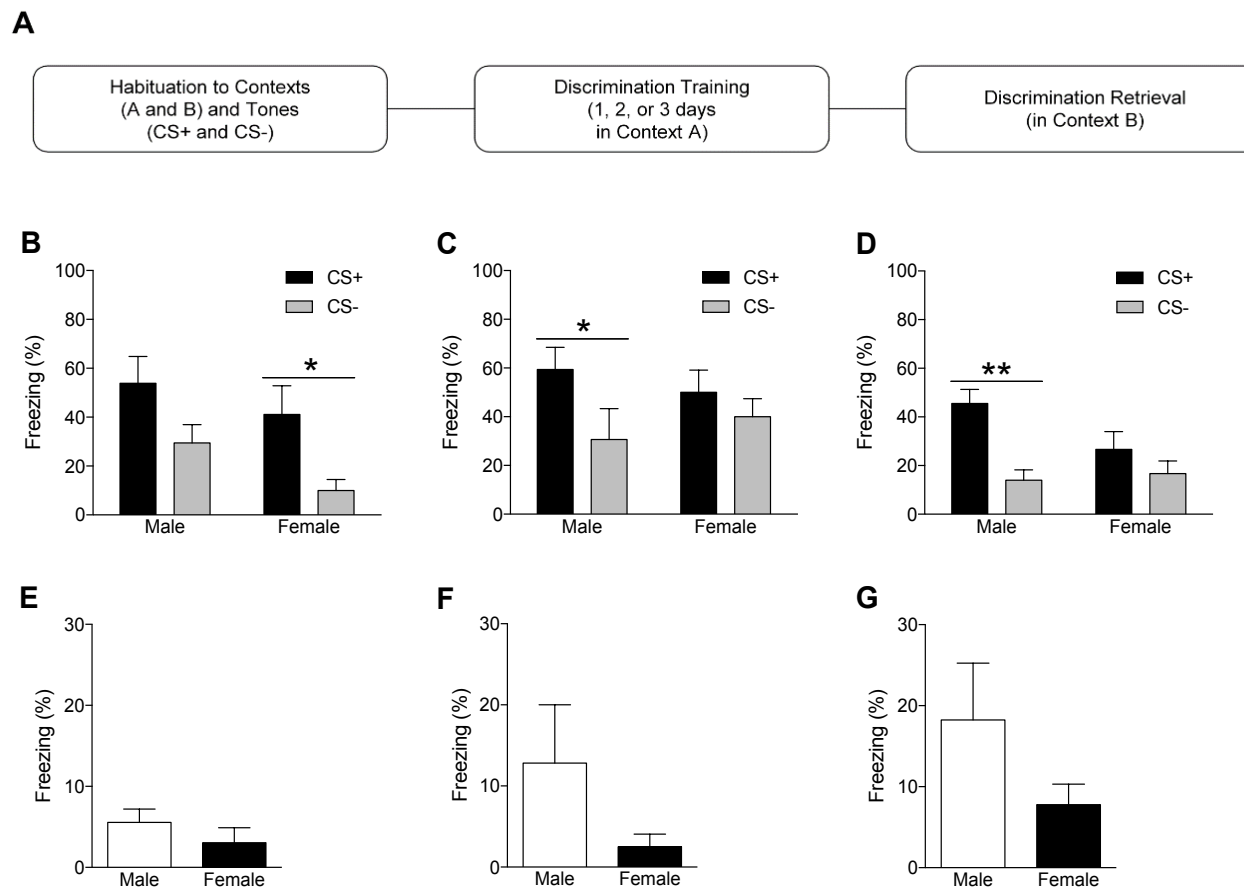
Figure 2.1. Sex differences in auditory fear discrimination depend on the extent of training received. (A) Schematic representation of the fear discrimination paradigm used. (B) Freezing in response to CS+ and CS- presentation during discrimination retrieval testing after one day of training. Males showed no significant difference in freezing between the CS+ and CS-, whereas freezing was significantly increased during CS+ compared to CS- presentation in females (*P < 0.05). (C and D) Freezing to the CS+ and CS- during retrieval testing after two (C) or three (D) days of training. Freezing was significantly increased to the CS+ compared to the CS- in males (*P < 0.05, **P < 0.01), while freezing during CS+ and CS- presentation showed no difference females. (E–G) Contextual freezing before CS+ and CS- presentations during retrieval testing after one (E), two (F), or three (G) days of training. There were no significant differences in freezing between any of the males and females during this time-period.

2.3.2 Experiment 1B: Females exhibit enhanced anxiety-like behaviour and locomotor activity in the open field

It is possible that the sex differences in freezing in response to CS+ and CS-presentation during fear discrimination retrieval reported in Experiment 1A could have resulted from non-specific effects on anxiety-like behaviour and/or locomotor activity. To address this possibility, we examined indices of these behaviours in males (n = 7) and females (n = 8) during open field testing in Experiment 1B. The time spent in, latency to enter, and frequency of entries into the centre of the open field are shown in Figures 2.2 (A–C). The two-way ANOVA for these anxiety-like behavioural measures revealed a significant main effect of measure ($F_{(2,26)}$ = 5.66, P = 0.009) and a significant sex × measure interaction ($F_{(2,26)}$ = 3.63, P = 0.041) but no main effect of sex ($F_{(1,16)}$ = 1.82, P = 0.20). Post-hoc analysis (Bonferroni multiple comparisons test) indicated that there was no difference between males and females in the time spent in the centre (P > 0.05; Figure 2.2 (A)). However, females took significantly longer to enter the centre, compared to males (P < 0.05; Figure 2.2 (B)). Females also had a reduction in the mean number of entries into the centre compared to males, but this did not reach statistical significance (P > 0.05; Figure 2.2 (C)). Locomotor activity in the open field is presented in Figure 2.2 (D). Females showed a significant increase in the horizontal distance moved, compared to males ($t_{(13)}$ = 2.45, P = 0.029; Figure 2.2 (D)). These results suggest that females displayed a subtle enhancement of anxiety-like behaviour and elevated locomotor activity in relation to males.
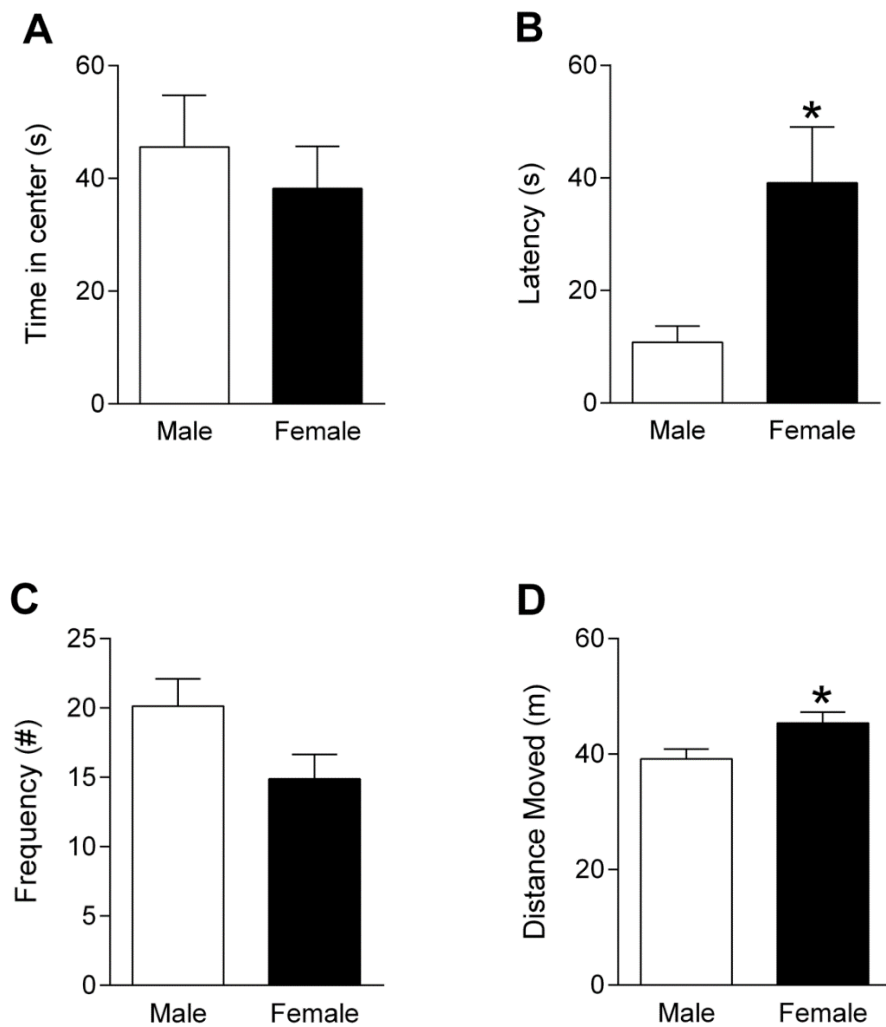
Figure 2.2. Females show enhanced anxiety-like behaviour and locomotor activity during open field testing. (A) There was no difference between males and females in the duration of time spent in the centre of the open field. (B) Females showed an increased latency to first enter the centre of the open field (*P < 0.05). (C) The frequency of entries into the centre of the open field did not differ significantly between males and females. (D) The horizontal distance moved in the open field was increased in females (*P < 0.05).

2.3.3 Experiment 2: There are no sex differences in shock sensitivity

The sex differences in fear discrimination retrieval reported in Experiment 1A could also have involved non-specific effects on nociception during fear discrimination training. To address this, we examined shock sensitivity in separate cohorts of males (n = 8) and females (n = 8) in Experiment 2 (Figure 2.3). The two-way ANOVA revealed a significant main effect of response type

$(F_{(1,14)} = 43.09,\ P < 0.0001)$ but no main effect of sex $(F_{(1,14)} = 0.23,\ P = 0.64)$ or sex × response type interaction $(F_{(1,14)} = 0.88,\ P = 0.36)$. These results indicate that there were no sex differences in shock sensitivity.
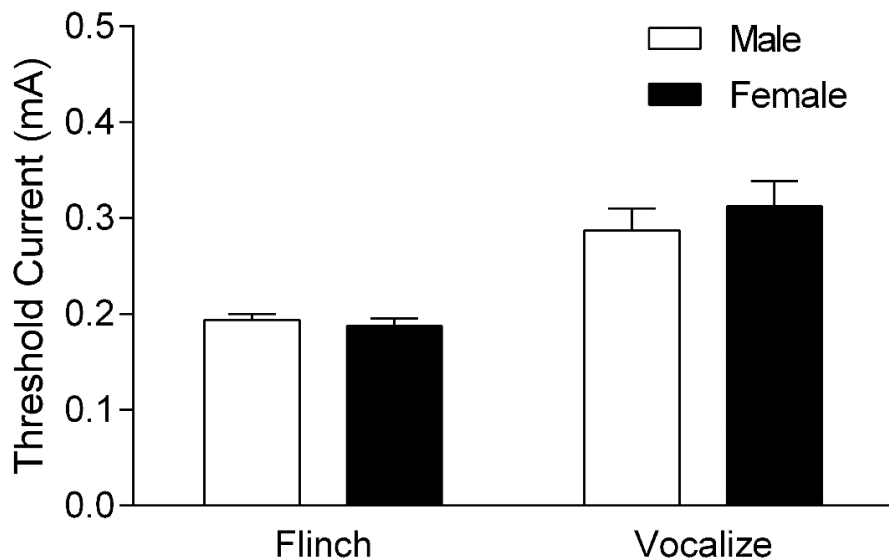
Figure 2.3. The threshold current eliciting flinch or vocalisation responses does not differ between males and females, indicating a lack of sex differences in shock sensitivity.

2.3.4 Experiment 3: Females show fear generalisation with extended discrimination training due to impaired safety signalling

The results from Experiment 1A indicated that males showed fear discrimination and females showed fear generalisation after three days of discrimination training (Figure 2.1 (D)). To determine if this sex difference in fear discrimination with extended training involved altered safety signalling by the CS-, we subjected another cohort of rats to three days of discrimination training followed by retardation testing in Experiment 3 (Figure 2.4 (A)). Freezing in response to the CS+ and CS- during fear discrimination retrieval testing after three days of training is shown in Figure 2.4 (B). The two-way

ANOVA analysis revealed a significant main effect of CS type ($F_{(1,16)} = 19.28$, $P = 0.0005$) and a significant sex × CS type interaction ($F_{(1,16)} = 7.43$, $P = 0.015$) but no main effect of sex ($F_{(1,16)} = 0.89$, $P = 0.36$). Post-hoc analysis (Bonferroni's multiple comparisons test) indicated that males (n = 9) showed a significant increase in freezing during CS+ compared to CS- presentation ($P < 0.001$). In contrast, females (n = 9) showed no difference in freezing in response to the CS+ and CS- ($P > 0.05$). These results replicate our finding from Experiment 1A, which showed that males discriminated, whereas females generalised, between the CS+ and CS- after three days of fear discrimination training.

For the retardation test, after discrimination retrieval testing the same rats underwent fear conditioning using the CS- as the conditioned cue and fear retrieval was then tested (Figure 2.4 (A)). If later conditioning to the CS- is retarded, as indicated by a reduction in freezing during cue presentation at a subsequent retrieval test, then this provides evidence that the CS- acquired the inhibitory properties of a safety cue during prior fear discrimination. Freezing in response to the cue during fear retrieval testing is presented in Figure 2.4 (C). The two-way ANOVA analysis revealed a significant main effect of CS history ($F_{(1,34)} = 5.77$, $P = 0.022$) but no main effect of sex ($F_{(1,34)} = 0.11$, $P = 0.74$) or sex × CS history interaction ($F_{(1,34)} = 1.15$, $P = 0.29$). Despite there being no significant interaction, we were interested in examining differences in freezing between discrimination trained vs cue pre-exposed controls in males and females. Therefore, direct comparisons were conducted using independent unpaired t-tests. Freezing was significantly decreased in response to the cue

in males that had previously undergone discrimination training (n = 9), compared to controls (n = 10) pre-exposed to the cue before conditioning ($t_{(17)}$ = 2.56, P = 0.021). In contrast, freezing during cue presentation in females previously subjected to fear discrimination (n = 9) did not differ from controls (n = 10) that underwent cue pre-exposure before conditioning ($t_{(17)}$ = 0.91, P = 0.38). These results suggest that the CS- acted as a safety cue during fear discrimination in males but not females.
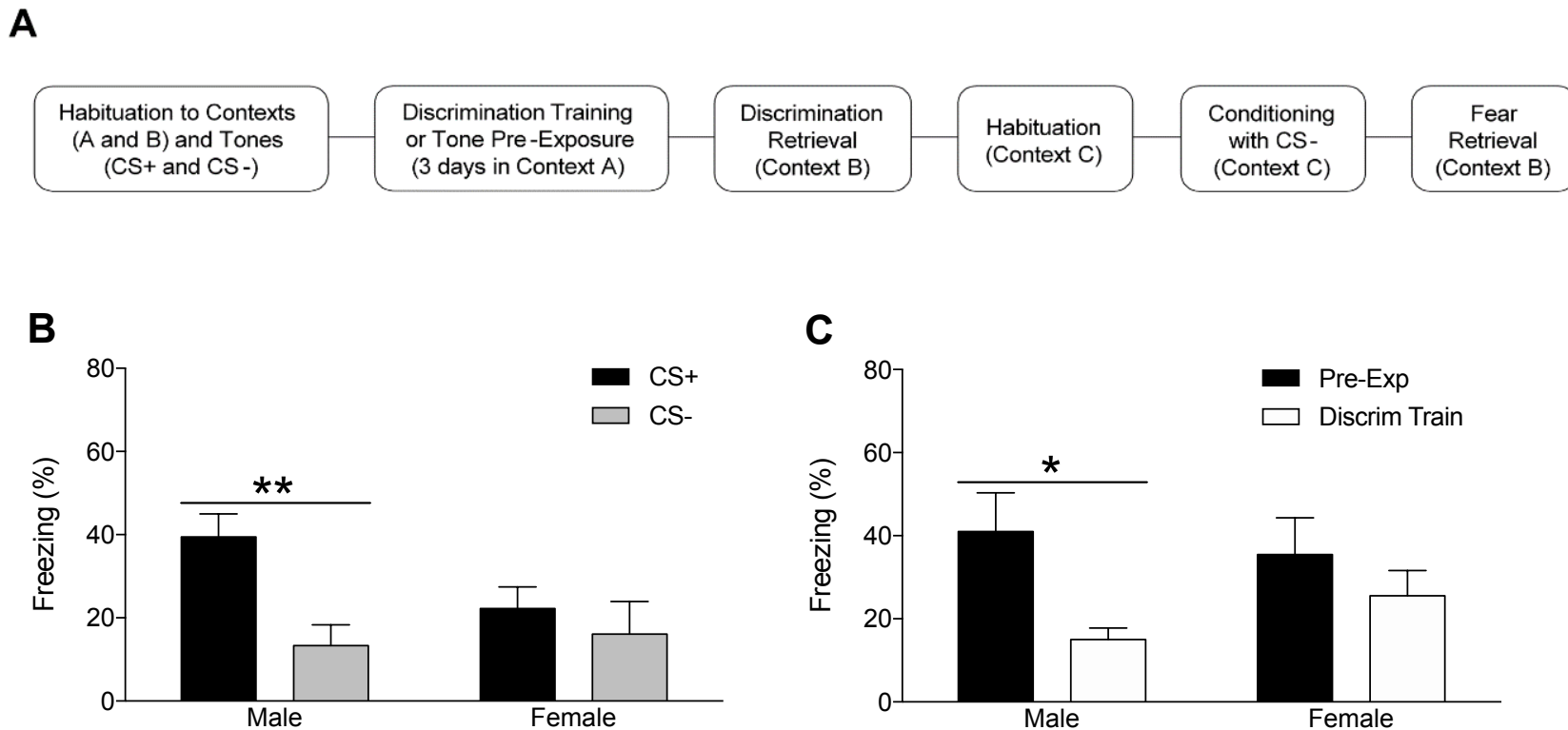
Figure 2.4. Sex differences in auditory fear discrimination with extended training involve altered safety signalling by the CS–. (A) Schematic representation of the discrimination and retardation testing paradigm used. (B) Freezing in response to the CS+ and CS- during discrimination retrieval testing after three days of training. Freezing was increased during CS+ compared to CS- presentation in males (**$P < 0.001$) but not females. (C) Males subjected to discrimination training (Discrim Train) followed by fear conditioning using the previous CS- as the cue showed decreased freezing to the cue during fear retrieval testing, compared to controls pre-exposed (Pre-Exp) to the cue before conditioning (*$P < 0.05$). There was no difference in freezing to the cue between females that underwent discrimination training and pre-exposed controls (note that the discrimination retrieval data in (B) is from the Discrim Train groups in (C).

2.4 Discussion

This study investigated sex differences in auditory fear discrimination. In Experiment 1A we found that males did not discriminate after limited training but did display successful discrimination with extended training. In contrast, females displayed fear discrimination with limited training, and generalisation after extended training. This indicates that sex differences in fear discrimination depended on the extent of training received. In Experiment 1B we found a subtle enhancement of anxiety-like behaviour and elevated locomotor activity in females during open field testing. In Experiment 2 we observed no sex differences in shock sensitivity. In Experiment 3 we again found that males showed fear discrimination while females showed fear generalisation after extended training. We also provided evidence that the CS- signalled safety with extended fear discrimination training in males, whereas in females this safety signalling was impaired. These results confirm previous findings indicating sex differences in the inhibition of learned fear and extend them to the domain of fear discrimination involving auditory stimuli.

Previous studies have also found that males receiving extended initial fear discrimination training show better discrimination during subsequent retrieval, whereas brief training paradigms lead to lower levels of stimulus specificity during fear learning (Dunsmoor & Paz, 2015). This has been shown in discrimination learning where the cues are tones, combinations of light and tone and distinct contexts (Antunes and Moita 2010; Foilb and Christianson 2016). Interestingly, we found opposing patterns of sex differences in fear discrimination with limited and extended training in the present study. In

contrast to the discrimination with extended training that we observed in males, females did not discriminate between the CS+ and CS- after two or three days of training. This lack of discrimination was not due to a learning deficit, because females clearly discriminated between the two cues after only one day of training. The fact that females were able to discriminate with only limited training suggests that sex differences in auditory perception are also unlikely to be involved, which is supported by previous evidence stating that males and females do not differ in auditory appetitive discrimination tasks (van Haaren et al., 1990).

Our results instead suggest that females show a rapid acquisition of fear discrimination, but that they develop fear generalisation across both cues with repeated training sessions. Comparative studies investigating sex differences in aversive learning have shown faster acquisition of eyeblink conditioning and active avoidance in females compared to males. For example, Dalla and Shors (2009) have shown that faster acquisition during fear conditioning observed in females is most evident early on during learning; a similar pattern to what we see in our study after one day of training. In addition, Toufexis et al. (2007) demonstrated that sham-implanted (i.e. naturally-cycling, control) females could discriminate between two discrete cues very early on in training. Although it is unclear why fear generalisation was observed after extended discrimination training in our females, it could be that the stressful experience of the first day of conditioning affected subsequent discrimination learning, and that this initial stressor had differential effects in males and females over the following day/s of training. This is supported by the finding that acute stress the

day before eyeblink conditioning improved learning in males but impaired learning in females (Wood & Shors, 1998), although chronic stress prior to initial training may reverse this effect (Baran et al., 2009). Similarly, Keller et al. (2015) demonstrated that single-prolonged-stress (SPS), a non-human animal model of PTSD, results in cued fear extinction retention deficits in male, but not female, rats. These studies indicate that there may be differential effects on learning in female rats with acute verses prolonged or chronic stress, but the underlying neurobiological mechanisms are still relatively unexplored.

Overall, however, our results agree with previous findings suggesting that stress and sex can interact to regulate learned fear and its inhibition through extinction. Further, recent research indicates that there may be sex differences in the social modulation of fear learning. For example, rats exposed to a novel tone in the presence of a cage-mate previously conditioned to that same tone showed increased freezing to the stimulus the next day, a phenomena known as fear conditioning by-proxy (Bruchey et al., 2010). Male rats exposed to a fear-conditioned conspecific showed an enhanced avoidance response when subsequently trained, but this effect was only present in females with high oestrogen levels (Mikosz et al., 2015). In addition, there is also evidence to support that familiarity and/or kinship influences the social transmission of fear to a higher degree in female rats (Jones et al., 2014). Mikosz et al. (2015) also identified that interaction with a recently fear-conditioned rat results in activation of the central and lateral amygdala and PFC, but only in male rats. This suggests that there may be sex differences in

how the social aspects of fear and the transfer of information about threat are modulated.

It is worth noting that females and, to a lesser extent, males, subjected to three days of discrimination training exhibited less freezing in response to the CS+ and CS- at discrimination retrieval test, compared to those that underwent one or two days of training. Although the reason for this is unclear, it could be that the females adopted less passive (i.e. freezing) and more active (i.e. escape-related) fear responding after extended discrimination training. Evidence in support of this comes from a recent study indicating that females were more likely to display active 'darting' movements as a type of fear response during auditory fear conditioning and its extinction, compared to males (Gruene et al., 2015). In addition, Dalla et al. (2008) also demonstrated that there are sex differences in learned helplessness; males exposed to uncontrollable stress prior to testing did not attempt to escape chambers in which they received footshocks (characterised as "helplessness") whereas females continued to display increased escape behaviour even when they had been exposed to uncontrollable stress. Therefore future studies characterising other fear responses in both sexes in addition to freezing during fear discrimination are needed, especially given that Gruene et al. (2015) and Dalla et al. (2008) used a different rat strain than the one used in the present study. Although not formally quantified at the time of writing this thesis, ongoing work in our laboratory is re-examining active fear behaviours in the females of this study in more detail. Here, initial qualitative observations highlight that the reduced levels of freezing seen in females to the CS+ and CS- cues after

extended training is not a reduction in fear, but instead is likely to be a change in passive vs active fear responding.

During open field testing, we also found subtlety enhanced anxiety-like behaviour and increased locomotor activity in females. However, these results are unlikely to explain the sex differences that we observed in fear discrimination. Previous studies have reported decreased, unaltered or increased anxiety-like behaviour in females tested in the open field, whereas the finding of increased locomotion in females is more consistent across studies (Aguilar et al., 2003; Baran et al., 2010; Gray and Lalljee 1974; Lehmann et al., 1999; Seliger 1977). There are several possible reasons for this discrepancy between studies, including the measures quantified to index fear behaviour, the conditions under which testing occurred, and the strain used for testing (Prut and Belzung 2003). In our experimental setup, we found no sex differences in the duration of time spent in or the frequency of entries into the centre of the open field, but we did find an increased latency to enter the centre in females. This was observed despite the increase in locomotor activity that they also displayed, suggesting that females showed a slight enhancement of anxiety-like behaviour. It could be argued that enhanced anxiety-like behaviour might contribute to fear generalisation, which we observed in females after two or three days of discrimination training. However, this would not explain the fear discrimination that we observed in females after one day of training. Similarly, while increased locomotor activity might result in decreased freezing during presentation of both the CS+ and the CS- in females, it cannot explain the

different patterns of fear discrimination observed with one or 2–3 days of training.

Sex differences in nociception during fear discrimination training are also unlikely to account for our results as we found that males and females did not differ in their shock sensitivity. In contrast to the present findings, most previous studies have reported increased shock sensitivity in females (Dalla and Shors 2009; Beatty and Fessler 1977), but there are also studies which show similar results to ours (Mikosz et al., 2015). Differences in the experimental conditions and the strain used between studies could account for this discrepancy.

In addition to the results discussed above, we also investigated the psychological process underlying sex differences in fear discrimination by determining if the CS- took on the inhibitory properties of a safety signal with extended training. Summation and retardation tests are used to demonstrate safety signalling by the CS- (Christianson et al., 2012; Sangha et al., 2013). During summation testing the CS+ and CS- are presented together; if the CS- acts as a safety signal, this results in a reduction of fear compared to presentation of the CS+ alone. In the present study, it was not possible to use a summation test as both cues were auditory stimuli of differing pitch. During retardation testing, the CS- is used as the cue (i.e. paired with the US) in subsequent fear conditioning. If the CS- signals safety then that subsequent conditioning is retarded, and fear in response to the CS- cue at retrieval test is reduced, in comparison to controls not subjected to prior discrimination training.

We pre-exposed control rats to the same number of cues that were presented during fear discrimination to rule out the possibility that any

differences in freezing during retrieval testing were attributable to an effect of latent inhibition, a form of learned irrelevance where cue pre-exposure impairs later conditioning to that cue (Young et al., 2005). This was also important to consider given that previous studies have shown sex differences in latent inhibition (Kaplan & Lubow, 2011). Compared to their respective controls, we found reduced fear in response to the prior safety cue in males but not females. This sex difference in the retardation test suggests that, with extended discrimination training, the CS- acted as a safety signal in males but that this safety signalling was impaired in females. An alternative interpretation is that females showed a deficit in latent inhibition rather than safety signalling. However, if latent inhibition was impaired then female controls would have been expected to show more fear at retrieval test compared to their male counterparts, which was not observed to be the case. Future studies examining sex differences in fear discrimination and safety signalling using cues from different sensory modalities, which would also allow for the assessment of summation testing, might prove useful in addressing this issue.

In fact, a previous study has examined sex differences and the role of oestrogen in fear discrimination involving auditory and visual cues but there were also other important differences between that study and ours. Toufexis et al. (2007) examined fear-potentiated startle in gonadectomised rats using an AX+/BX- discrimination paradigm, where presentation of A and X together predicted the US and B presented together with X signalled non-occurrence of the US. They also used a slow acquisition protocol, in which rats were subjected to fewer cue and US presentations over more days of training than in our study,

to track changes in discrimination learning over time. Under these conditions both male and female shams showed fear discrimination over the course of training and during later retrieval testing. During summation testing, both male and female shams also exhibited less fear in response to the presentation of A and B together than when A was presented alone, providing evidence that B signalled safety. Furthermore, fear discrimination and safety signalling both depended on oestrogen receptor signalling in females. Evidence indicates that sex differences in contextual fear discrimination also depend on oestrogen (Lonsdorf et al., 2015; Lynch et al., 2013). A limitation of our study is that we did not account for variations in the oestrous cycle phase of females, yet we were still able to replicate our finding of fear generalisation with extended training in a separate cohort of naturally cycling females. Moreover, a recent study in traumatised children found that girls showed impaired visual fear discrimination compared to boys (Gamwell et al., 2015), suggesting that sex differences in fear discrimination may involve the organisational effects of gonadal hormones during development and/or genetic factors that are independent of any hormonal effects. Nevertheless, when taken together with other evidence our results suggest that the generalised fear observed in intact females may have involved oestrogen.

In conclusion, we found that females showed auditory fear discrimination with limited training and generalisation with extended training due to impaired safety signalling. Our findings add to accumulating evidence indicating important sex differences in learned fear inhibition. From an adaptive perspective, there might be different circumstances which favour discrimination

or generalisation in relation to salient stimuli. Rapid discrimination between threat-related and harmless stimuli may conserve resources by restricting appropriate behavioural responding to a limited number of cues. On the other hand, generalising across cues may enhance survival by promoting defensive responding to a wider range of stimuli that potentially predict threat, perhaps under more uncertain or stressful environmental conditions. However, when the balance tips too far towards generalisation then this can lead to inappropriate fear in response to innocuous stimuli (Dunsmoor & Paz, 2015). Crucially, impaired fear discrimination and safety signalling are hallmark features of PTSD, which is also much more prevalent in women. Recent studies have begun to elucidate the neurobiological basis of sex differences in fear inhibition via extinction and further work is needed to determine if sex differences in fear discrimination involve similar, distinct or overlapping mechanisms.

Chapter 3. Computational Modelling of Sex Differences in Behaviour

3.1 Introduction

As discussed in Chapter 1, there are multiple, interconnected brain regions involved in the processes of fear learning, retrieval and inhibition, including the PL and IL of the mPFC and the BLA. A schematic diagram of some of these connections is detailed in Figure 3.1. below:
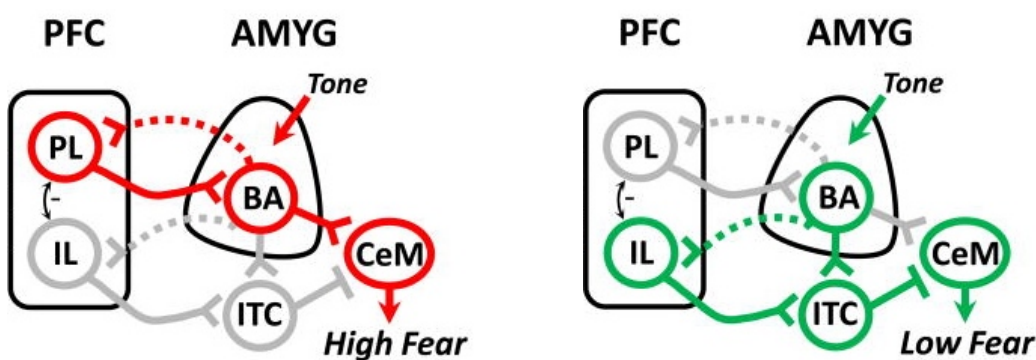
Figure 3.1 PL and IL contributions to the control of learned fear (left, red) and its inhibition (right, green). Learned fear involves PL projections to the BA, which excites neurons in the CeM to produce fear. Fear inhibition involves IL projections to the amygdala ITCs. ITCs inhibit amygdala output neurons, inhibiting fear responses. Here, conditioned stimuli (e.g. a tone) can produce either a high fear state (e.g. post-conditioning) or a low fear state (e.g. post-extinction), depending on the associative nature of the stimulus with either a US or no-US. Figure adapted from Sotres-Bayon & Quirk, (2010).

However, exactly how these regions influence each other in response to auditory fear and safety cues is still poorly understood. Because of this, we aimed to use computational models (this chapter) in combination with experimental data (Chapter 4) to better understand the underlying activity and connectivity of this network. Although learning and synaptic plasticity within the amygdala has been modelled using simple learning paradigms (Li et al., 2009; Vlachos et al., 2011; Pendyam et al., 2013), a reduced model of how neural

populations within the BLA respond to cued auditory threat and safety stimuli has yet to be examined. Here, a reduced model simulates dynamical "information" about real neurons (i.e. activity rates), without having to model the more complex and computationally intensive elements of neuronal activity, such as membrane current fluctuations (Gutkin et al., 2003). Although an extrapolation, results from a reduced model can be interpreted to make tangible hypotheses about *in vivo* phenomena, such as behaviour. This is despite compelling evidence to support the BLA as a crucial locus for the acquisition and inhibition of learned fear, with both 'fear' and 'extinction' neurons existing within the same subnuclei (reviewed in Giustino & Maren, 2015). The relative activity rates produced by these neural ensembles strongly correlates with the level of fear expression. In particular, there is a dearth of models investigating potential sex differences in neural activity and connectivity (Chapter 4) which may underlie differences observed in behaviour (Chapter 2).

LFP recordings in animals, combined with computational modelling, can provide insight into the co-operative behaviour of neurons, both locally and between brain areas (Rasch et al., 2009; Friston & Dolan, 2010). In turn, these measures can increase our understanding of how these processes contribute to behaviour (Buzsáki et al., 2012). Originally, the dynamics of ion channels were developed in the Hodgkin–Huxley model (Hodgkin & Huxley, 1952), which described how action potentials were initiated and propagated in giant squid axons by means of a set of non-linear ordinary differential equations (reviewed in Platkiewicz & Brette, 2010). Although action potentials and spike modelling are important to the understanding of the fear memory network (Schmidt et al.,

2015; Li et al., 2016), the oscillatory activity of locally connected neural populations as described previously (Chapter 1) and measured directly (Chapter 4), will be the main focus of this chapter. LFPs provide additional information on neuronal activity between brain areas, making it easier to link this activity to behaviour than the activity of individual neurons alone (Carlson et al., 2014). For example, by using measures of synchrony between LFP signals in two different brain areas, we are able to interpret potential neural networks, in addition to how those networks correlate with fear behaviours, such as freezing (Stratton et al., 2012).

From further investigations of the Hodgkin-Huxley model, it was found that different patterns of oscillatory activity could be extrapolated using bifurcation analysis (reviewed in Sase et al. (2017)). Bifurcation analysis is commonly used to study changes in the qualitative behaviour of dynamical systems, for example the interplay of oscillations described by several differential equations (Kazarinoff, 1990). Bifurcation analysis has led to a classification of different types of responses within the neural population, such as excitatory and inhibitory activity, which have been utilised in further *in silico* experiments (Foster et al., 2008; Vanvinckenroye et al., 2016). For example, modelled neuronal activity generated by populations of inter-connected inhibitory and excitatory cells can show spontaneous oscillations (Terman et al., 2002). These spontaneous oscillations have been well-described by the Wilson-Cowan model (Wilson & Cowan, 1972; reviewed by Destexhe & Sejnowski, 2009). In addition to this, it has been found that modelled oscillatory dynamics of brain activity closely agree with experimental findings, wherein

models based on these principles have been used to provide descriptions of neural oscillations and EEG rhythms (David & Friston, 2003; Baker & Cowan, 2009; Cabral et al., 2014).

The Wilson-Cowan model was first described in 1972, and extensions of the original framework are now standard practice in the modelling of neuronal populations. In this model, simple representations of neuronal sub-groups can be simulated, and stimulus-dependent evoked responses within these neurons can be predicted (reviewed in Cowan et al., (2016). For example, the Wilson-Cowan model can describe activity from excitatory (E) and inhibitory (I) sub-populations of neurons. The activity from each neural sub-population can be represented as an oscillator, where E and I can be coupled through connections to form a network (Ueta & Chen, 2003). Here, rhythmic oscillations can be represented by a non-linear dynamical system. In this instance, the connections of and between E and I can be wired up as such:
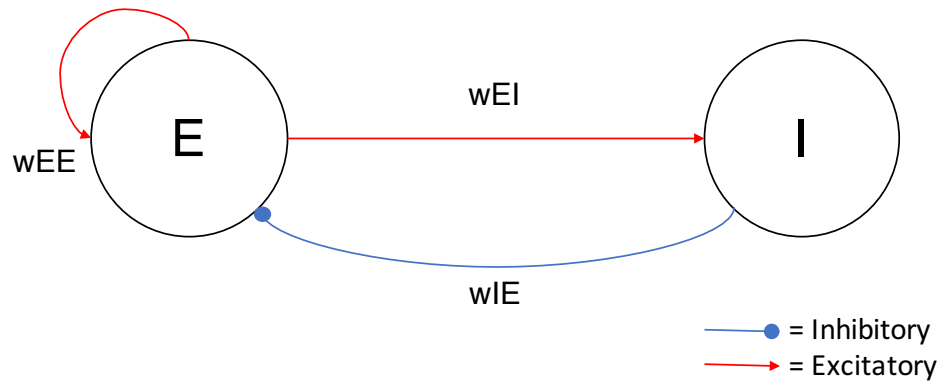
Figure 3.2 Neural circuitry of a pair of network oscillators representing excitatory (E) and inhibitory (I) neurons. Excitatory connections are shown by red arrows and inhibitory connections are shown by blue solid circles. The weight of the self-excitatory connection from E to E is shown by the weight wEE, the excitatory connection from E to I is shown by the weight wEI and the inhibitory connection from I to E is shown by the weight wIE. Here, 'weight' is defined as the influence of one neuronal group on another Figure adapted from Wilson & Cowan, (1972).

The change in the activity rates generated by the neuronal groups E and I over time can be described by the following first order, non-linear differential equations:

Equation 1 (a):

$$\tau_E \frac{dE}{dt} = (-E(t) + Sig(wEE_E - wIE_I + K_E(t)))$$

Equation 1 (b):

$$\tau_I \frac{dI}{dt} = (-I(t) + Sig(wEI_E + K_I(t)))$$

Here, $\frac{dx}{dt}$ depicts that change in x over time (t). Time is defined by the variable τ_x , where in Equation 1 (a) the change in the activity level of the neuronal sub-group E is defined by the decay of E, plus a sigmoidal function of the weight (or influence) of the self-propagating wEE connection depicted in Figure 3.2 above, minus the inhibitory connection of wIE from the I neuronal population. Similarly, in Equation 1 (b) the change in the activity level of the neuronal subgroup I is defined by the decay of I, plus a sigmoidal function of the weight (or influence) of the excitatory connection wEI depicted in Figure 3.2 above. In addition to the weights on E and I, there is also a constant, K, which prevents system collapse resulting from either runaway excitation or inhibition. The source of the non-linearity in these differential equations is the sigmoidal function (Sig), which acts as the threshold value for activity of these two groups. This function has a steepness parameter (p) and a threshold value (θ, theta), meaning that unless

the Sig function contains satisfactory values of p and/or θ, neuronal activity will not be sustained. The sigmoid function is shown by Equation 2, below:

Equation 2:

$$Sig(x) = \frac{1}{1 + e^{-p(x-\theta)}}$$

The use of a sigmoidal function to describe a threshold for neural activity within the Wilson-Cowan framework is well supported and is now a mainstream of neural population modelling. For example, similar equations are found in Maass (1997) and Platkiewicz & Brette (2010). Variations on the sigmoid function in Equation 2 are represented graphically in Figure 3.3, below. Here, changing the values of θ changes the steepness of the curve, making it easier (f(x)) or harder (g(x)) for the threshold of activity to be reached. This means that there will be more, or less, overall activity within the system of E and I, respectively.
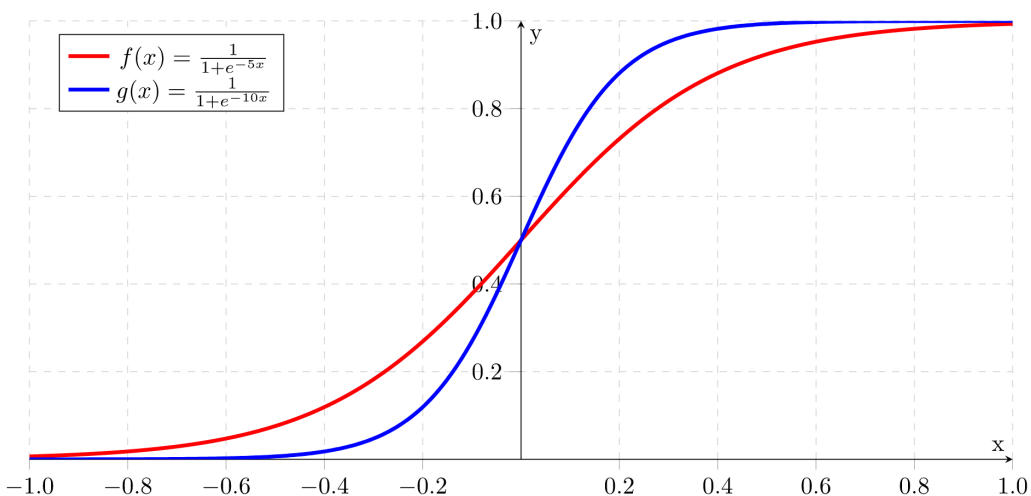
Figure 3.3 Sigmoid curve function detailed in Equation 2, above. This sigmoid function (f(x)) provides the threshold limit for activity in E and I neural sub-populations. This sigmoid curve is bound by parameters p and θ to govern the slope. A reduction in either of these values (i.e. (g(x))) will describe a lower threshold for activity (i.e. higher rates of activity produced by the same input); similarly, an increase in either of these values will describe a higher threshold for activity (i.e. lower rates of activity produced by the same input).

Together, **Equations 1 and 2** describe the activity produced by E and I. Here, E and I both have a baseline level of activity from the constant, K. E will excite both itself and I via the wEE and wEI connections, whereas I will inhibit E via the wIE connection. This means that when E initially becomes active, it will then become more active (via the self-propagating wEE connection), but the activity will not exponentially increase, as the more E becomes active, the more it will activate its own inhibitor, I. From this, the relative activity levels of E and I increase and decrease in a cyclical pattern. By performing phase-plane analysis, we can solve Equations 1a and 1b to graphically show how the relative activity levels of E and I change over time. Here, this can be achieved by making **Equations 1a and 1b** both equal 0. This results in two functions being produced, which, when plotted, produce the nullclines of E and I. A nullcline is a function satisfied by a set of points produced when derivative of x = 0 (i.e. when the rate of change is zero) (Hankins et al., 2013). In the case wherein the derivatives of E and I equal zero and are then plotted, the result is two lines (the nullclines) which intercept at a point, or points. The point/s of interception depict when the system achieves equilibrium. A representation of this is shown in Figure 3.4, below:
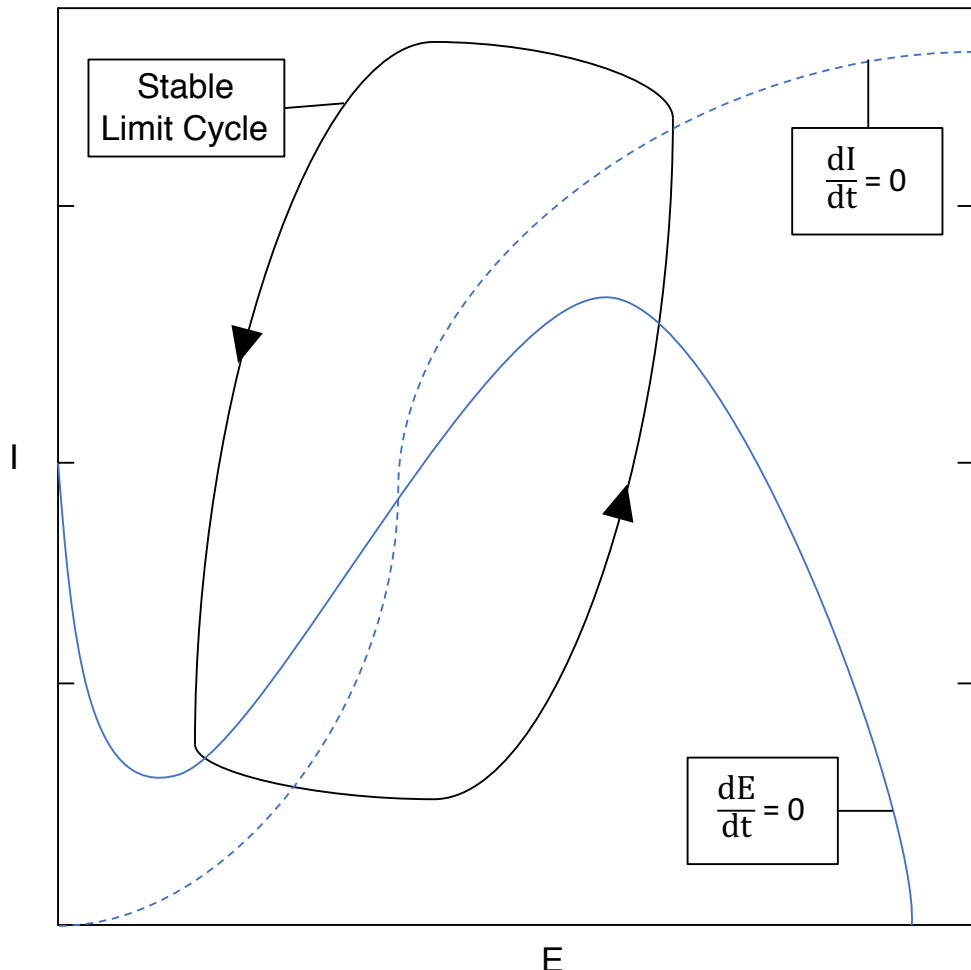
Figure 3.4. Limit cycle oscillations of a pair of Wilson–Cowan oscillators. The solid blue line represents the nullcline of E (i.e. dE/dt = 0) and the dashed blue line represents the nullcline of I (i.e. dI/dt = 0) from Equation 1a and 1b in the phase plane. Here, the solid and dashed blue lines are satisfied by the functions produced when $\frac{dE}{dt}$ or $\frac{dI}{dt}$ are equal to 0, respectively. The intersection of the two nullclines is an unstable equilibrium point, or spiral point, for these equations. At this intersection, the equilibrium is periodic, producing a limit cycle (i.e. the limit cycle describes the oscillatory activity of E and I). Figure adapted from Cowan et al., (2016).

These two nullclines of E and I are plotted in solid and dashed blue lines respectively in Figure 3.4, above. In this example, the nullclines only cross at a single point, depicting stability in the system. However, with different parameters, it is possible for one, three or five intersections to exist, meaning that the system can reach (stable) equilibrium at other points (Onslow et al., 2014). In Figure 3.4, the interception of the E and I nullclines depicts an

as a limit

from the

E excites

becomes
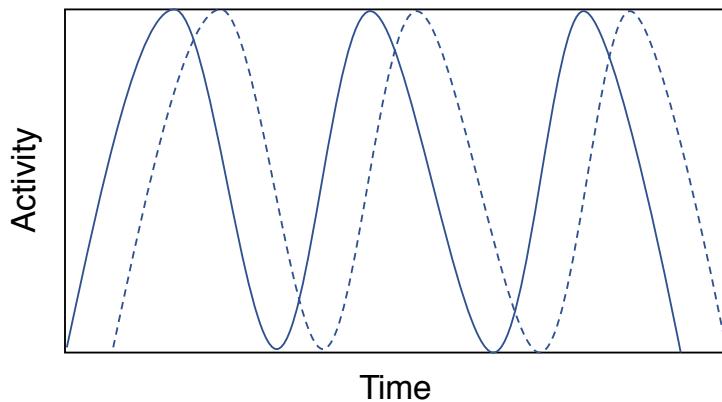
activity

Figure 3.5. The activity levels of E and I are plotted as functions of time (E(t) and I(t)). E is depicted as a solid blue line, and I is depicted as a dashed blue line, respectively. Each neuronal population goes through a cycle of increasing activity, followed by inhibition and a reduction of activity, only to begin again. This is akin to neurons within those populations initially residing in a resting state (low levels of activity), firing together (increasing levels of activity), then being inhibited (reducing levels of activity) phase before returning to a resting state again. In this instance, one cycle of pre-firing, firing and return to the basal state would be the period of the oscillation created (Akam & Kullmann, 2014).

Modelled oscillators, similar to those described above, generate a wide range of activity, such as excitation or inhibition of themselves and/or other oscillators (Campbell & Wang, 1996; Ermentrout & Chow, 2002; Neves & Monteiro, 2016). From this, the dynamics of these Wilson and Cowan modelled oscillators can be studied to make predictions, which can either be inspired by, or tested in, *in vivo* experiments. Previously, Herry et al. (2008) showed that there are two distinct neuronal populations in the BLA; 'fear' and 'extinction' neurons. *In vivo* stimulation of these populations revealed that they each receive differential

functional input from the hippocampus and mPFC. In the seminal paper by Vlachos et al. (2011), this experimental work was expanded into a computational model to describe contextual fear discrimination. In their model, sub-populations of these 'fear' and 'extinction' BLA neurons were created by utilising similar differential equations used to describe the original Wilson-Cowan paired oscillators. These sub-populations of BLA neurons received input from the hippocampus and mPFC to represent the current context; either the conditioning (pro-fear) or the extinction (anti-fear) context. In addition to contextual input, all BA neurons could receive input from the LA, which itself received US inputs during conditioning. From this, the population of BA neurons receiving simultaneous US input from the LA combined with context-specific input (i.e. context A, the conditioning context) from the hippocampus/mPFC become responsive during conditioning (i.e. acting similarly to 'fear' neurons observed *in vivo*). A simplified diagram of this network is shown below:
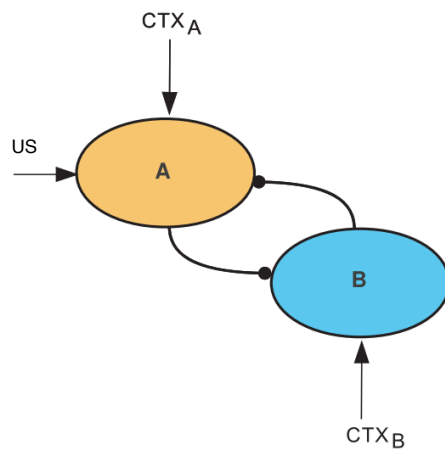
Figure 3.6. A firing rate model of contextual fear discrimination. Two neuron populations, A ('fear') and B ('extinction') have US and/or contextual inputs. These external inputs influence the relative activity rates of A and B. Both populations negatively inhibit one another, with high activity in B inhibiting activity in A and vice versa. This model bears resemblance to the original E and I populations from the Wilson-Cowan oscillatory model, described above. Figure adapted from Vlachos et al., (2011).

From this, Vlachos et al. (2011) proposed that contextual input modulates neuronal activity within the BA, resulting in the formation of associations between the CS, US, and/or context, which then, in turn, modulate behavioural output. During fear conditioning, the US paired with the Context A representation signals danger, causing a high fear state, whereas during extinction, the newly formed no-US paired with Context B representation signals safety and suppresses the fear state. However, this model only investigated the neural populations of A and B with relation to contextual cues during conditioning and extinction; how similar sub-populations of neurons respond to cued (i.e. CS+ or CS-) stimuli during a fear discrimination paradigm, and how sex can influence these responses, remains to be established.

3.1.2 Objectives

In the model described within this chapter, we used the basic Wilson-Cowan framework and inspiration from the Vlachos et al. (2011) model to investigate the influence of CS+, US and CS- inputs on two distinct neural populations in the BLA; 'fear' (F) and 'safety' (S) neurons. Initially, each sub-population of 'fear' and 'safety' neurons received information of either the CS+ and US (F neurons) or the CS- alone (S neurons). Connections from the CS+, US and CS- to F and S were plastic and produced LTP to influence both F and S activity levels. F and S were also inter-connected, with both connections being mutually inhibitory (i.e. when activity in F was high, activity in S was suppressed, and vice versa). From this, we expanded the model to include both excitatory and inhibitory neural sub-populations and connections within F and S. Here, F+ and

S+ were created with the aim to represent excitatory glutamatergic pyramidal sub-populations, whereas F- and S- were created with the aim to represent inhibitory GABAergic interneuron sub-populations, within F and S. In both models, we assumed high levels of activity from the F population were indicative of a 'high fear' state, whereas high levels of activity from the S population were indicative of a 'low fear' state. This is similar to outputs from the BLA to either the CEm or ITC (see Figure 3.1, above), which represent the dominant outputs during either high or low fear states, respectively.

By utilising these models, our overall aim was to simulate the distinct 'discrimination' and 'generalisation' phenotypes we have observed in males and females with extended training (described in Chapter 2). Initially, we aimed to describe the 'discrimination' phenotype (i.e. high fear in response to the CS+ and low fear in response to the CS-) in our first Model, Model 1. Following this, we then aimed to represent the 'generalisation' phenotype (i.e. similar, high levels of fear to both the CS+ and CS-) by changing the parameters of Model 1. The parameter changes which produced the 'switch' from the discrimination phenotype to the generalisation phenotype would then form the basis for further modelling. In the second iteration of our model, Model 2, we aimed to produce biologically plausible connections between F+ and S+ pyramidal neurons and F- and S- interneurons, which we hypothesised would produce the discrimination phenotype. We then aimed to reduce the amount and/or weight of the inhibitory connections to model the generalisation phenotype observed in females with extended training for two reasons. Firstly, because most forms of brain rhythms are inhibition-based, wherein interneurons produce rhythmic

inhibitory inputs to principal cell populations (Buzsáki & Watson, 2012). Secondly, we wanted to simulate a relative reduction in GABA signalling, which has been previously reported in females (Milad et al., 2009; Cholanian et al., 2014; Fernandez de Velasco et al., 2015; Möller et al., 2016), and has been linked to fear generalisation (Shaban et al., 2006; Bergado-Acosta et al., 2008; Sangha et al., 2009; Lange et al., 2014).

3.2 Model Methods and Results

3.2.1 Model 1: Methods

To make our results comparable to the LFP data presented in Chapter 4, we created our computational models to represent neural activity at the population level. In order to do this, we utilised and built upon the Wilson-Cowan equations described above to create two identical neural sub-populations, 'fear' (F) and 'safety' (S) within the BLA (Model 1, described in Figure 3.7, below). All computational models were made using MATLAB (MATLAB and Statistics Toolbox Release 2012b, The MathWorks, Inc., USA), and all code is provided in the appendix (Chapter 6). In the initial stages of creating Model 1, we first derived examples of the original differential equations of the Wilson-Cowan model to show that the limit cycle at the intercept of the nullclines (i.e. when the derivatives of **Equation 1** are set to 0) produced oscillatory activity. Once we established that we could satisfactorily describe oscillatory activity utilising the Wilson-Cowan equations, we built Model 1, consisting of a pair of inter-connected, mutually inhibitory neuronal sub-populations (F and S) with external

inputs CS+, CS- and US. The equations defining the activity levels for F and S are described below:

Equation 3 (F neuronal activity):

$$\tau_F \frac{dF}{dt} = -F + (k_F - r_F F) Sig(wCP_F(CSPlus) + wCU_F(US)) + wSF(S))$$

Equation 4 (S neuronal activity):

$$\tau_S \frac{dS}{dt} = -S + (k_S - r_S S) Sig(wCP_S(CSMinus)) + wFS(F))$$

In addition to the external inputs and connections between F and S, we also programmed a time constant (τ; Tau) as well as the relative maximum firing rate (*k*) and refractoriness (*r*) of the neurons within F and S. *Sig* represents the Sigmoid function outlined in **Equation 2**, wherein parameters 'p' and θ define the threshold of activity for both F and S. *wCP$_F$*, *wCU$_F$* and *wCM$_S$* represent the connections to F and S from the CS+, US and CS- inputs, respectively, and *wSF* and *wFS* represent the inhibitory interconnections from S to F and F to S, respectively. The evolution of the weights of the CS+, US and CS- inputs to F and S are described below:

Equation 5:

$$\frac{dwCP, CU, CM}{dF} = \alpha_F(CSPlus) + (CSMinus) + (US)$$

Equation 6:

$$\frac{dwCP, CU, CM}{dS} = \alpha_s(CSPlus) + (CSMinus) + (US)$$
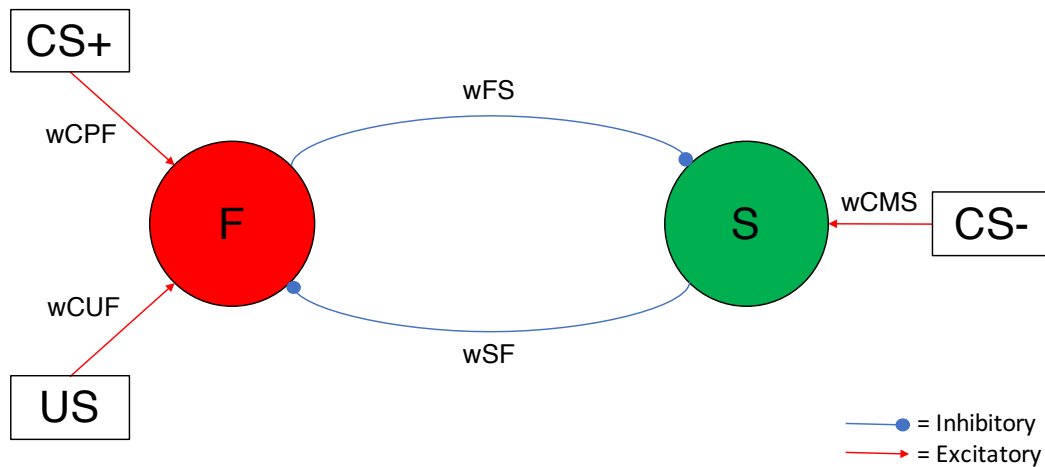
Figure 3.7 Model 1 of 'fear' (F) and 'safety' (S) neural sub-populations in the BLA. Based on the original Wilson-Cowan equations (Wilson & Cowan, 1972), we created two neural sub-populations; 'fear' neurons (F) and 'safety' neurons (S). The activity of each sub-population was influenced by excitatory plastic connections from CS+, US and CS- inputs (red arrows), determined by the weights wCPF, wCUF (CS+ and US→F) and wCMS (CS-→S). In addition, there were mutually inhibitory connections between F and S (blue circles), determined by the weights wFS (F→S) and wSF (S→F). The thresholds of activity for F and S were determined by the sigmoid function detailed in **Equation 2**. Both F and S were identical in their initial conditions (described by the differential equations presented in **Equations 3 and 4**, above). Inputs from the CS+, US and CS- were created to replicate the fear discrimination paradigm described in (Chapter 2) represented by **Equations 5 and 6**, above.

From these parameters, we aimed to describe the activity of F and S during a similar behavioural fear discrimination paradigm described in Chapter 2. We designed an initial 'conditioning' phase, wherein the CS+ input was always paired with the US input and the CS- was never paired with the US. This was then followed by a period of no stimulus input, to represent the interval between conditioning and retrieval, followed by a 'retrieval' phase, wherein both CS+ and CS- were presented with no US. To better represent the behavioural fear discrimination paradigm described in Chapter 2, we simulated the same number of CS+, US and CS- presentations during conditioning and an increased number of CS+ and CS- presentations during retrieval in the computational models as we used experimentally. Here, there was a total of 15 CS+ with US presentations and 15 CS- presentations modelled during

conditioning, with the retrieval period consisting of 5 further presentations of the CS+ and CS-, with no US. Additional presentations were used during retrieval to allow the model to adjust to further input following the ITI.

In line with the behavioural paradigm, we designed the F and S sub-populations of Model 1 to receive either CS+ or CS- stimuli, with an additional US stimulus applied at the termination of each CS+, during the conditioning period. These external inputs, presumed to originate from other brain regions such as the LA (Armony et al., 1995; LeDoux, 2000), were programmed to modulate the activity of F and S.

Overall, although F and S are able to receive a general input from the CS+, CS- and US (as cells in the BLA would do *in vivo* prior to conditioning), we wanted the activity of F to only be modulated when the CS+ and US were presented together, and the activity of S to only be modulated when the CS- was present, during conditioning. To do this, we designed the responsiveness and relative activity rates of F and S to be identical prior to CS/US input, following experimental data from Herry et al., (2008) and the Vlachos et al., (2011) model. Then, to create a basis for the 'discrimination' or 'generalisation' phenotypes, we designed weights of the CS+ and US input to modulate only the activity of F by increasing in an additive fashion when they temporally coincided (**Equations 5 and 6**, above). Similarly, we designed the weight of the CS- to only modulate the activity of S neurons. This means that, during conditioning, only when the CS+ and US temporally coincided was activity produced within F, and only when the CS- was presented was activity produced within S.

Effectively, this meant that the F and S neurons only gained the identity of 'Fear'- and 'Safety'-responsive neurons post-conditioning. Prior to this, they were identical. Over the period of conditioning, repeated presentations of the CS+, US and CS- would generate a model of an engram, or 'associative learning' in F and S. For example, after conditioning, the CS+ would be associated with the US in the F neurons, whereas the CS- would be associated with no-US in the S neurons. This means that the activity rates observed within F and S would be a direct consequence of the stimulus inputs during conditioning. Post-conditioning, we halted the active 'associative learning' process in F and S. In biological terms, this is similar to the process of consolidation, wherein the learning process halts, and the memory of that learning is preserved to be utilised in future scenarios (Payne & Nadel, 2004). During retrieval (i.e. the presentations of the CS+ and CS- without the US), we allowed the modelled activity of F and S to evolve only from the last point in time at the end of conditioning. This meant that the activity levels of F and S were generated by the 'retrieval' of the 'associative learning' gained by F and S during conditioning, instead of being directly modulated by the US and CS inputs. From this, we hoped to model a better representation of the process of learning during conditioning, followed by the retrieval of that learning, in the populations of F and S neurons.

In addition to these external inputs, F and S were also inter-connected, with the connections between the two groups being mutually inhibitory. We chose these mutually inhibitory connections between F and S to simulate the interplay between fear expression and fear inhibition *in vivo* during successful

discrimination; a 'high fear' state will preside over a 'low fear' state when a threat is perceived and vice versa when safety is perceived. This is based on similar results observed from the A and B populations detailed in Vlachos et al., (2011) (Figure 3.7, above) during recall of the fear conditioning and extinction contexts.

3.2.2 Model 1: Results

Once we had established a discrimination paradigm within the computational model, we observed the relative activity rates produced by the F and S sub-populations during conditioning and retrieval. As previously described, the CS+ and US (when presented together) would produce activity within the population of F neurons, whereas the CS- would produce activity within the population of S neurons. With the connections outlined in Figure 3.7 (Model 1, above), we observed a 'discrimination' phenotype in the F and S neurons in response to CS+, CS- and US input. These results are outlined in Figure 3.8, below:

Figure 3.8. Evolution of the firing rates of fear (F, red) and safety (S, green) neurons from Model 1 during fear discrimination conditioning and retrieval. Activity of F (red) and S (green) is shown (bottom panel) in response to the input stimuli of CS+ (red), CS- (blue) and US (yellow), (top panel). As a result of the connections in Model 1 (Figure 3.7, above), the 'discrimination' phenotype emerges. This is described by high F activity during the CS+ and low F activity during the CS-, in addition to high S activity during the CS- and low S activity during the CS+, presentations throughout conditioning and retrieval.

From this, we then aimed to perturb the model, both in terms of changing the relative connection strengths from the internal (i.e. connections between F and S) and external (i.e. CS+, CS- and US) inputs, to the nature of these connections (i.e. removing excitatory connections or making them inhibitory). By doing this, we wanted to test how we could change the parameters of Model 1 to change the 'discrimination' phenotype outcome (i.e. F activity was greater than S activity during the CS+, whereas S activity was greater than F activity during the CS-) to a 'generalisation' phenotype outcome (i.e. F activity was greater than S activity regardless of cue type). We were able to produce the 'generalisation' phenotype from Model 1 in two different ways.

Initially, we increased the mutual inhibition between F and S by increasing the negative weight of F → S and the negative weight of S → F. By slightly increasing the mutual inhibition of F and S, the 'discrimination' phenotype still presided, although the relative activity of S was subtly decreased. This is shown in Figure 3.9:

Figure 3.9. Evolution of the firing rates of fear (F, red) and safety (S, green) neurons from Model 1 during fear discrimination conditioning and retrieval. Activity of F (red) and S (green) is shown (bottom panel) in response to the input stimuli of CS+ (red), CS- (blue) and US (yellow), (top panel). A small increase in mutual inhibition between F and S preserves the 'discrimination' phenotype, albeit with lower levels of S activity during the CS-.

However, when we increased the strength of the mutual inhibitory connections between F and S further, we then eventually observed a 'generalisation' phenotype emerge. Here, there is initial discrimination between the CS+ and CS- early on in conditioning (i.e. high F activity, but low S activity, to the CS+ and low F activity, but high S activity, to the CS-), but the activity of F overtakes the activity of S with extended training. Here, F activity is higher than S activity regardless of which CS is presented and remains high throughout the retrieval phase. These results are shown in Figure 3.10, below:
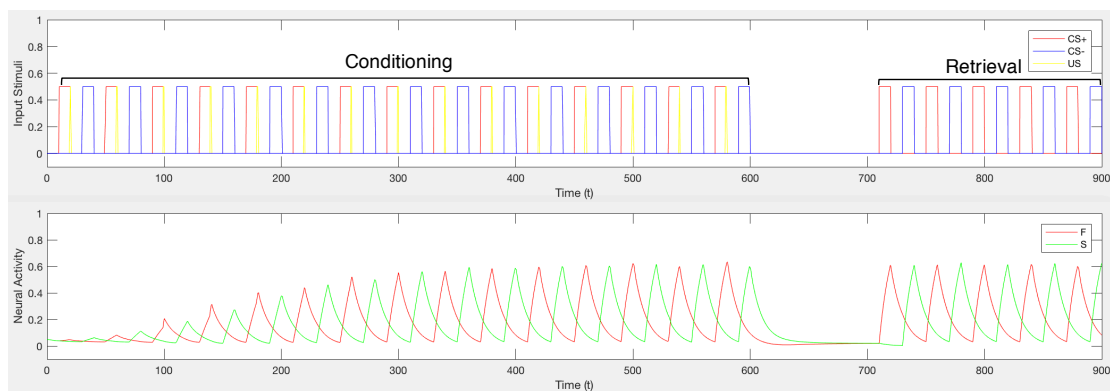

Figure 3.10. Evolution of the firing rates of fear (F, red) and safety (S, green) neurons from Model 1 during fear discrimination conditioning and retrieval. Activity of F (red) and S (green) is shown (bottom panel) in response to the input stimuli of CS+ (red), CS- (blue) and US (yellow), (top panel). A larger increase in mutual inhibition between F and S generates a 'switch' from the 'discrimination' phenotype to the 'generalisation' phenotype, where discrimination is observed in the early stages of conditioning, but generalisation occurs with extended training.

The results shown in Figure 3.10 bear a strong resemblance to the initial discrimination behaviour with limited training, followed by generalisation behaviour after extended training, that we have previously reported in females (Chapter 2). Therefore, one of the ways the 'generalisation' phenotype can be produced in this model is by increasing the overall amount of mutual inhibition between F and S. *In vivo*, this may be similar to relatively higher levels of mutual

inhibition between certain subpopulations of BLA neurons (akin to 'fear' and 'extinction' neurons; Herry et al., (2008)). However, the neurobiological factors underlying these behaviours are likely to be complex in nature as this was not the only way we were able to model the 'generalisation' phenotype.

Interestingly, we were also able to generate the 'generalisation' phenotype by changing the connection from S➔F from inhibitory to excitatory (i.e. the 'safety' neurons exciting the 'fear' neurons, instead of inhibiting them. These connections are outlined by Model 1 (B), shown in Figure 3.11, below:
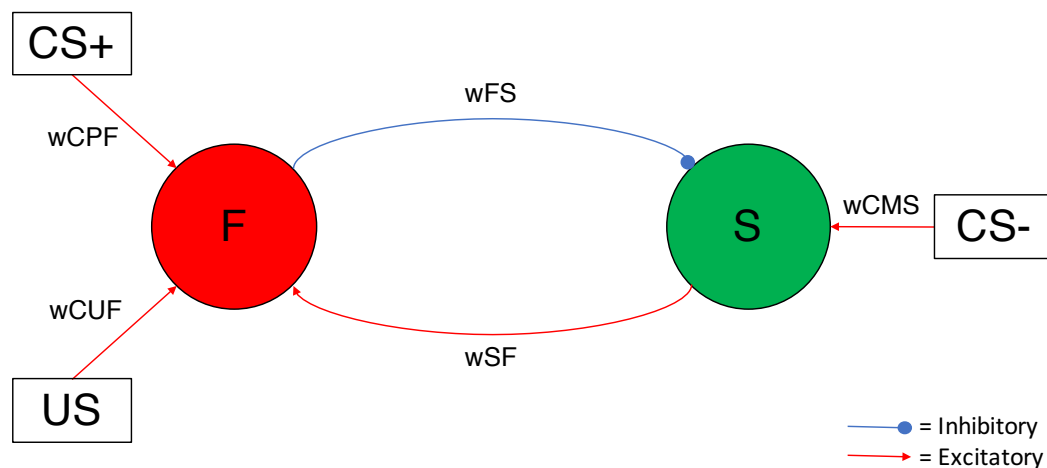
Figure 3.11. Model 1 (B). Excitation of F neurons by S neurons (wSF changed from inhibitory to excitatory). The thresholds of activity of the two neural sub-populations F and S, in addition to the inputs from CS+, US and CS-, were all as described for Model 1 (Figure 3.7). However, the sign of wSF was reversed from inhibitory to excitatory.

In this instance, reversing the sign of S➔F from negative to positive increased the excitation of F. However, in addition to increasing the excitation of F, this change simultaneously also reduced the relative inhibition of F. The activity rates of F and S produced by Model 1 (B) are presented in Figure 3.12, below:
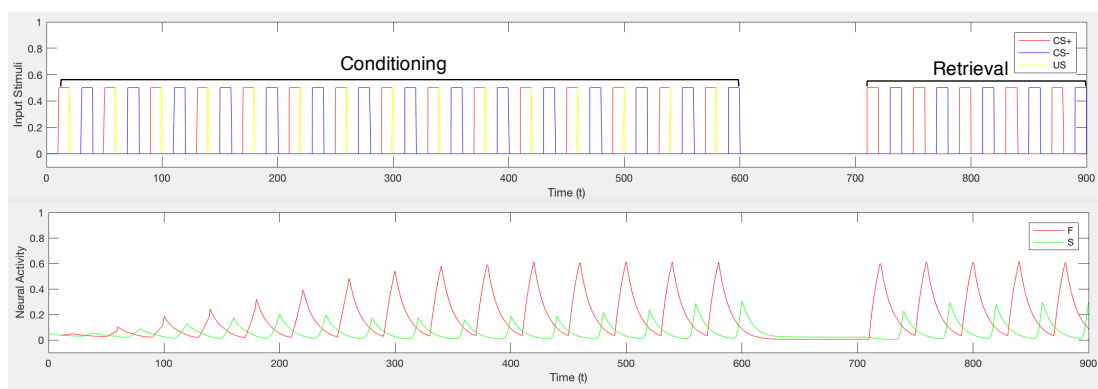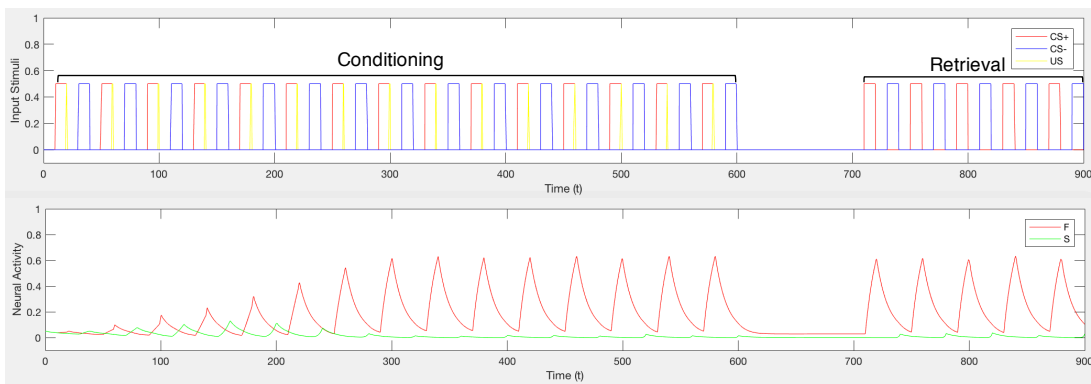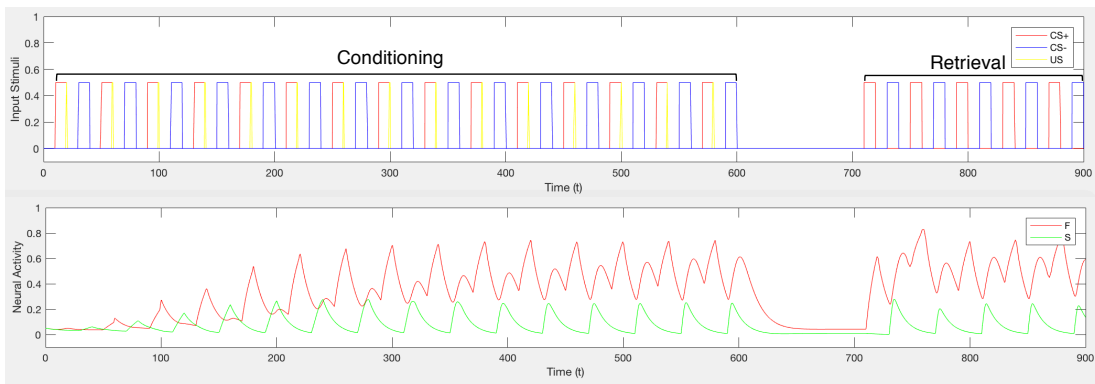
Figure 3.12. Evolution of the firing rates of fear (F, red) and safety (S, green) neurons from Model 1 during fear discrimination conditioning and retrieval. Activity of F (red) and S (green) is shown (bottom panel) in response to the input stimuli of CS+ (red), CS- (blue) and US (yellow), (top panel). Reversal of the wSF connection from inhibitory to excitatory (shown in Model 1 (B), Figure 3.11, above). Again, discrimination in the early stages of conditioning switches to generalisation with extended training. Although F neural activity reduces when there is no stimulus input, it remains higher than S throughout retrieval, regardless of the type of stimulus input.

Here, we still see the initial 'discrimination' phenotype at the beginning of conditioning (where there is more relative F activity during presentations of the CS+ and S activity during presentations of the CS-), but this pattern rapidly changes to 'generalisation' with further conditioning. However, the 'generalisation' we see here if different to the 'generalisation' we observed in Figure 3.10. In Figure 3.10, there was a suppression of S activity whilst F activity remained above baseline, whereas in Figure 3.12, there appeared to be a distinct activation of F neurons by both the CS+ and CS- cues. This distinction in the type of 'generalisation' phenotype produced by the two models is an important outcome to consider, as it may reflect subtle differences in the underling neurobiology of the sex differences in behaviour outlined in Chapter 2.

Taken together, these results indicate that there is likely to be a fine balance of excitation and inhibition of the fear and safety neurons; both too much and too little mutual inhibition within the model was able to perturb the

'discrimination' phenotype into 'generalisation' across the CS+ and CS- stimuli. In addition, 'safety' neurons may be unlikely to excite 'fear' neurons *in vivo*, due to the disparate nature of the 'discrimination' and 'generalisation' phenotypes. To further investigate the influences of excitation and inhibition on fear and safety neurons, we decided to develop Model 1 further to include both excitatory and inhibitory components of F and S. The result of these developments was Model 2, which is described below.

3.2.3 Model 2: Methods

Similar to Model 1 described above, Model 2 also had sub-populations of F and S neurons. However, each of these sub-populations was further split into excitatory (F+ and S+) and inhibitory (F- and S-) neurons, meaning that there were now four inter-connected neural sub-populations in total. As Model 1 only had mutual inhibitory connections between F and S, and since differing levels of inhibition produced either a discrimination or generalisation phenotype, we wanted to create more connections in Model 2. The equations describing F+(Fp), F-(Fm), S+(Sp) and S-(Sm) model neurons are detailed below:

Equation 7:

$$\tau_{Fp}\frac{dFp}{dt} = -Fp + \left(k_{Fp} - r_{Fp}Fp\right)Sig\left(wCP_{Fp}(CSPlus) + wCU_{Fp}(US)\right)$$
$$+ wFpFp(Fp) + wFmFp(Fm) + wSpFp(Sp) + wSmFp(Sm)$$

Equation 8:

$$\tau_{Fm}\frac{dFm}{dt} = -Fm + (k_{Fm} - r_{Fm}Fp)Sig\left(wCP_{Fm}(CSPlus) + wCU_{Fm}(US)\right)$$
$$+ wFmFm(Fm) + wFpFm(Fp) + wSpFm(Sp) + wSmFm(Sm)$$

Equation 9:

$$\tau_{Sp}\frac{dSp}{dt} = -Sp + (k_{Sp} - r_{Sp}Sp)Sig\left(wCP_{Sp}(CSMinus)\right) + wSpSp(Sp)$$
$$+ wSmSp(Sm) + wFpSp(Fp) + wFmSp(Fm)$$

Equation 10:

$$\tau_{Sm}\frac{dSm}{dt} = -Sm + (k_{Sm} - r_{Sm}Sm)Sig\left(wCP_{Sm}(CSMinus)\right) + wSmSm(Sm)$$
$$+ wSpSm(Sp) + wFpSm(Fp) + wFmSm(Fm)$$

Similar to **Equations 3 and 4** for F and S (above), the activities of F+, F-, S+ and S- are described in terms of the CS+, US and CS- external inputs, in addition to the internal connections between each sub-population. Again, the activity is governed by the same Sigmoid function given by **Equation 2**, above. The weights of the internal connections between F+, F-, S+ and S- are shown in Table x, below:

F+/- and S+/- weights	F+ (Fp)	F- (Fm)	S+ (Sp)	S- (Sm)
F+ (Fp)	wFpFp	wFpFm	wFpSp	wFpSm
F- (Fm)	wFmFp	wFmFm	wFmSp	wFmSm
S+ (Sp)	wSpFp	wSpFm	wSpSp	wSpSm
S- (Sm)	wSmFp	wSmFm	wSmSp	wSmSm

Table 3.1. Connection weights between F+, F-, S+ and S-. Each of F+, F-, S+ and S- are interconnected in accordance to **Equations 7-10**, described above.

In the first iteration of Model 2, we assumed that the excitatory sub-populations F+ and S+ would have primarily excitatory outputs, whereas F- and S- would have primarily inhibitory outputs, to other sub-populations. Further to this, we also designed F+, F-, S+ and S- to be self-regulating, with additional collateral inhibitory connections to themselves (i.e. an inhibitory connection from F+ to

F+). As for Model 1 before, we designed the external inputs from the CS+, CS- and US to converge on the F and S neurons during conditioning, with the CS+ and CS- in the absence of the US being presented during retrieval.

In Model 2, we again designed weights of the CS+ and US input to modulate only the activity of F neurons (i.e. F+ and F-) by increasing in an additive fashion when they temporally coincided during conditioning. Similarly, the activity in S neurons (i.e. S+ and S-) was modulated in response to the CS- input during conditioning. As in Model 1, we used this framework to generate 'associative learning' in all four sub-populations (i.e. F+, F-, S+ and S-), which would then affect their relative activity rates during the retrieval period where the CS+ and CS- were presented in absence of the US. The connections between the four sub-populations and the external CS+, CS- and US inputs are detailed in Figure 3.13, below:
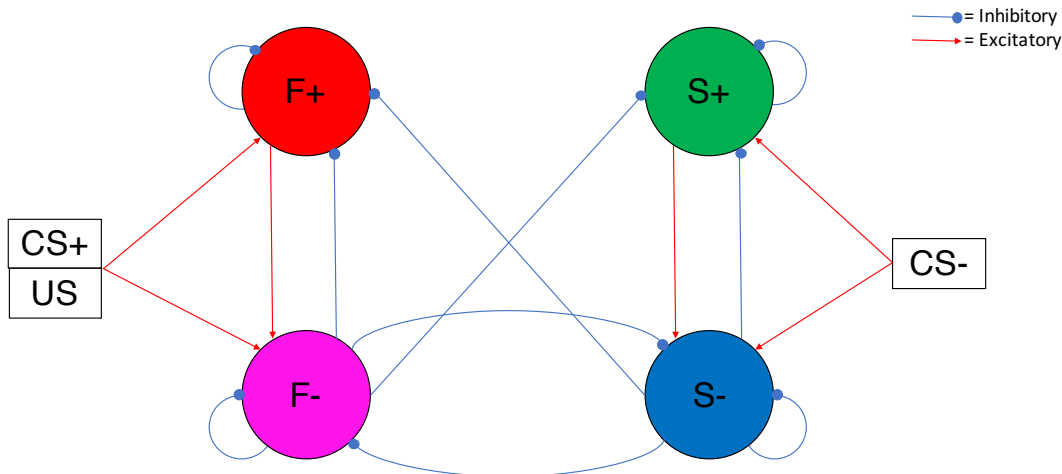
Figure 3.13. Model 2. Connections between excitatory and inhibitory 'fear' (F+, F-) and 'safety' (S+, S-) neural sub-populations in the BLA. Based on Model 1, we split each of the original homogenous F and S neural populations into excitatory (F+, S+) and inhibitory (F-, S-) neural sub-populations. Here, we determined that F+ and S+ would have predominantly excitatory outputs, whereas F- and S- would have predominantly inhibitory outputs (blue circles) to the other sub-populations. The weights of these connections are outlined in Table 3.1, above. As in Model 1, the activity of each sub-population was also influenced by excitatory plastic connections from CS+, US and CS- inputs (red arrows), determined by the weights wCPF, wCUF (CS+ and US→F+, F-) and wCMS (CS-→S+, S-). The thresholds of activity for F+, F-, S+ and S- were again determined by the sigmoid function detailed in **Equation 2**, above. All sub-populations were identical in their initial conditions prior to conditioning, and their relative levels of activity throughout training and retrieval were described by the differential equations presented in **Equations 7-10**, above. Inputs from the CS+, US and CS- were created to replicate the fear discrimination paradigm described in Chapter 2, and are represented by **Equations 5 and 6**, above.

As shown by Figure 3.13, above, F+ and S+ have excitatory connections to F- and S-, whereas F- and S- have inhibitory connections between each other and to F+ and S+. Each of F+, F-, S+ and S- also have self-inhibitory connections. As before, the CS+ and US modulates the activity of the F neurons, whereas the CS- modulates the activity of the S neurons. In this iteration of Model 2, the relative weights of all connections remain the same as in Model 1, with the activity of each of the neural sub-populations also governed by the same Sigmoid function outlined in **Equation 2**. Although the connections in Model 2 are more complex than Model 1, we aimed to, again, produce 'high fear' during the CS+ (i.e. high activity in F+ neurons) and 'low fear' during the CS- (i.e. low

activity in the F+ neurons and/or high activity in the S+ neurons) to model the 'discrimination' phenotype and 'high fear' (i.e. high activity in F+ neurons) regardless of the CS type presented to model the 'generalisation' phenotype.

3.2.4 Model 2: Results

From the connections shown in Figure 3.13 above, we were again able to model

Here, the 'discrimination' phenotype is shown by a relative increase in the F neurons during the CS+ (compared to the S neurons) and a relative increase in the S neurons during the CS- (compared to the F neurons). As before, once we had successfully modelled the 'discrimination' phenotype, we tried to perturb Model 2 to describe the 'generalisation' phenotype. In Model 1 this was achieved in two ways; either through increased mutual inhibition between F and S, or through reduced inhibition of F by S. These two produced two subtly

distinct variations on the 'generalisation' phenotype, either the relative suppression of S neurons whilst F neuronal activity remained above baseline or more of an activation of F neurons by CS- cue itself.

Therefore, to help decipher whether the generalisation phenotype is generated from too much and/or too little inhibition we aimed to describe these two processes in Model 2 by manipulating the additional excitatory and inhibitory connections between F+, F-, S+ and S-. To increase global inhibition in Model 2, we added weight to all the inhibitory connections from F- and S-, effectively making these connections stronger. Here, this means that F- and S- are themselves more inhibited, but also have a greater ability to inhibit F+ and S+. Although the inhibition weights have been increased, the configuration of the connections in Model 2 remain the same as described in Figure 3.13, above.

Overall, increasing global inhibition in Model 2 did reduce the activity rates of all neural sub-populations. However, instead of generating the pattern of 'generalisation' observed in Model 1 with increased inhibition (Figure 3.10), increasing inhibition within the Model 2 framework still produced a 'discrimination' phenotype during the retrieval phase (albeit with reduced activity in all neural sub-populations). Therefore, an increase in global inhibition is probably unlikely to underlie the 'switch' from discrimination to generalisation. This result in the activity levels of F+, F-, S+ and S- is outlined in Figure 3.15, below:

a 'switch' from discrimination to generalisation in a more biologically realistic representation of fear and safety neurons within the BLA.

Further to increasing inhibition, the 'generalisation' phenotype (i.e. high activity in F neurons regardless of CS type) was also observed in Model 1 when there was either a promotion and/or a lack of inhibition to F neurons by S neurons. With Model 2, we achieved a reduction in the inhibition of F neurons by removing the inhibitory connection from F- to F+. Here, we assumed the driving force ultimately resulting in fear behaviours would originate from the excitatory F+ neurons, rather than the inhibitory F- neurons. In addition to removing the inhibitory connection from F- to F+, we also removed the self-inhibiting connection from F+ to F+. The changes in connections in Model 2 are shown in Figure 3.16, below:
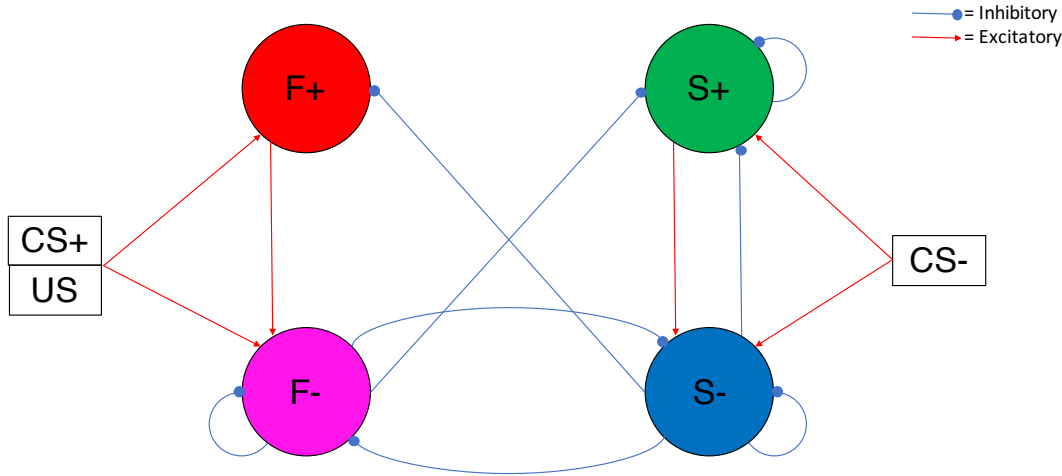
Figure 3.16. Changes in the connections of Model 2 to describe the 'generalisation' phenotype in activity output. Based on Model 1 and original connections detailed in Model 2 (Fig 3.13 above), we perturbed Model 2 to produce the 'generalisation' phenotype. This was achieved in two ways: **(A) Less inhibition of F+.** This was generated by removing the inhibitory connection from F- to F+ and removing the self-inhibitory connection from F+ to F+.

In this instance, a lack of inhibition of F+ resulted in initial 'discrimination' followed by a switch to 'generalisation' (Figure 3.17, below). Although there is a relative increase in F+ activity during CS+ presentations, and a relative reduction in this activity during CS- presentations, during both conditioning and retrieval, by the end of conditioning (and throughout retrieval) the activity of F+ has overtaken the activity of all other neural sub-populations. We interpreted this as initial discrimination, as during early conditioning there is high F+ activity during presentations of the CS+ and US, but low F+ activity during presentations of the CS- (in addition, there is still comparatively more activity in the S+ neurons, compared to F+ neurons, during presentations of the CS-). However, during late conditioning and retrieval, the activity of the F+ population remains comparatively higher than all other sub-populations. We interpreted this result to represent 'generalisation', as the dominant response generated during retrieval would be fear, regardless of the type of CS being presented.

Here, this is similar to the type of 'generalisation' we saw in Figure 3.10, where the activity of F neurons is higher than S neurons, regardless of CS type, but that the CS- did not appear to generate any promotion of activity in the F neurons. Indeed, the opposite appears to be true, wherein the activity of both the F+ and F- neurons have relatively lower levels of activity when the CS- is presented. Moreover, this result is again comparable to the behavioural pattern of initial discrimination followed by generalisation that we saw in females with

response, regardless of the type of CS presented.

We also observed the generalisation phenotype in Model 1 when F neurons were excited, instead of inhibited, by S neurons. Therefore, we decided to switch the sign of the FpFp weight (see Table 3.1; above) from negative (inhibitory) to positive (excitatory) in Model 2. This means that, instead of the F+ neurons being self-inhibitory (i.e. having an inhibitory connection from F+ to

F+), F+ neurons are self-excitatory (i.e. self-promoting). This change represents the comparative lack of inhibition and addition of excitation we saw in Model 1, where we changed the sign of the connection from S→F from inhibitory to excitatory. The change to this connection is shown in Figure 3.18:
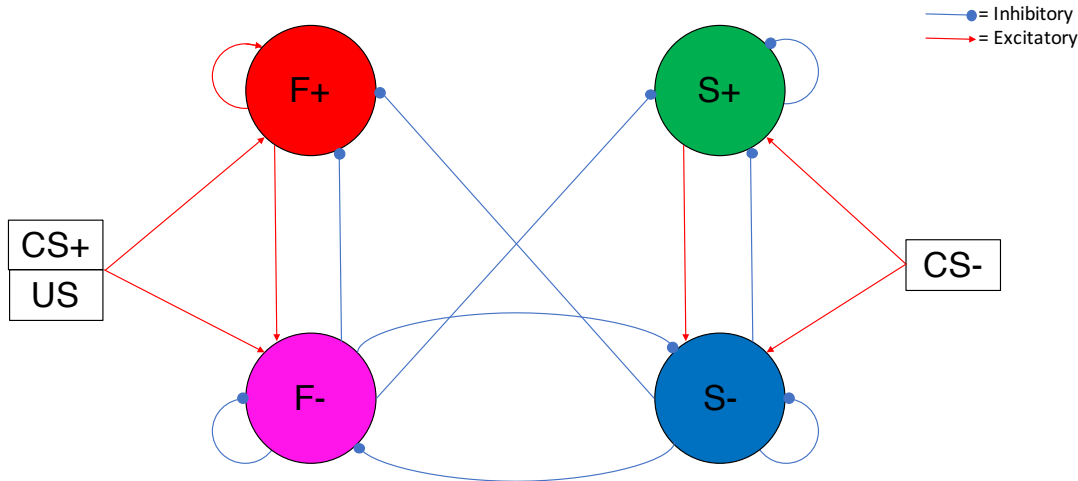
Figure 3.18. Changes in the connections of Model 2 to describe the 'generalisation' phenotype in activity output. (B) Excitation of F+. This was generated by reversing the sign of the self-inhibitory connection from F+, such that it became self-excitatory.

The activity of all neural sub-populations as a result of the perturbations to the connections of Model 2 (outlined in Figure 3.18, above) is presented in Figure 3.19, below:

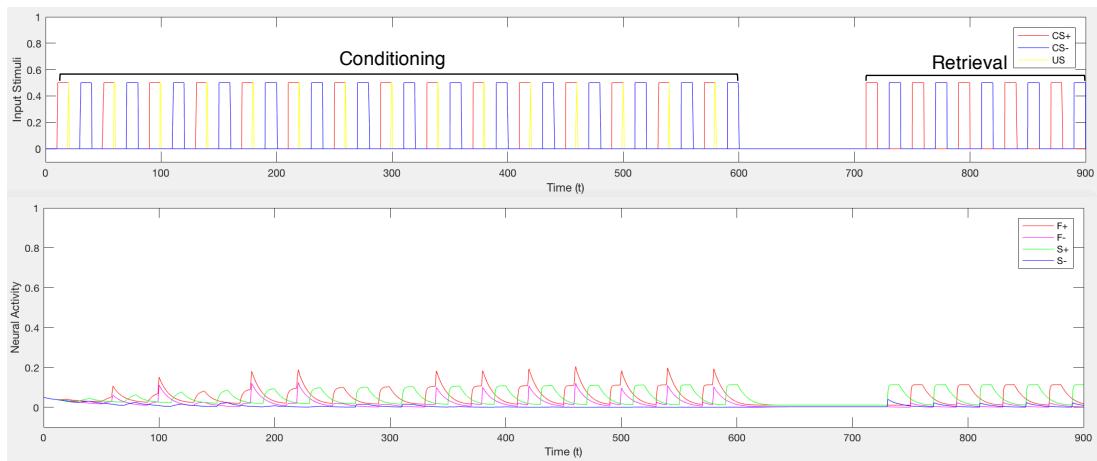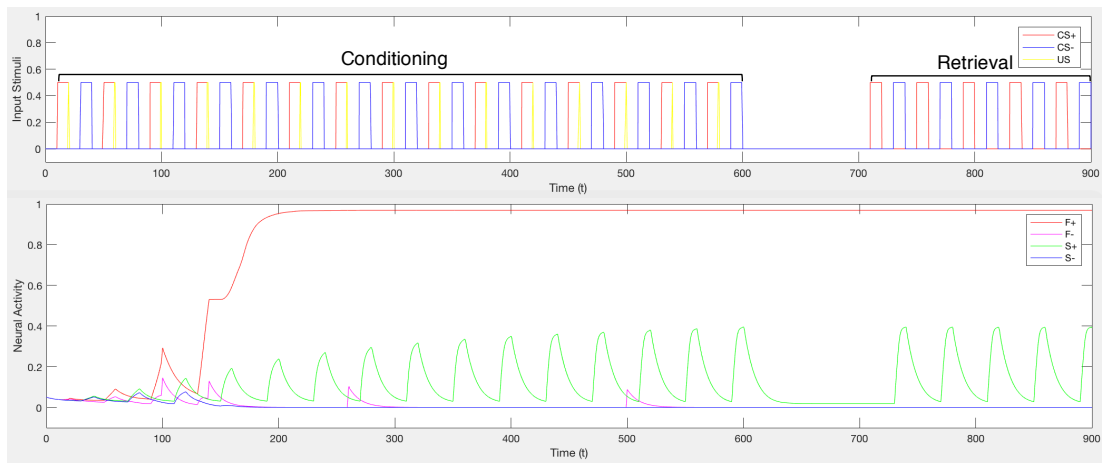**Figure 3.19. Evolution of the firing rates of fear (F+ F-) and safety (S+, S-) neurons during fear discrimination conditioning and retrieval in response to perturbations of Model 2. Excitation of F+ by reversing the wFpFp connection from inhibitory to excitatory also produces the 'generalisation' phenotype.** Activity of F+ (red), F- (magenta), S+ (green) and S- (blue) is shown (bottom panel) in response to the input stimuli of CS+ (red), CS- (blue) and US (yellow), (top panel). Here, feed-forward excitation of F+ produces large amounts of F+ activity, which remain high during conditioning and retrieval regardless of CS type, and even with no stimulus input.

Similar to what we observed in Model 1 when this change was made, we here observe a large, and rapid, increase in F+ activity in the early stages of conditioning. This increase in F+ activity then remains throughout the remainder of conditioning, does not reduce in the absence of stimulus input, and continues to remain high throughout retrieval. We also interpreted the results of this change in Model 2 to represent the 'generalisation' phenotype, although there does not seem to be as much initial discrimination activity compared to a relative reduction in F+ neurons without the additional excitatory promotion. Further, as the level of activity of the F+ neurons is at a peak throughout the majority of conditioning, the ITI and retrieval, it cannot be said that there is an additional promotion of F neurons as a result of the CS- presentations similar to the 'generalisation' phenotype observed in Figure 3.12

3.2.5 Model 3: Methods

By considering the results of Models 1 and 2, we also wanted to investigate the effect of additional excitation of F+ neurons without altering the levels of local inhibition within the BLA. This is because the BLA receives multiple inputs from other brain areas (Coplan & Lydiard, 1998), yet these inputs may or may not change the nature of the connections between F and S neurons. From this, we designed Model 3, wherein all the connections between F+, F-, S+ and S- are the same as the original iteration of Model 2 (Figure 3.13, above), with the addition of a PL input. This is detailed in Figure 3.20, below:
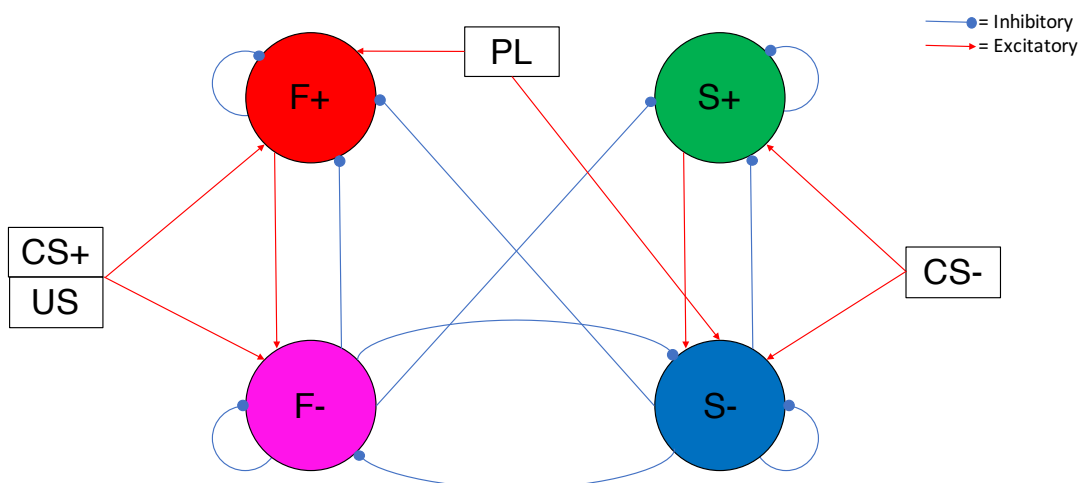
Figure 3.20. Model 3. Connections between excitatory and inhibitory 'fear' (F+, F-) and 'safety' (S+, S-) neural sub-populations in the BLA with additional external output from the PL. Based on Model 2 and experimental evidence, we hypothesised and modelled likely targets of the PL within the fear and safety BLA neural network. Here, we assumed that the PL would send excitatory projections to excitatory fear neurons (F+) and inhibitory safety neurons (S-).

Here we assumed that the PL would have excitatory connections to the F+ neural population in addition to the S- neural population. This assumption is based on the evidence that the PL and BLA are inter-connected (Sotres-Bayon et al. 2012; Choi et al., 2010), and that the PL sends primarily glutamatergic

(excitatory) projections to the BLA (Cheriyan et al., 2016). Further, there is considerable literature that implicates the PL region with the promotion of fear behaviours and the inhibition of extinction (Baeg et al., 2001; Rosenkranz et al., 2003; Vidal-Gonzalez et al. 2006; Burgos-Robles et al., 2009; Choi et al., 2010; Graham & Milad, 2011). Differences in PL activity have also been reported between males and females. Recently, there has been evidence to show that there is more theta and gamma activity present in the PL region in females during learned fear expression, compared to males (Fenton et al., 2014; 2016). Importantly, the PL has also been implicated in context-and cue-dependent fear discrimination (Kim et al., 2013; Piantadosi & Floresco, 2014).

3.2.6 Model 3: Results

By including the PL module in Model 3, we could modulate the activity of F+ and S+ without disturbing the inter-connective dynamics between F+, F-, S+ and S-. Initially, we added PL input to both F+ and S-. Here, levels of PL input were the same as the strengths of connections between F+, F-, S+ and S-. The resulting activity levels of F+, F-, S+ and S- from the addition of a PL input are described below:
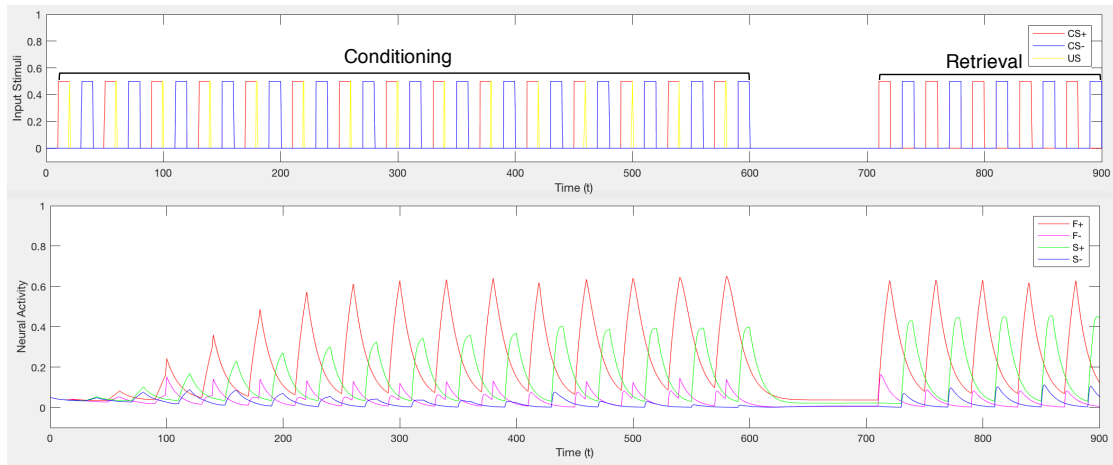
Figure 3.21. Evolution of the firing rates of fear (F+, F-) and safety (S+, S-) neurons from Model 3, which is the same neuronal network as in Model 2 but includes additional external input from the PL, during fear discrimination conditioning and retrieval. Low-level input from the PL still results in the 'discrimination' phenotype. Activity of F+ (red), F- (magenta), S+ (green) and S- (blue) is shown (bottom panel) in response to the input stimuli of CS+ (red), CS- (blue) and US (yellow), (top panel). Although there is more overall F+ activity, the activity levels of F-, S+ and S- do not greatly change compared to previous 'discrimination' phenotypes, meaning that F+ activity levels are kept low enough during presentations of the CS- to still resemble discrimination.

Initial input from the PL does appear to increase the activity of the F+ neurons, and slightly reduce the activity of S+ neurons, but not so much that the phenotype of 'discrimination' is lost. Instead, there are still relatively high levels of F+ activity during presentations of the CS+ and US during conditioning and CS+ during retrieval, but activity levels of F+ are lower than activity levels of S+ during presentations of the CS-. This means that a 'high fear' state would preside during presentations of the CS+, but that a 'low fear' state would preside during presentations of the CS- (i.e. discrimination).

As before, we wanted to perturb Model 3 to produce the 'generalisation' phenotype of high F activity regardless of CS type. In order to do this, we wanted to investigate the effects of additional excitation of F+ (and the resultant inhibition of S+). We therefore slightly increased the PL influence on F+ and S-

described above. The resultant activity levels in F+, F-, S+ and S- of increasing the influence of the PL on the BLA circuit are described in Figure 3.22, below:
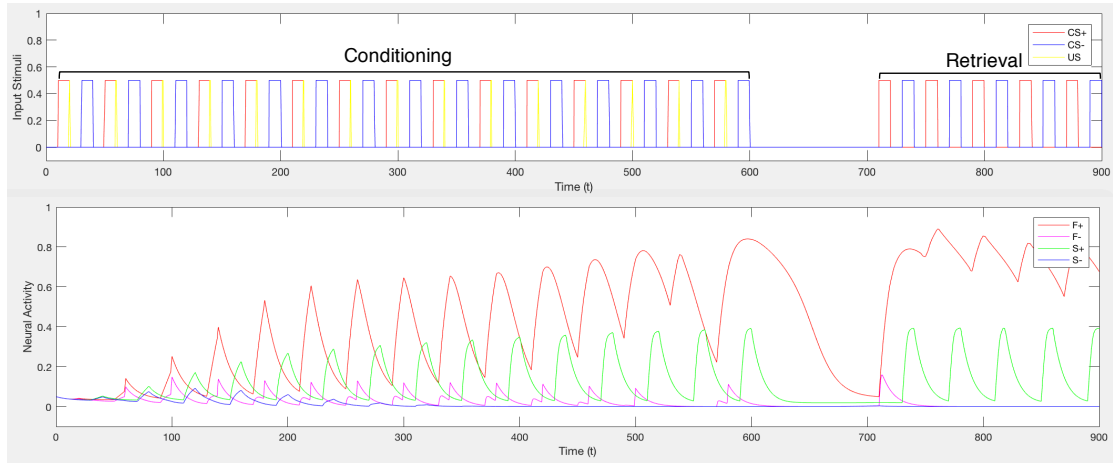
Figure 3.22. Evolution of the firing rates of fear (F+, F-) and safety (S+, S-) neurons from Model 3, which is the same neuronal network as in Model 2 but includes additional external input from the PL, during fear discrimination conditioning and retrieval. Increased input from the PL region results in the 'generalisation' phenotype. Activity of F+ (red), F- (magenta), S+ (green) and S- (blue) is shown (bottom panel) in response to the input stimuli of CS+ (red), CS- (blue) and US (yellow), (top panel). Again, there is discrimination at the start of conditioning, but activity of F+ neural population rapidly rises to become the dominant response. Although activity of F+ neurons does decrease to almost baseline levels with no stimulus input, and S+ neurons are still active during presentations of the CS-, activity in F+ neurons remains the dominant response during retrieval, regardless of stimulus input.

From this, we see initial 'discrimination' between the CS+ and CS- during the early stages of conditioning, where there is a relative increase in F neurons during the CS+ and a relative increase in S neurons during the CS-. However, with extended training, the activity of F+ neurons increases until it overtakes the activity levels of all other neural sub-populations. Even though there is a relative reduction in F+ activity when there is no stimulus input, F+ activity remains the dominant response during retrieval. This means that we see initial discrimination, followed by generalisation in Model 3 as a direct result of increased external influence from the PL, despite unchanged levels of local inhibition and excitation between the F+, F-, S+ and S- within the BLA circuit. Overall, Models 1, 2 and 3 have been shown to successfully produce

representations of both discriminatory and generalisation behaviour in BLA neurons in response to threat and safety cues, as well as showing similar phenotypes associated with both male and female behaviour described in Chapter 2.

3.3 Discussion

In the present chapter we have presented three computational models of fear and safety neurons in the BLA based on Wilson-Cowan oscillatory dynamics in order to create a potentially biologically plausible explanation for the neural network mechanisms underlying the behavioural results described in Chapter 2 (Wilson & Cowan, 1972; Herry et al., 2008; Destexhe & Sejnowski, 2009; Vlachos et al., 2011; Cowan et al., 2016). We initially presented Model 1, where 'fear' (F) and 'safety' (S) neurons received excitatory plastic inputs from the CS+, US and CS- during a representation of a fear discrimination and retrieval paradigm (based upon the experimental paradigm used in Chapter 2). Here, we modelled the dynamics of the F and S neurons similarly to the A and B neuronal populations described in Vlachos et al., (2011), where mutually inhibitory projections between fear and extinction neurons in BLA were modelled. In addition to receiving inputs from CS+, US and CS- inputs, F and S were also linked via mutually inhibitory connections, which additionally influenced the resultant activity levels of these two neural populations. Within Model 1 we represented both the 'discrimination' and the 'generalisation' phenotypes, similar to what we observed in male and female rats in Chapter 2 (Figures 3.8, 3.9, 3.10 and 3.12, above). Initially, we modelled BLA network

activity underlying the 'discrimination' phenotype, which we defined as high levels of F activity during presentations of the CS+ and US, and low F activity during presentations of the CS- during conditioning (and during presentations of the CS+ and CS- alone during retrieval), in addition to high levels of S activity during presentations of the CS-, and low levels of S activity during presentations of the CS+ and US during conditioning and retrieval. From this, we then increased mutual inhibition in the network by increasing the weight of inhibitory connections between F and S. This appeared to model network activity underlying the discrimination phenotype observed initially with limited training followed by the 'generalisation' phenotype observed with extended training in females. Here, the 'generalisation' phenotype was defined as relatively high F activity (i.e. higher than S activity) during retrieval, regardless of the CS type presented. In this instance, activity of S was suppressed whereas activity of F remained higher than baseline levels, regardless of which cue type was presented. We were also able to produce the 'generalisation' phenotype by increasing the activity of the F neurons by reversing the sign of the wSF weight (i.e. the connection from S→F) from inhibitory to excitatory (Figure 3.11, above). Here, we again saw a large increase in the activity of F neurons, which remained high regardless of the type of CS being presented, in addition to an apparent promotion of F+ activity during presentations of the CS- (Figure 3.12). In this instance, the activity of F was increased both by additional excitatory input and a relative lack of inhibition.

However, from the results generated from Model 1, we were unable to determine whether it was a relative increase in global inhibition of the F and S

neurons, a lack of inhibition, or an increase in excitation, of F neurons specifically, that contributed to the 'switch' from discrimination to generalisation. In order to investigate this further, we developed Model 2, which split the initially homogenous populations of F and S neurons into excitatory (F+, S+) and inhibitory (F-, S-) sub-populations (Figure 3.13, above). In Model 2, we assumed that the excitatory neurons would represent glutamatergic pyramidal neurons, whereas the inhibitory neurons would represent local GABAergic interneurons (Muller et al., 2006; Wolff et al., 2014; Capogna, 2014). Therefore, F+ and S+ neuronal sub-types were modelled to have excitatory connections, whereas F- and S- neuronal subtypes were modelled to have inhibitory connections. Here, we assumed that the F+ and S+ neurons would be the main force to drive excitation of either the CEm/l or ITC to model either a 'high fear' or 'low fear' behavioural output, respectively. Therefore, high F+ activity during the CS+, but not the CS-, and high S+ activity during the CS-, but not the CS+, would be interpreted as 'discrimination', whereas a high level of F+ activity (i.e. higher than the activities of all the other sub-populations) regardless of the type of CS presented would be interpreted as 'generalisation'.

From this, we increased global inhibition within the network by enhancing the weights of the inhibitory connections to emulate the increase in the mutual inhibition of F and S described in Model 1. When the global inhibition was increased in Model 2, however, we did not see the 'generalisation' phenotype as described in Model 1. Instead, we observed a retention of the 'discrimination' phenotype, albeit at comparatively lower activity levels (Figure 3.15).

Here, we can interpret that the 'switch' from discrimination to generalisation is unlikely to result from an increase in global inhibition within the BLA. This is supported by evidence demonstrating that inhibition plays a central role in gating synaptic plasticity in the BLA, and is reduced during fear conditioning (reviewed in Ehrlich et al., (2009); Szinyei et al., (2007)).

In addition to increasing global inhibition, we also reduced the inhibition of the F+ neurons specifically (Figure 3.16, above). By reducing the inhibition of these F+ neurons, we now observed the 'generalisation' phenotype (Figure 3.17, above). Here, we saw initial discrimination during the early stages of fear discrimination training, but this was rapidly followed by an increase in the activity rate of the F+ neurons until F+ neural activity was the dominant response, regardless of CS input. This result was similar to the 'generalisation' phenotype we observed in Model 1 (Figure 3.10), wherein the activity of F was high regardless of CS input type but was not additionally promoted by the CS-. Indeed, the relative activity of the F neurons in Figure 3,17 appeared to be reduced during presentations of the CS-.

In line with Model 1, we also increased the relative excitation of F+ neurons by reversing the sign of the wFpFp connection (Table 3.1) from negative to positive. This means that F+ now generated reciprocal excitation, rather than reciprocal inhibition. Perhaps unsurprisingly, this change also caused a rapid generation of the 'generalisation' phenotype, with F+ neural activity showing a large increase early in the conditioning period, which then remained high until and including retrieval, even when there was no stimulus input. Here again this result was similar to the 'generalisation' phenotype we

observed in Model 1 (Figure 3.10), wherein the activity of F was high regardless of CS input type but, as the activity of F neurons was at a peak throughout the majority of conditioning, the ITI and retrieval, it cannot be said that these F neurons were additionally promoted by the CS-.

Taken together, these results are in line with the literature, wherein a reduction in GABA signalling (i.e. less inhibition) in the BLA has been linked to fear generalisation (Shaban et al., 2006; Bergado-Acosta et al., 2008; Sangha et al., 2009; Lange et al., 2014). Interestingly, there is also evidence to support that there may be less GABA signalling in females (Milad et al., 2009; Cholanian et al., 2014; Fernandez de Velasco et al., 2015; Möller et al., 2016). Therefore, the switch from discrimination to generalisation observed in females (Chapter 2), and the reduction in inhibition in Model 2 (this chapter), may be in part due to a difference in local levels of GABA signalling in the BLA of males and females.

To further model the external regulation of BLA neurons, we added the outside influence of the PL to act upon both fear and safety neurons in the BLA (Model 3, Figure 3.20). Here, we assumed that the PL would have primarily excitatory connections to the fear pyramidal neurons (i.e. F+) and safety interneurons (i.e. S-). This is due to the involvement of the PL in both the promotion of fear expression and the inhibition of extinction (Baeg et al., 2001; Rosenkranz et al., 2003; Vidal-Gonzalez et al. 2006; Laurent & Westbrook, 2009; Burgos-Robles et al., 2009; Choi et al., 2010; Graham & Milad, 2011; Fenton et al., 2014, 2016) and that the PL has primarily glutamatergic

projections to the BLA (Choi et al., 2010; Sotres-Bayon et al. 2012; Cheriyan et al., 2016).

From this, we observed that comparatively low levels of PL input (representative of its normal function) did not perturb the 'discrimination' phenotype, although there were comparatively higher levels of F+ activity, and lower levels of S+ activity, generated overall (Figure 3.21). However, when PL input was increased (representative of an 'over-active' PL), we again observed the 'switch' from the 'discrimination' to the 'generalisation' phenotype (Figure 3.22), even when there is no direct reduction in the local inhibition of fear neurons in the BLA. Similar effects of persistent PL activity have been observed previously in females which failed to successfully extinguish their fear, in comparison to males (Fenton et al., 2014, 2016). From Model 3, we can hypothesise that the 'switch' from discrimination to generalisation may also, in part, be mediated by regulation of the 'fear' and 'safety' neuronal network in the BLA by additional brain regions, such as the PL. In summary, we hypothesised that generalisation may involve either a lack of local inhibition in fear neurons in the BLA, and/or an over-active PL (i.e. PL excitation of F+ and S-).

Overall, these results provide a novel representation of fear discrimination learning and retrieval in a computational framework. Although we started by modelling a specific fear discrimination paradigm based on our behavioural results (Chapter 2), this chapter has presented three models which are able to describe a biologically plausible framework for the neural architecture within the BLA, which could be used to make predictions on which to base future work (Sah et al., 2003). From these results, we have been able

to model both 'discrimination' and 'generalisation' phenotypes resulting from changes made to connections between fear and safety neurons within the BLA. In addition, we have made several relevant observations on which we have based hypotheses as to how discrimination and generalisation can occur in response to different perturbations of the fear and safety neuronal network in the BLA, including the consideration of altered inhibition mediated by relative GABA levels and the influence from other brain regions, such as the mPFC.

From these models it is important to consider the relevant outcomes of the results produced. For example, although we were able to produce phenotypes of both 'discrimination' and 'generalisation', we did observe subtly different patterns in the 'generalisation' result. In some cases (e.g. Figures 3.10, 3.17, 3.19 and 3.22) the activity of F neurons throughout the majority of conditioning and retrieval was higher than the activity of S neurons, regardless of CS input type. Here, although the activity of F neurons was high, there did not appear to be a distinct promotion of their activity by the CS-. However, in the case of Figure 3.12 the activity of F neurons was high regardless of CS type, but there appears to be an additional small promotion or activation of F neurons by the safety cue. Both of these instances were still considered 'generalisation', as the activity of F neurons was relatively higher than S neurons, regardless of CS type input, but each iteration could potentially signify a subtly different neurobiological process.

Overall, it is more likely that the type of 'generalisation' observed in Figure 3.12 is a result of large changes in model structure prior to being run, rather than a reflection of a potential neurobiological change. Figure 3.12 was

produced from reversing the sign of S→F from negative to positive, which increased the excitation of F and simultaneously reduced the relative inhibition of F. In biological terms, this means that the 'safety' neurons would have switched from inhibitory GABAergic neurons to excitatory glutamatergic neurons, which would not occur in adult rats *in vivo*. Further, this pattern of generalisation occurs only once out of all the iterations of models described throughout this chapter, and only occurs with the most dramatic change to the underlying model connections, in the simplest model (Model 1).

It is more likely that the pattern of 'generalisation' seen in Figures 3.10, 3.17, 3.19 and 3.22 is of relative importance to the behaviour observed in Chapter 2. Here, this pattern of 'generalisation' was produced from more subtle changes in the dynamics of Model 2, where both excitatory and inhibitory subpopulations of F and S were considered, and in Model 3, where the PL was also considered. This meant that no neuronal group switched function from inhibitory to excitatory and, perhaps consequently, that pattern of 'generalisation' was no longer subsequently observed.

Further to this, it could be argued that the iteration of Model 2 which produced Figure 3.17 (as shown by Figure 3.16), was the most 'successful' at demonstrating the process of generalisation seen in females with extended training in Chapter 2. Here, there is an initial discrimination between the CS+ and CS-, as shown by high F+ activity, but low S+ activity, during presentations of the CS+, as well as low F+ activity, but high S+ activity, during presentations of the CS-. Upon extended training however, the activity of F+ soon becomes the dominant response, regardless of the type of CS presented. Further to this,

the S neurons still fire in response to presentations of the CS-, meaning that they haven't necessarily changed or lost function, but are 'drowned out' by the relative increase in F+ activity. Similarly, the activity of the F+ neurons still appears to be inhibited by presentations of the CS-, but not to such a degree that their activity is overtaken by the S neurons to produce discrimination. Both the 'fear' and 'safety' neurons are performing similarly to how they perform when the 'discrimination' phenotype is produced, yet there is enough of a reduction in the inhibition of the 'fear' neurons to generate the 'discrimination' phenotype.

By looking at the retrieval phase of Figure 3.17 specifically, it appears that the activity of each subgroup of fear and safety neurons is in a fine balance. Here, a slight increase in the amount of inhibition of the F+ neurons, say by having slightly more GABA in the system (as males may have), could produce discrimination instead of generalisation, whereas lower overall GABA levels (which females may have) would maintain the 'generalisation' phenotype (Milad et al., 2009; Cholanian et al., 2014; Fernandez de Velasco et al., 2015; Möller et al., 2016). This iteration of Model 2 therefore provides an arguably excellent platform to conceive a potential biological mechanism for the 'switch' from discrimination to generalisation. Further, Model 2 may be slightly more biologically relevant than Model 3, as here we did not include the IL as a modulator of the PL and/or the 'fear' and 'safety' neurons of the BLA. Without this important component, Model 3 may not be as realised as Model 2, and may therefore not provide the most useful basis for forthcoming predictions.

Although certain iterations of Model 2 may be slightly more biologically relevant to *in vivo* behaviour, information produced from all three models has helped to provide a potential biological explanation for a cue-dependent instruction to downstream structures, such as the CEm or the ITC, to enable the switch of behavioural states from high to low fear during CS+ and CS- presentation, respectively.

Chapter 4. Sex Differences in *In vivo* Electrophysiology

4.1 Introduction

As discussed above (Chapter 1), LFPs are generated from the summated EPSPs and IPSPs arising from the synchronised excitation of large groups of neurons. As such, LFPs can be used as a measure of brain activity in areas known to be involved in the learning, consolidation and retrieval of fear memories, including the mPFC, hippocampus, and amygdala (Giustino & Maren, 2015). As well as neuronal activity, it is also important to consider functional connectivity between these inter-connected regions, as fear memory processing involves functional interactions in the mPFC-HIPP-BLA circuit. This functional connectivity can be inferred via measuring the synchronisation of activity between brain regions over different frequency ranges. Oscillations can synchronise activity within multiple brain regions, forming large-scale brain networks that allow for the functional integration of distributed information (Bartos et al., 2007).

In general, high-frequency brain activity (e.g. gamma oscillations; 30-120Hz) reflects higher-level processing in local domains of the cortex and will be discussed further below, whereas lower-frequency brain activity (e.g. theta oscillations; 4-12Hz) is typically used to entrain synchronised activity across distributed brain regions. Both high and low frequency oscillations can be generated by and modified in response to external (e.g. a CS) and internal (e.g. input from another brain region) stimuli (Buzsaki & Draguhn, 2004; Watson et al., 2016; Pevzner et al., 2016).

4.1.1 Theta Oscillations

Oscillations in the theta frequency range were first isolated in the dorsal hippocampus (reviewed in Likhtik & Gordon, 2014), where they have been linked to learning and memory retrieval. In this region, theta oscillations are thought to allow the occurrence of Hebbian plasticity to take place, meaning that they are an integral part of the induction of LTP, as well as organising neural coding for memory formation and spatial navigation (Lisman & Jensen, 2013). In humans, oscillations within this frequency range have been shown to be positively associated with the induction of synaptic plasticity as well as memory retrieval. For example, the strength of certain memories in humans is predicted by how tightly co-ordinated the spike timing of single neurons is to local theta oscillations (Rutishauser et al., 2010).

In addition to the hippocampus, theta oscillations are found in multiple structures throughout the brain, including the mPFC and amygdala (Buzsáki, 2002). For example, increased synchronisation within the theta-frequency range between the ventral hippocampus and the mPFC was observed during anxiety, wherein the firing of mPFC neurons became more phase-locked to ventral hippocampal theta input as anxiety levels increased (Adhikari et al., 2011). Further, pyramidal cells of the BLA can intrinsically resonate at the theta frequency, generating prominent theta oscillations (Pape & Driesang, 1998). In addition to this, the LA has been shown to display increased theta frequency oscillations and synchronous activity (i.e. coherence) with the DH during subsequent presentations of previously fear-conditioned stimuli (Seidenbecher et al., 2003). Coherence is defined as a measure of neural synchrony to

determine how similar oscillations in different brain regions are to one another (Halliday et al., 1995), from the two signals having no relationship (i.e. completely asynchronous) to the two signals being identical at a particular frequency (Stevenson et al., 2007). In addition to hippocampus-mPFC and hippocampus-amygdala interactions, synchronisation between the mPFC and amygdala is also involved in fear memory consolidation and retrieval. For example, bi-directional changes in the coherence of theta oscillations between these areas during paradoxical sleep correlate with inter-individual variability in fear memory consolidation in rats (Popa et al., 2010). In this study, rats with increased theta coherence between the amygdala and mPFC showed a corresponding increase in conditioned fear responding during later retrieval testing, whereas the opposite was true for rats which showed decreased theta coherence between these structures. Further, Courtin et al., (2014a) have shown that fear expression is causally related to the phasic inhibition of prefrontal parvalbumin interneurons (PVINs) in mice. Inhibition of PVIN activity disinhibits prefrontal projection neurons and synchronises their firing by resetting local theta oscillations, leading to fear expression. Taken together, these results demonstrate a key role for theta synchrony in mediating functional interactions between these regions underlying fear and fear memory processing.

In addition to fear conditioning, theta oscillations in, and theta coherence between, the mPFC and LA have been implicated in fear extinction. For example, Lesting et al. (2011) found that theta coupling increased between these areas during retrieval of conditioned fear, yet showed a significant

decrease during extinction learning. Interestingly, theta coupling between the LA and mPFC partially rebounded during extinction recall, and conditioned fear and extinction recall could be modulated by interfering with theta coupling through local electrical micro-stimulation in a theta phase-dependent manner. Further, an additional study by Lesting et al., (2013) makes an intriguing link between theta coupling of the mPFC to the different types of neurons in the amygdala which appear to be differentially linked to fear memory expression or extinction memory/fear inhibition (Herry et al., 2008;Chapter 1). Here, when the CS evoked no fear during successful extinction recall, activity in the mPFC-amygdala circuit was characterized by mPFC→amygdala directionality as indicated by mPFC spike firing temporally leading LA theta oscillations. They hypothesised that, during extinction recall, theta coupling may functionally connect the relevant populations of 'extinction' neurons in the amygdala with the IL, a region known to be integral to the extinction process (Sierra-Mercado et al., 2011).

Studies are also now considering theta activity separately in the PL and IL. A study by Fenton et al., (2014) showed that males display a significant decrease in PL theta activity during late compared to early extinction. Conversely, male IL activity was significantly increased during late compared to early extinction. Males were also shown to have successful extinction recall (i.e. low freezing). In contrast, females displayed increased theta activity in the PL during late relative to early extinction in addition to increased IL activity during late relative to early extinction recall. Further, females showed more learned fear expression during extinction and its recall compared to males.

Contrary to the IL, the PL is involved in the expression of conditioned fear and potentially the inhibition of extinction (Vidal-Gonzalez et al., 2006; Sierra-Mercado et al., 2011). From these observations, theta oscillations are likely to participate in shifting the balance between the relative expression or inhibition of fear after conditioning and/or extinction, in turn promoting or inhibiting corresponding fear behaviours, such as freezing.

More recently, there has been compelling evidence to indicate that prefrontal inputs to the amygdala use theta frequency oscillations and coherence as a mechanism for communicating not only about fear and anxiety, but about safety. It appears that the relationship between the mPFC and BLA is of importance to the behavioural 'switch' between successful discrimination or generalisation between cues that signal threat (CS+) or safety (CS-). For example, Likhtik et al. (2014) recorded activity from the mPFC, hippocampus and BLA during CS+ and CS- stimuli. Although no link was found between hipp-BLA or hipp-mPFC, or VH/DH power, it was found that (in 'discriminators') neuronal firing in the BLA only becomes entrained to incoming mPFC theta when mice are presented with the CS- or when they are in the relatively safe periphery of an open field. This means that activity in the mPFC and BLA is more synchronous when mice respond to a learned safety signal or show an inhibition of innate fear in a relatively safe environment. Indeed, as the communication is directional (mPFC → BLA), these results support the notion of an inhibitory influence from the mPFC on the BLA that regulates behavioural fear responding appropriately.

4.1.2 Gamma Oscillations

Compared to theta oscillations, there has been relatively little research investigating the potential role of gamma oscillations in anxiety, fear learning and retrieval, and extinction. Gamma oscillations are generated by the synchronous firing of fast-spiking inhibitory interneurons (Puig et al., 2008), and are involved in long-term (episodic) memory (Nyhus & Curran, 2010), visual awareness, rapid eye movement during sleep and anaesthesia (Vanderwolf, 2000), attention and cognitive task performance (Tallon-Baudry et al., 1999), which all reflect higher-level processing (Hughes et al., 2008). In a recent study, Courtin et al. (2014b) found that gamma oscillations in the BLA are enhanced following fear conditioning. Interestingly, a predictive relationship was found between variations in the strength of gamma power within the BLA between the early and late stages of extinction and the level of post-extinction spontaneous fear recovery. These data suggest that maintenance of gamma oscillations in the BLA during extinction learning is a strong indicator of long-term spontaneous fear recovery. In addition, significantly more gamma power was found in the PL of an extinction-deficient mouse strain compared to control mice. The extinction-deficient mouse strain also showed exaggerated single-unit firing in the IL region compared to control mice, potentially reflecting a (failed) over-compensation of the IL to control fear-promoting activity in other regions, such as the PL or BLA (Fitzgerald et al., 2014b). In humans, only extinguished (compared to non-extinguished) stimuli evoked a relative increase in vmPFC-localised gamma power. Moreover, individuals who failed to show a suppressed skin conductance response to the extinguished versus non-

extinguished stimuli also failed to show the otherwise observed alterations in vmPFC gamma power to the extinguished stimulus (Mueller et al., 2014).

Gamma oscillations have also been coupled to theta oscillations in the mPFC-BLA network (reviewed in Harris & Gordon, (2015)) One of the more recent studies by Stujenske et al., (2014) builds upon research by Likhtik et al., (2014) described above. Here, it was discovered that there were two distinct bands of gamma oscillations present in the BLA: slow (40-70 Hz) and fast (70-120 Hz). Each gamma band was also found to be coupled to distinct phases of the theta cycle, reflecting cross-frequency coupling in that area. Cross-frequency coupling occurs when the phase of one frequency is linked to the amplitude of another (i.e. phase-amplitude coupling (PAC) (Terada et al., 2013)). For example, the phase of theta oscillations biases the amplitude of the gamma waves (reviewed in Belluscio et al., (2012)). In addition to this, Stujenske et al., (2014) found that BLA fast gamma power was suppressed, yet local BLA theta to fast gamma-coupling was shown to be enhanced, during periods of fear relative to periods of safety. During periods of relative safety, however, BLA fast gamma power was increased and shown to be entrained to mPFC theta oscillations.

Importantly, there is a distinct lack of research detailing the potential sex differences in neural activity which may underlie the distinct and opposing patterns of behaviour observed during the retrieval of cued fear and safety memories outlined in (Chapter 2). There is evidence to suggest sex differences in gamma oscillations in the mPFC in relation to extinction training and its subsequent recall (Fenton et al., 2016). In this study, they showed that females

displayed enhanced learned fear expression, compared to males, which was linked to elevated levels of gamma activity in the PL. Further, females also showed impaired extinction retrieval compared to males, which in turn was linked to reduced levels of gamma activity in the IL. However, there is little research investigating activity in and synchrony between the PL, IL and BLA in cued fear and safety learning and retrieval. For example, although Stujenske et al., (2014) examined activity in both the gamma and theta frequency ranges during recordings of neural activity from the BLA, hippocampus and mPFC during discriminatory fear conditioning, extinction, and exposure to an open field, they did not specify any distinction of separate areas of the mPFC.

4.1.3 Objectives

The present study aims to investigate sex differences in PL-IL-BLA oscillations and synchronisation underlying the fear discrimination and generalisation phenotypes seen in males and females, respectively, with extended discrimination training reported in Chapter 2. To do this, we used *in vivo* electrophysiology to record LFPs simultaneously from the IL, PL, and BLA in male and female rats during the retrieval of auditory fear discrimination after a three-day training paradigm. Our primary aim was to determine any potential sex differences in PL-IL-BLA circuit function which may underpin the behavioural differences observed between males and females in Chapter 2. We investigated the differences in LFP power and coherence of frequencies in the theta (4-12 Hz) and gamma (30-120 Hz) ranges in the PL, IL and BLA during retrieval of the CS+ and CS-. Overall, we aim to investigate how theta and

gamma LFP activity in the PL, IL and BLA in generalisers (females) differs from their discriminator (male) counterparts. We hypothesise that our study may show differences in PL activity in the theta and gamma ranges in females compared to males, as similar observations have been seen in females during fear extinction (Fenton et al. 2014b, 2016). In addition, the PL has also been implicated in discriminative reward seeking, as well as fear discrimination (Sangha et al., 2013; 2014). Further, as the IL is involved in the recall of extinction learning (Quirk et al., 2000; Do-Monte et al., 2015), we hypothesise that this region may also be specifically activated by the CS- during discrimination retrieval. Finally, we aim to replicate the results discussed by Stujenske et al., (2014), wherein gamma power in the BLA was suppressed or increased with regards to periods of relative threat or safety in male mice. Importantly, we aim to build upon the data produced from Stujenske et al., (2014) by investigating how activity in the PL, IL and BLA changes in a discrimination paradigm in females.

4.2 Materials and Methods

4.2.1 Animals

We surgically implanted recording electrodes into the PL and IL cortices of the mPFC and the BLA of young adult male and naturally cycling female Lister hooded rats (Charles River, UK) prior to behavioural testing. Rats weighed between 200 to 325g prior to surgery and were group housed according to sex on a 12 hr light/dark cycle (lights on at 7am), with a room temperature of ~22°C

and free access to food and water. All experimental procedures were conducted during the animals' light cycle and with internal ethical approval and in accordance with the Animals (Scientific Procedures) Act 1986, UK.

4.2.2 Surgical Procedure

Animals were administered pre-operative analgesia (buprenorphine) then induced into anaesthesia via 3.5% isoflurane in medical air and maintained at ~2% during surgery. Throughout the surgical procedure rats were secured in a stereotaxic frame (World Precision Instruments) and held in place with blunt ear and incisor bars, adjusted accordingly to ensure the skull was kept horizontal. Rat body temperature was maintained at approximately 37°C using a homoeothermic heating blanket (Harvard Apparatus Ltd, UK). Once a complete lack of withdrawal of the hind paw reflex had been confirmed, an initial incision was made in the scalp to expose the skull and 4-6 metal screws were inserted to secure the implanted electrodes to the skull. Small holes (~2mm in diameter) were created over the right mPFC and BLA to expose the dura mater, which was then removed. Prior to electrode insertion, all exposed areas of cortex were kept moist using sterile 0.9% sodium chloride solution. An eight-wire multi-electrode array (NBLabs; Teflon-coated stainless-steel wires, 50 μm diameter, four wires 1 mm longer than the other four) was implanted into the PL and IL (2.5 mm anterior and 0.5 mm lateral to Bregma, and 3.1 mm and 4.1 mm ventral to the brain surface for the PL and IL, respectively). Another eight-wire multi-electrode array (as above except all eight wires were identical in length and constrained to a single bundle) was inserted into the BLA (2.8 mm posterior

and 4.7 mm lateral to Bregma, 7.4 mm ventral to the brain surface). Once lowered to the appropriate depth the electrodes were given time (~15min) to acclimatise to the tissue environment. We recorded activity during surgery to ensure that the LFPs observed were characteristic of activity previously reported in mPFC and BLA under anaesthesia (Stevenson et al., 2007), before cementing MEAs in place using dental cement. On the day of surgery rats received post-operative analgesia (meloxicam). Immediately after surgery, animals were singly housed overnight and then pair- or group-housed during recovery prior to behavioural testing. During the recovery period immediately after surgery (~2-3 days), rats also received post-operative analgesia (buprenorphine and meloxicam).

4.2.3 Behavioural Testing and LFP Recording

Between 10-14 days after electrode implantation, we examined sex differences in behaviour during auditory fear discrimination and retrieval as described previously (Chapter 2). Male and female rats underwent one day of habituation, followed by three days of discrimination training, with discrimination retrieval on day five. During discrimination retrieval, all rats received five presentations each of the CS+ and CS− in context B to test discrimination retrieval. This is an increase from the two presentations each of the CS+ and CS- presented in (Chapter 2) to provide additional data for subsequent LFP analysis.

4.2.4 Behavioural Data Analysis

As before (Chapter 2), freezing was used as the behavioural index of conditioned fear and scored manually during the first 2 minutes of retrieval to determine contextual fear and during each 30s CS. Sex differences were then analysed using two-way ANOVA, with sex and cue type as between-subject factors. Here, CS+ vs CS- was analysed with a 2-way ANOVA and contextual fear was analysed separately with a *t*-test (see Chapter 2 for further details). All data are presented as the mean plus the standard error of the mean. The level of significance for all comparisons was set at $P < 0.05$.

4.2.5 LFP Recording

LFPs were recorded from the implanted electrodes in PL, IL and BLA during discrimination retrieval testing, where an event marker was used to indicate the beginning of each session and each CS+ and CS- presented. The implanted electrodes were connected by a unity-gain multichannel headstage (HTS/8m-G1) to a cable and a commutator to a preamplifier linked to a Recorder system (all Plexon Inc.). LFPs were band-pass filtered at 0.7–170 Hz and then digitized at 1 kHz. Post-recording, one representative channel from each area of the PL, IL and BLA was selected from each rat for further analysis. Each selected channel was chosen based on minimising noise artefacts. Initially, the raw LFP traces were band-pass filtered at ~50Hz and high-pass filtered at 4Hz to remove interference from electrical mains and LFP activity below frequencies of interest. Further to LFP data, we also attempted to record extracellular action potential unit spikes. Unfortunately, even though unit spiking was observed

during surgery under anaesthesia, we could not detect reliable spiking activity during behavioural testing 10-14 days post-implantation. This was most likely due to microglial repair and tissue deposition in the perimeter of neurons surrounding the electrode shaft, which has been previously reported to reduce the number of high-amplitude spikes seen during chronic implantation (reviewed in Scott et al., (2012)).

4.2.6 Histology

After completing the experiments, all rats were deeply anesthetised with sodium pentobarbital. Current (0.1 mA) was passed for 7-10s through a random pair of recording electrodes in the PL, IL and BLA using an electrical stimulator (Grass Technologies, USA) to deposit ferric ions at the electrode tip sites. Rats were then transcardially perfused with 0.9% saline followed by a mix of 4% paraformaldehyde (PFA) containing 4% potassium ferrocyanide (Sigma, UK) to mark the recording sites in PL, IL and BLA via a Prussian blue reaction (Green, 1958), (Figure 4.2). Brains were then removed and stored at 4°C for a minimum period of 48hrs in the same 4% PFA / 4% potassium ferrocyanide solution used for perfusion. To confirm electrode placements in the PL, IL, and BLA, brains were sliced into sections between 80-200μm using either a vibratome or microtome. Brain slices were stained for acetylcholinesterase to delineate the basal nucleus of the amygdala (Stevenson et al., 2007) and placements in the PL, IL and BLA were determined using the rat brain atlas (Paxinos and Watson, 1998). Example slices demonstrating electrode placements within these brain

regions are shown in Figure 4.2, below. Only rats with confirmed histology were included in the LFP analysis.

4.2.7 LFP Data Analysis

Filtered LFPs from each rat were examined by a trained observer and individual trials with large noise artefacts were manually removed. All representative LFPs from each region were grouped separately in males and females and then averaged over combined trials of either CS+ or CS-. We initially focused our analyses on the inter-group differences to the two tones (i.e. CS+ vs CS-) and then expanded our examinations of LFP activity to qualitative between-group (i.e. sex) differences. Resultant LFP signals were analysed to determine changes in multiple frequency domains using continuous wavelet transformations with Morlet wavelets and multi-taper spectral analysis. Both Morlet transformations and multi-taper spectral analysis were conducted using custom MATLAB scripts (Mathworks, MA, USA; Halliday, 1995; Fenton et al., 2013) to generate spectral estimates of oscillatory activity (i.e. power) in and coherence between the PL, IL and BLA during fear discrimination retrieval. Morlet wavelets were first used to produce LFP colour plots for the pooled CS+ and CS- for each sex. These were visually examined to characterise any qualitative inter-group differences seen during CS+ in comparison to CS-, which were then analysed quantitatively using multi-taper analysis.

4.2.8 Power

For power analyses using Morlet wavelet transformations, colour spectra of the averaged LFPs (i.e. taken from the five CS+ and CS- presentations during discrimination retrieval) were initially generated between 1-150 Hz. Wavelet transformations use a wave-like scalable function that is well-localised in both time and frequency, meaning that multiple frequency bands can be examined over a specified time period (reviewed in Le Van Quyen & Bragin, 2007). In this instance, by contracting the wavelet function, it is possible to increase the depth of focus, from coarser (e.g. low-frequency; theta) to finer (e.g. high-frequency; gamma) signal structures (Oren et al., 2006).

Initially, the LFP signal was low-pass filtered (at 4 Hz), then extracted and decomposed into segments according to distinct frequency bands to produce estimates of how LFP power in the PL, IL and BLA regions changed dynamically over the 30 second time windows for either CS+ or CS-. This was conducted separately for males and females, wherein CS+ and CS- presentations could be analysed within each sex. Given the recently established role of mPFC and BLA theta and gamma oscillations in mediating fear discrimination (Likhtik et al., 2014; Stujenske et al., 2014), we focused our analysis on frequencies between 4 and 120 Hz. For multi-taper analyses, the same averaged LFPs used for the Morlet transformations were initially split into segments of equal length across each 30 second CS for each animal, with multi-taper windows applied to each segment. Multi-taper windows are applied to each segment to obtain a spectral estimate of frequencies across a time series without a loss of information (Percival & Walden, 1993). The number of

tapers was determined as the integer, *K*, nearest to the value 2*NW*-1 (where *NW* equals the time-bandwidth product (Percival & Walden, 1993; Cox, 1996; Fenton et al., 2013)). Pooled spectra for each group of either male or female animals were generated by taking *K* for each segment, which was then averaged across segments and animals using multitaper windows. This analysis produced estimates of LFP power in the PL, IL and BLA at 4-120 Hz, where CS+ and CS- presentations could again be analysed separately within each sex. Differences in LFP power during CS+ in comparison to CS- were determined using the log ratio difference of spectra test (Diggle, 1990; Halliday, 1995) and quantified statistically using 95% confidence intervals (Fenton et al., 2014a, 2014b, 2016; Stevenson et al., 2007).

4.2.9 Coherence

To produce estimates of wavelet coherence, Morlet transformations were again used over the time-frequency domain of the averaged CS+ or CS- LFPs for each sex. This analysis was performed using custom MATLAB scripts (Rosenberg et al., 1998; Amjad et al., 1997; Fenton et al., 2013; Halliday, 2015; Halliday et al., 2016). Coherence was determined for each pair of regions (PL-BLA, IL-BLA and PL-IL) and was then compared between CS type separately for males and females. Multi-taper spectrograms were then calculated across multiple frequency domains to quantify the relative levels of coherence between the PL-BLA, IL-BLA and PL-IL during either the CS+ or CS- for each sex. Initially, coherence between each pair of regions was calculated as a value from 0 to 1, wherein a value of zero indicates no coherence and a value of one

indicates perfect coherence at a particular frequency (Halliday et al., 1995; Stevenson et al., 2007). Differences in LFP coherence between PL, IL and BLA during CS+ in comparison to CS- for each sex were determined using the comparison of coherence test (Rosenberg et al., 1989) and 95% confidence intervals (Fenton et al., 2014a, 2014b, 2016; Stevenson et al., 2007).

4.3 Results

4.3.1 Behaviour

Freezing in response to CS+ and CS- presentations during fear discrimination retrieval is shown in Figure 4.1. The two-way ANOVA revealed a significant main effect of CS type ($F_{(1,29)}$ = 30.89, P = 0.0001) and a significant Sex × CS type interaction ($F_{(1,29)}$ = 7.334, P = 0.0112) but no main effect of sex ($F_{(1,29)}$ = 2.223, P = 0.1467). Post-hoc analysis indicated that males (n = 18) showed significantly increased freezing during CS+ compared to CS- presentations (****P < 0.0001), while females (n = 13) showed no such difference (P > 0.05). In line with the results shown in Chapter 2, these results again replicate discrimination in males and generalisation in females resulting from extended fear discrimination training. Freezing before CS+ and CS- presentations during fear discrimination retrieval testing is also shown in Figure 4.1, below. Although males did show more freezing than females, this did not reach significance ($t_{(18)}$ = 1.72, P = 0.0964). Again, in line with the results presented in (Chapter 2), we found no sex differences in contextual fear before testing auditory fear discrimination retrieval.
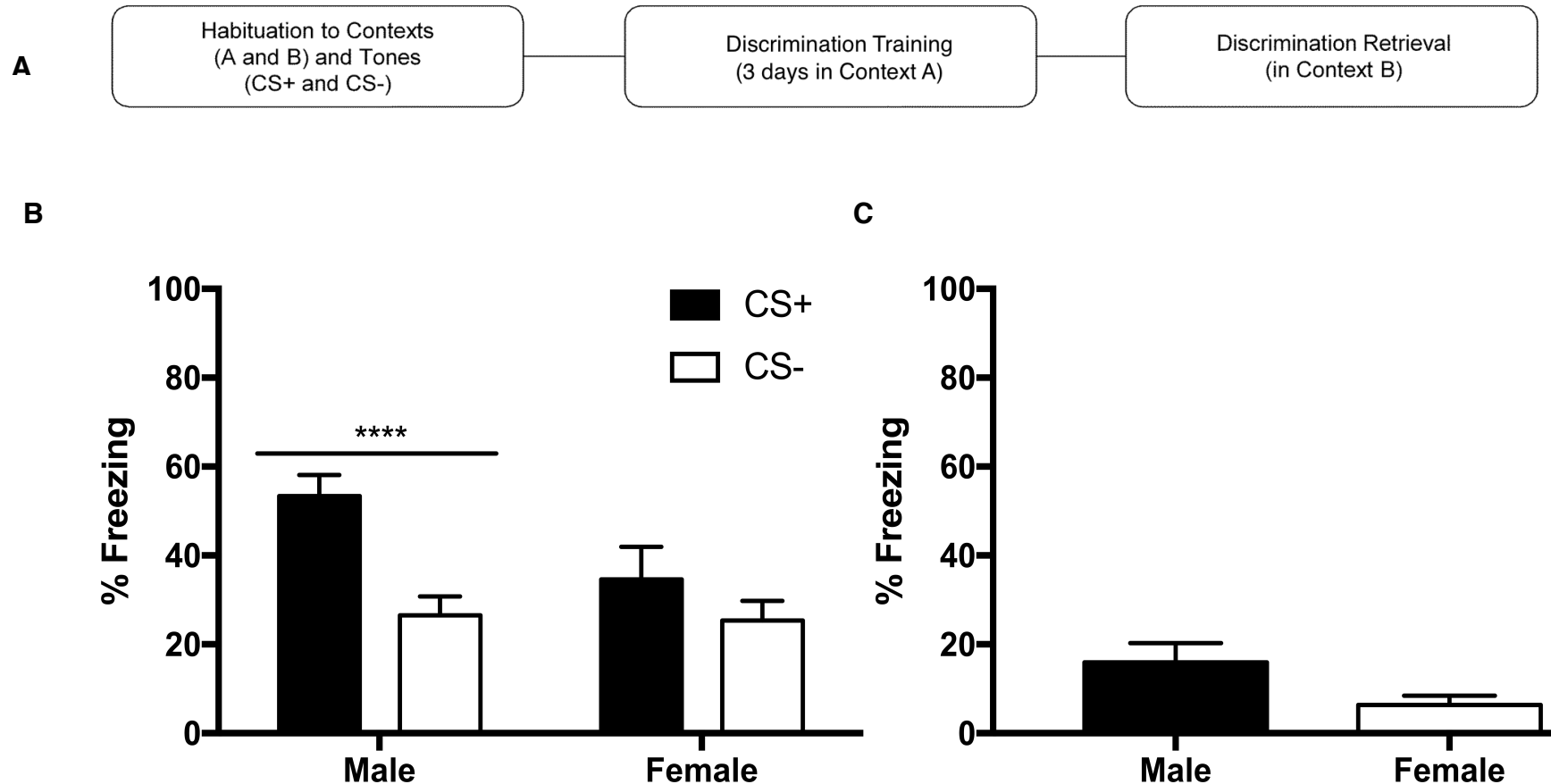
Figure 4.1. Sex differences in auditory fear discrimination (A) Schematic representation of the fear discrimination paradigm used. **(B)** Freezing in response to CS+ and CS− presentations during discrimination retrieval testing after three days of training. Males showed significantly higher freezing to presentations of the CS+ compared to the CS- (****$P < 0.0001$) whereas freezing during CS+ and CS- presentation did not differ in females. **(C)** Freezing before CS+ and CS- presentations during retrieval testing. There were no significant differences in freezing between the males and females.

4.3.2 Histology

Electrode placements within the PL, IL, and BLA in males and females are shown in Figure 4.2. Of the 18 males, n = 7 had good placements in PL, n = 7 had good placements in IL, and n = 6 had good placements in BLA. Of the 13 females, n = 9 had good placements in PL, n = 8 had good placements in IL, and n = 9 had good placements in BLA. For pairwise coherence analysis for comparisons between all three regions (PL-IL, PL-BLA, IL-BLA) we only included animals with good placements in PL, IL, and BLA, even though this meant that we excluded data from some animals that had good placements in only 1-2 of these regions. After exclusion, n = 5 male and n = 5 female rats with good placements in all three areas were included in subsequent analysis. All histology is outlined in Figure 4.2, below:
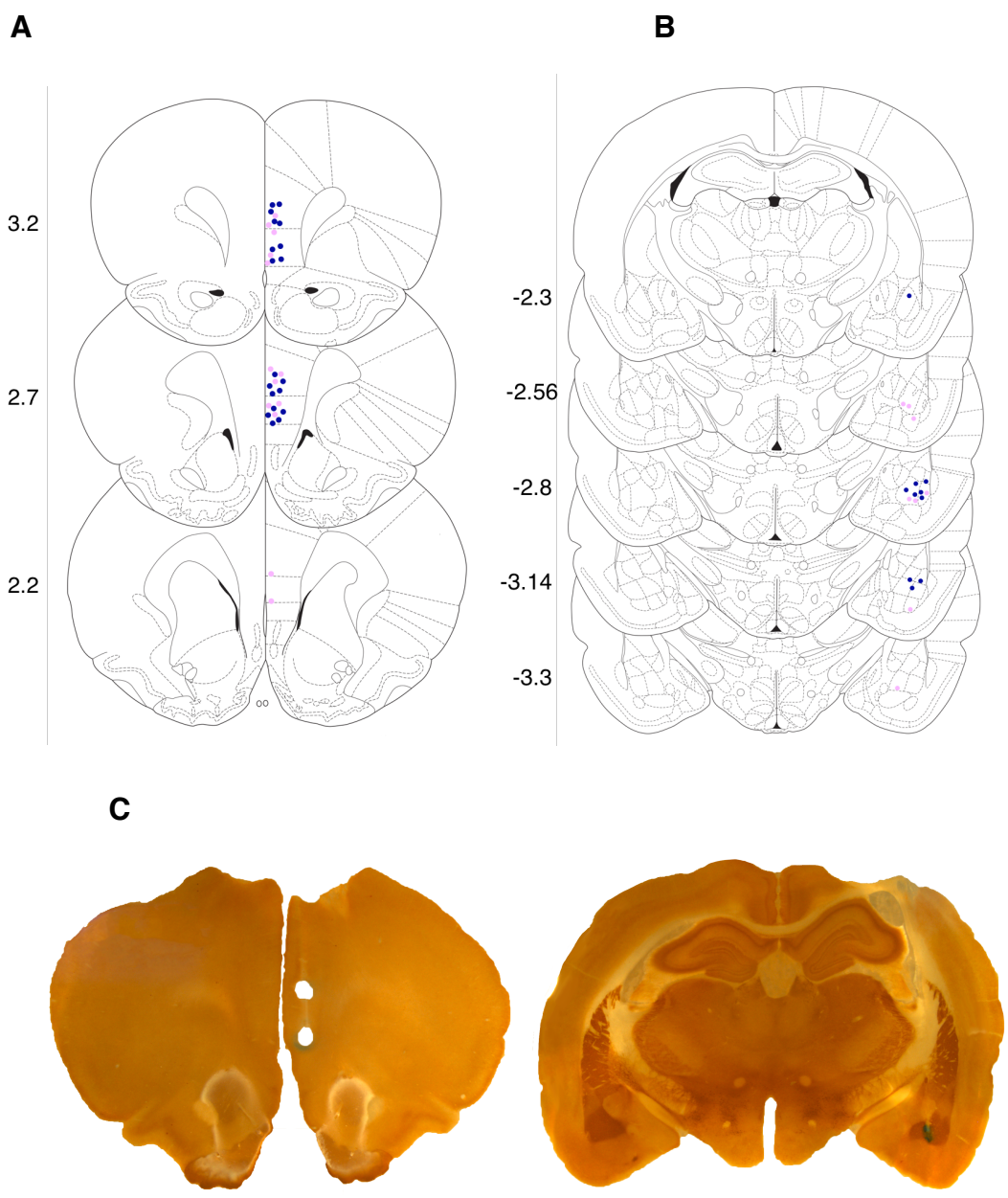
Figure 4.2. Histological verification of electrode placements in the PL, IL, and BLA. (A) Schematic representations of male (blue) and female (pink) electrode locations in the PL and IL (numbers represent the distance (mm) anterior to Bregma). **(B)** Schematic representations of male (blue) and female (pink) electrode locations in the BLA (numbers represent the distance (mm) posterior to Bregma). **(C)** Representative acetylcholinesterase-stained coronal sections showing electrode placements in the PL and IL (left) and BLA (right).

4.3.3 Differences in power and coherence in the theta frequency band

4.3.4 Theta Power colour plots

PL, IL and BLA theta power during CS+ and CS- presentations in males is presented in Figure 4.3, below. Upon visual inspection, it appeared that males showed decreased theta power in both the PL and IL regions during the CS+ compared to the CS-, although this effect is subtler in the IL. Males also appeared to display a marked decrease in BLA power during presentations of the CS+ compared to the CS-.

PL, IL and BLA theta power during CS+ and CS- presentations in females is presented in Figure 4.4, below. In females, theta power also appeared to be slightly decreased during presentations of the CS+ compared to the CS- in the PL, IL and BLA. However, these differences were of smaller magnitude compared to males.
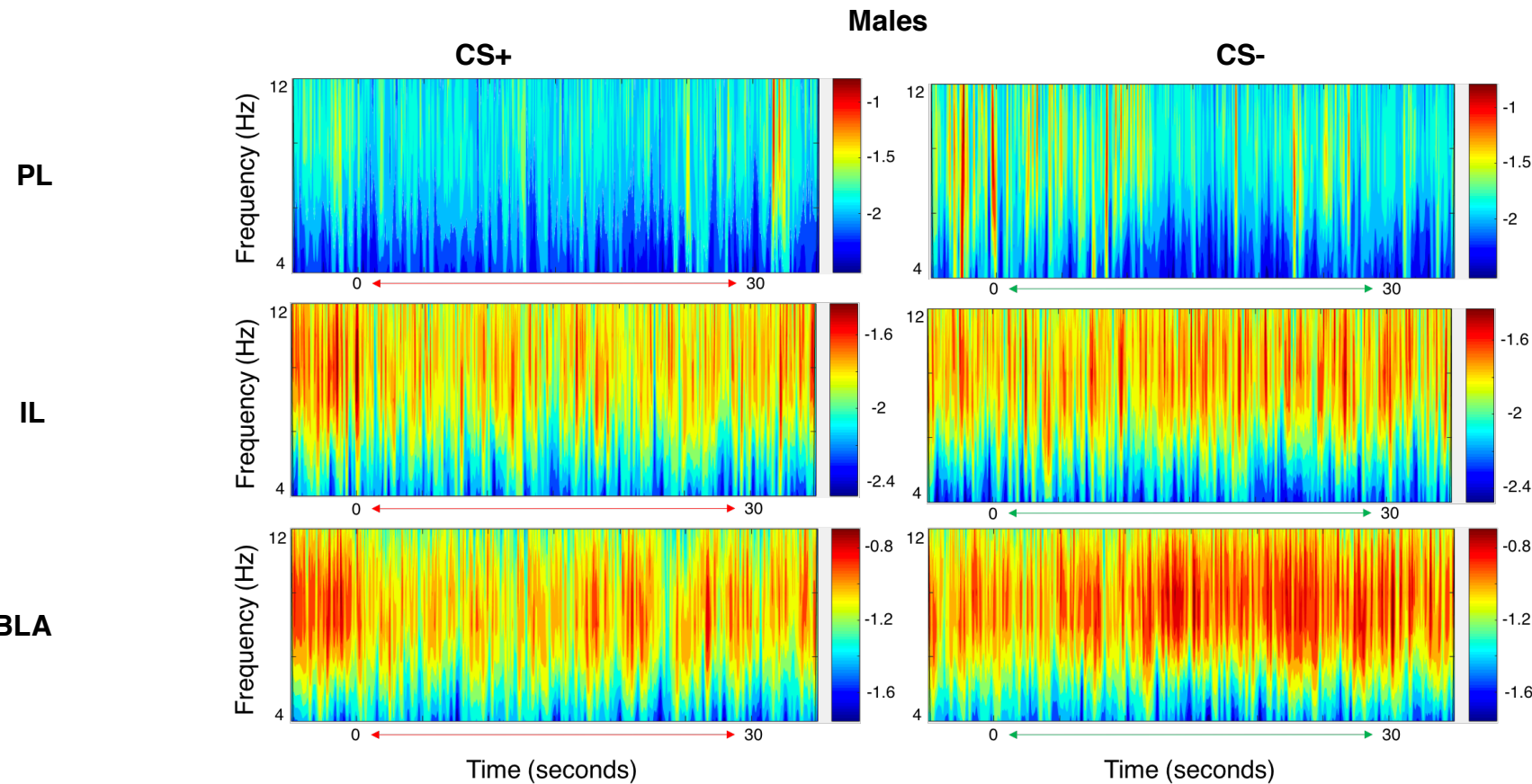
Figure 4.3. PL (top), IL (middle) and BLA (bottom) theta power spectra during CS+ (left) vs CS- (right) presentation in males. In accordance with the colour scale (right), more power is represented by warmer colours (i.e. orange/red) whereas less power is indicated by cooler colours (i.e. blue).

Figure 4.4. PL (top), IL (middle) and BLA (bottom) theta power spectra during CS+ (left) vs CS- (right) presentation in females. In accordance with the colour scale (right), more power is represented by warmer colours (i.e. orange/red) whereas less power is indicated by cooler colours (i.e. blue).

4.3.5 Power Multi-taper analysis

Differences in PL theta power between the CS+ and CS- in males and females are presented in Figures 4.5-4.7, below. In the PL, males displayed a relative decrease in power during presentations of the CS+ compared to the CS-. This decrease in power reached significance for multiple frequencies throughout the theta range, with the biggest difference seen ~6-9.5Hz and ~11-12Hz, but smaller, significant differences were also seen at 4 and 10 Hz ($P < 0.05$). In females, however, there was only one significant, small decrease in PL power for CS+ compared to CS- at ~8.5 Hz ($P < 0.05$). Moreover, females also showed significant, but small, increases in PL power during presentations of the CS+ compared to the CS- between 4.5-5.5 Hz and at ~7 and 11.5 Hz ($P < 0.05$). Yet, the differences seen in male PL are almost three times the magnitude of any differences observed in female PL.

In the IL, males again showed a decrease in power during presentations of the CS+ compared to the CS-, but this decrease only reaches significance at certain frequencies (~7-10 Hz ($P < 0.05$)) instead of the broader frequency range seen in PL. Females also showed a significant, but smaller, decrease in IL power during presentations of the CS+ compared to the CS- at around ~8 Hz ($P < 0.05$). Additionally, females also again showed a significant, small increase in IL power during presentations of the CS+ compared to CS- at ~10.5 Hz ($P < 0.05$), whereas males showed no such increase.

In the BLA, males showed a large, significant, decrease in power for presentations of the CS+ compared to the CS- from ~6.5-12 Hz. Interestingly, males also showed a significant, but subtle, increase in BLA power during the

CS+ compared to the CS- at ~5.5-6 Hz. Conversely, females showed no increases in BLA power, but did show a significant decrease during presentations of the CS+ compared to CS- from ~5-10 Hz.
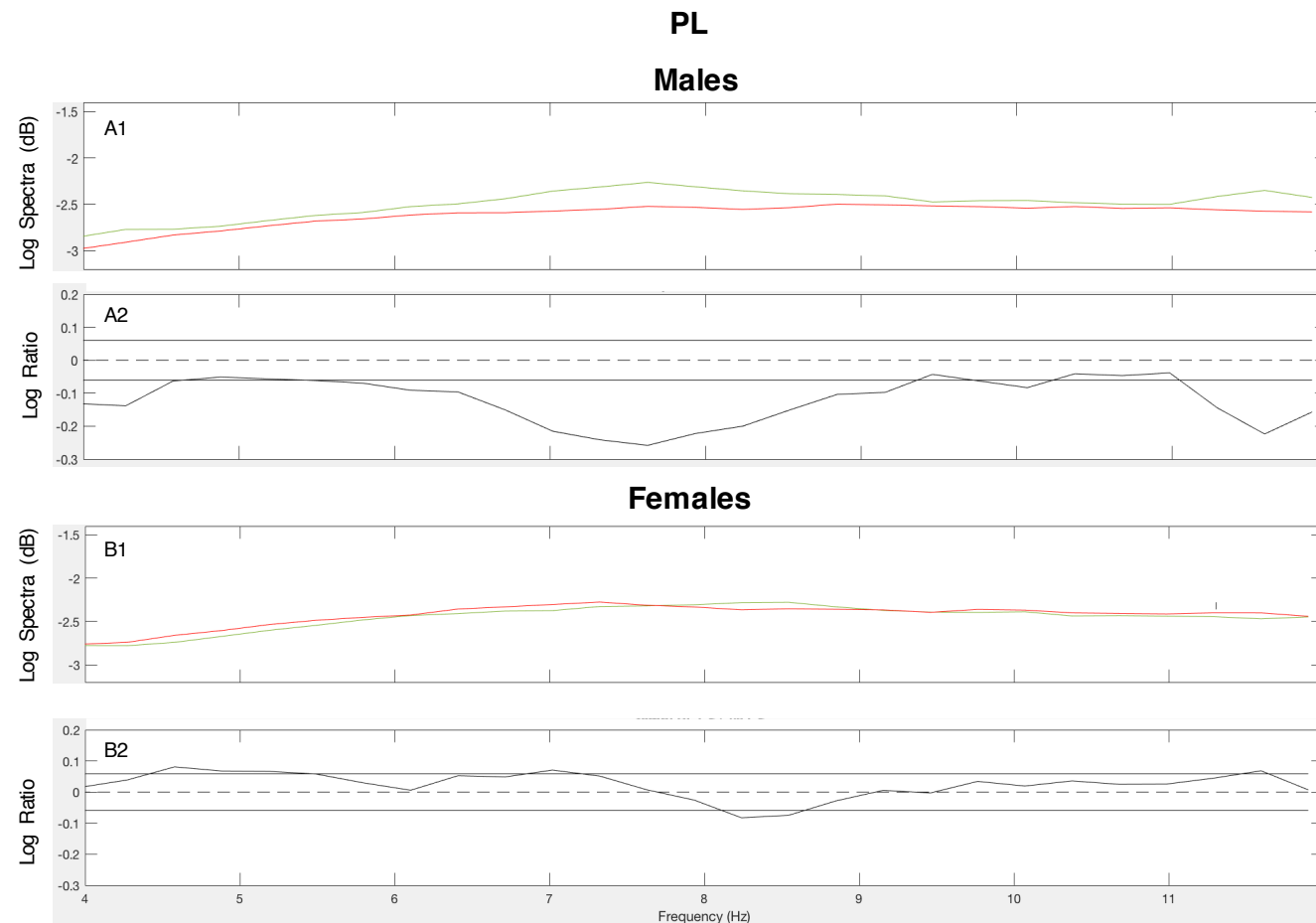
Figure 4.5. Pooled PL theta power spectra for males (A1) and females (B1) for CS+ (red) vs CS- (green) and log ratio tests quantifying differences in power during the CS+ vs CS- for males (A2) and females (B2). The solid horizontal lines in the log ratio plots represent the upper and lower 95% confidence limits; positive log ratio values indicate increased power, whereas negative values indicate decreased power, during the CS+ vs CS-. Males showed a large and consistent decrease in PL power during presentations of the CS+ compared to the CS- at various frequencies, whereas females showed both increases and decreases in PL power during presentations of the CS+, compared to the CS-.
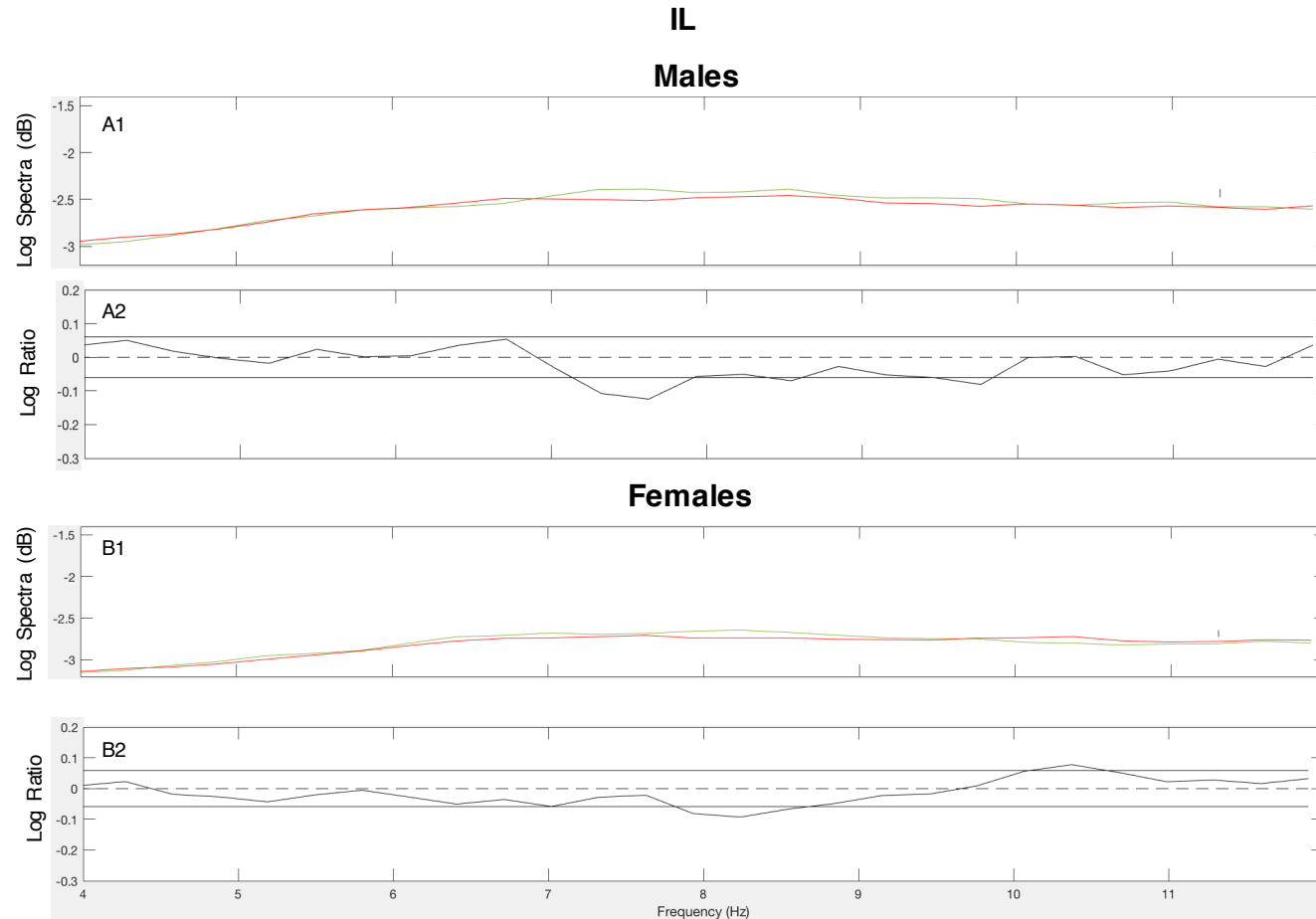
Figure 4.6. Pooled IL theta power spectra for males (A1) and females (B1) for CS+ (red) vs CS- (green) and log ratio tests quantifying differences in power during the CS+ vs CS- for males (A2) and females (B2). The solid horizontal lines in the log ratio plots represent the upper and lower 95% confidence limits; positive log ratio values indicate increased power, whereas negative values indicate decreased power, during the CS+ vs CS-. Males showed decreased IL power during presentations of the CS+ compared to the CS- ~7-8 Hz, whereas females showed both slight decreases and increases in IL power during presentations of the CS+, compared to the CS-.
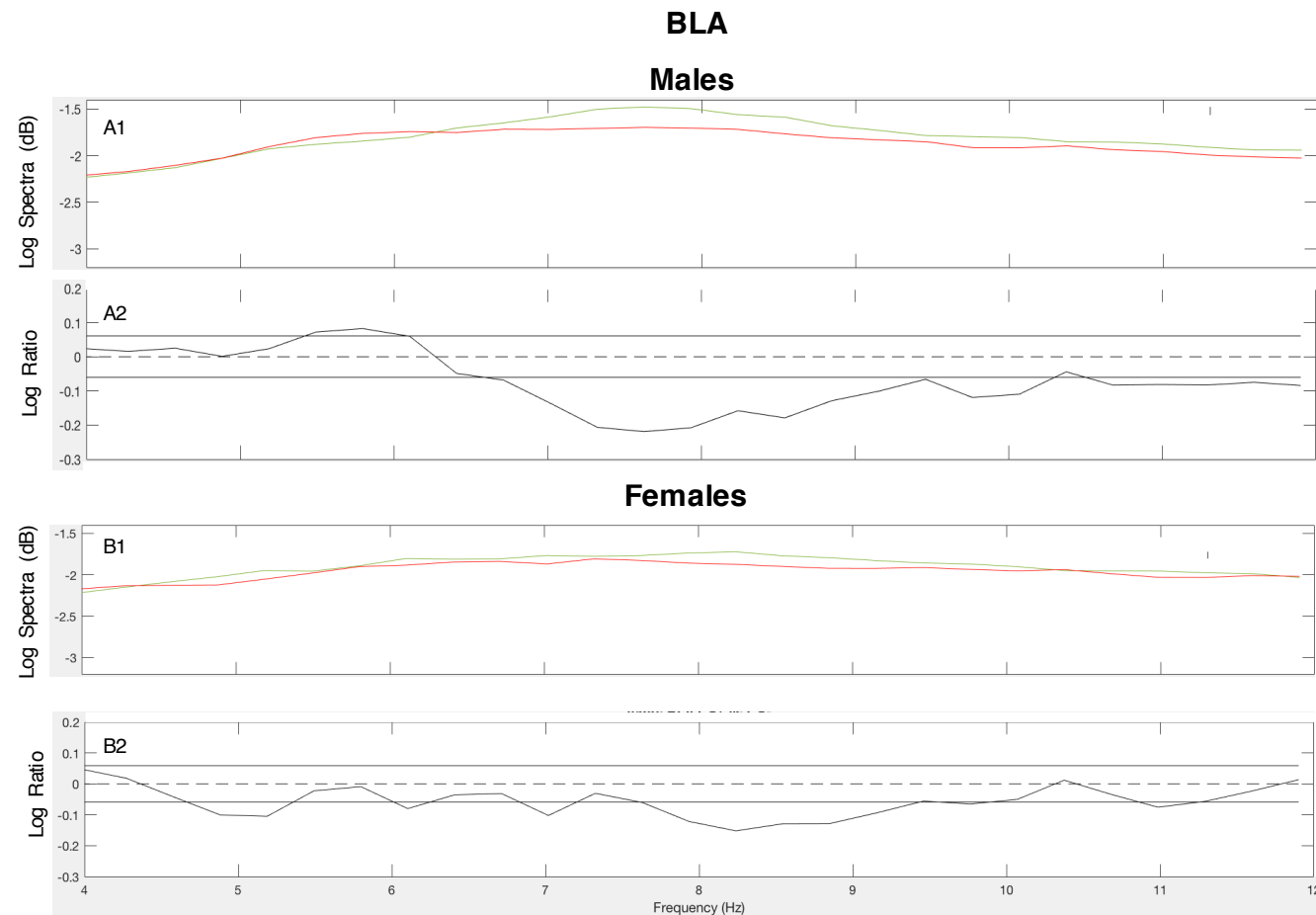
Figure 4.7. Pooled BLA theta power spectra for males (A1) and females (B1) for CS+ (red) vs CS- (green) and log ratio tests quantifying differences in power during the CS+ vs CS- for males (A2) and females (B2). The solid horizontal lines in the log ratio plots represent the upper and lower 95% confidence limits; positive log ratio values indicate increased power, whereas negative values indicate decreased power, during the CS+ vs CS-. Males showed a small increase at lower, and a larger decrease at higher, frequencies during presentations of the CS+, compared to the CS-. Females showed decreased BLA power during presentations of the CS+ compared to the CS-, which became significant at ~7.75-10 Hz.

4.3.6 Coherence Colour Plots

PL-BLA, IL-BLA and PL-IL theta coherence during CS+ and CS- presentations in males is presented in Figure 4.8 below. Overall, much of the coherence seen between brain areas was transient in nature. Although there were hardly any continuous epochs of coherence that last for the whole 30 second stimulus, there were still some interesting observations featured in these data. In males, it appeared that there was slightly less coherence between the PL and BLA during presentations of the CS+ compared to the CS-, similar to the relative decreases in power observed in both these regions during the CS+ compared to the CS- in figures 4.5-4.7, above. In contrast, there appeared to be slightly less coherence between IL and BLA during presentations of the CS- compared to the CS+. Coherence between the PL and IL seemed similar during presentations of both the CS+ and CS-.

PL-BLA, IL-BLA and PL-IL theta coherence during CS+ and CS- presentations in females is presented in Figure 4.9. In females, there seemed to be less coherence between the PL and BLA during the CS- in comparison to the CS+. As the colour spectra plots for coherence are directly comparable between sexes due to absolute scaling, it appeared that there was considerably less coherence between the PL and BLA in females compared to males. Females also appeared to show a subtle increase in coherence between the IL and BLA during presentations of the CS+ in comparison to the CS-, with stronger coherence in the upper frequencies of theta during the middle and last third of CS+ presentation. Coherence between PL and IL appeared to be slightly increased during presentations of the CS+ compared to the CS-.
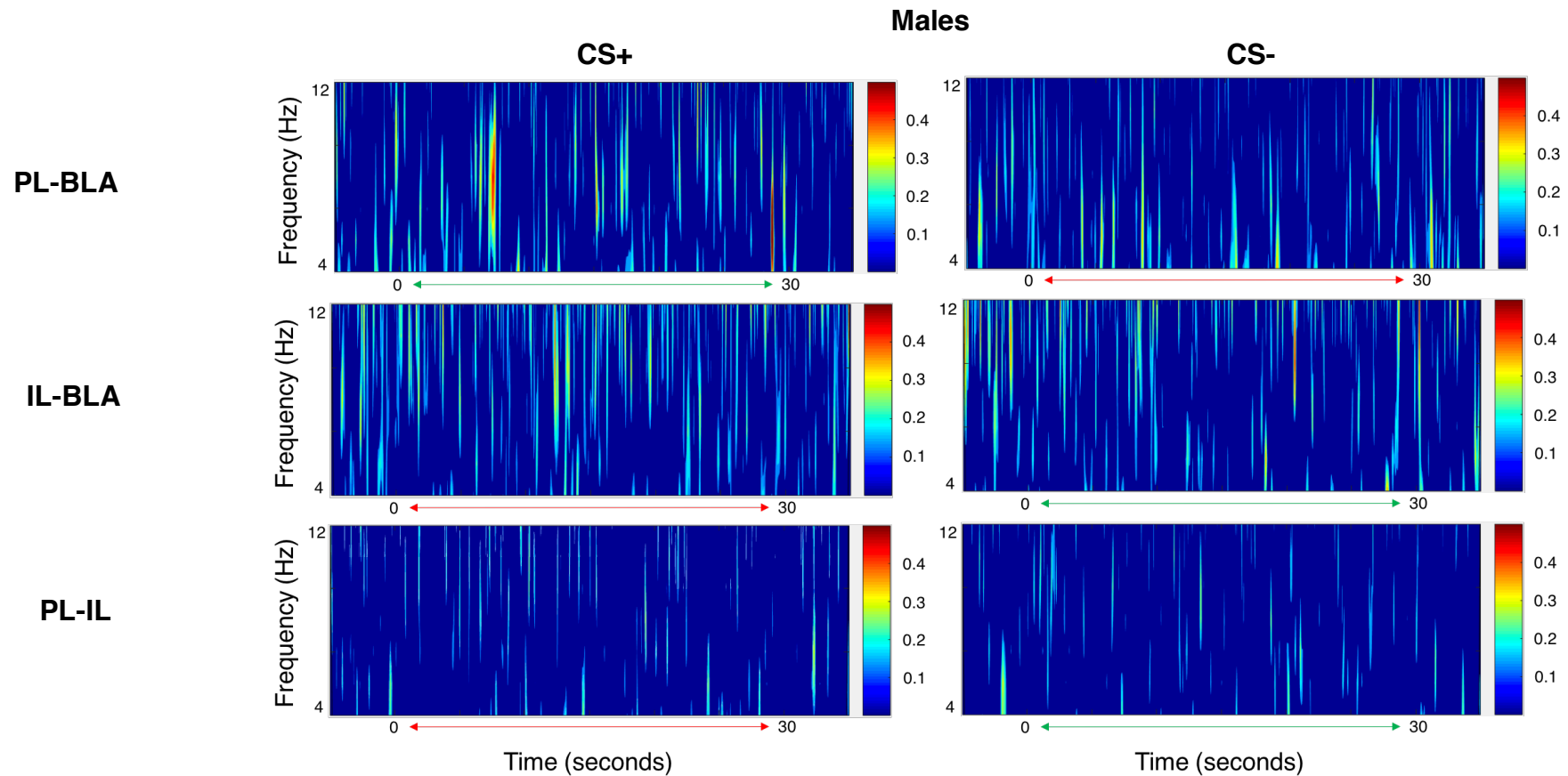
Figure 4.8. PL-BLA (top), IL-BLA (middle) and PL-IL (bottom) theta coherence spectra during CS+ (left) vs CS- (right) for males. In accordance with the colour scale (right), more power is represented by warmer colours (i.e. orange/red) whereas less power is indicated by cooler colours (i.e. blue).
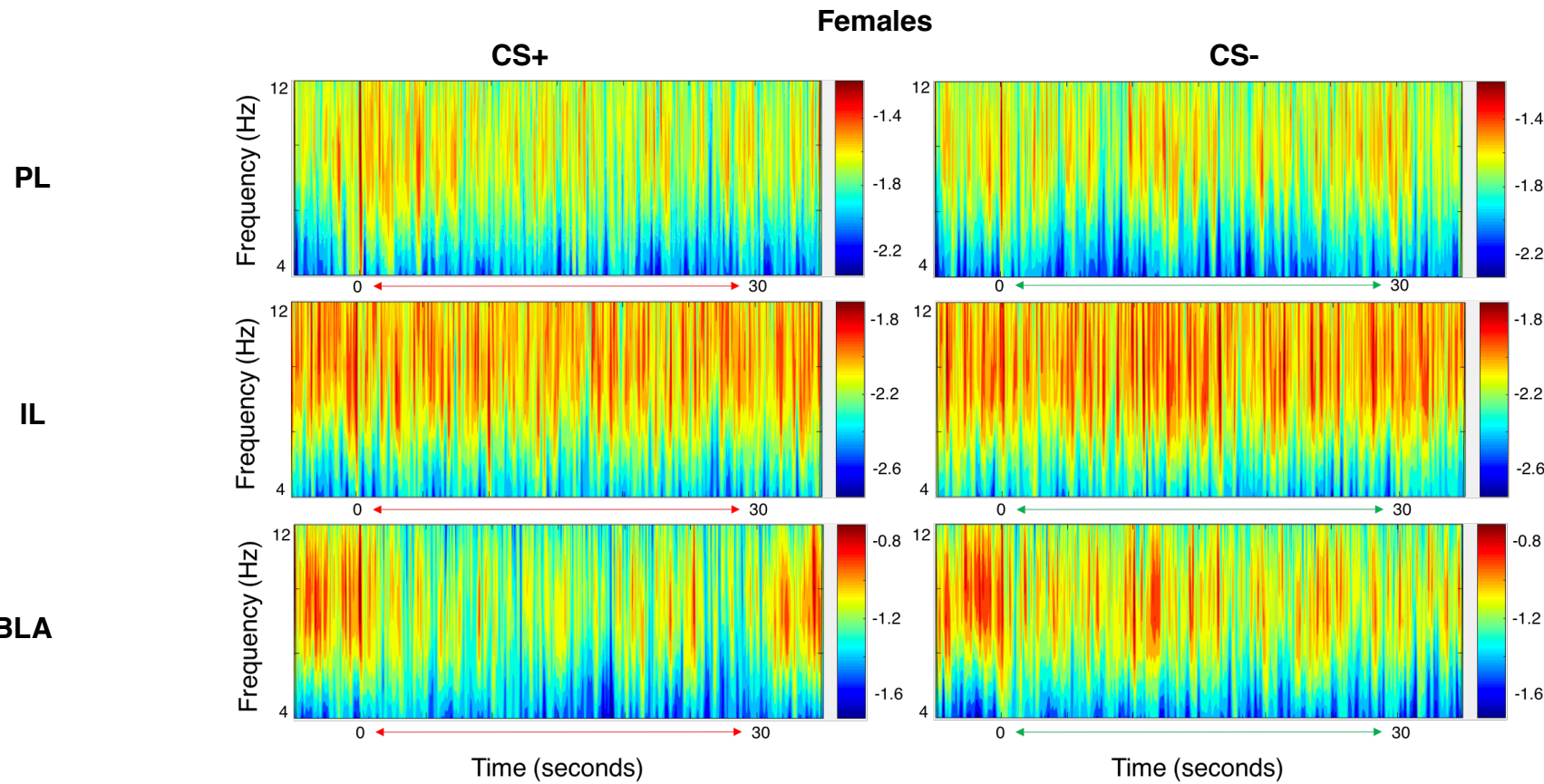
Females

CS+

CS-

PL-BLA

IL-BLA

PL-IL

Time (seconds)

Time (seconds)
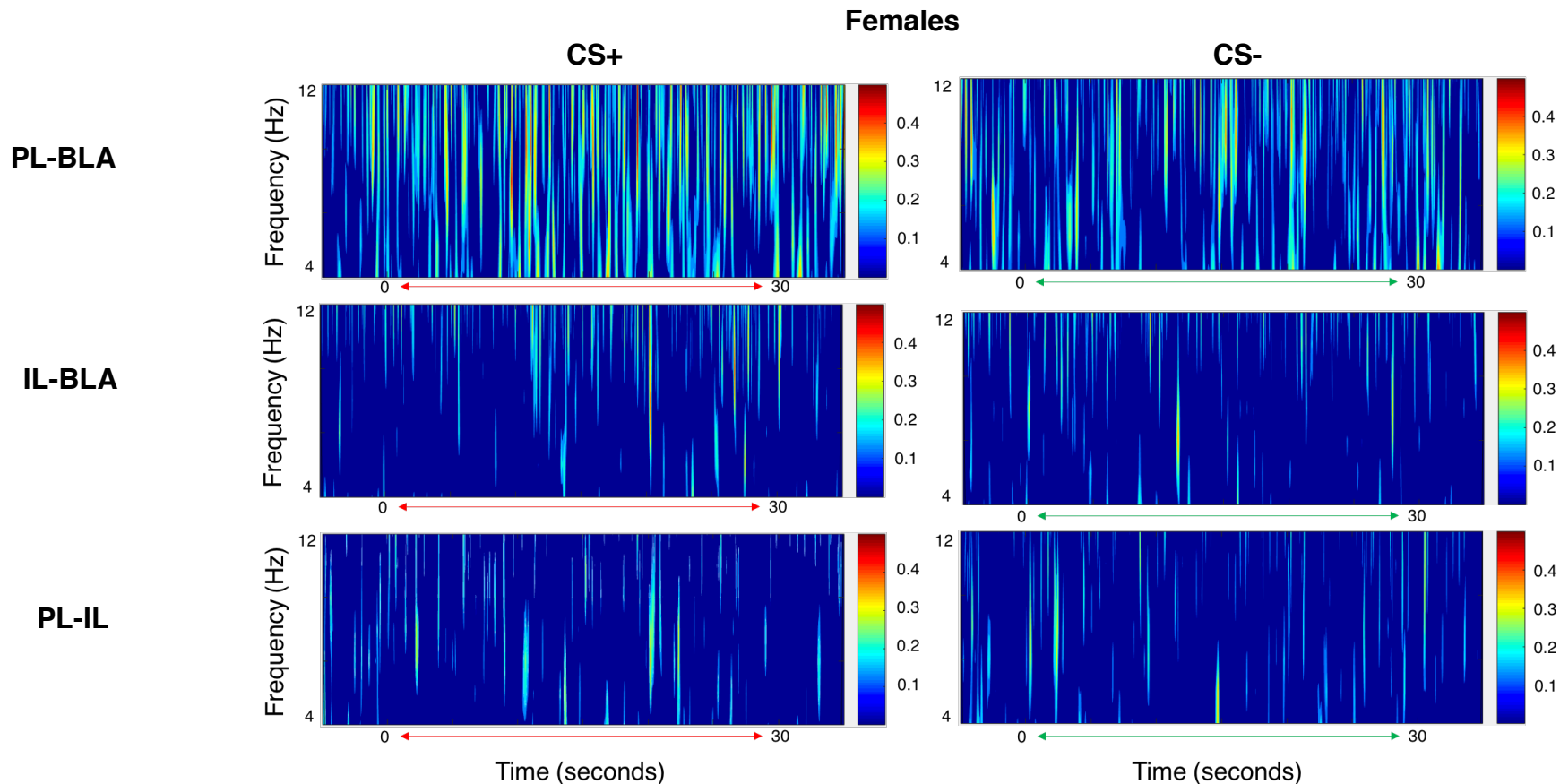
Figure 4.9. PL-BLA (top), IL-BLA (middle) and PL-IL (bottom) theta coherence spectra during CS+ (left) vs CS- (right) for females. In accordance with the colour scale (right), more power is represented by warmer colours (i.e. orange/red) whereas less power is indicated by cooler colours (i.e. blue).

167

4.3.7 Coherence Multi-taper Analysis

Differences in PL-BLA theta coherence during CS+ and CS- presentation in males and females are presented in Figures 4.10-4.12, below. Overall coherence (4.10, top panel) between the PL-BLA regions in males was significant at lower theta (less than ~7.5 Hz) during presentations of both stimuli. However, there were no significant increases in coherence between these regions during presentations of CS+ vs CS- (4.10, lower panel). In contrast, females showed more overall PL-BLA coherence at all frequencies in the theta range. Further, females showed a significant increase in PL-BLA coherence during presentations of the CS+, compared to the CS- at ~7-9 Hz, with additional significant, but smaller, increases at ~ 4.75 and 10.5 Hz ($P < 0.05$).

In males, coherence between the IL and BLA showed significant, but low, levels of coherence at all theta frequencies, with a marked increase in coherence at frequencies above ~ 7.5 Hz. However, males again also showed no significant increases in coherence between the IL and BLA during presentations of the CS+ vs CS- (4.11, lower panel). Interestingly, in females, the IL and BLA were only significantly coherent at higher theta frequencies (above ~ 7.5 Hz). Again, females also showed a significant difference in coherence between the IL and BLA during presentations of the CS+ compared to the CS- at ~8 Hz ($P < 0.05$).

In males, there was an overall lack of coherence between the PL and IL in addition to no significant increases in PL-IL coherence to either stimulus. Again, females, showed low, but still significant, levels of coherence between

the PL and IL at the majority of theta frequencies. Females also again showed a significant increase in PL-IL coherence during presentations of the CS+ compared to CS- at ~ 6.75 Hz (P < 0.05).

Overall, females displayed higher levels of coherence between all pairs of brain regions in comparison to males. In addition, males showed no significant increases in coherence between any pair of regions during presentations of the CS+ compared to the CS-, whereas females showed significant increases in coherence between all three pairs of regions during presentations of the CS+, compared to the CS-, with the largest increase in coherence occurring between the PL and BLA.
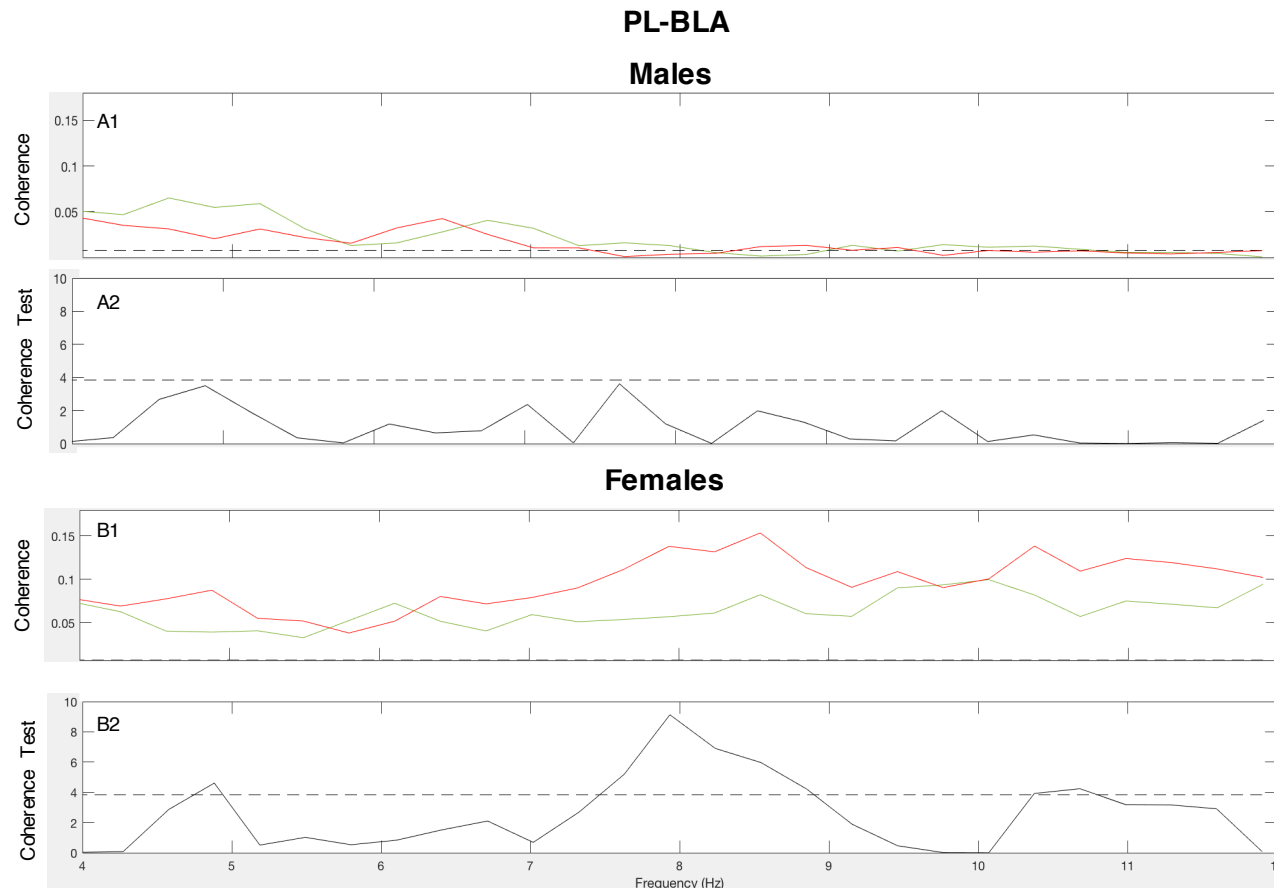
Figure 4.10. Pooled PL-BLA theta coherence for males (A1) and females (B1) for CS+ (red) vs CS- (green) and comparison of coherence tests quantifying differences in coherence during the CS+ vs CS- for males (A2) and females (B2). The dashed line denotes the 95% confidence limit. Upper panel: above this line shows significant overall coherence between regions during presentations of the CS+ (red) and CS- (green) (P < 0.05). Lower panel: peaks above this line show a significant increase in coherence between regions during presentations of either the CS+ or CS-. In males, there were no differences in coherence between presentations of the CS+ vs CS-. In females, PL-BLA coherence at increased during CS+ vs CS- between 7.5-9 Hz and again at approximately 4.75 and 10.5 Hz.

Figure 4.11. Pooled PL-BLA low gamma coherence for males (A1) and females (B1) for CS+ (red) vs CS- (green) and comparison of coherence tests quantifying differences in coherence during the CS+ vs CS- for males (A2) and females (B2). The dashed line denotes the 95% confidence limit. Upper panel: above this line shows significant overall coherence between regions during presentations of the CS+ (red) and CS- (green) (P < 0.05). Lower panel: peaks above this line show a significant increase in coherence between regions during presentations of either the CS+ or CS-. In males, there were no differences in coherence. In females, there was a significant difference in IL-BLA coherence, with an increase in coherence seen during presentations of the CS+ compared to the CS- at ~8 Hz.

Figure 4.12. Pooled PL-BLA low gamma coherence for males (A1) and females (B1) for CS+ (red) vs CS- (green) and comparison of coherence tests quantifying differences in coherence during the CS+ vs CS- for males (A2) and females (B2). The dashed line denotes the 95% confidence limit. Upper panel: above this line shows significant overall coherence between regions during presentations of the CS+ (red) and CS- (green) (P < 0.05). Lower panel: peaks above this line show a significant increase in coherence between regions during presentations of either the CS+ or CS-. In males, there were no significant increases in PL-IL coherence. In females, these regions become significantly more coherent during the CS+ at ~ 6.75 Hz.

4.3.8 Differences in power and coherence in the gamma frequency band

As for theta frequencies, LFPs recorded during discrimination retrieval were initially analysed using Morse Wavelet transformations to generate colour spectrograms of the changes in power and coherence seen in the PL, IL and BLA of both males and females during presentations of the CS+ and CS- at gamma frequencies (~ 30-120 Hz). As this frequency band is much larger than theta (4-12 Hz), and differences within this large band are difficult to observe when all frequencies are taken into consideration, gamma was split into low (32-45 Hz), mid (45-64 Hz) and high (64-128 Hz) bands. This is similar to the splitting of gamma into slow (40-70 Hz) and fast (70-120 Hz) oscillations in Stujenske et al., (2014). Further, low gamma is also the frequency band where Fenton et al., 2016 saw changes in PL and IL during learned fear expression and extinction.

4.3.9 Low gamma (32-45 Hz)

4.3.10 Low Gamma Power Colour Plots

PL, IL and BLA low gamma power during CS+ and CS- presentations in males is presented in Figure 4.13, below. Upon visual inspection, there appeared to be slightly more PL power during presentations of the CS+ compared to the CS-. There did not appear to be any visible changes in IL power during presentations of either the CS+ or CS-. However, in the BLA, there appeared to be a moderate increase in power during presentations of the CS- compared to the CS+, although this overall change looks to be due to intermittent epochs

of increased power during the 30 second stimulus, rather than a steady increase throughout the tone.

PL, IL and BLA low gamma power during CS+ and CS- presentations in females is presented in Figure 4.14, below. In females, there appeared to be subtle differences between CS+ and CS- for the PL, IL and BLA. Arguably, there was slightly more power in the PL region during the CS- compared to the CS+, but this may have been due to the comparatively large increase in power seen towards the end of the CS- tone. There appeared to be slightly more IL power during presentations of the CS- compared to the CS+. Moreover, there seemed to be slightly more BLA power during presentations of the CS+ compared to the CS-.
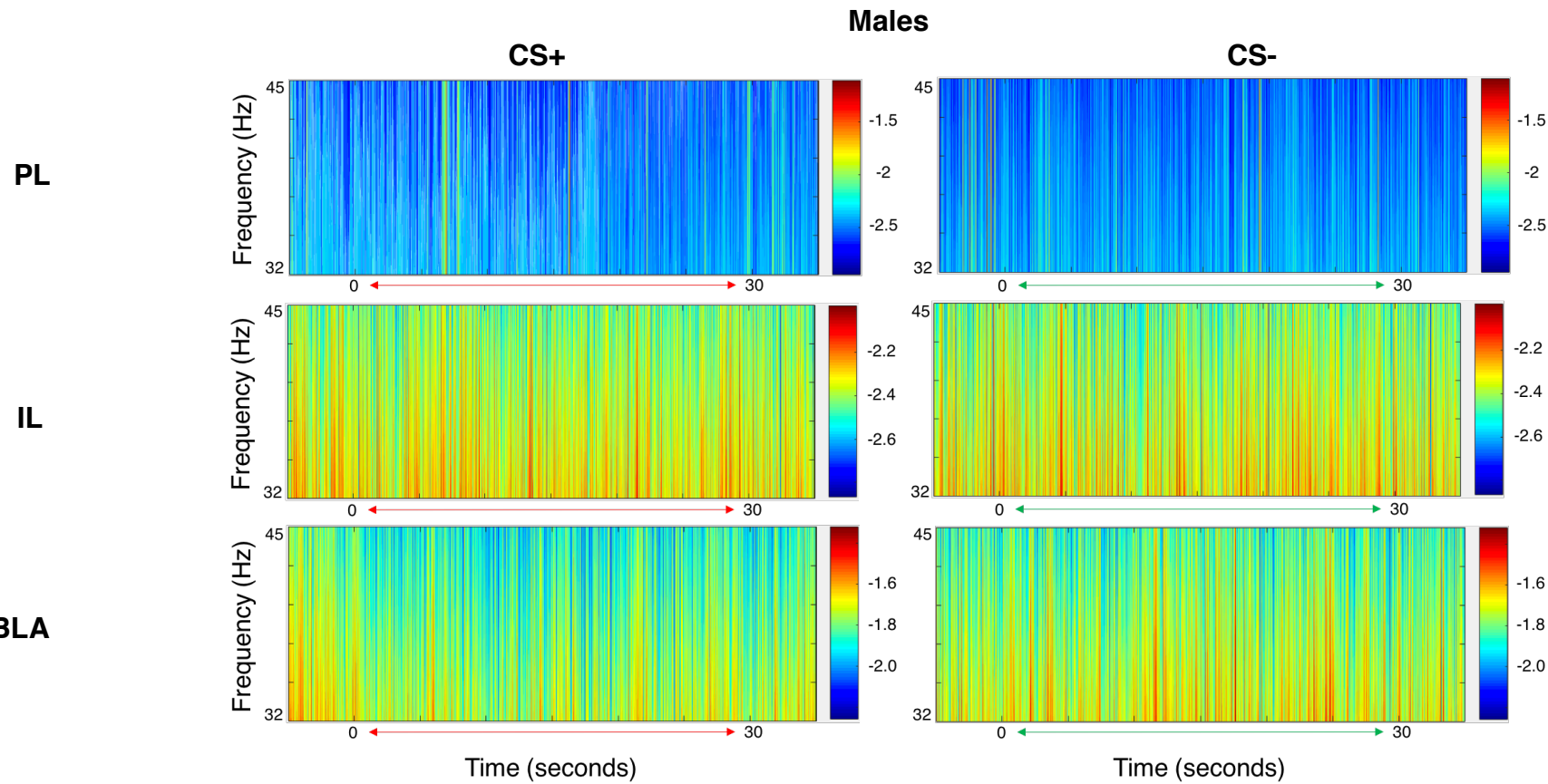
Figure 4.13. PL (top), IL (middle) and BLA (bottom) low gamma power spectra during CS+ (left) vs CS- (right) presentation in males. In accordance with the colour scale (right), more power is represented by warmer colours (i.e. orange/red) whereas less power is indicated by cooler colours (i.e. blue).

Figure 4.14. PL (top), IL (middle) and BLA (bottom) low gamma power spectra during CS+ (left) vs CS- (right) presentation in females. In accordance with the colour scale (right), more power is represented by warmer colours (i.e. orange/red) whereas less power is indicated by cooler colours (i.e. blue).

4.3.11 Low Gamma Power Multi-taper Analysis

Differences in PL, IL and BLA low gamma power between the CS+ and CS- in males and females are presented in Figures 4.15-4.17, below. In the PL, there did not appear to be a large difference between presentations of the CS+ compared to the CS- for either sex. In males, there were two instances where there was slightly less power in the PL during the CS+ compared to the CS- at approximately 41 and 45 Hz. Similarly, females also showed a slightly larger, significant, decrease in PL power during the CS+ compared to the CS- at $\sim$ 42 Hz. However, as these decreases were at only 1-2 frequencies across this entire range, it is hard to conclude that there was an overall difference.

Similarly, there were no large differences in power between presentations of the CS+ compared to the CS- in the IL region for either sex. Both sexes did show a significant, but small, decrease in IL power during presentations of the CS+ compared to CS- at $\sim$ 30 Hz, but there were no other significant differences in IL power.

In males, there was a significant decrease in BLA low gamma power across multiple frequencies during presentations of the CS+ compared to the CS-. The biggest difference occurred at $\sim$35-37 Hz, with significant, but smaller, differences occurring at 31, 32-32, 38, 40, and 43-44 Hz ($P < 0.05$). In females, there were also several instances where there was a significant decrease in BLA power during the CS+ compared to the CS- ($\sim$31-42 Hz), but these decreases were smaller in magnitude, and occurred more infrequently, compared to males.
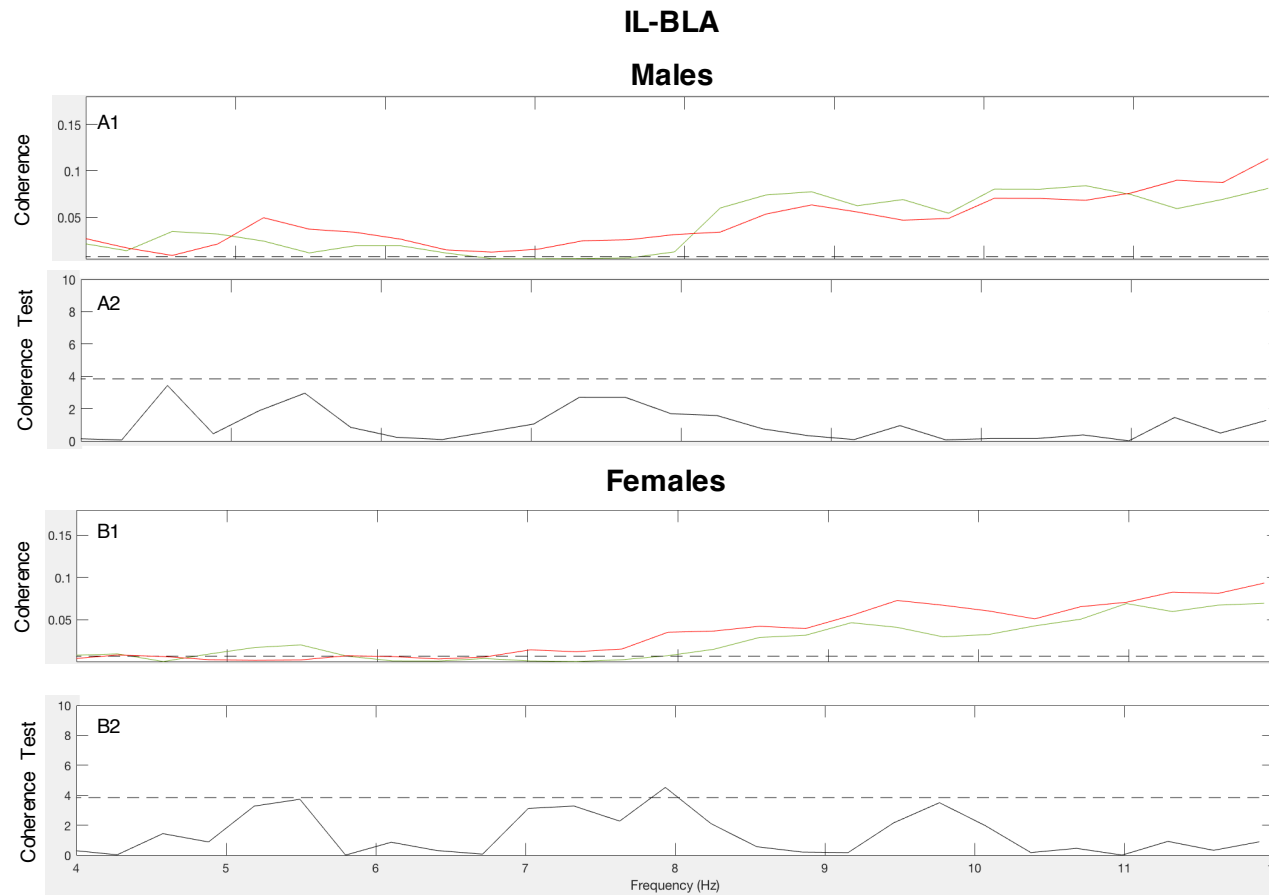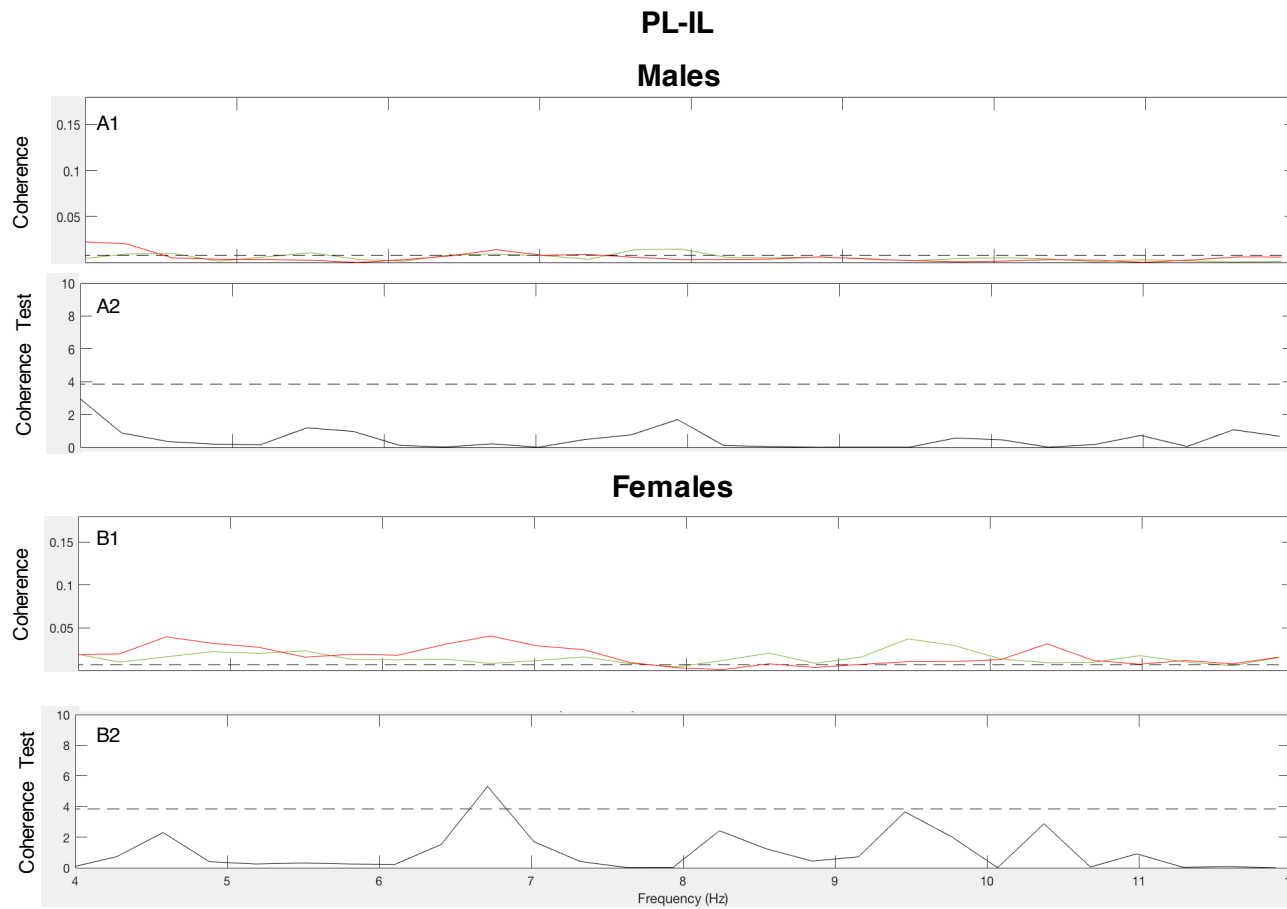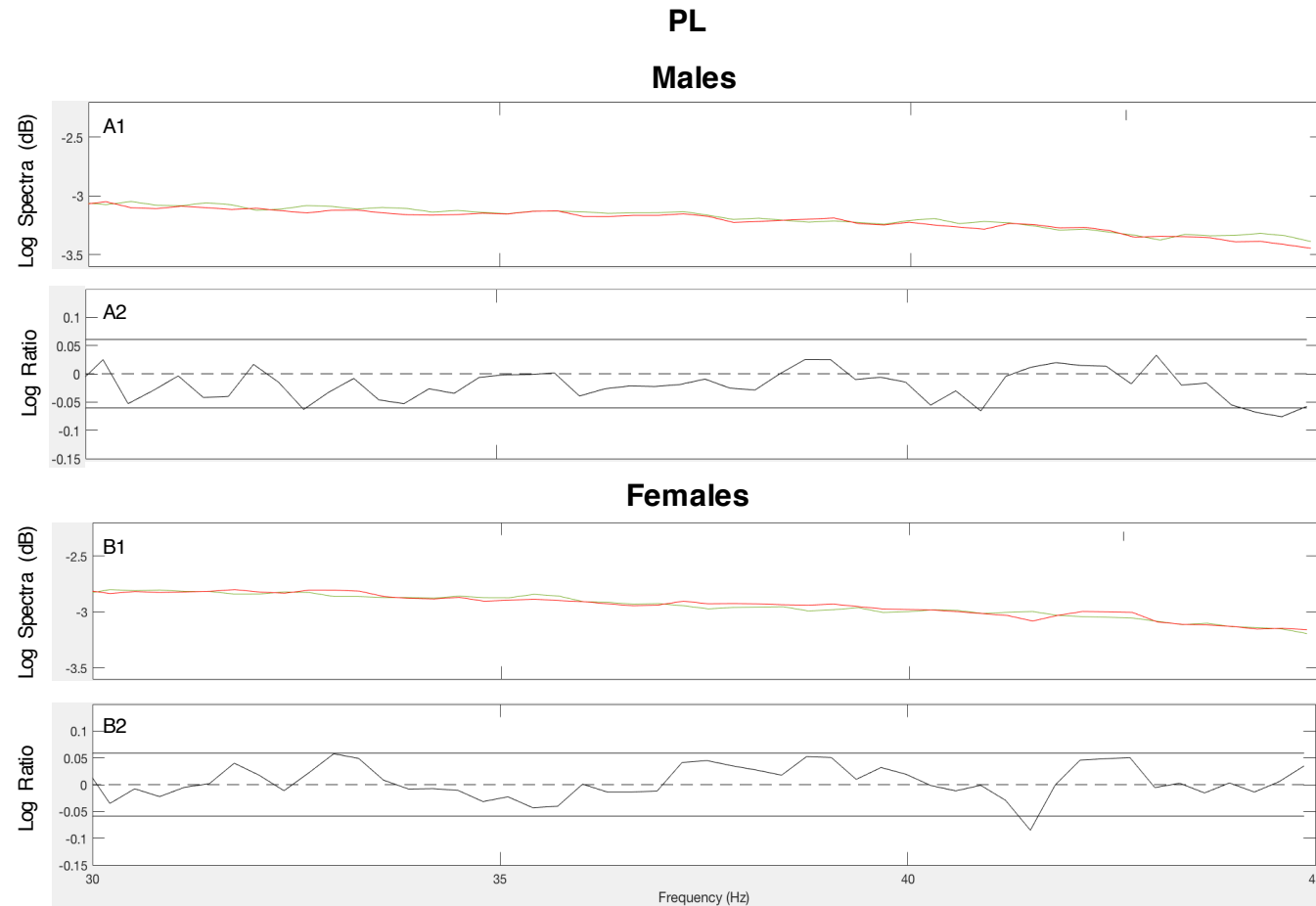
Figure 4.15. Pooled PL low gamma power spectra for males (A1) and females (B1) for CS+ (red) vs CS- (green) and log ratio tests quantifying differences in power during the CS+ vs CS- for males (A2) and females (B2). The solid horizontal lines in the log ratio plots represent the upper and lower 95% confidence limits; positive log ratio values indicate increased power, whereas negative values indicate decreased power, during the CS+ vs CS-. Both males and females showed an overall lack of changes in power for CS+ compared to CS-, apart from slight decreases in power during the CS+ compared to the CS- at ~44 and 42 Hz, respectively.
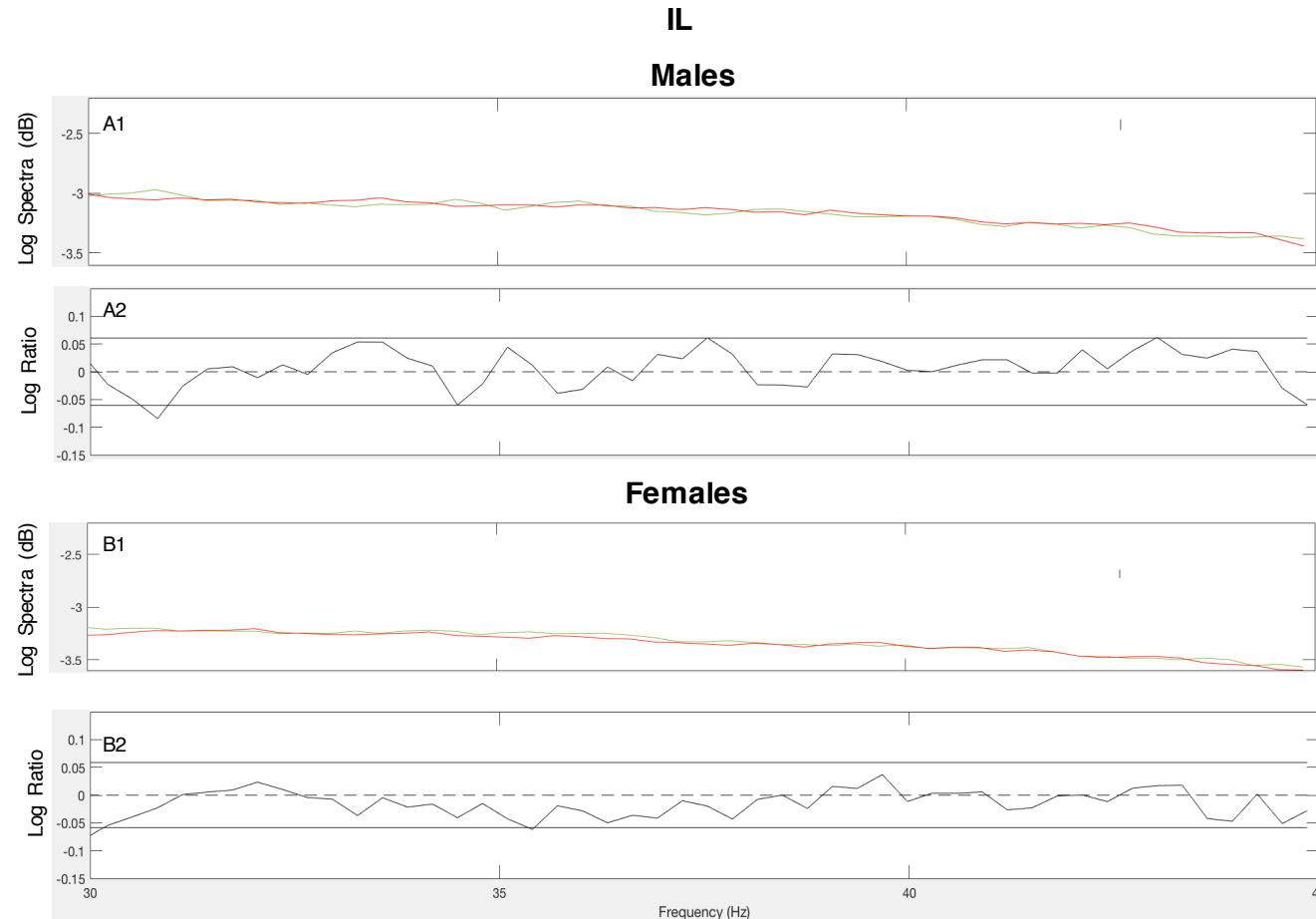
Figure 4.16. Pooled IL low gamma power spectra for males (A1) and females (B1) for CS+ (red) vs CS- (green) and log ratio tests quantifying differences in power during the CS+ vs CS- for males (A2) and females (B2). The solid horizontal lines in the log ratio plots represent the upper and lower 95% confidence limits; positive log ratio values indicate increased power, whereas negative values indicate decreased power, during the CS+ vs CS-. Both males and females showed an overall lack of changes in low gamma power in the IL region for CS+ compared to CS-. However, males and females showed slight decreases in low gamma power during the CS+ compared to the CS- at ~31 and 30 Hz, respectively.

179
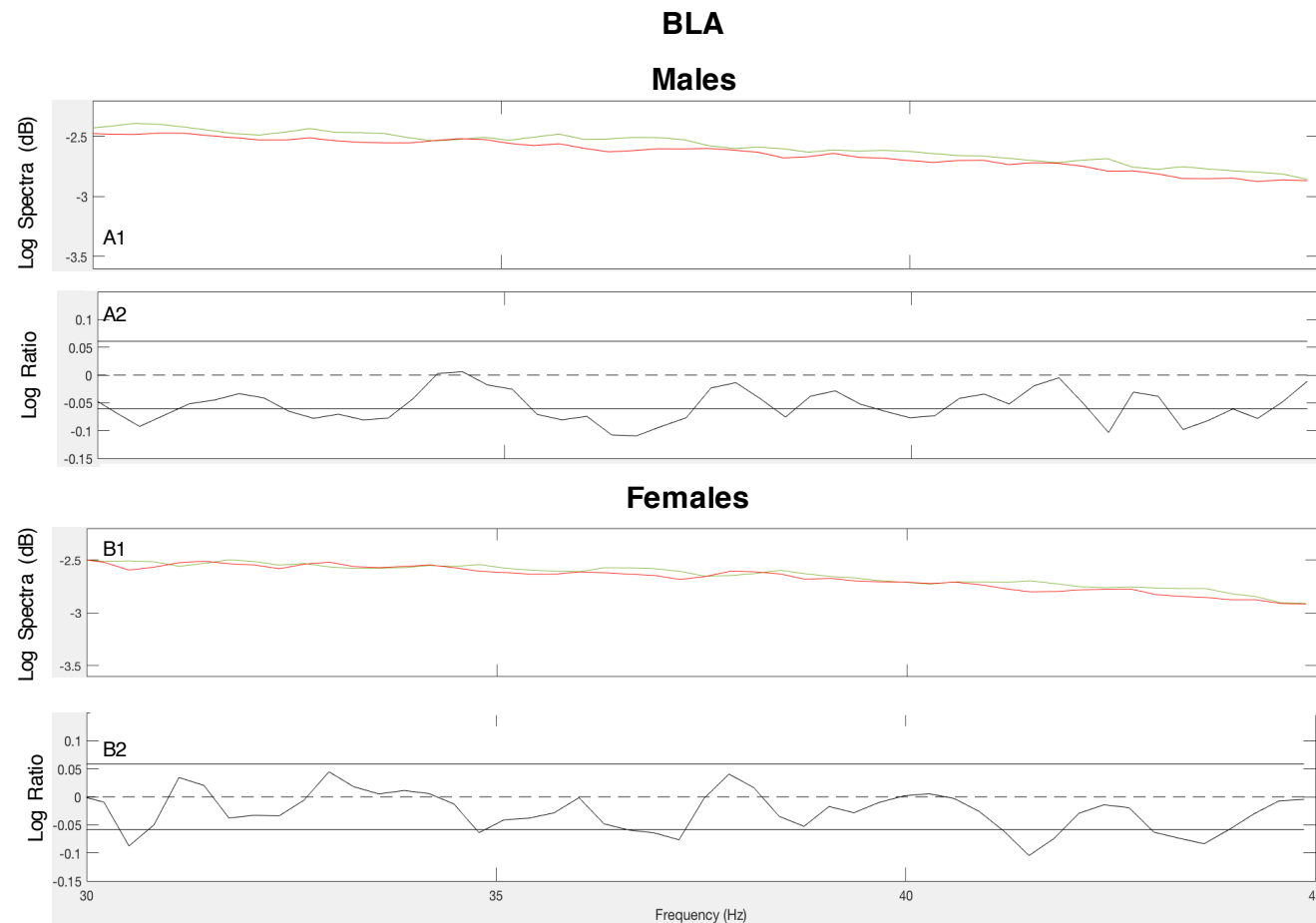
Figure 4.17. Pooled BLA low gamma power spectra for males (A1) and females (B1) for CS+ (red) vs CS- (green) and log ratio tests quantifying differences in power during the CS+ vs CS- for males (A2) and females (B2). The solid horizontal lines in the log ratio plots represent the upper and lower 95% confidence limits; positive log ratio values indicate increased power, whereas negative values indicate decreased power, during the CS+ vs CS-. Males showed a decrease in BLA power during presentations of the CS+ compared to the CS- at multiple frequencies. Females also showed a decrease in BLA low gamma power during the CS+ compared to the CS-, but these differences were less frequent and of smaller magnitude than the differences seen in males.

4.3.12 Low Gamma Coherence Colour Plots

PL-BLA, IL-BLA and PL-IL low gamma coherence during CS+ and CS-presentations in males is presented in Figure 4.18. In males, coherence between the PL and BLA regions showed no clear differences during presentations of the CS+ compared to the CS-. In contrast, coherence between the IL and BLA appeared to increase during presentations of the CS+ compared to presentation of the CS-. Finally, coherence between the PL and IL did not appear to show any clear differences between either tone.

PL-BLA, IL-BLA and PL-IL low gamma coherence during CS+ and CS-presentations in females is presented in Figure 4.19. There seemed to be little to no difference in coherence between the PL and BLA in females, although there appeared to be a very subtle increase in IL-BLA coherence during presentations of the CS+ compared to the CS-. However, as there was less overall coherence between the IL and BLA in females compared to males, this is difficult to determine. There appeared to be no clear differences in PL-IL coherence in females for presentations of the CS+ compared to presentations of the CS-.
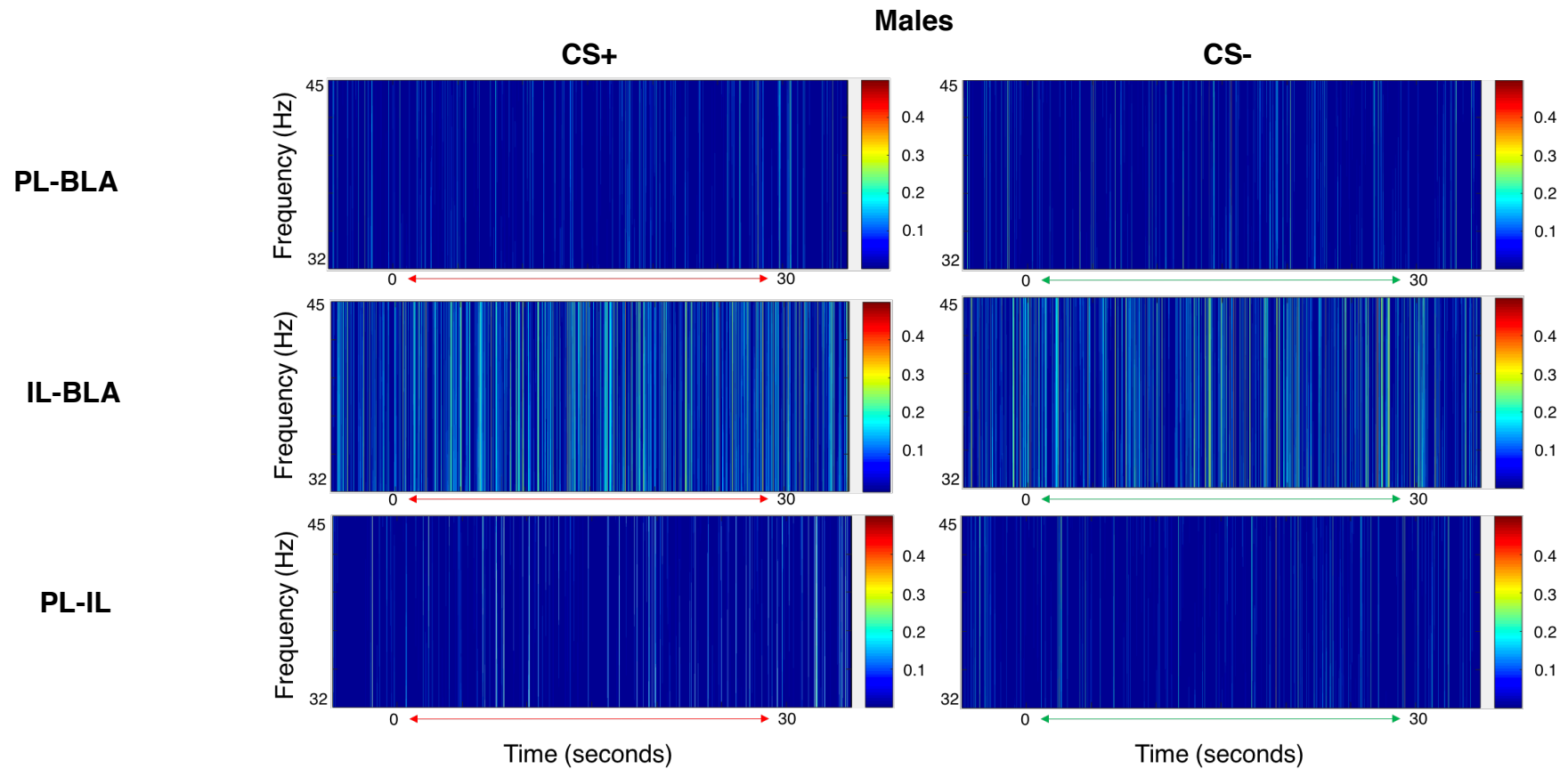
Figure 4.18. PL-BLA (top), IL-BLA (middle) and PL-IL (bottom) low gamma coherence spectra during CS+ (left) vs CS- (right) for males. In accordance with the colour scale (right), more coherence is represented by warmer colours (i.e. orange/red) whereas less coherence is indicated by cooler colours (i.e. blue).
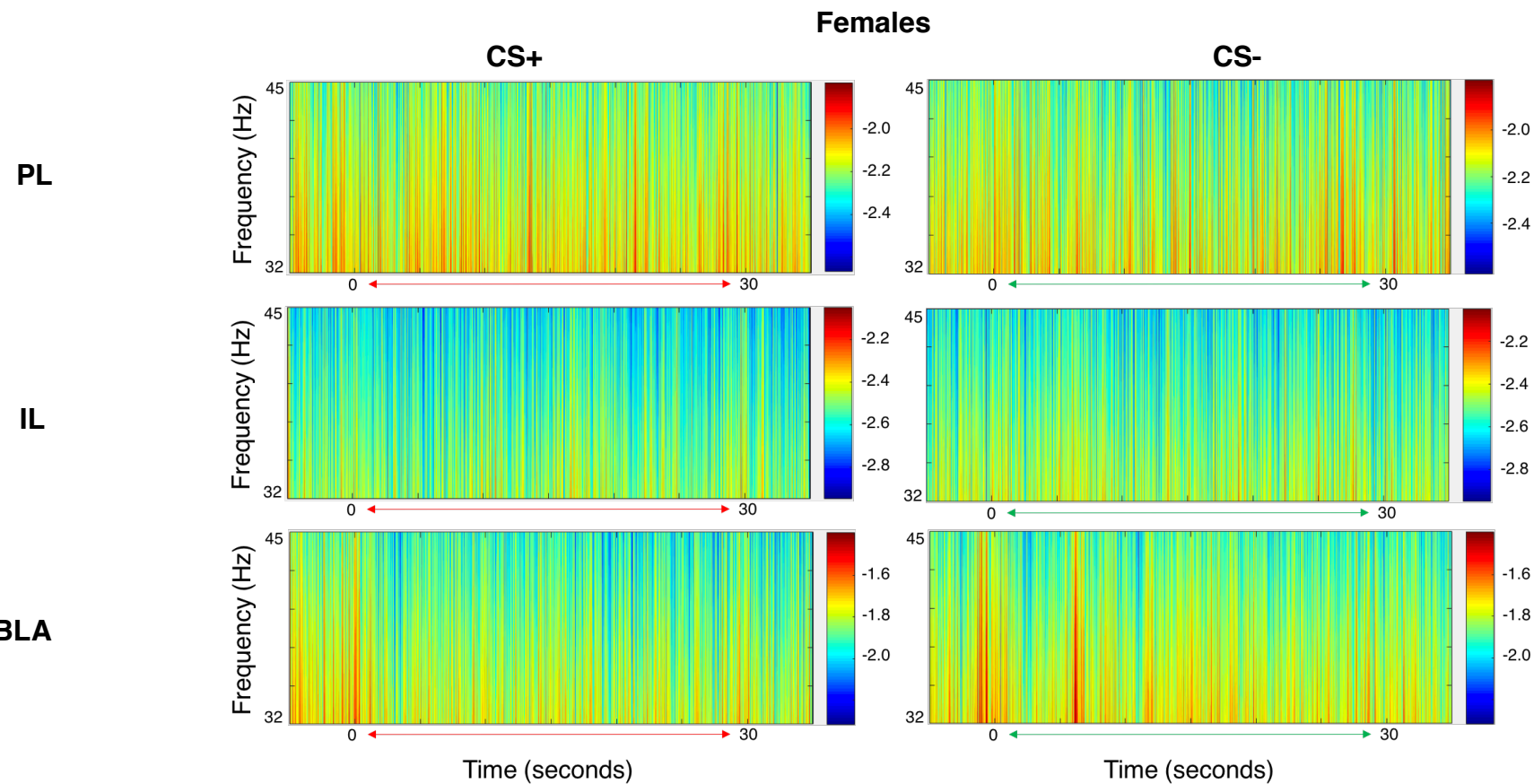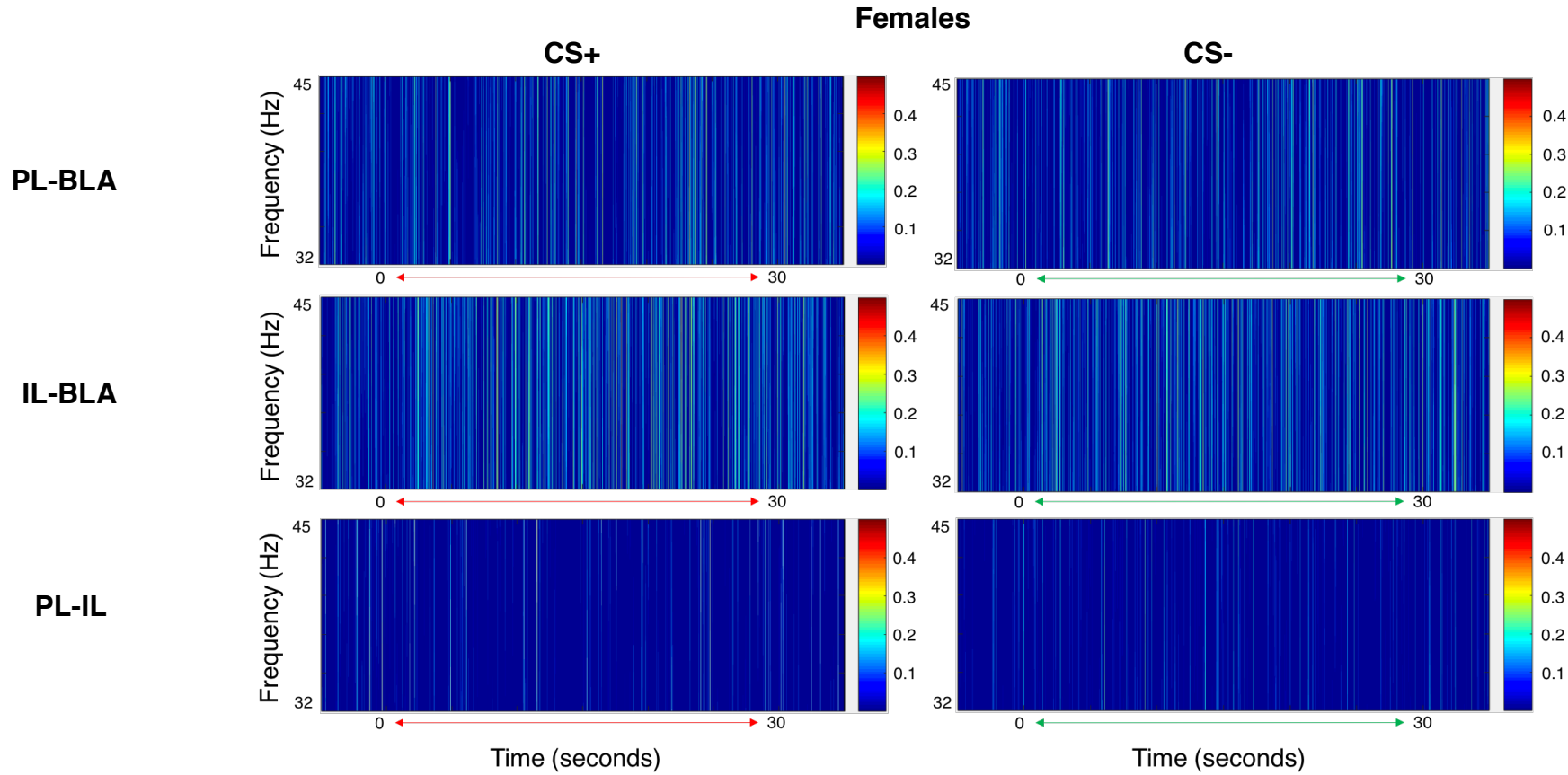
Figure 4.19. PL-BLA (top), IL-BLA (middle) and PL-IL (bottom) low gamma coherence spectra during CS+ (left) vs CS- (right) for females. In accordance with the colour scale (right), more coherence is represented by warmer colours (i.e. orange/red) whereas less coherence is indicated by cooler colours (i.e. blue).

4.3.13 Low Gamma Coherence Multi-Taper Analysis

PL-BLA, IL-BLA and PL-IL low gamma coherence during CS+ and CS-presentations in males and females is presented in Figures 4.20-4.22, below. In males, the overall level of PL-BLA coherence was low, dropping below significance at multiple points throughout the range. However, there was a significant decrease in PL-BLA coherence during the CS+ compared to the CS-at ~ 31, 33 and 44 Hz. Yet, PL-BLA coherence in males also showed a significant increase during the CS+ compared to the CS- at ~33 and 43 Hz ($P < 0.05$). Although they showed higher overall PL-BLA coherence, females only show a significant increase in PL-BLA coherence at ~44 Hz, where there is more coherence during presentations of the CS+, compared to the CS- ($P < 0.05$). Males also showed a moderate overall level of IL-BLA coherence, with a significant increase in IL-BLA coherence during the CS+ in comparison to the CS- at ~30, 37 and 42 Hz ($P < 0.05$). Females also showed a moderate overall level of IL-BLA coherence, with a significant increase in IL-BLA coherence during presentations of the CS+ in comparison to the CS- at ~33, 37 and 44Hz ($P < 0.05$). Interestingly, these frequencies correspond approximately with the frequencies at which decreases in BLA low power were observed in the females during the CS+ compared to the CS- (see Figure 4.19, above). Finally, there was a lack of PL-IL coherence in males. Despite this, males show a significant, but small, increase in PL-IL coherence during the CS+ compared to the CS- at ~ 38 Hz ($P < 0.05$). Females only showed overall PL-IL coherence at frequencies higher than ~40 Hz, but, unlike males, showed no significant increases in PL-IL coherence between presentations of the CS+ vs CS-.

PL-BLA
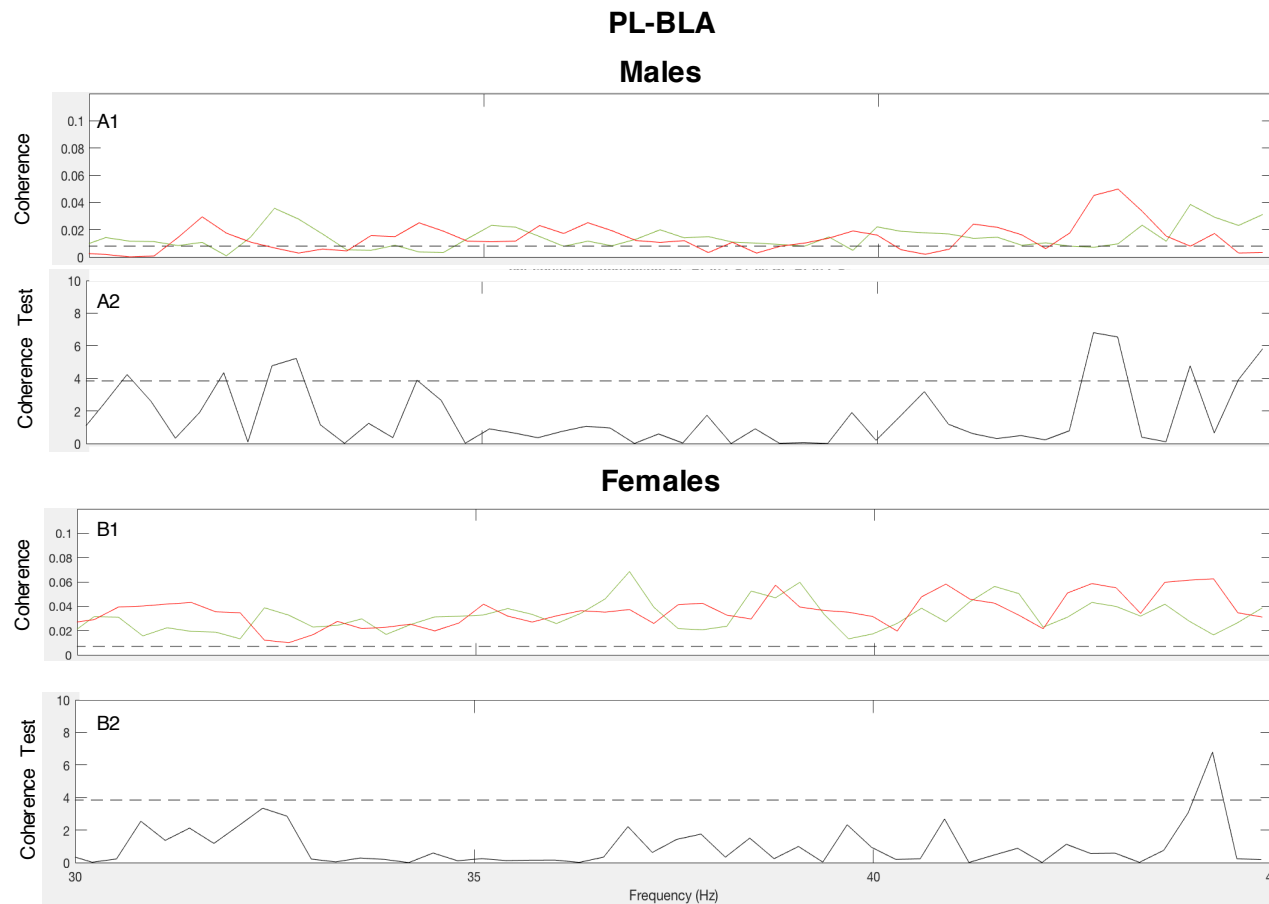
Males

Females

Figure 4.20. Pooled PL-BLA low gamma coherence for males (A1) and females (B1) for CS+ (red) vs CS- (green) and comparison of coherence tests quantifying differences in coherence during the CS+ vs CS- for males (A2) and females (B2). The dashed line denotes the 95% confidence limit. Upper panel: above this line shows significant overall coherence between regions during presentations of the CS+ (red) and CS- (green) (P < 0.05). Lower panel: peaks above this line show a significant increase in coherence between regions during presentations of either the CS+ or CS-. Males showed increases in coherence during presentations of the CS+ (vs CS-) at ~32 and 43 Hz, but also during presentations of the CS- (vs CS+) at ~31, 33 and 44 Hz. Females showed an increase in coherence during presentations of the CS+ (vs CS-) at ~ 44 Hz.
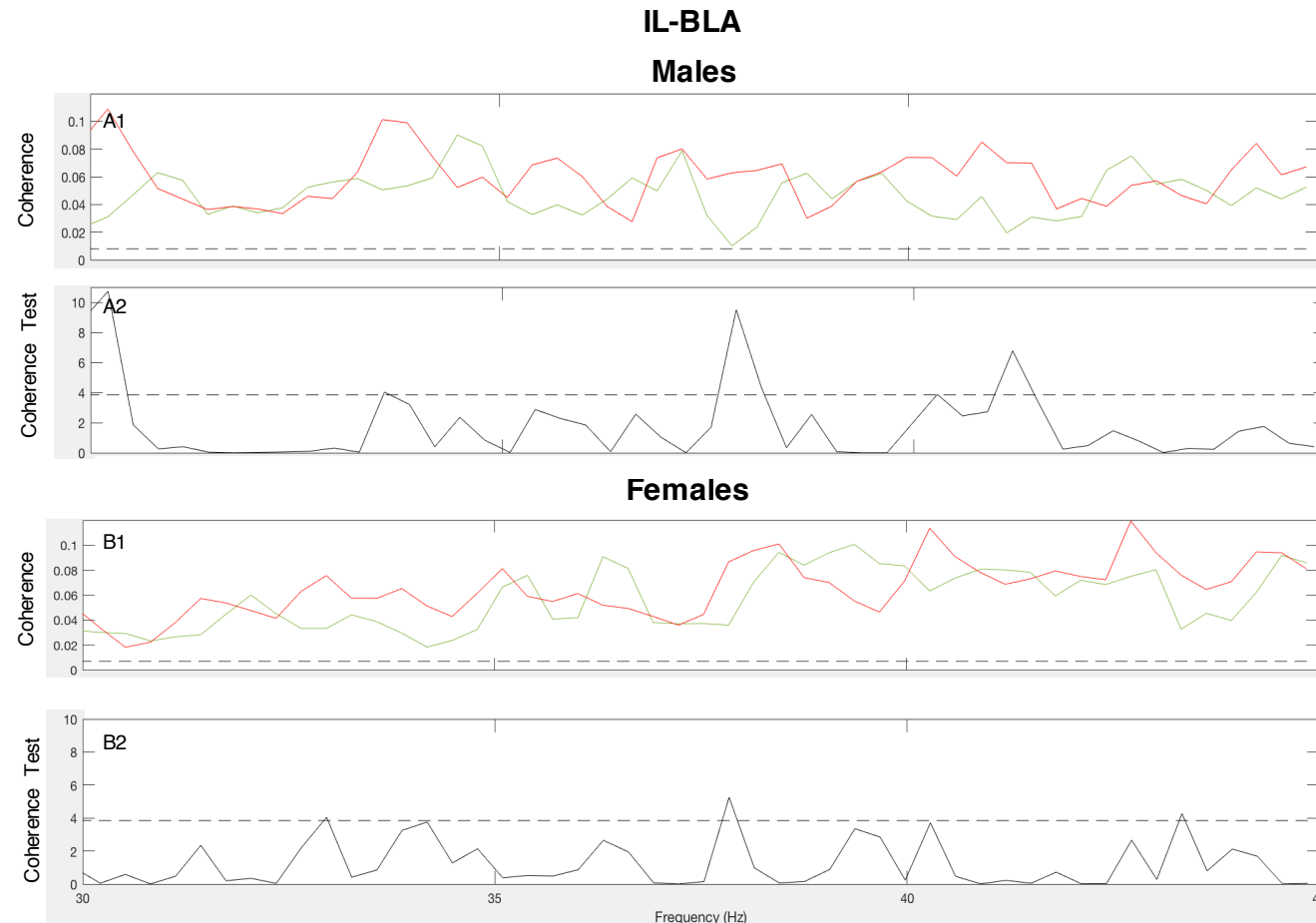
Figure 4.21. Pooled IL-BLA low gamma coherence for males (A1) and females (B1) for CS+ (red) vs CS- (green) and comparison of coherence tests quantifying differences in coherence during the CS+ vs CS- for males (A2) and females (B2). The dashed line denotes the 95% confidence limit. Upper panel: above this line shows significant overall coherence between regions during presentations of the CS+ (red) and CS- (green) ($P < 0.05$). Lower panel: peaks above this line show a significant increase in coherence between regions during presentations of either the CS+ or CS-. Males showed increases in coherence during presentations of the CS+ at ~30, 38 and 42 Hz. Females showed significant, small, increases in coherence during the CS+ at ~38 and 43 Hz.
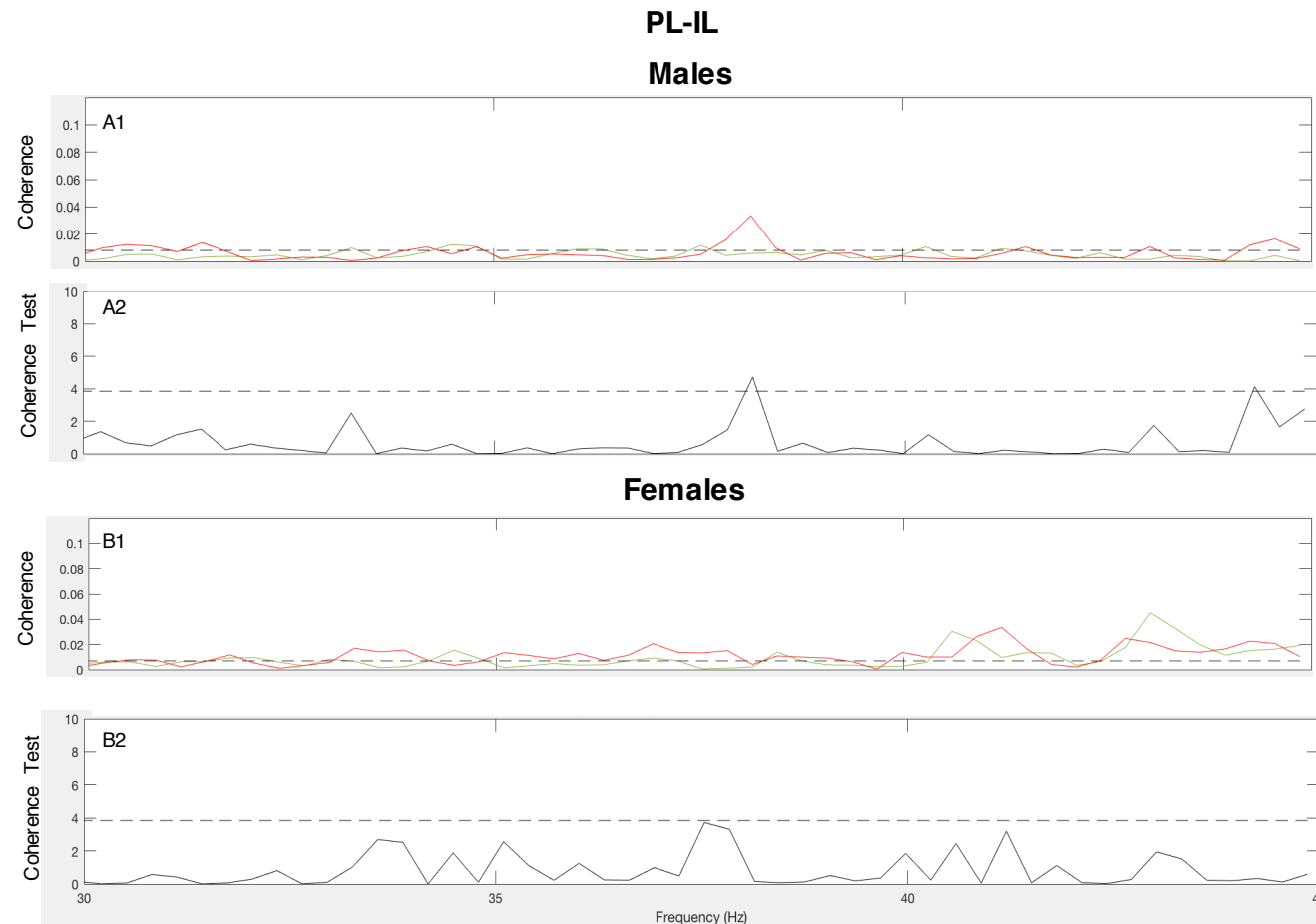
Figure 4.22. Pooled PL-BLA low gamma coherence for males (A1) and females (B1) for CS+ (red) vs CS- (green) and comparison of coherence tests quantifying differences in coherence during the CS+ vs CS- for males (A2) and females (B2). The dashed line denotes the 95% confidence limit. Upper panel: above this line shows significant overall coherence between regions during presentations of the CS+ (red) and CS- (green) ($P < 0.05$). Lower panel: peaks above this line show a significant increase in coherence between regions during presentations of either the CS+ or CS-. Males showed a small increase in coherence during presentations of the CS+ (vs CS-) at ~38 Hz, whereas females showed no tone-dependent significant changes in coherence.

187

4.3.14 Mid Gamma (45-64 Hz)

4.3.15 Mid Gamma Power Colour Plots

PL, IL and BLA mid gamma power during CS+ and CS- presentations in males is presented in Figure 4.23, below. In males, there appeared to be an overall decrease in PL power during presentations of the CS+ compared to the CS-. This is despite the presence of a few narrow bands of increased power during the CS+. For the IL, there did not appear to be any differences between the CS+ and CS- in males. In the BLA however, it appeared that there was a moderate increase in power during the CS+ compared to the CS-.

PL, IL and BLA mid gamma power during CS+ and CS- presentations in females is presented in Figure 4.24, below. In females, it appeared that there was a slight increase in PL power during the CS+ compared to the CS-, but overall differences in power between the two stimuli seemed to be marginal. There appeared to be a slight decrease in IL power during presentations of the CS+ compared to the CS-. In the BLA, there appeared to be a slight decrease in power for presentations of the CS+ compared to the CS-.
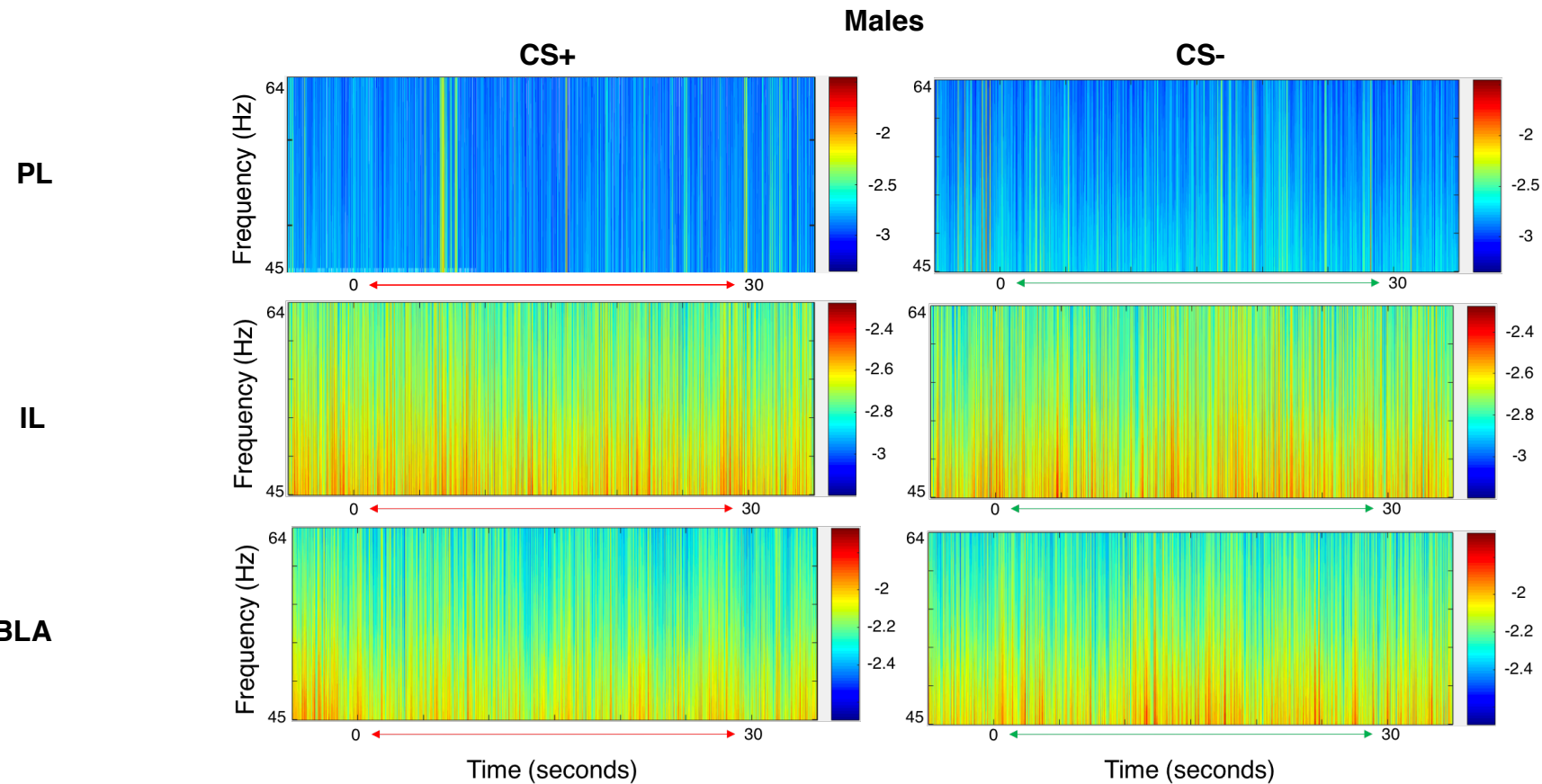
Figure 4.23. PL (top), IL (middle) and BLA (bottom) mid gamma power spectra during CS+ (left) vs CS- (right) presentation in males. In accordance with the colour scale (right), more power is represented by warmer colours (i.e. orange/red) whereas less power is indicated by cooler colours (i.e. blue).
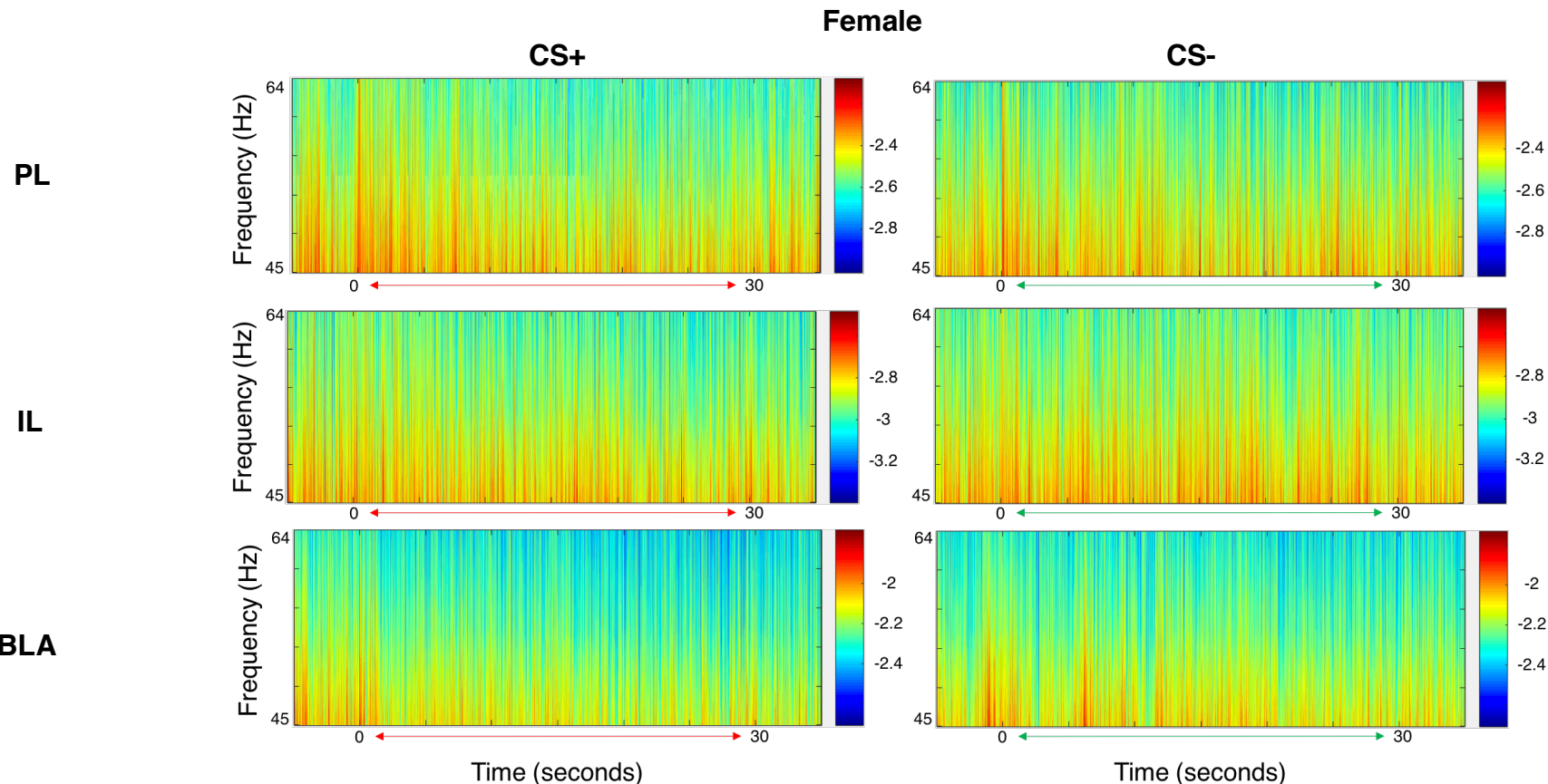
Figure 4.24. PL (top), IL (middle) and BLA (bottom) mid gamma power spectra during CS+ (left) vs CS- (right) presentation in males. In accordance with the colour scale (right), more power is represented by warmer colours (i.e. orange/red) whereas less power is indicated by cooler colours (i.e. blue).

4.3.16 Mid Gamma Power Multi-taper Analysis

Differences in PL, IL and BLA mid gamma power between the CS+ and CS- in males and females are presented in Figures 4.25-4.27, below. Overall, the difference of the largest magnitude observed in the gamma frequency range occurs in mid-gamma, wherein males showed a decrease in PL power during presentations of the CS+ compared to the CS- between ~48 and 54 Hz ($P < 0.05$). In addition to this large difference, males showed another significant, but smaller, decrease in PL mid gamma power during the CS+ compared to the CS- at ~57 Hz ($P < 0.05$). In contrast, even though females showed higher overall PL power, they showed only a few significant, but small, decreases in power during the CS+ compared to the CS- at ~45, 50 and 63 Hz ($P < 0.05$). Further, females also showed a small, but still significant, increase in PL power during the CS+ compared to the CS- at ~ 61 Hz.

Males show a significant, but small, increase in IL power during presentations of the CS+ compared to the CS- at ~48 Hz ($P < 0.05$), whereas females show significant decreases in IL power during presentations of the CS+ compared to the CS- at multiple frequencies (~49, 51, 61 and 63 Hz, $P < 0.05$). Males also showed higher overall levels of IL mid-gamma power than females, which was consistent across all frequencies.

Further to the PL and IL, mid-gamma power in the BLA region also highlighted some interesting sex differences. In males, BLA power showed significant decreases during presentations of the CS+ compared to the CS- at frequencies ~46, 49 and 51 Hz ($P < 0.05$), but also showed significant decreases during presentations of the CS- compared to the CS+ at slightly

higher frequencies of ~57, 58 and 61 Hz (P < 0.05). There was also a significant, but subtle, decrease in BLA power during presentations of the CS+ compared to the CS- at ~63 Hz in males (P < 0.05). Females also showed significant, but smaller, decreases in BLA mid-gamma power during presentations of the CS+ compared to the CS- at frequencies ~46, 48, 51 and 52 Hz (P < 0.05). Further, females also showed a subtle increase in BLA power during presentations of the CS+ compared to the CS- at ~62 Hz (P < 0.05). However, all significant differences in BLA mid-gamma power in females were much smaller in magnitude compared to the differences in power observed in males.

PL
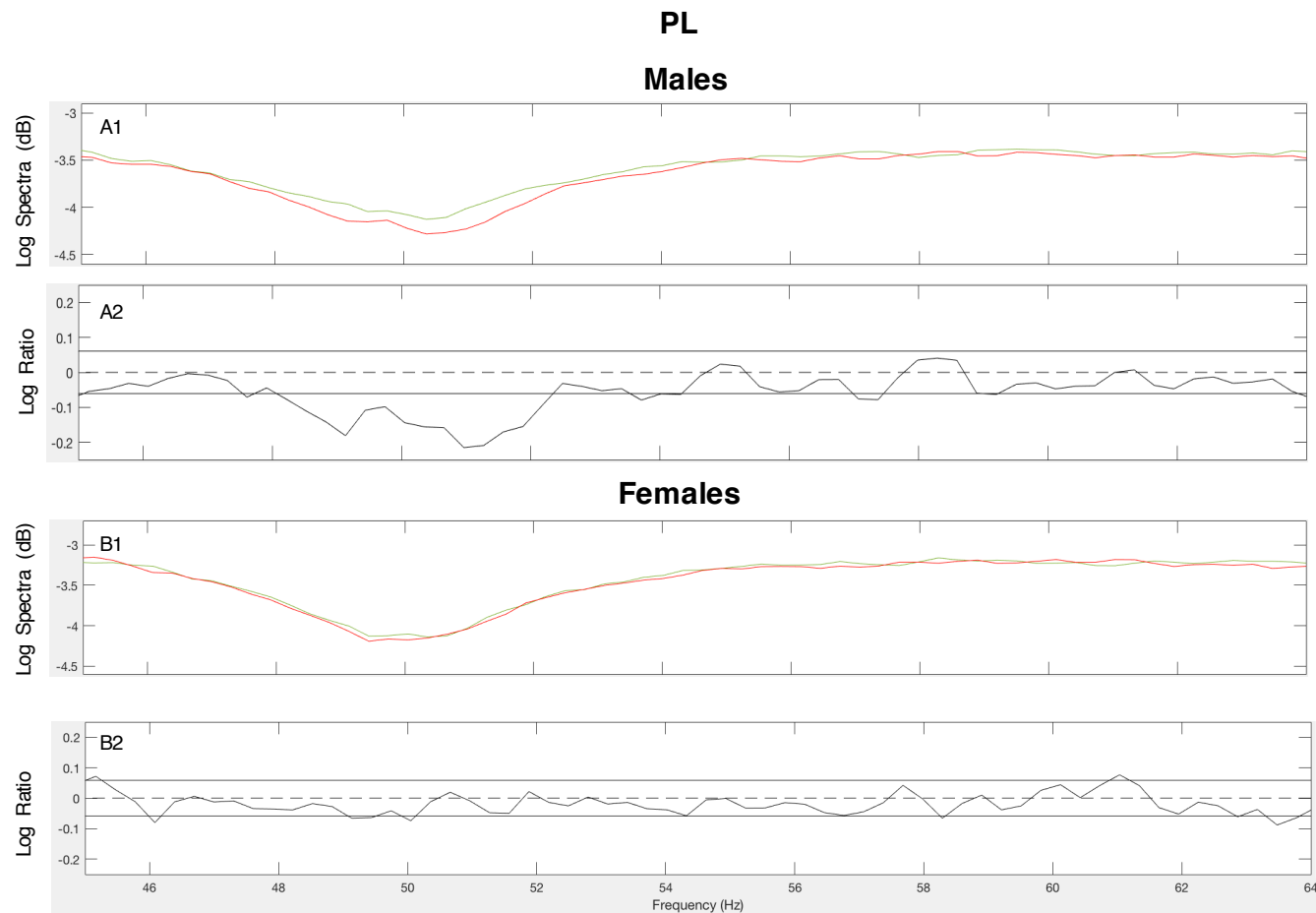
Males

Females

Figure 4.25. Pooled PL mid gamma power spectra for males (A1) and females (B1) for CS+ (red) vs CS- (green) and log ratio tests quantifying differences in power during the CS+ vs CS- for males (A2) and females (B2). The solid horizontal lines in the log ratio plots represent the upper and lower 95% confidence limits; positive log ratio values indicate increased power, whereas negative values indicate decreased power, during the CS+ vs CS-. Males showed a decrease in PL power during presentations of the CS+ vs CS- between ~48-54 Hz and at ~57 Hz. Females showed small decreases during CS+ compared to the CS- at ~45, 50 and 63 Hz. Females also showed a small increase in PL mid-gamma power during the CS+ compared to the CS- at ~61 Hz.

193
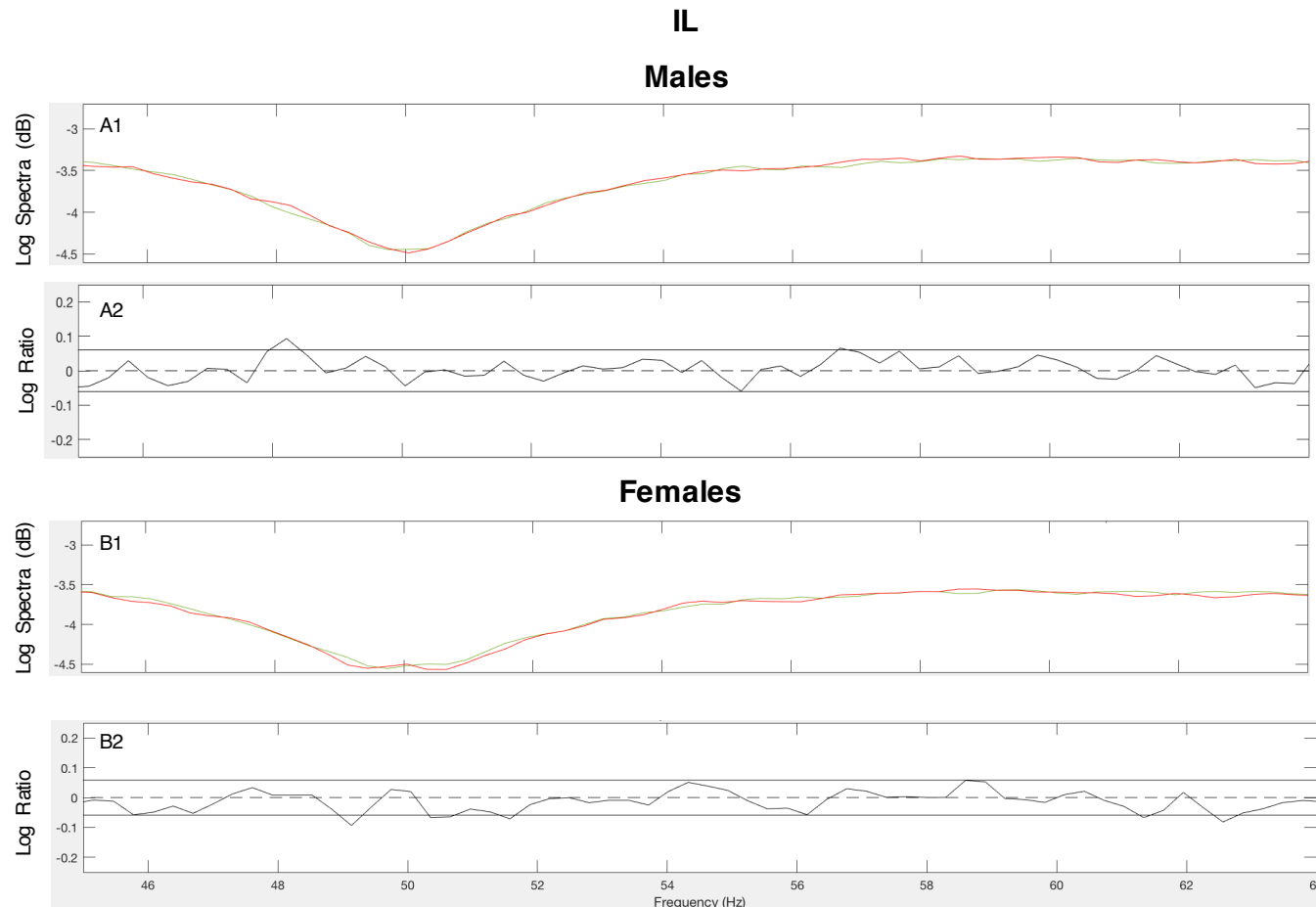
Figure 4.26. Pooled IL mid gamma power spectra for males (A1) and females (B1) for CS+ (red) vs CS- (green) and log ratio tests quantifying differences in power during the CS+ vs CS- for males (A2) and females (B2). The solid horizontal lines in the log ratio plots represent the upper and lower 95% confidence limits; positive log ratio values indicate increased power, whereas negative values indicate decreased power, during the CS+ vs CS-. Males showed an increase in IL mid gamma power during presentations of the CS+ compared to the CS- at ~48 Hz. In contrast, females showed small decreases during the CS+ compared to the CS- at ~49, 51, 52 and 63 Hz.
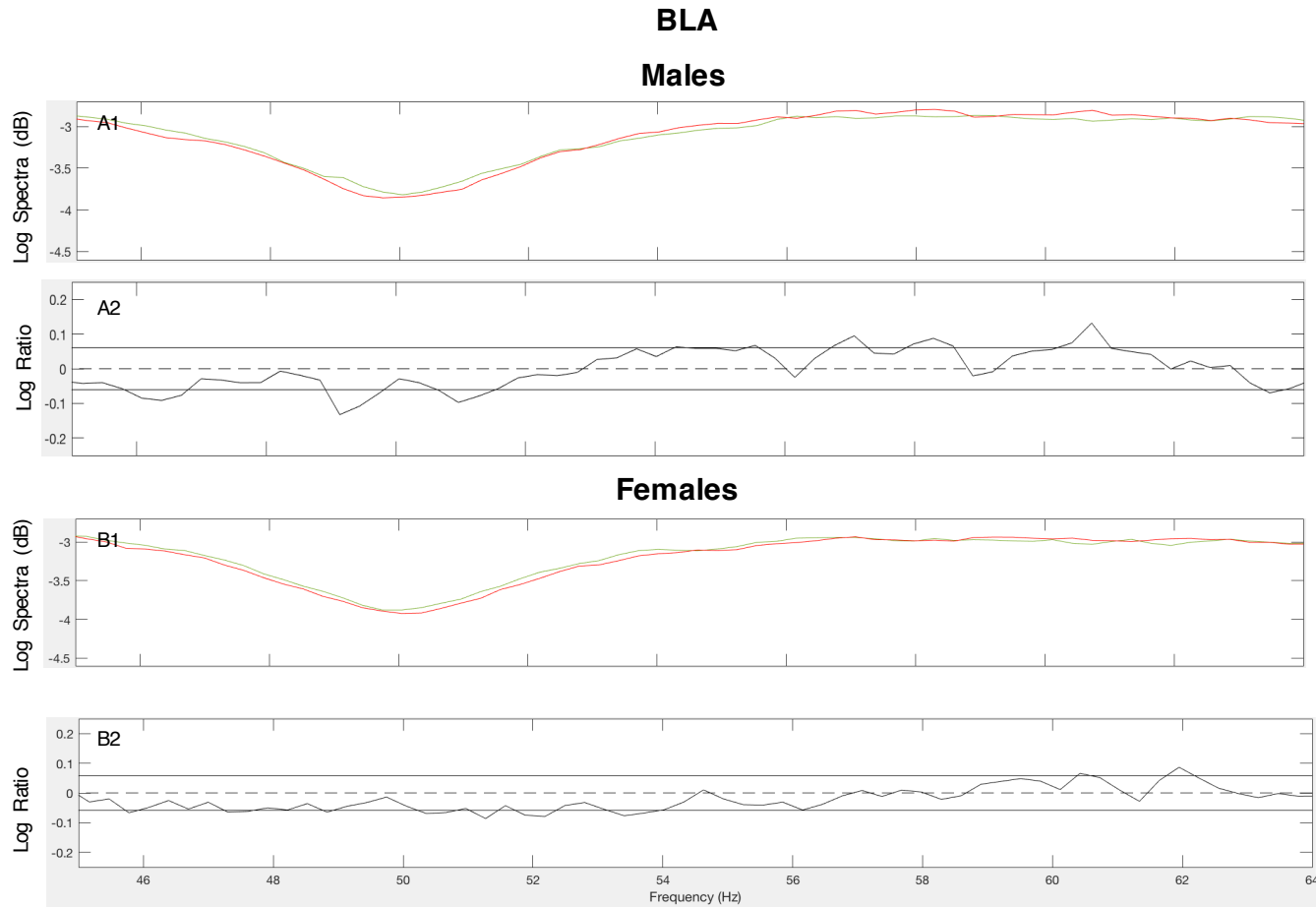
Figure 4.27. Pooled BLA mid gamma power spectra for males (A1) and females (B1) for CS+ (red) vs CS- (green) and log ratio tests quantifying differences in power during the CS+ vs CS- for males (A2) and females (B2). The solid horizontal lines in the log ratio plots represent the upper and lower 95% confidence limits; positive log ratio values indicate increased power, whereas negative values indicate decreased power, during the CS+ vs CS-. Males showed a decrease in BLA power during presentations of the CS+ compared to the CS- at ~46, 49 and 51 Hz, but also showed increases during presentations of the CS+ compared to the CS- at ~57, 58 and 61 Hz. Females showed a similar pattern, but to a lesser magnitude.

4.3.17 Mid Gamma Coherence Colour Plots

PL-BLA, IL-BLA and PL-IL mid gamma coherence during CS+ and CS- presentations in males is presented in Figure 4.28, below. In males, there appeared to be a decrease in PL-BLA coherence during presentations of the CS+ compared to the CS-. In contrast, it appeared that there was slightly more coherence between the IL and BLA during the CS+ in comparison to the CS-. In addition, there did not appear to be any significant differences in PL-IL coherence in males between the CS+ and CS-.

PL-BLA, IL-BLA and PL-IL mid gamma coherence during CS+ and CS- presentations in females is presented in Figure 4.29, below. In females, there appeared to be slightly more coherence between the PL and BLA during presentations of the CS+ in comparison to the CS-. Similarly, there also appeared to be slightly more IL-BLA coherence during presentations of the CS+ compared to the CS-. However, there did not appear to be any significant differences in PL-IL coherence between the CS+ and CS-.
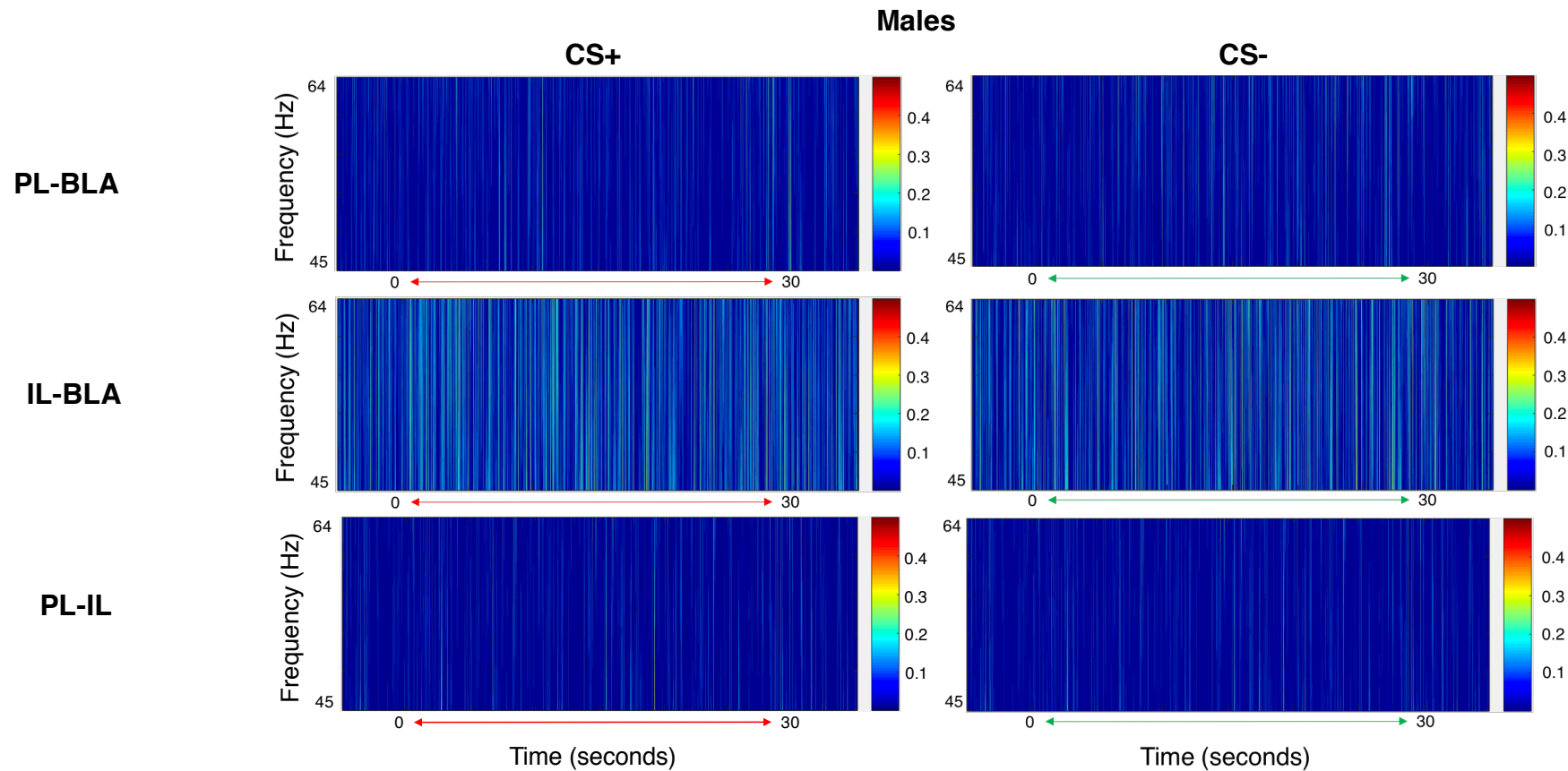
Figure 4.28. PL-BLA (top), IL-BLA (middle) and PL-IL (bottom) mid gamma coherence spectra during CS+ (left) vs CS- (right) for males. In accordance with the colour scale (right), more coherence is represented by warmer colours (i.e. orange/red) whereas less coherence is indicated by cooler colours (i.e. blue).
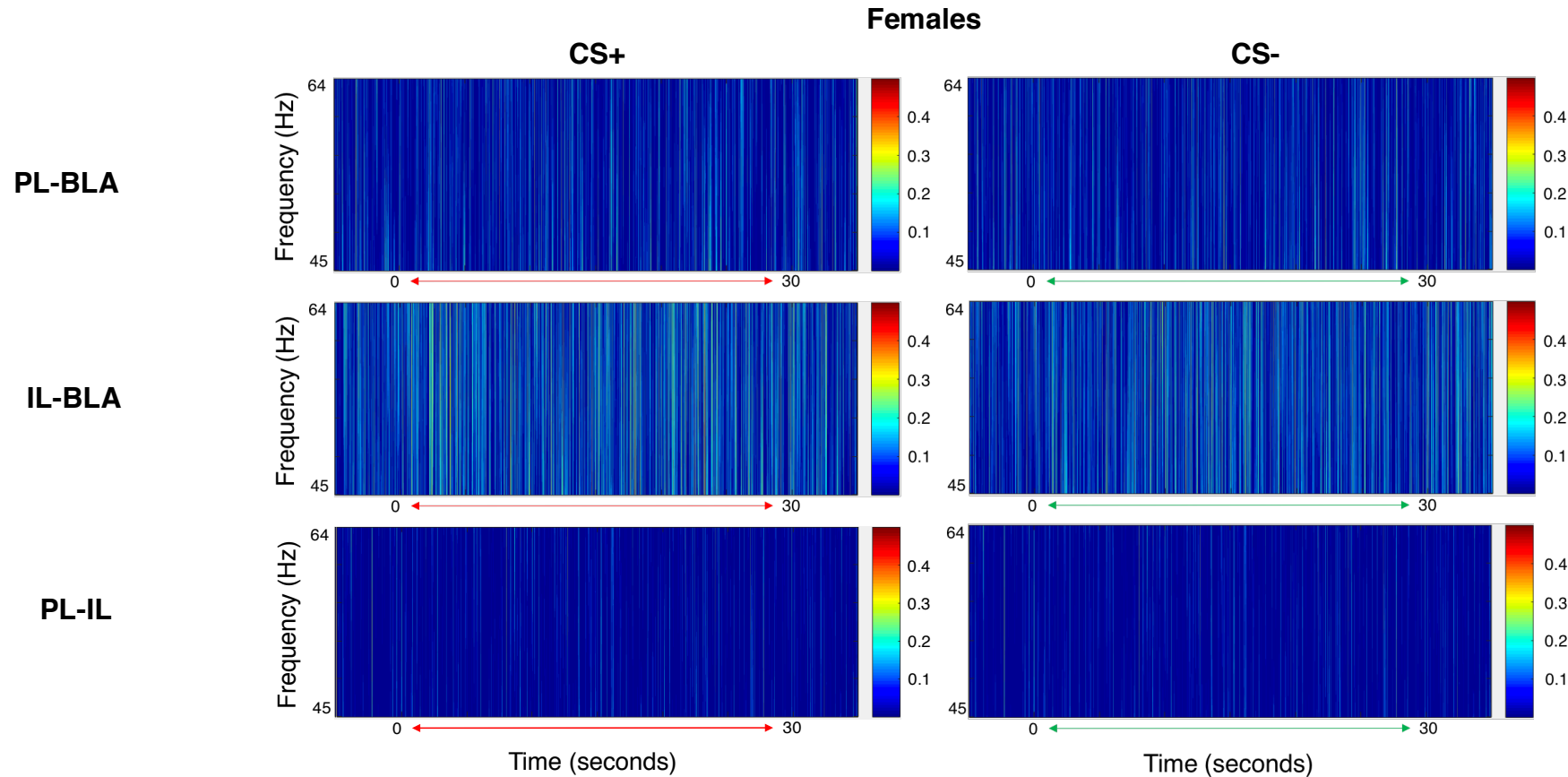
Figure 4.29. PL-BLA (top), IL-BLA (middle) and PL-IL (bottom) mid gamma coherence spectra during CS+ (left) vs CS- (right) for females. In accordance with the colour scale (right), more coherence is represented by warmer colours (i.e. orange/red) whereas less coherence is indicated by cooler colours (i.e. blue).

4.3.18 Mid Gamma Coherence Multi-Taper Analysis

PL-BLA, IL-BLA and PL-IL mid gamma coherence during CS+ and CS- presentations in males and females is presented in Figures 4.30-4.32, below. In males, coherence between the PL and BLA was mostly decreased during presentations of the CS+ compared to the CS- (at ~49, 51, 54, 56 and 60 Hz, $P < 0.05$). However, male PL-BLA coherence also showed a small, but significant, increase in coherence during the CS+ compared to the CS- at ~47 Hz ($P < 0.05$). In contrast, females only showed a single instance of increased coherence during the CS+ compared to the CS- between the PL and BLA at ~57 Hz ($P < 0.05$). Coherence between the IL and BLA showed an increase during the CS+ compared to the CS- at ~49, 51 and 57 Hz in males and at ~61 Hz in females ($P < 0.05$), although the difference observed in the females is much smaller.

As previously shown at theta and low gamma frequencies, coherence between the PL and IL at mid-gamma frequencies was relatively low for both sexes in comparison to coherence between other regions. In males, although the overall coherence between the PL and IL only reached significance at ~50 and 57 Hz, there is a significant decrease in coherence during presentations of the CS+ compared to the CS- at ~ 50 Hz ($P < 0.05$). This may relate to the significant increase in PL power seen during presentations of the CS- compared to the CS+, which was absent in the IL region in males. Interestingly, females also showed two peaks of increased PL-IL coherence at ~50 Hz during presentations of the CS- compared to the CS+ ($P < 0.05$).

PL-BLA
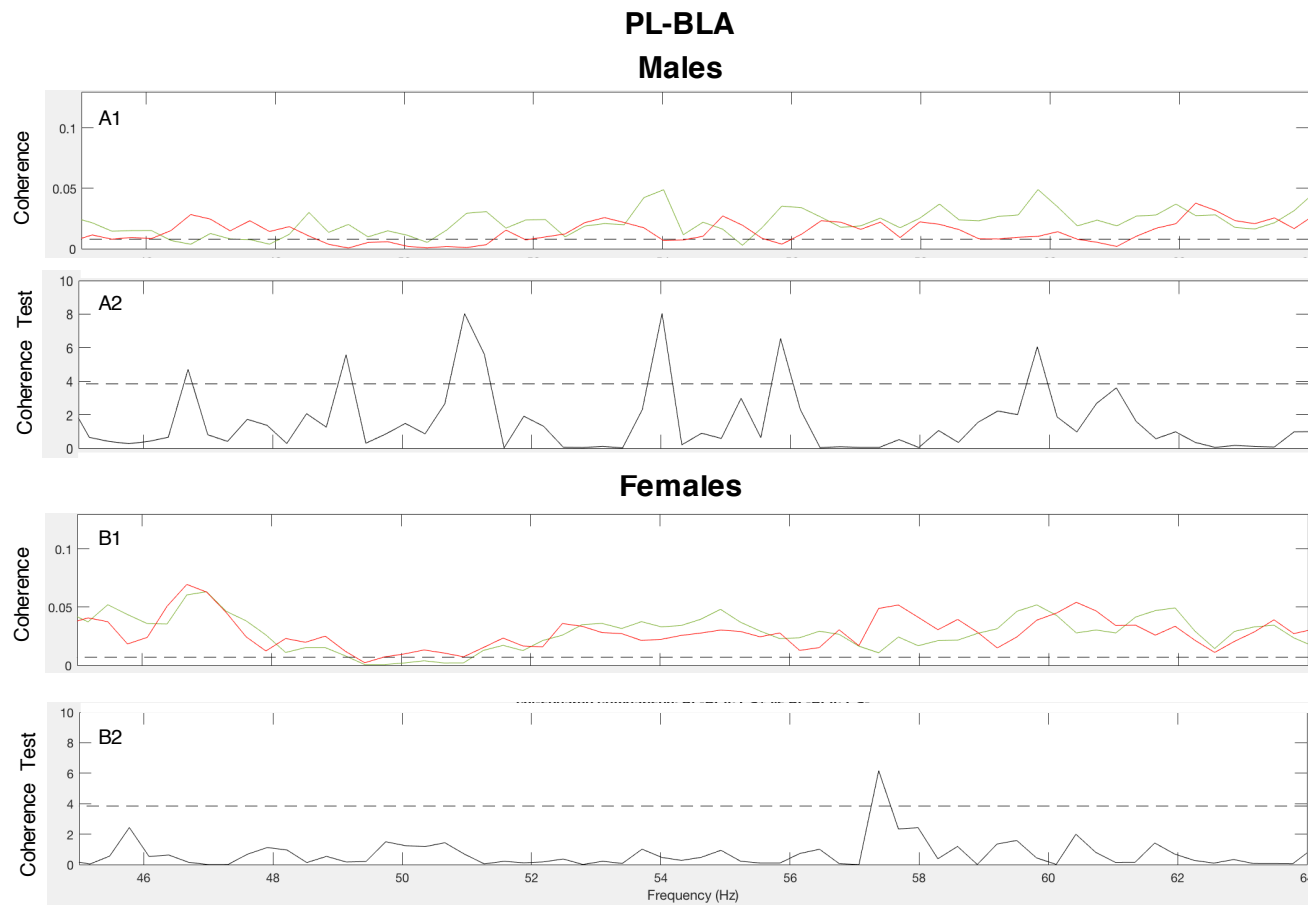
Males

Females

Figure 4.30. Pooled PL-BLA mid gamma coherence for males (A1) and females (B1) for CS+ (red) vs CS- (green) and comparison of coherence tests quantifying differences in coherence during the CS+ vs CS- for males (A2) and females (B2). The dashed line denotes the 95% confidence limit. Upper panel: above this line shows significant overall coherence between regions during presentations of the CS+ (red) and CS- (green) (P < 0.05). Lower panel: peaks above this line show a significant increase in coherence between regions during presentations of either the CS+ or CS-. Males showed a decrease in coherence during presentations of the CS+ at ~49, 51, 54, 56 and 60 Hz, but also showed a small increase in coherence during the CS+ at ~47 Hz. Females showed a small increase in coherence during the CS+ at ~57 Hz
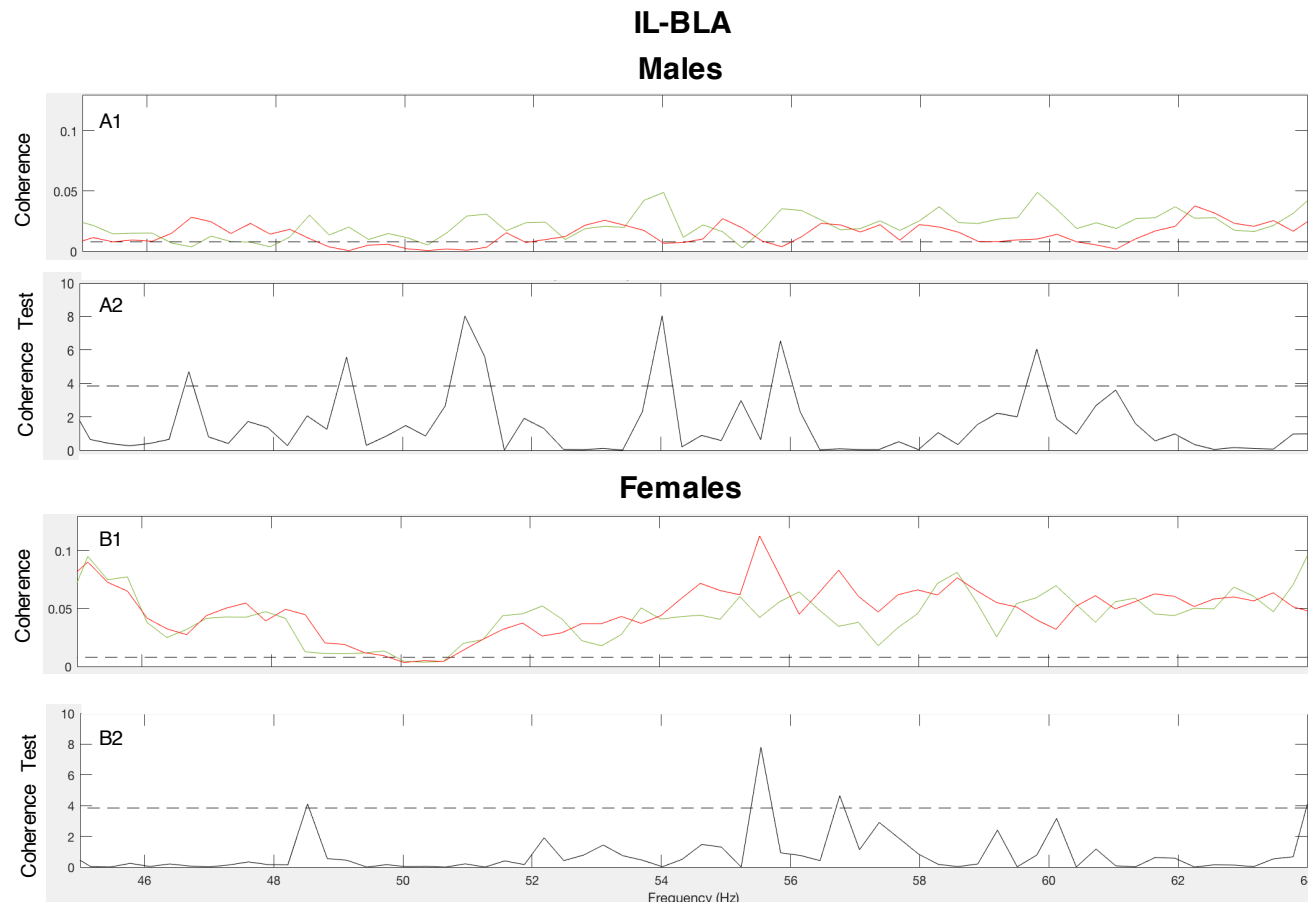
Figure 4.31. Pooled IL-BLA mid gamma coherence for males (A1) and females (B1) for CS+ (red) vs CS- (green) and comparison of coherence tests quantifying differences in coherence during the CS+ vs CS- for males (A2) and females (B2). The dashed line denotes the 95% confidence limit. Upper panel: above this line shows significant overall coherence between regions during presentations of the CS+ (red) and CS- (green) (P < 0.05). Lower panel: peaks above this line show a significant increase in coherence between regions during presentations of either the CS+ or CS-. Males showed multiple increases in coherence during presentations of the CS+ at ~48, 55 and 57 Hz. Females showed two small increases in coherence during the CS+ at ~55 and 57 Hz.
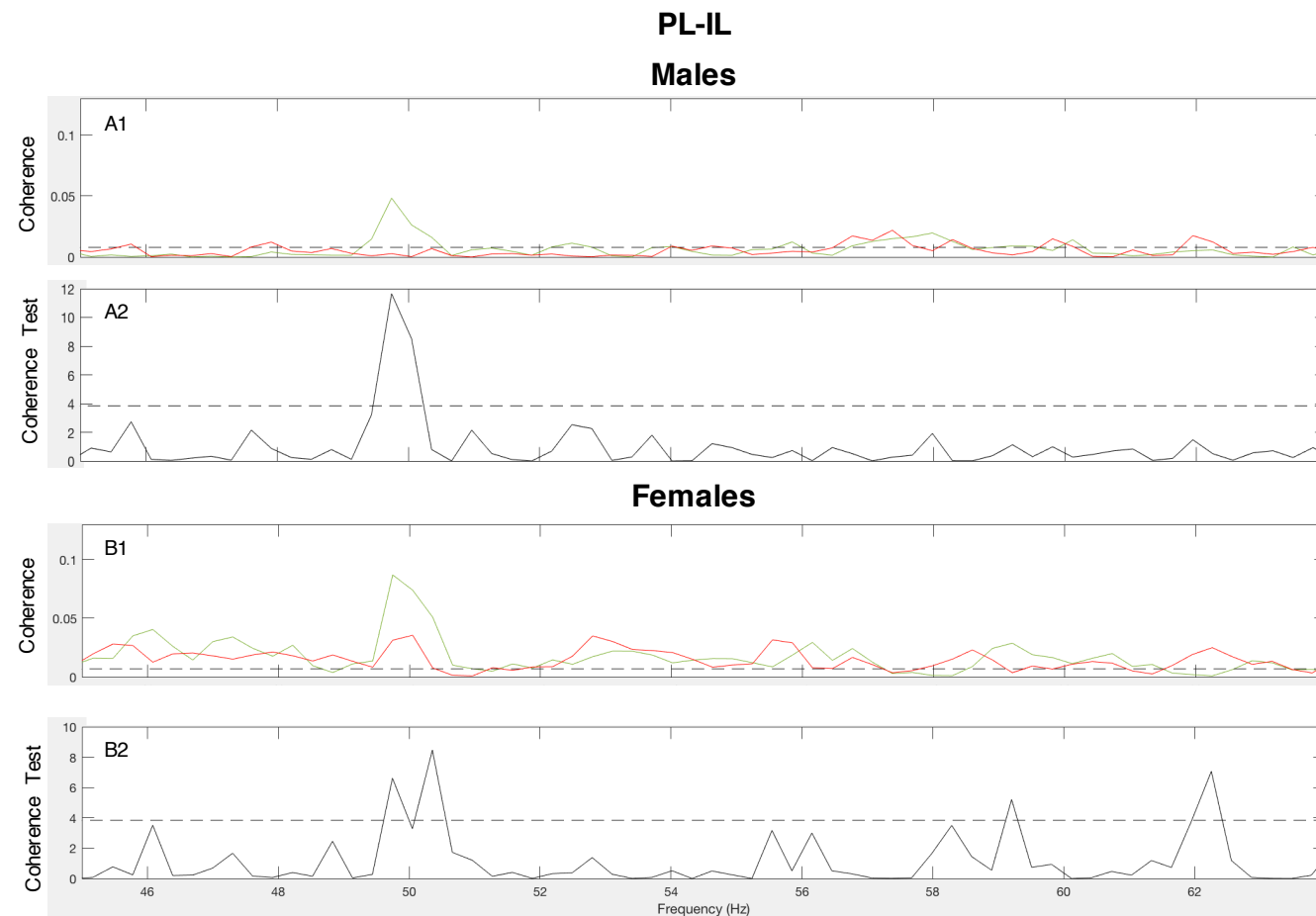
PL-IL

Males

Females

Figure 4.32. Pooled PL-IL mid gamma coherence for males (A1) and females (B1) for CS+ (red) vs CS- (green) and comparison of coherence tests quantifying differences in coherence during the CS+ vs CS- for males (A2) and females (B2). The dashed line denotes the 95% confidence limit. Upper panel: above this line shows significant overall coherence between regions during presentations of the CS+ (red) and CS- (green) (P < 0.05). Lower panel: peaks above this line show a significant increase in coherence between regions during presentations of either the CS+ or CS-. Both males and females showed low levels of overall coherence in addition to a significant decrease in coherence shown during CS+ compared to CS- at ~50 Hz.

4.3.19 High Gamma (64-128 Hz)

4.3.20 High Gamma Power Colour Plots

PL, IL and BLA high gamma power during CS+ and CS- presentations in males is presented in Figure 4.33, below. In males, it appeared that there was slightly less overall PL power during the CS+ compared to the CS-, but this may due to the small, transient increases in power seen near the start of the tone. It also appeared that there was a slight decrease in IL power during the CS+ compared to the CS- in males, wherein this increase appeared to be localised to the last half second of the CS- tone. In the BLA, it also appeared that there was less power during the CS+ compared to the CS- in males.

PL, IL and BLA high gamma power during CS+ and CS- presentations in females is presented in Figure 4.34, below. Despite a large increase in power at tone onset, there appears to be little overall change in PL power during the CS+ in comparison to the CS- in females. In contrast, it appeared that there was a slight decrease in IL power during the CS+ compared to the CS- in females. Further, there appeared to be more high gamma power during the CS- compared to the CS+ in the BLA in females.

Males

CS+

CS-

PL

IL

BLA

Frequency (Hz)

Time (seconds)

Time (seconds)
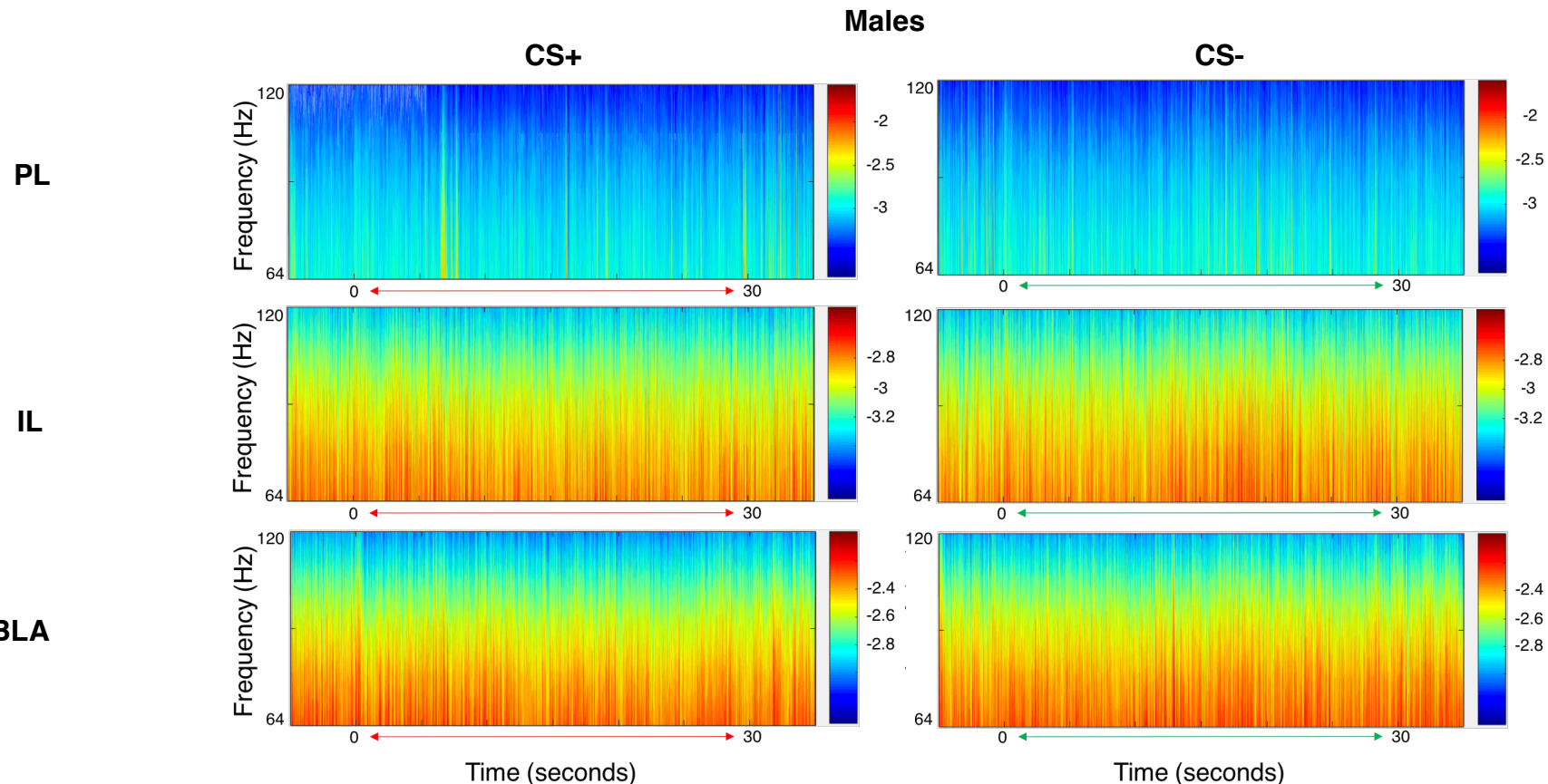
Figure 4.33. PL (top), IL (middle) and BLA (bottom) high gamma power spectra during CS+ (left) vs CS- (right) presentation in males. In accordance with the colour scale (right), more power is represented by warmer colours (i.e. orange/red) whereas less power is indicated by cooler colours (i.e. blue)
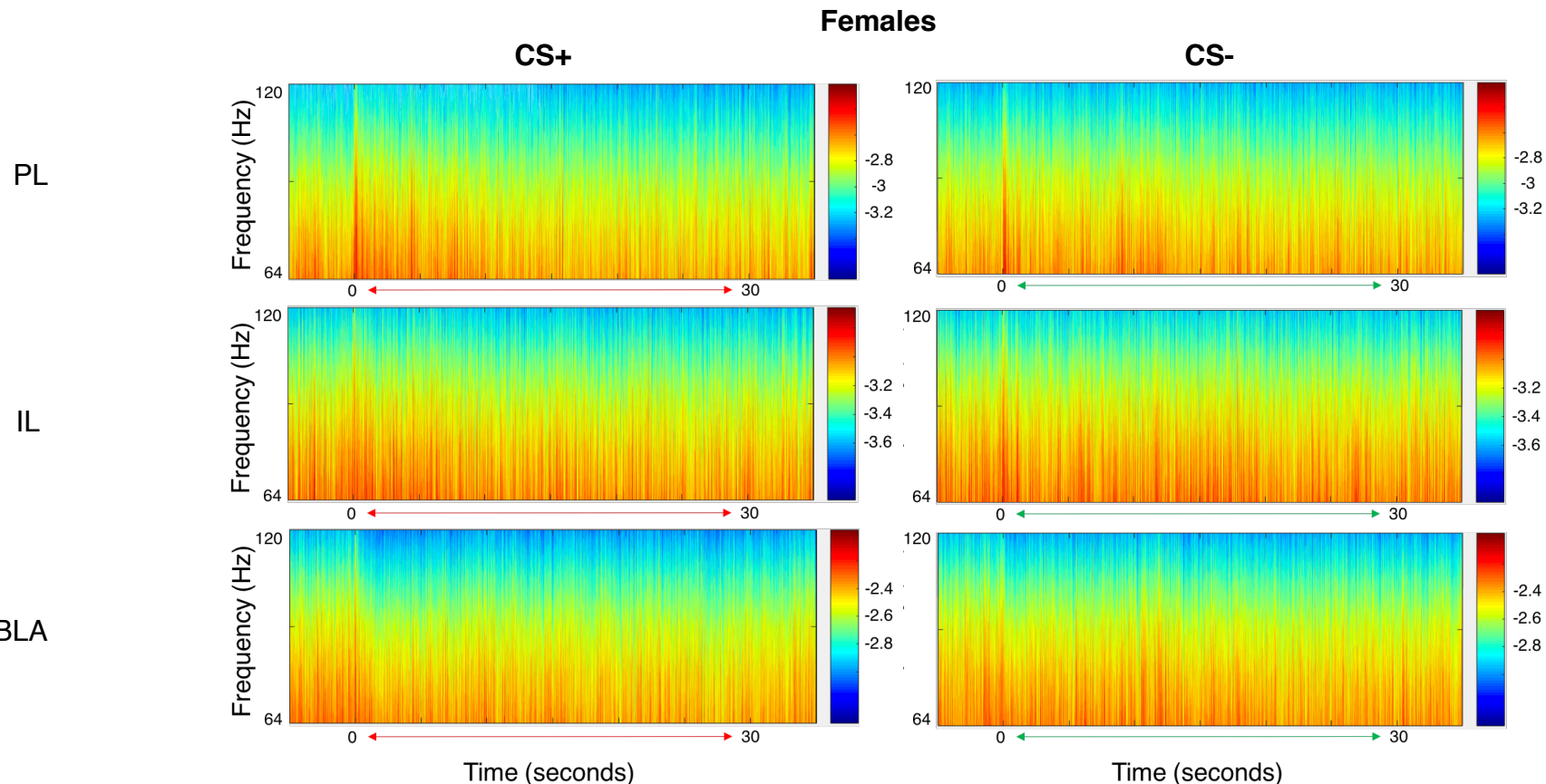
Females

Figure 4.34. PL (top), IL (middle) and BLA (bottom) high gamma power spectra during CS+ (left) vs CS- (right) presentation in females. In accordance with the colour scale (right), more power is represented by warmer colours (i.e. orange/red) whereas less power is indicated by cooler colours (i.e. blue).

4.3.21 High Gamma Power Multi-taper analysis

Differences in PL, IL and BLA high gamma power between the CS+ and CS- in males and females are presented in Figures 4.35-4.37, below. Both males and females showed significant decreases in PL power during presentations of the CS+ compared to the CS- at multiple frequencies, although males showed more significant differences, which were also greater in magnitude. Overall, these differences were present at higher frequencies (>90 Hz) in males than in females (~90 Hz).

For the IL, both sexes showed significant decreases in power during presentations of the CS+ compared to the CS-, where males again showed more differences of a greater magnitude.

Overall, the biggest differences in power at high gamma occurred in the BLA. In this region, males showed a significant decrease in BLA high gamma power during the CS+ compared to the CS- for multiple frequencies. Females also showed significant decreases in BLA high gamma power during the CS+ compared to the CS-, but for fewer frequencies compared to males. In addition, these differences are again smaller in magnitude compared to males.
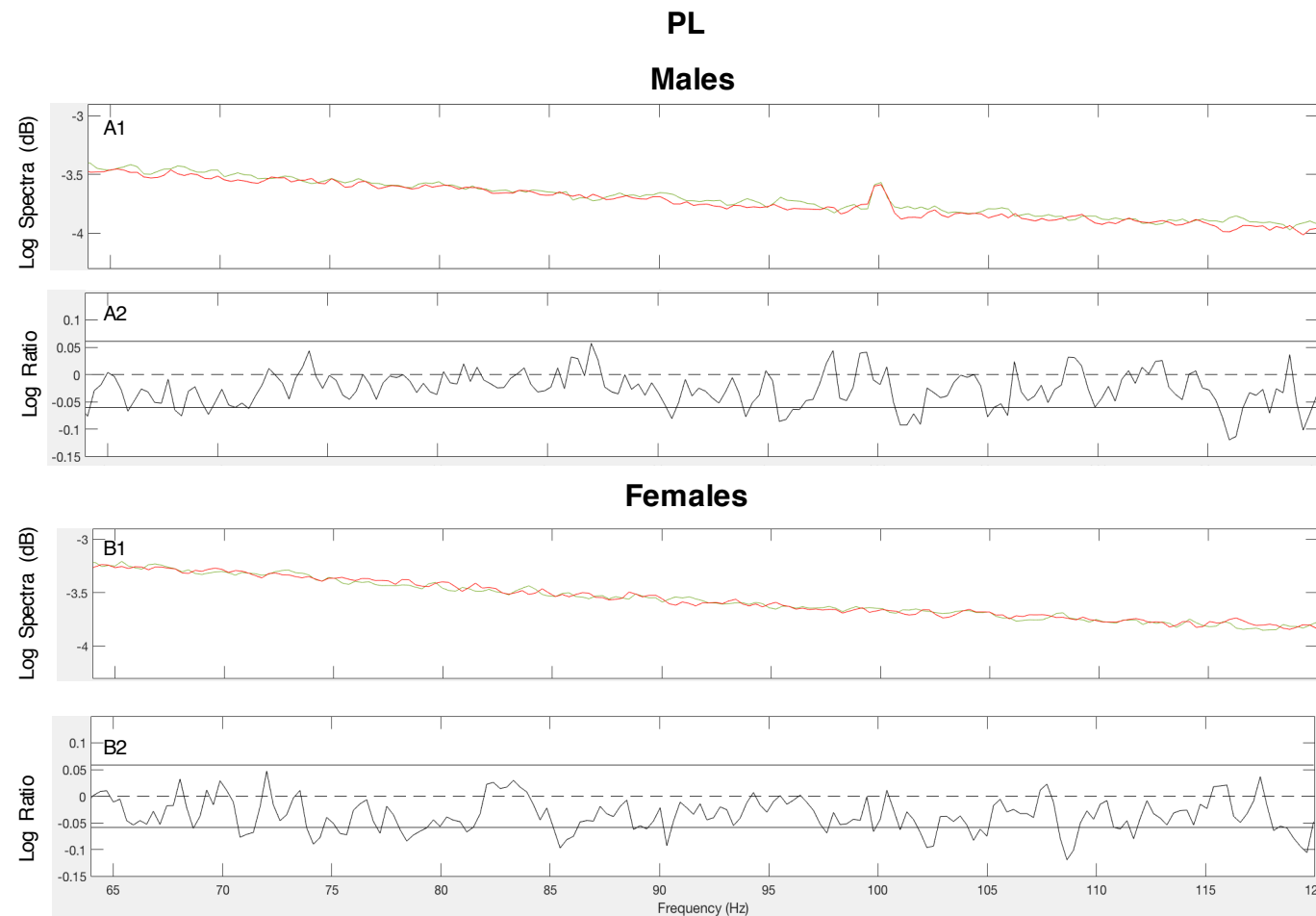
Figure 4.35. Pooled PL high gamma power spectra for males (A1) and females (B1) for CS+ (red) vs CS- (green) and log ratio tests quantifying differences in power during the CS+ vs CS- for males (A2) and females (B2). The solid horizontal lines in the log ratio plots represent the upper and lower 95% confidence limits; positive log ratio values indicate increased power, whereas negative values indicate decreased power, during the CS+ vs CS-. Both males and females showed significant decreases in PL power during presentations of the CS+ compared to the CS-.

IL
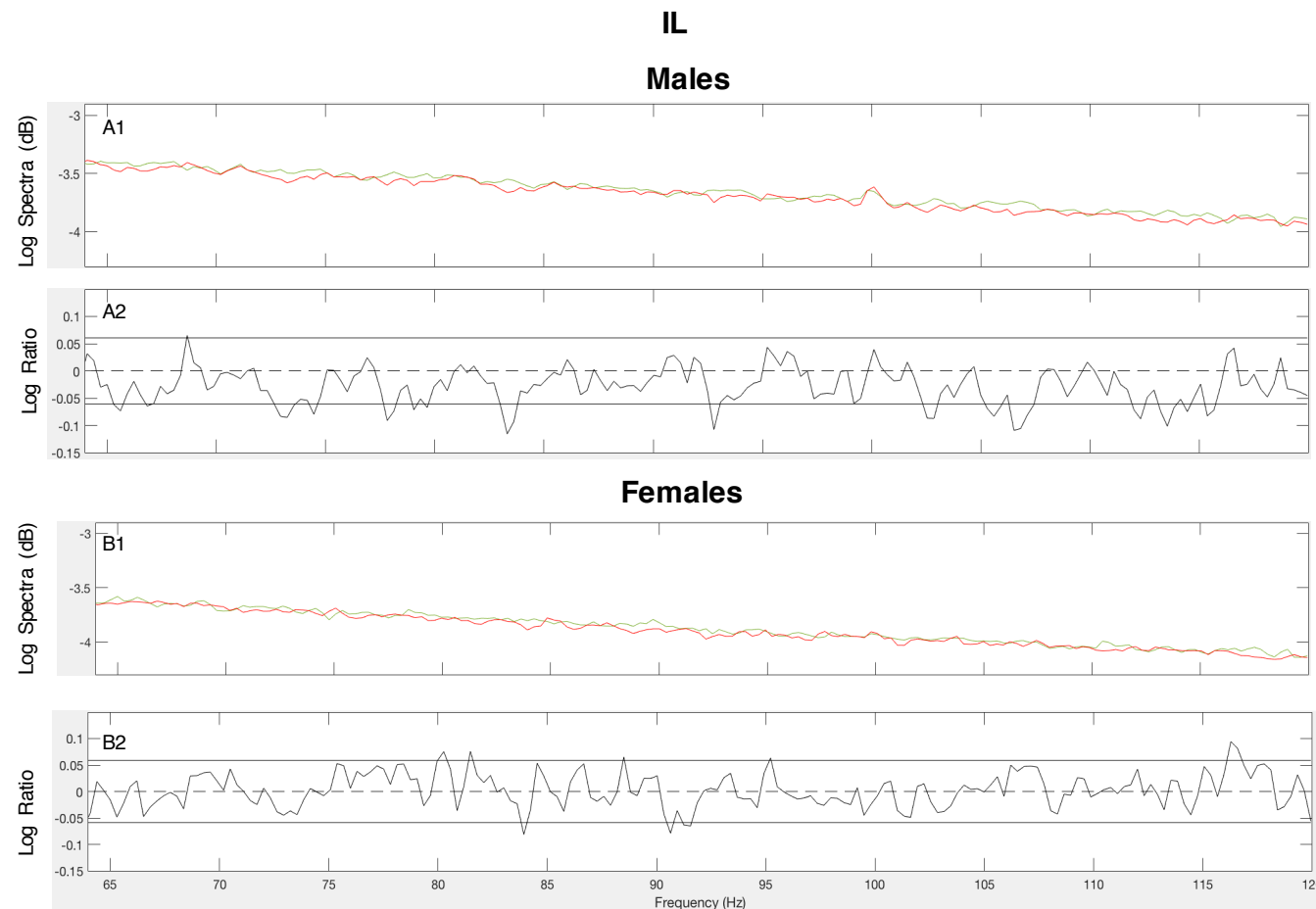
Males

Females

Figure 4.36. Pooled IL high gamma power spectra for males (A1) and females (B1) for CS+ (red) vs CS- (green) and log ratio tests quantifying differences in power during the CS+ vs CS- for males (A2) and females (B2). The solid horizontal lines in the log ratio plots represent the upper and lower 95% confidence limits; positive log ratio values indicate increased power, whereas negative values indicate decreased power, during the CS+ vs CS-. Males and females showed decreases in IL power during presentations of the CS+ compared to the CS-, although these differences are more numerous and larger in magnitude in males compared to females. Females also showed an increase in IL power during presentations of the CS+ at ~80-82 and 117 Hz.

208

BLA
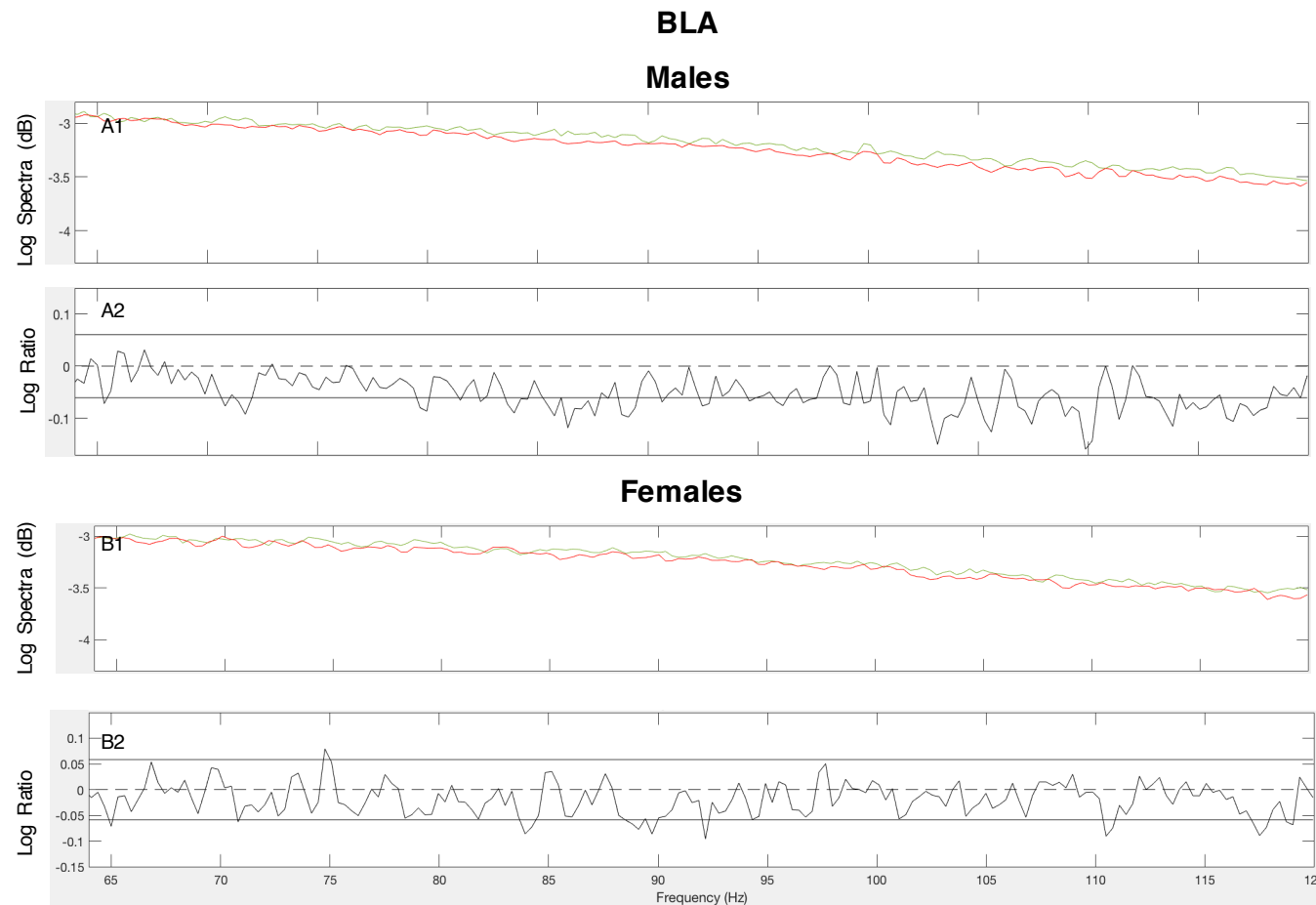
Males

Females

Figure 4.37. Pooled BLA high gamma power spectra for males (A1) and females (B1) for CS+ (red) vs CS- (green) and log ratio tests quantifying differences in power during the CS+ vs CS- for males (A2) and females (B2). The solid horizontal lines in the log ratio plots represent the upper and lower 95% confidence limits; positive log ratio values indicate increased power, whereas negative values indicate decreased power, during the CS+ vs CS-. Males showed a significant decrease in BLA power during the CS+ compared to the CS- for multiple frequencies. Females also showed significant decreases in BLA power during the CS+, but for fewer frequencies compared to males.

4.3.22 High Gamma Coherence Colour Plots

PL-BLA, IL-BLA and PL-IL high gamma coherence during CS+ and CS-presentations in males and females are presented in Figures 4.38-4.39, below. As there are no discernible visual differences in coherence for high gamma, qualitative observations of these data will not be discussed here. Instead, quantitative differences in coherence are described in detail with regards to multi-taper analysis below.
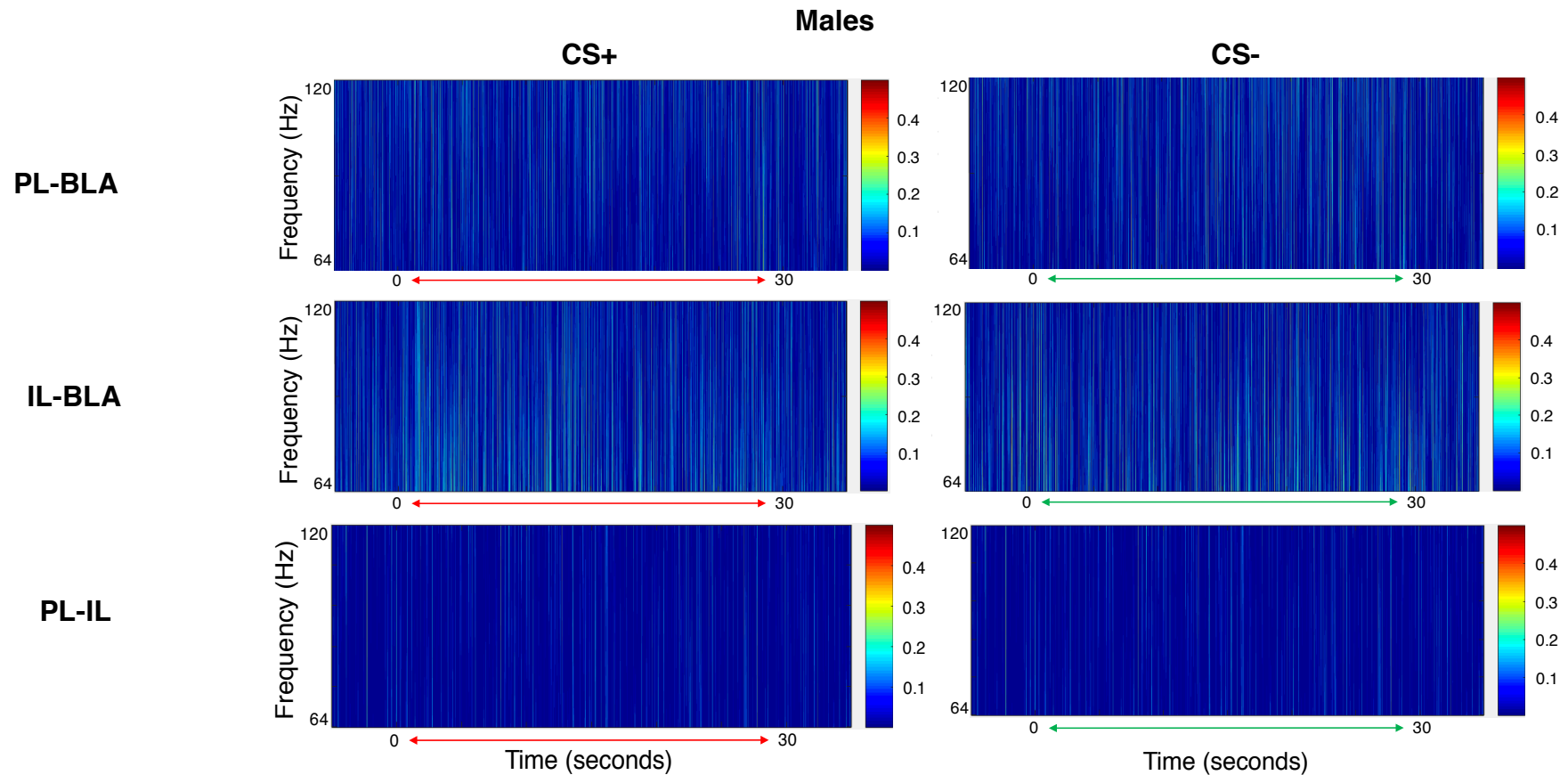
Figure 4.38. PL-BLA (top), IL-BLA (middle) and PL-IL (bottom) high gamma coherence spectra during CS+ (left) vs CS- (right) for males. In accordance with the colour scale (right), more coherence is represented by warmer colours (i.e. orange/red) whereas less coherence is indicated by cooler colours (i.e. blue).
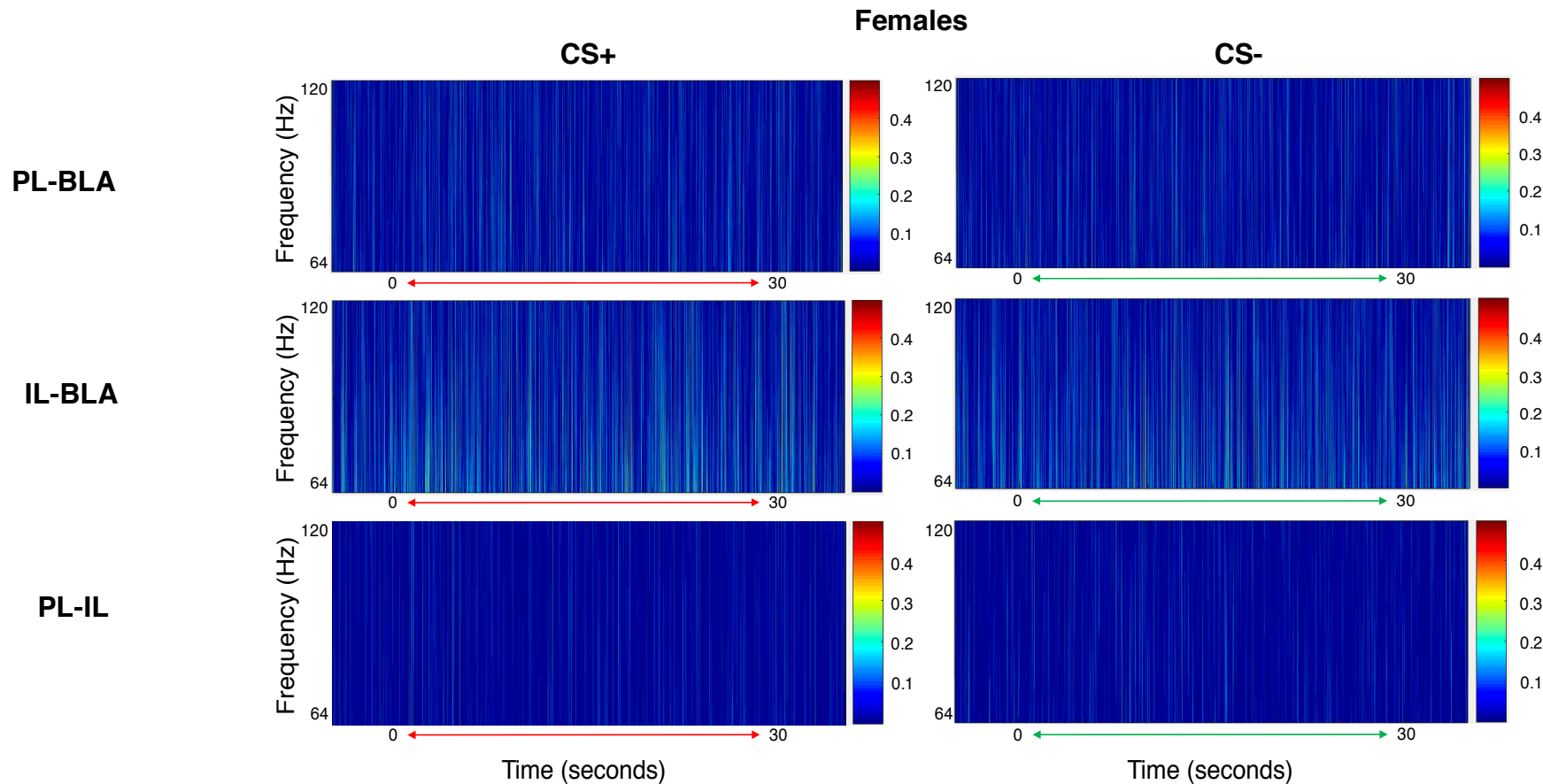
Figure 4.39. PL-BLA (top), IL-BLA (middle) and PL-IL (bottom) high gamma coherence spectra during CS+ (left) vs CS- (right) for females. In accordance with the colour scale (right), more coherence is represented by warmer colours (i.e. orange/red) whereas less coherence is indicated by cooler colours (i.e. blue).

4.3.23 High Gamma Coherence Multi-Taper Analysis

PL-BLA, IL-BLA and PL-IL high gamma coherence during CS+ and CS-presentations in males and females is presented in Figures 4.40-4.42, below. In males, coherence between the PL and BLA was significantly decreased during presentations of the CS+ compared to the CS- (~69 and 71, 102, 117 Hz). However, PL-BLA coherence was also significantly increased during presentations of the CS+ compared to the CS- (~100 Hz) ($P < 0.05$) Similarly, females also showed several instances of significantly decreased coherence during the CS+ relative to the CS- (~ 79 and 119 Hz) in addition to significantly increased coherence during the CS+ relative to the CS- (~110 Hz) ($P < 0.05$).

In males, there were multiple instances where coherence between the IL and BLA was significantly decreased during the CS+ compared to the CS- (~67, 73, 83, 88, 113 Hz) ($P < 0.05$), but there were also instances where IL-BLA coherence was decreased during the CS+ compared to the CS- (~ 68, 74, 89 Hz) ($P < 0.05$). In contrast, coherence between the IL and BLA regions only showed a significant decrease during the CS+ compared to the CS- in females (~ 69, 83, 92 Hz) ($P < 0.05$).

As previously shown at theta and low/mid gamma frequencies, there were also lower levels of coherence between the PL and IL at high-gamma frequencies. In males, the overall coherence between the PL and IL only reached coherence at approximately ~100 and 105 Hz. Similar to the 50 Hz spike seen at mid-gamma in males, there was significantly less coherence at 100 Hz during presentations of the CS+ compared to presentations of the CS-. However, this difference was only borderline significant. Males also showed

other multiple, but very subtle, increases in coherence, but as overall coherence between these two regions was very low, it was difficult to determine whether these were meaningful. Female PL-IL coherence was significantly decreased during presentations of the CS+ compared to the CS- (~ 66, 69, 82, 86, 90 Hz) (P < 0.05). However, females also showed significantly increased PL-IL coherence during presentations of the CS+ compared to the CS- (~ 81 and 87 Hz) (P < 0.05), meaning that females again showed increased PL-IL coherence during both fear and safety cues.
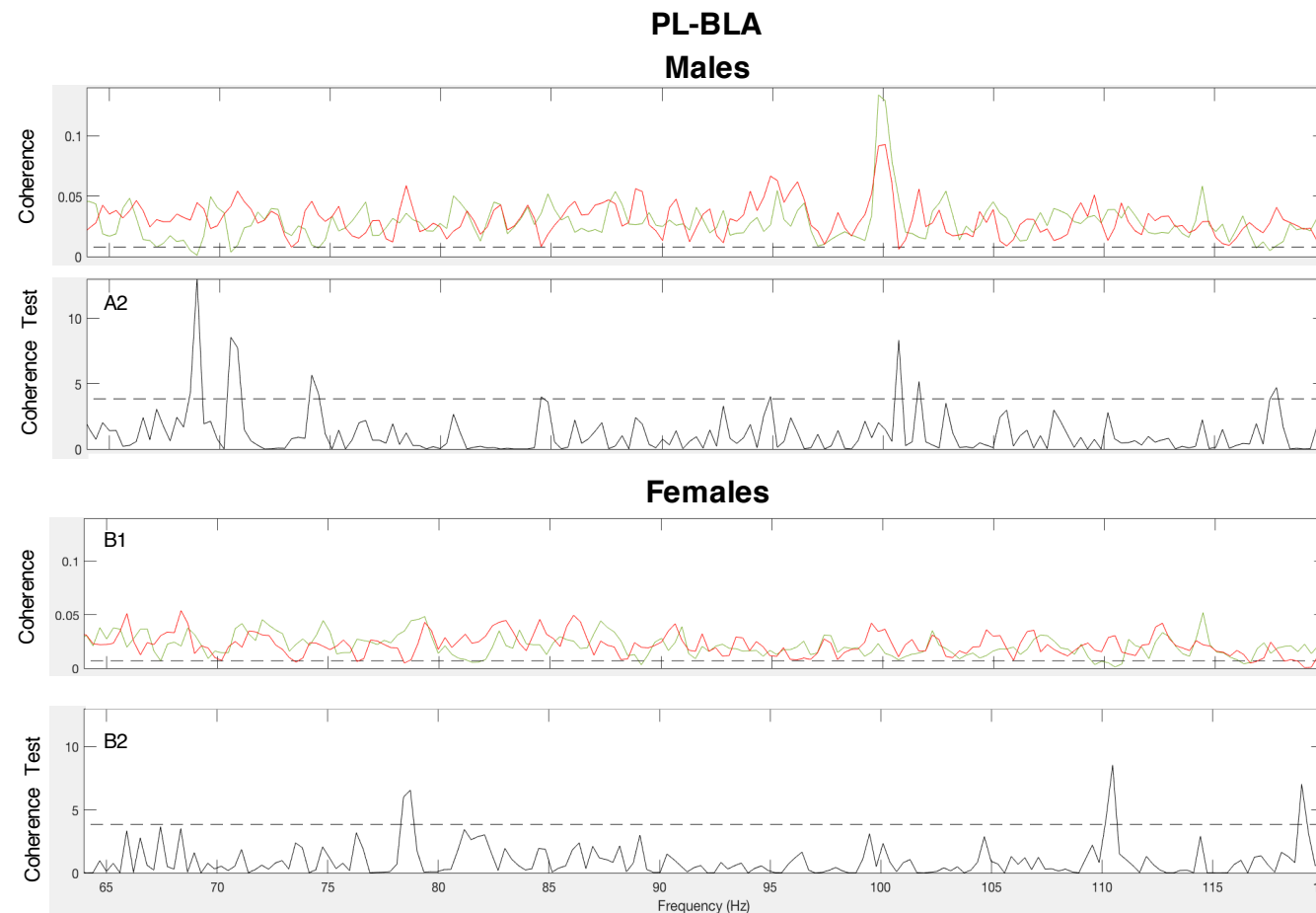
Figure 4.40. Pooled PL-BLA high gamma coherence for males (A1) and females (B1) for CS+ (red) vs CS- (green) and comparison of coherence tests quantifying differences in coherence during the CS+ vs CS- for males (A2) and females (B2). The dashed line denotes the 95% confidence limit. Upper panel: above this line shows significant overall coherence between regions during presentations of the CS+ (red) and CS- (green) ($P < 0.05$). Lower panel: peaks above this line show a significant increase in coherence between regions during presentations of either the CS+ or CS-. Males showed multiple increases in PL-BLA coherence during both CS+ and CS- at multiple frequencies. Females also showed a similar pattern, albeit at smaller amplitudes.

IL-BLA
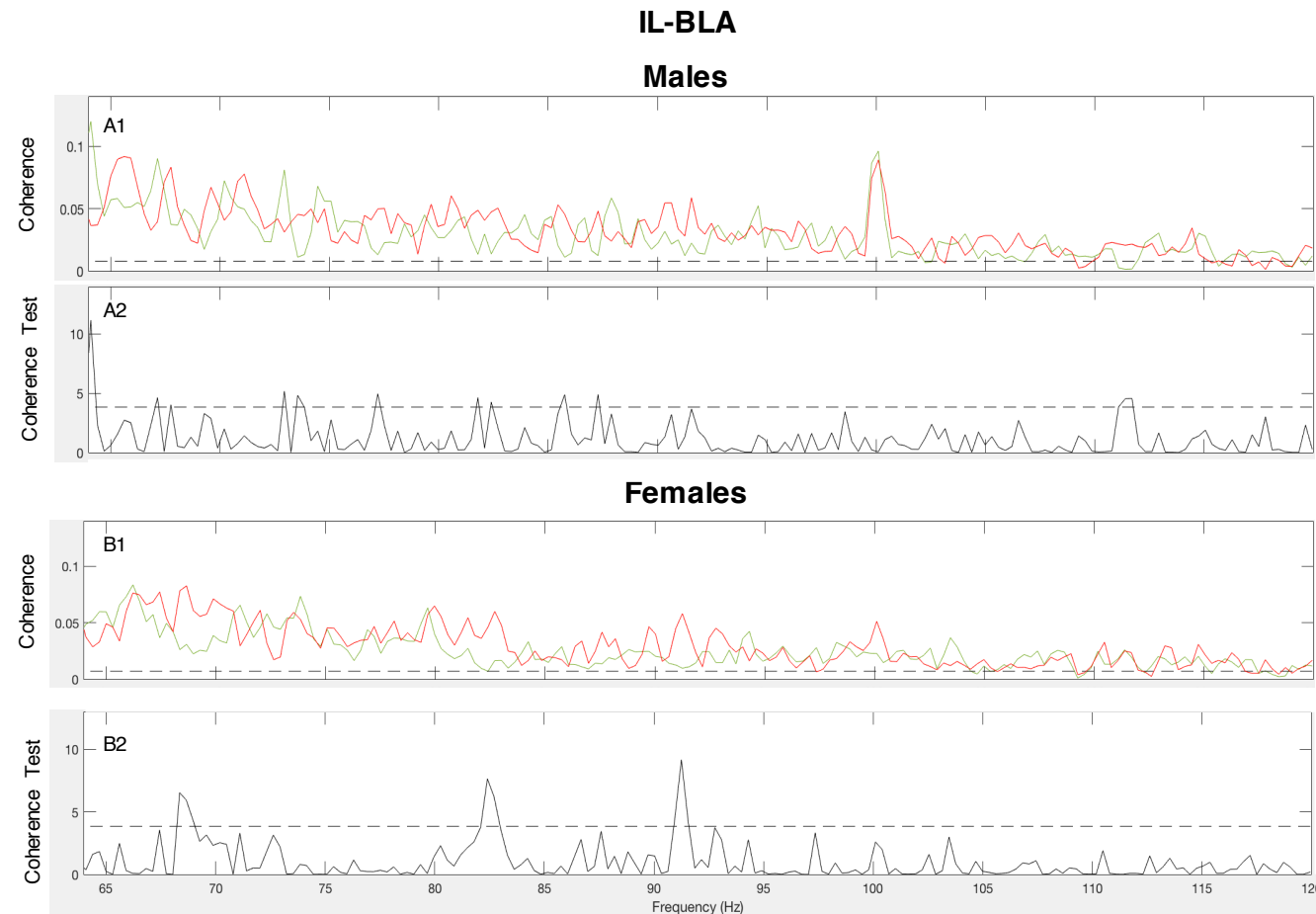
Males

Females

Figure 4.41. Pooled IL-BLA high gamma coherence for males (A1) and females (B1) for CS+ (red) vs CS- (green) and comparison of coherence tests quantifying differences in coherence during the CS+ vs CS- for males (A2) and females (B2). The dashed line denotes the 95% confidence limit. Upper panel: above this line shows significant overall coherence between regions during presentations of the CS+ (red) and CS- (green) (P < 0.05). Lower panel: peaks above this line show a significant increase in coherence between regions during presentations of either the CS+ or CS-. Males showed multiple increases in IL-BLA coherence during both CS+ and CS-. Females showed only significant increases in IL-BLA coherence during presentations of the CS+.
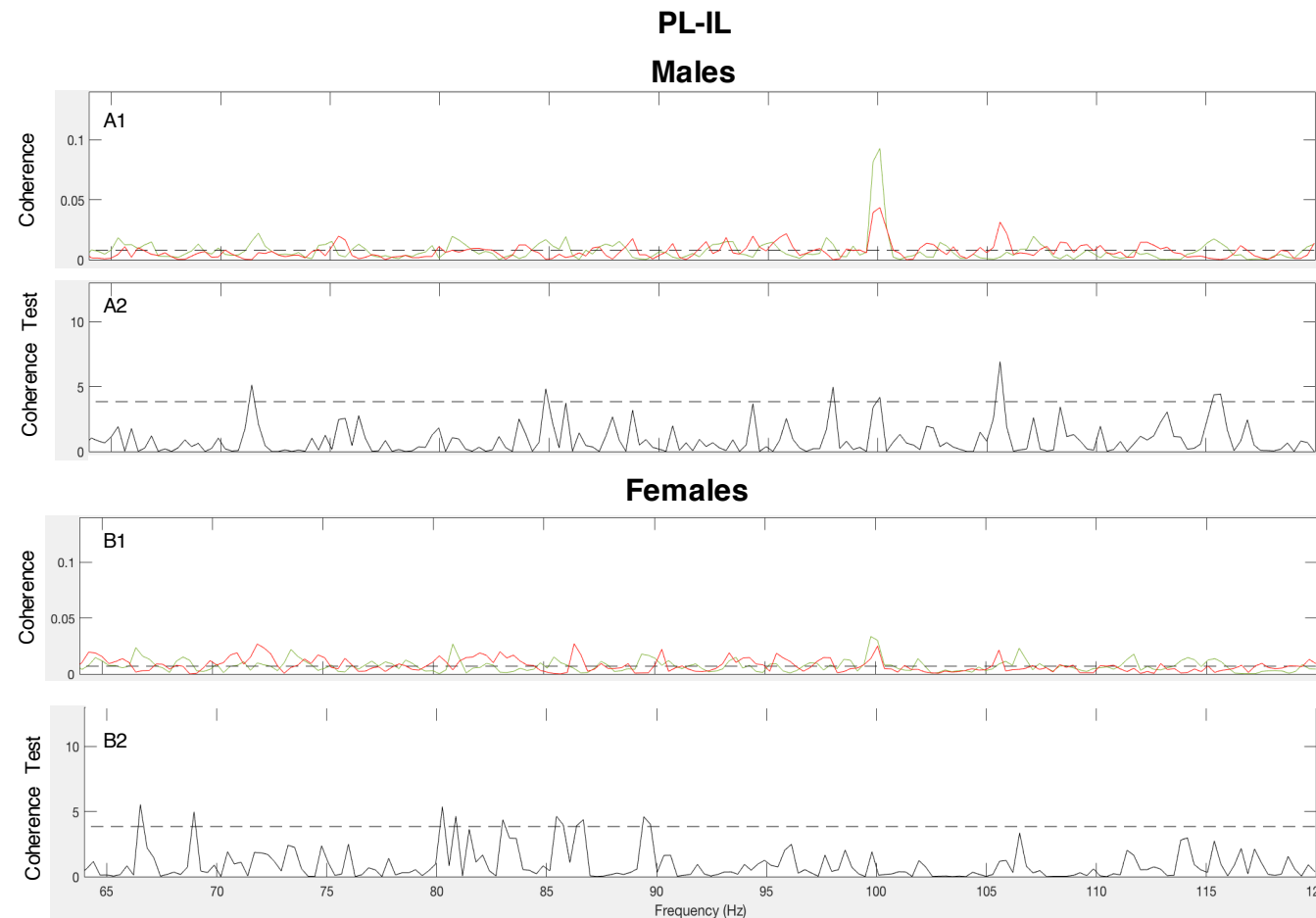
PL-IL

Males

Females

Figure 4.42. Pooled PL-IL high gamma coherence for males (A1) and females (B1) for CS+ (red) vs CS- (green) and comparison of coherence tests quantifying differences in coherence during the CS+ vs CS- for males (A2) and females (B2). The dashed line denotes the 95% confidence limit. Upper panel: above this line shows significant overall coherence between regions during presentations of the CS+ (red) and CS- (green) (P < 0.05). Lower panel: peaks above this line show a significant increase in coherence between regions during presentations of either the CS+ or CS-. Both males and females showed several small increases in PL-IL coherence during presentations of both the CS+ and CS-.

4.4 Discussion

In the present chapter, we investigated sex differences in PL-IL-BLA oscillations and synchronisation underlying the fear discrimination and generalisation phenotypes seen in males and females, respectively, with extended discrimination training. We provided further evidence for the sex differences seen in Chapter 2, showing again that extended training results in fear discrimination in males but fear generalisation in females. This is the third instance of the occurrence of this pattern, which indicates that this is a robust finding.

We also investigated sex differences in LFP power and coherence at frequencies in the theta (4-12 Hz) and gamma (30-120 Hz) ranges in and between the PL, IL and BLA during retrieval to determine how PL-IL-BLA activity and synchrony in generalisers (females) differs from their discriminator (male) counterparts. Key differences in power and coherence are summarised in Tables 4.1 and 4.2, below:

Theta Power	Males	Females
PL	CS- > CS+	CS+ > CS- and CS+ > CS-
IL	CS- > CS+	CS+ > CS- and CS+ > CS-
BLA	CS+ > CS- and CS+ > CS-	CS- > CS+
Low Gamma Power	**Males**	**Females**
PL	CS- > CS+	CS- > CS+
IL	CS- > CS+	CS- > CS+
BLA	CS- > CS+	CS- > CS+
Mid Gamma Power	**Males**	**Females**
PL	CS- > CS+	CS+ > CS- and CS+ > CS-
IL	CS+ > CS-	CS- > CS+
BLA	CS+ > CS- and CS+ > CS-	CS+ > CS- and CS+ > CS-
High Gamma Power	**Males**	**Females**
PL	CS- > CS+	CS+ > CS- and CS+ > CS-
IL	CS- > CS+	CS+ > CS- and CS+ > CS-
BLA	CS- > CS+	CS- > CS+

Table 4.1. Differences in power in PL, IL and BLA for males and females during presentations of the CS+ and CS- at theta, and low, mid and high gamma frequencies. CS-/CS+ > CS+/CS- represents increases in region power during presentations of the CS-/CS+ compared to the CS+/CS-, respectively. CS+ > CS- and CS+ > CS- represents increases in region power to both stimuli relative to one another at different frequencies.

Theta Coherence	Males	Females
PL-BLA	CS+ ↔ CS-	CS+ > CS-
IL-BLA	CS+ ↔ CS-	CS+ > CS-
PL-IL	CS+ ↔ CS-	CS+ > CS-
Low Gamma Coherence	**Males**	**Females**
PL-BLA	CS+ > CS- and CS+ > CS-	CS+ > CS-
IL-BLA	CS+ > CS-	CS+ > CS-
PL-IL	CS+ > CS-	CS+ ↔ CS-
Mid Gamma Coherence	**Males**	**Females**
PL-BLA	CS+ > CS- and CS+ > CS-	CS+ > CS-
IL-BLA	CS+ > CS- and CS+ > CS-	CS+ > CS-
PL-IL	CS- > CS+	CS- > CS+
High Gamma Coherence	**Males**	**Females**
PL-BLA	CS+ > CS- and CS+ > CS-	CS+ > CS- and CS+ > CS-
IL-BLA	CS+ > CS- and CS+ > CS-	CS+ > CS-
PL-IL	CS+ > CS- and CS+ > CS-	CS+ > CS- and CS+ > CS-

Table 4.2. Differences in coherence between PL-BLA, IL-BLA and PL-IL for males and females during presentations of the CS+ and CS- at theta, and low, mid and high gamma frequencies. CS-/CS+ > CS+/CS- represents increases in region power during presentations of the CS-/CS+ compared to the CS+/CS-, respectively. CS+ > CS- and CS+ > CS- represents increases in region power to both stimuli relative to one another at different frequencies. CS+ ↔ CS- represents no significant increases in coherence to either tone (i.e. no differences).

4.4.1 Sex Differences in Theta Power and Coherence

4.4.2 Theta Power

In males, we found that PL theta power was increased during presentations of the CS- compared to the CS+. In contrast, there were no clear differences in females due to subtle increases in PL power during presentations of the CS+ compared to the CS- (~4, 7 Hz) in addition to subtle increases in PL power during presentations of the CS- compared to the CS+ (~ 8-9 Hz). In the IL region, males again showed a significant increase in theta power during presentations of the CS- compared to the CS+, although this increase was restricted to a narrower band of frequencies compared to the PL. Females again showed no clear differences in IL power, as they showed both increases in power during presentations of the CS+ compared to the CS- (~ 10-11 Hz) as well as increases in power during presentations of the CS- compared to the CS+ (~ 8 Hz). Similar to female PL power, the differences seen in female IL power were very subtle. In the BLA, males showed a large, significant, increase in theta power during presentations of the CS- compared to the CS+ (~ 7-12 Hz). However, males also showed a significant, but very subtle, increase in BLA theta power during the CS+ compared to the CS- at a lower theta frequency (~ 5-6 Hz). Conversely, females only showed increases in BLA theta power during presentations of the CS- compared to the CS+, although these differences were much smaller in magnitude than in males.

Interestingly, the increases in mPFC theta power shown in males during periods of relative safety seemed to disagree with studies showing that

increases in mPFC theta power predicted avoidance of aversive compartments and is linked to anxiety-like behaviour (Tsujimoto et al., 2003; Adhikari et al., 2010). Further, in humans, non-extinguished versus extinguished stimuli was linked to increased skin conductance and dACC-localised theta power, wherein the dACC is a homolog of rodent PL (Mueller et al., 2014). Because of this, the increased PL theta seen in males during presentations of the CS- compared to the CS+ also seemed at odds with results from studies showing that the PL is involved in learned fear expression. For example, Corcoran & Quirk, (2007) found that inactivation of PL reduced freezing to both a tone and a context that had been previously paired with footshock. In addition, sustained activity in the PL is correlated with heightened fear expression and extinction failure (Burgos-Robles et al., 2009; Fenton et al., 2014b). Further studies have also shown that PL (and potentially IL) theta activity increases during CS+ vs CS- presentation (Laviolette et al., 2005; Fenton et al., 2014a), which is in opposition to these data presented here. However, it is important to note that activity in in these cases was recorded under anaesthesia, which may have produced different results compared to awake behaving studies.

In contrast, other studies have shown that, in a behavioural discrimination paradigm, PL (and potentially IL) activity may be needed to suppress inappropriate fear responding (Lee & Choi, 2012; Giustino & Maren, 2015). Further to this, IL lesions have been shown to impair retardation (Rhodes & Killcross, 2007), but also to enhance performance of appetitive, context-dependent discrimination learning (Ashwell & Ito, 2014). Taken together, these studies could indicate that the increased PL theta we saw in males during

presentations of the CS- compared to the CS+ may reflect the role of the PL in suppressing inappropriate fear responding during the CS-, in turn leading to the suppression of freezing during the safety tone and successful discrimination in males.

Further to this, the mPFC is known to be involved in decision making (Vertes, 2004; Iordanova et al., 2007), wherein theta activity in the mPFC and communication with the sub-thalamic nucleus (STN) is thought to control the shift from automatic to controlled action selection when conflict is present in humans. Here, increased mPFC theta power was observed during high conflict trials relative to low conflict trials (Zavala et al., 2016). As we have shown that males selected the appropriate response during fear discrimination retrieval (i.e. freezing during the CS+ vs not freezing during the CS-), perhaps the increased PL and IL theta power we observed during presentations of the CS- is involved with correct choice-making. As we observed no clear differences in power between presentations of the CS+ and CS- in female mPFC, the lack of difference in IL and PL theta power between CS+ and CS- presentation may have potentially interfered with this choice-making process in females.

In addition, learned safety has rewarding properties (Masuda et al., 1994; Ganguly & Kleinfeld, 2004; Rogan et al., 2005; reviewed in Kong et al., (2014)), and mPFC theta power has been shown to increase during retrieval of conditioned stimuli which had predictive value for reward (Paz et al., 2008). Therefore, the CS- in our study may be interpreted as a reward in males, resulting in concurrent increases in mPFC theta, which are absent in females. Our study is also the first to distinguish between PL and IL activity in the mPFC

during a discrimination retrieval paradigm involving both males and females, meaning that there may be a level of discrepancy when comparing our results to other prior studies.

In males, BLA theta power showed a large, significant increase during presentations of the CS- compared to the CS+ (~ 7-12 Hz), but also showed a smaller increase during presentations of the CS+ compared to the CS- at lower theta frequencies (~ 5-6 Hz). BLA theta power was also subtly increased during presentations of the CS- compared to the CS+ in females. As both males and females showed more BLA theta activity during CS- vs CS+ overall, there is less of a sex difference seen in this region compared to theta power in the mPFC. Yet, this lack of sex differences in BLA theta activity, combined with the presence of sex differences observed in PL theta activity, might mean that downstream structures are instead involved in mediating freezing during threat and safety cues rather than direct modulation of freezing by the BLA alone. In males, downstream structures which are modulated by the PL, may be acting to modulate the appropriate behavioural response (i.e. promoting freezing during the CS+ and inhibiting freezing during the CS-). Although mPFC theta oscillations regulate BLA activity differently during fear vs safety (Likhtik & Gordon, 2014), it is possible that the mPFC may 'bypass' the BLA to regulate other areas directly to control behavioural responding instead. For example, the PAG, which controls freezing (Kim et al., 2013), receives direct PL input (reviewed in Vianna & Brandão, (2003)). Further, the BNST also receives direct PL input (Radley et al., 2009; Marek et al., 2013), and this area has also been implicated in fear discrimination (reviewed in Radke, (2009)).

4.4.3 Theta Coherence

Here, females showed a significant increase in PL-BLA theta coherence during presentations of the CS+ compared to the CS-, whereas males showed no such difference. Again, females showed a significant increase in IL-BLA coherence during presentations of the CS+ compared to the CS-, although this increase was smaller in magnitude compared to PL-BLA theta coherence. Males again showed no significant cue-dependent differences in IL-BLA theta coherence. Further, females showed low, but significant, basal levels of PL-IL coherence in addition to a significant increase in PL-IL coherence during presentations of the CS+ compared to the CS-. In males, we observed low to no overall basal PL-IL theta coherence, and again no significant cue-dependent differences in PL-IL theta coherence. Overall, males showed a lack of significant differences in coherence between all three structures between stimuli, whereas females consistently displayed increased coherence during presentations of the CS+ compared to the CS-.

Theta coherence between the amygdala and mPFC has been shown to increase in relation to fear memory consolidation during paradoxical sleep (Popa et al., 2010). Interestingly, increased theta coherence between the IL and LA has been linked to freezing in response to aversive stimuli (Lesting et al., 2013). In our study, we saw increased IL-BLA coherence only in females during presentations of the CS+, compared to the CS-, yet we did not see increased freezing during presentations of the CS+ compared to CS- (i.e. a lack of discrimination), meaning that there are likely to be additional contributions to the behavioural generalisation we see in females with extended training.

One plausible explanation for increased circuit coherence, accompanied by a lack of freezing differences between the CS+ and CS-, in females could be a failure of a compensatory mechanism. For example, Fitzgerald et al., (2014) investigated PL and IL activity in extinction deficient (S1) and control (B6) mice, where they found that impaired extinction in S1 mice was also associated with exaggerated IL activity. Here, they hypothesised that, although IL activity has been linked to the promotion of extinction, increased IL activity in S1 mice could reflect a (failed) compensatory effort by this region to mitigate fear-promoting activity in other regions, such as the PL or the amygdala. In our study, it could be that females show increased coherence in the PL-IL-BLA circuit during presentations of the CS+ compared to CS- as an attempt to compensate for the inappropriate response selection and failure to suppress fear during the safety tone.

Moreover, we did see opposing patterns of mPFC-BLA theta coherence in the males of our study compared to Likhtik et al, (2014). Their study showed an increase in mPFC-BLA coherence in male mice which discriminated between threat and safety cues (discriminators), whereas mice which froze equally to both the CS+ and CS- (generalisers) showed no differences in mPFC-BLA theta coherence between these tones. In our study, we instead saw no significant changes in mPFC-BLA coherence in males (discriminators) and increases in mPFC-BLA theta coherence during presentations of the CS+ compared to CS- in females (generalisers).

Yet, Likhtik et al, (2014) did not specify which region of the mPFC they recorded from, meaning that the individual contributions of the PL and IL to the

discriminatory behaviours described was unknown. We also showed increased PL-IL theta coherence in females during presentations of the CS+ compared to the CS-, which is not present in males. As PL-IL theta coherence was unreported by Likhtik et al, (2014), it is possible that increased PL-IL theta coherence could potentially interfere with discrimination. For example, although the PL and IL have previously been linked primarily to the promotion and inhibition of fear, respectively (Quirk et al., 2000; Do-Monte et al., 2015), we have highlighted that these regions may have more complex roles during discrimination learning and retrieval.

As the mPFC is involved in strategy switching and choice selection it at first seems unclear how increased mPFC coherence during presentations of the CS+ compared to the CS- could also be linked to failed discrimination. However, the combined involvement of the PL and IL regions in this process may change with extended training (Rich & Shapiro, 2007). Further, as the PL and IL also have increased coherence with the BLA, which is lacking in males, it may be that the BLA is interfering with the normal function of one, or both, of these regions during presentations of the CS+ in females. In combination with this, the enhanced PL-IL coherence in females may also be inhibiting the individual contributions of these regions during presentations of the CS+ compared to CS-. Further, both strain and species differences have been reported in discrimination and fear inhibition (Andrews et al., 1995; Camp et al., 2012), meaning that the sex differences observed in PL-IL-BLA theta coherence could potentially be strain and/or species-specific to the Lister-Hooded rats used in this study.

4.4.4 Sex Differences in Gamma Power and Coherence

4.4.5 Gamma Power

Overall, we only reported very subtle increases in low gamma (30-45 Hz) power in the PL and IL during presentations of the CS- compared to CS+ in both sexes. In the BLA, we observed a slightly larger increase in low gamma power during presentations of the CS- compared to the CS+ in both sexes, although this increase was marginally bigger in magnitude in males compared to females. In general, these differences were relatively minor compared to the differences observed at theta and higher gamma frequencies.

For mid gamma (45-64 Hz), males showed a large increase in PL power during presentations of the CS- compared to the CS+, whereas females showed no clear differences in PL power between presentations of the CS+ and CS-. In contrast, in IL we observed a small, but significant, increase in mid gamma power during presentations of the CS+ compared to the CS- in males, whereas in females IL mid gamma power was significantly, but subtly, increased during presentations of the CS- compared to the CS+. In the BLA, we saw moderate increases in mid gamma power during presentations of the CS- compared to the CS+ and smaller, but still significant, increases in power during presentations of the CS+ compared to the CS- in males. A similar pattern was observed in BLA mid gamma power in females, but to a much smaller magnitude compared to males.

The PL and IL appear to have differential increases in mid gamma power in males and females, depending on stimulus presentation. For example,

although the PL is involved with the memory of learned fear and fear expression (Burgos-Robles et al., 2009; Choi et al., 2010), and males showed increased freezing during the CS+ compared to the CS-, males in our study showed a significant increase in PL mid gamma power during the CS- compared to the CS+. In contrast, females displayed no clear differences in PL mid gamma power during presentations of the CS+ vs CS-. As these results are similar to what was observed for PL theta (i.e. increase in PL power in males during presentations of the CS- compared to the CS+, with no clear differences present in females), it may be that the PL mid gamma is also is potentially involved in suppressing inappropriate fear responding during the CS- in males, whereas this is absent in females (Lee & Choi, 2012; Giustino & Maren, 2015). Further, the PL projects to the ITC of the amygdala, albeit more weakly than the IL (Pape & Pare, 2010). This could mean that, during discrimination retrieval, activity of the PL potentially causes increases in freezing via excitation of the ITC during presentations of the CS-. Interestingly, Fenton et al., (2016) found that persistent PL (albeit low) gamma activation in females contributed to heightened fear expression and extinction failure, highlighting that there may be differing roles for the PL during extinction and discrimination recall in males and females.

In the IL, males showed an increase in IL mid gamma power during presentations of the CS+ compared to the CS-, whereas females showed the opposite pattern, displaying subtly increased IL mid gamma power during presentations of the CS- compared to the CS+. However, it should be noted that the increase in IL mid gamma power in males during presentations of the

CS+ compared to CS- is also in opposition to the increase in IL power in males during presentations of the CS- compared to the CS+ at other theta and gamma frequencies. There is evidence to suggest that altered IL gamma power is linked to impaired extinction retrieval and impulsive behaviour, which could mean that, in females, increased IL mid gamma power during presentations of the CS- compared to the CS+ may be causing impulsive, or habitual, inappropriate freezing to the safety tone. Nevertheless, these sex differences in IL mid gamma power are of much smaller magnitude to other sex differences seen in the PL, both at this frequency and overall. Therefore, it is difficult to interpret how meaningful other sex differences in IL mid gamma power are.

As we saw similar increases in BLA mid gamma power during presentations of both the CS+ compared to the CS- and during presentations of the CS- compared to the CS+ in both males and females, there were no clear sex differences in this region, meaning that changes in BLA mid gamma power were unlikely to be the underlying cause of the sex differences we see in freezing behaviour.

In the high gamma range, we observed subtle increases in PL power during presentations of the CS- compared to the CS+ for both sexes, with slightly larger increases observed in females compared to males. In the IL, we also saw moderate increases in high gamma power during CS- compared to CS+ in males. In contrast, females showed small increases in IL power during presentations of the CS+ compared to the CS-, in addition to small increases in IL power during presentations of the CS- compared to the CS+. In the BLA we observed increases in high gamma power during presentations of the CS-

compared to CS+ in both sexes, although these differences were much subtler in females.

Although the sex differences described above are subtle, they may still play a role in the sex differences we have observed in behaviour. For example, the fact that we see increased IL power in males during presentations of the CS- compared to the CS+, yet in females we see increases in IL high gamma power to presentations of both the CS+ (compared to the CS-) and the CS- (compared to the CS+) at various frequencies may suggest a potential over activity of the IL in females. There are studies to suggest that the PL is broadly responsible for voluntary responding (i.e. choosing the appropriate response) whereas the IL mediates the ability to override this goal-directed behaviour (i.e. acting on instinct, impulse, or habitually. (Chudasama et al., 2003: Killcross & Coutureau, 2003; Sharpe & Killcross, 2015)).

As we have shown that there are subtle increases in innate, anxiety-like behaviours in females in the open field in comparison to males (Chapter 2), it may be that the instinctual response in females is to freeze and/or perform escape behaviours, whereas males have a greater capacity for voluntary responding as they have lower levels of innate anxiety. Therefore, an increase in IL high gamma power during presentations of the CS+ and CS- relative to one another may potentially be driving a pro-instinctual-freezing response (i.e. generalisation) to both stimuli in females. This is supported by the fact that we saw elevated PL power in males during presentations of the CS- compared to the CS+ at all frequencies, which is not seen in females, suggesting that they may have more overall voluntary control of their response selection during

periods of relative safety, compared to females. Further, as the IL is linked to fear suppression (Bloodgood et al., 2017), and that males showed specific increases in IL high gamma power only during presentations of the CS- compared to the CS+, this may have contributed to their ability to suppress fear behaviours during the safety tone compared to females, who showed no clear tone-dependent differences in IL high gamma power.

Interestingly, the results we observed in BLA high gamma power agree with a similar study by Stujenske et al., (2014). Both in their study and in the present study, BLA fast gamma power (between 70-120 Hz) was found to be suppressed in animals which could successfully discriminate between fear and safety cues (i.e. 'discriminators' in their study and males in the present study). In their study, BLA fast gamma power was also reported to be enhanced with periods of relative safety. Here, we have shown that males display significantly increased BLA high (or fast) gamma power in response to presentations of the CS- compared to the CS+. Conversely, females only show very minor (borderline significant) increases in BLA high gamma power during periods of relative safety, which may in part, contribute to their inability to discriminate between presentations of CS+ and CS-.

4.4.6 Gamma Coherence

At low gamma, males showed significant increases in PL-BLA coherence during presentations of the CS+ compared to the CS-, as well as increases during presentations of the CS- compared to the CS+, whereas females only showed significant increases in PL-BLA coherence during presentations of the

CS+. Both sexes showed significant increases in IL-BLA coherence during presentations the CS+ compared to the CS-, although these increases were greater in magnitude in males. Males showed significant, but subtle, increases in PL-IL low gamma coherence during presentations of the CS+ compared to the CS-, whereas females did not.

Increased PL-IL coherence during presentations of the CS+ in males, which is absent in females, may reflect increased spatial and goal encoding in males (Hok et al., 2005). Even though we did not see sex differences in contextual fear prior to tone presentation, there are reported differences in how males and females use contextual cues in addition to discrete cues for processing associative meaning (Gresack et al., 2009). Further, the mPFC is linked to the contextual regulation of learned fear expression and inhibition (Orsini et al., 2011; Xu et al., 2013), meaning that the increased PL-IL coherence at low gamma we observed may be involved in these processes, and could therefore potentially contribute to better discrimination in males. Further, a recent study has shown that rats tended to increase their choice of a disadvantageous option and decrease their choice of an optimal option following inactivation of either the PL or IL (Zeeb et al., 2015), suggesting that both regions (potentially working in tandem) may contribute to better, or more appropriate, choice making, which may play a larger role in males compared to females.

Interestingly, we saw generally opposing trends in mPFC-BLA coherence in males compared to females in the mid gamma range. In males, the majority of significant increases in PL-BLA and IL-BLA coherence occurred

during presentations of the CS- compared to the CS+, although there was one instance where PL-BLA and IL-BLA coherence were very subtly increased during presentations of the CS+ compared to CS- at ~ 46 Hz. Conversely, females only showed significant increases in coherence between these regions during presentations of the CS+ compared to the CS-. Both sexes showed a significant increase in PL-IL coherence during presentations of the CS-compared to CS+, although there were more differences at a greater in magnitude in females.

As mPFC-BLA mid gamma coherence in males is significantly increased during presentations of mainly the CS- compared to the CS+, whereas this is not present in females, these results could potentially describe a modulatory effect of the mPFC on the BLA in males, wherein fear behaviours are suppressed during presentations of relative safety. However, as we observed mostly increases in BLA power across all gamma ranges during presentations of the CS- compared to the CS+ in both sexes, it is unclear how these differences in mPFC-BLA mid gamma coherence contribute to the behavioural sex differences. It may be that sex differences in PL-IL-BLA coherence, or PL, IL and BLA power, across other, or multiple, frequency ranges are more important in modulating behaviour than the sex differences in mPFC-BLA mid gamma coherence observed.

At high gamma, both sexes also showed significantly increased PL-BLA coherence during presentations of the CS+ (vs CS-), in addition to increased coherence during presentations of the CS- (vs CS+), at different frequencies. For coherence between the IL and BLA, males again showed significant

increases in high gamma coherence during presentations of the CS+ (vs CS-) in addition to increased coherence during presentations of the CS- (vs CS+) at different frequencies. In contrast, females only showed significantly increased coherence during presentations of the CS+ compared to the CS-. Similar to other gamma frequencies, PL-IL high gamma coherence was very low or borderline in both sexes. Both sexes again also showed significant increases in PL-IL coherence during presentations of the CS+ compared to the CS- in addition to increased coherence during presentations of the CS- compared to the CS+ at different frequencies.

Sex differences in coherence in the high gamma range were therefore restricted to between the IL and BLA, wherein females showed increased IL-BLA coherence during presentations of the CS+ compared to the CS- and males did not. Here, this increase in IL-BLA coherence during the fear tone in females may reflect the concurrent increase in IL high gamma power we saw during presentations of the CS+, compared to CS-, that were absent in males. It may be that this general increase in IL power and coherence in females during periods of fear is potentially another instance of increased (failed) compensatory activity of the IL to control fear-promoting activity in other regions (Fitzgerald et al., 2014b).

In the present chapter we have presented several sex differences in LFP power and coherence at frequencies in the theta (4-12 Hz) and gamma (30-120 Hz) ranges in the PL, IL and BLA during retrieval in response to the CS+ and CS-. Here, we observed a clear increase in PL power in males during presentations of the CS- compared to the CS+ at all frequencies, which was

mostly absent in females. We also saw increased IL power in males during presentations of the CS- compared to the CS+ at both theta and high gamma frequencies, which was absent in females. Further to this, we also observed an overall increase in PL-BLA coherence to the CS+, compared to the CS-, in females at theta, low and mid gamma frequencies, which was not present in males. In addition, there was a significant increase in IL-BLA coherence during presentations of the CS+, compared to the CS-, at all frequencies in females, whereas this was mostly absent in males. Finally, we observed that PL-IL coherence showed sex differences at lower frequencies (i.e. theta and low gamma) but showed a similar pattern in both sexes at higher frequencies (mid and high gamma).

5. General Discussion

In this thesis we have investigated sex differences in cued fear discrimination and generalisation by looking at behaviour (Chapter 2), computational models of BLA network activity potentially underlying this behaviour (Chapter 3) and *in vivo* activity in the PL-IL-BLA circuit during this behaviour (Chapter 4). A brief summation of the findings from each chapter will be presented below, along with further reasoned explanations of these results, potential refinements to the experiments conducted, and a proposed rationale for future work.

5.1 Sex Differences in Behaviour

Initially, we observed clear differences in behaviour between males and females during retrieval after extended fear discrimination training (Chapter 2). Here we observed that males displayed appropriate fear behaviour preferentially during the CS+ compared to the CS- wherein they were successfully able to discriminate between the two stimuli with extended training. However, males did not show successful discrimination with limited training. Conversely, females showed successful discrimination after limited training, yet they showed a generalised fear response (i.e. similar freezing to both stimuli) after extended training. Following this, we also observed that the CS-, when subsequently conditioned with an aversive stimulus after initial extended discrimination training, retarded learning in males but not in females. This suggested that the CS- acts as a safety signal in males, but not in females. As we saw no sex differences in shock sensitivity, we concluded that the sex

differences observed in extended fear discrimination training were likely to be a result of impaired safety cue processing in females. Although we did see increased locomotor activity in females, as well as subtle increases in innate fear behaviours in the open field, these differences are unlikely to underpin the sex differences observed during discrimination retrieval.

5.1.1 Suggested Future Behavioural Studies

Summation and retardation tests are used to demonstrate conditioned inhibition, a form of which is safety signalling by the CS- during fear discrimination (Christianson et al., 2012; Sangha et al., 2013). During summation testing the CS+ and CS- are presented together and, if the CS- acts as a safety signal, this reduces fear compared to CS+ presentation alone. In Chapter 2, we could not use a summation test given that both cues used were auditory stimuli. Therefore, it would be useful for additional future studies to use cues from different sensory modalities, such as a combination of light and tone, which would also allow for the assessment of summation testing, to further investigate the sex differences in safety signalling.

In addition, as previous research has examined the potential role of oestrogen in sex differences and in fear discrimination and CI via summation testing involving auditory and visual cues (Toufexis et al., 2007), a potential limitation of our study is that we did not account for variations in the oestrous cycle phase. However, we still replicated our finding of fear generalisation with extended training in a separate cohort of naturally cycling females when looking at the effects of the CS- as a safety signal during retardation. Moreover, we

replicated this finding again in Chapter 4, with another cohort of implanted animals for *in vivo* electrophysiology recordings during behavioural testing. Here, it is likely that the three different cohorts would have been in different phases of the cycle, but similar effects were observed across all females. Therefore, although research has shown that oestrogen may modulate the fear extinction network and fear inhibition in females (Lebron-Milad & Milad, 2012), it is unlikely that hormone status has a defining influence during extended fear discrimination training. However, it must be noted that, for limited training, these data were generated from one cohort. Because training (and retrieval) occurred on only one day, it is possible that different oestrogen/progesterone levels at different points in the cycle could result in different levels of discrimination. We did perform vaginal swabbing to determine oestrous phase in a separate cohort of females undergoing limited discrimination training and retrieval, and there may have been an effect of high vs low oestrogen (analysis ongoing).

A similar argument could be made to investigate the changes in testosterone and/or progesterone and allopregnanolone in males and females. For example, female rats in the proestrous (i.e. high oestrogen and progesterone) phase of the oestrous cycle exhibited significantly less overall freezing during extinction learning compared to female rats at different points of the cycle and to male rats (reviewed in Gruene et al., 2015). Allopregnanolone (a metabolite of progesterone) is a positive modulator of $GABA_A$ receptors (reviewed in Wang, (2011)), and women with PTSD have been shown to have reduced cerebrospinal fluid levels of allopregnanolone (Rasmusson et al., 2006). Therefore, it would be interesting to test the

influences of these hormones on fear discrimination and generalisation in males and females.

Interestingly, there may be sex-specific impacts of oxytocin on fear learning and anxiety. For example, repeated intranasal oxytocin administered at an early stage post-trauma reduced subsequent PTSD symptom development in emergency department patients with high acute PTSD symptoms (Frijling, 2017). In addition to this, it has been shown that there are sex-specific routes for the effects of oxytocin administration on the potential to diminish fear expression in PTSD patients (Olff, 2017). In this study, it was found that oxytocin administration increased inhibitory control of the vmPFC over the CEm in men but resulted in less functional regulation of BLA by the dACC in women. From this, it would be valuable to test the effects of oxytocin on fear discrimination and generalisation in male and female rats in future studies.

In addition to this, it may also be beneficial to investigate fear discrimination training and safety learning in juvenile and aged rats. For example, using juvenile (i.e. prepubescent) rats to further investigate the potential effects of gonadal hormones, such as oestrogen, on fear discrimination and generalisation in male and female rats. As we have previously highlighted, women in the general population are twice as likely to develop PTSD compared to men over the course of a lifetime (Koenen & Widom, 2009), and that PTSD is linked with impaired safety cue learning (Jovanovic et al., 2012). However, at some ages females were almost three

times as likely to develop PTSD (21-25 year old), whereas at other ages there is a reduced risk for both sexes and less of a sex difference (70-75 years old) (reviewed in Ditlevsen & Elklit, 2010). This may be because there are sex differences in the biological aspects of age-related brain development, such as response to psychological stress (Wang et al., 2007), which could influence how fear and safety cues are processed. For example, many of the cognitive deficits of normal ageing (forgetfulness, distractibility, inflexibility in decision making and impaired executive functions) involve PFC dysfunction (reviewed in Wang et al., 2011), meaning that there could also be effects on discrimination vs generalisation. There has also been little research investigating age-related changes in the availability of basic amino acid neurotransmitters (such as glutamate and GABA). GABA signalling, as we described in Chapter 3, may have an impact on fear discrimination and generalisation, meaning that a focus on studies involving cohorts of wider age ranges, in addition to sex, are likely to be helpful in determining the neurobiological factors underlying anxiety and fear-based disorders, such as PTSD.

5.2 Computational Modelling of Sex Differences in Behaviour

To investigate the potential neural circuitry behind the sex differences observed in behaviour after extended fear discrimination training we wanted to compare differences in neural circuit function underlying discrimination (males) vs generalization (females). To achieve this, we utilised two complementary approaches; computational modelling and *in vivo* electrophysiological recordings of brain activity. *In silico*, we created three models to simulate the

relative activity rates of populations of fear and safety neurons within the BLA, with additional external input from the PL in one model, throughout a similar extended fear discrimination training and retrieval model paradigm (Chapter 3) to the one used *in vivo* (Chapters 2 and 4).

From these reduced models of representative neuronal activity, we were able to simulate both 'discrimination' (i.e. male) and 'generalisation' (i.e. female) phenotypes. If 'fear' and 'safety' neurons residing in the BLA were preferentially active only during the respective CS+ and CS- inputs, then this was described as 'discrimination', whereas if fear neurons were preferentially active over safety neurons, regardless of input stimuli, then this was described as 'generalisation'. We found that we were able to induce a 'switch' from discrimination to generalisation by increasing overall inhibition (Model 1), reducing inhibition/increasing excitation of fear neurons (Model 2) and by modulating the activity of fear and safety neurons with external input from the PL (Model 3). These models were initially inspired by the model described by Vlachos et al. (2011) in combination with oscillatory neural population dynamics described by the Wilson-Cowan equations to detail mutually inhibitory connections between fear and extinction neurons.

By comparing results from all three models, we hypothesised that the switch from discrimination to generalisation may be mediated, in part, by a reduction in the inhibition of fear neurons within the BLA. Specifically, we proposed that the generalisation phenotype seen with a reduction in the inhibition of fear neurons may be influenced by differences in GABA signalling

in males and females, as modelled by an extension of Model 1 to include excitatory (GLU) and inhibitory (GABA) fear and safety neurons (Model 2). This hypothesis is in line with the reduction in GABA signalling (i.e. less inhibition) in the BLA that has been linked to fear generalisation (Shaban et al., 2006; Bergado-Acosta et al., 2008; Sangha et al., 2009; Lange et al., 2014). In addition, there is also evidence to support that there may be less GABA signalling in females (Milad et al., 2009; Cholanian et al., 2014; Fernandez de Velasco et al., 2015; Möller et al., 2016). Therefore, the change from initial discrimination with limited training to generalisation with extended training in females could potentially be linked to a difference in local GABA signalling within the BLA between males and females.

Further, as a lack of local inhibition of fear neurons appears to generate the 'generalisation' phenotype, this may provide additional evidence to investigate the use of benzodiazepines in the treatment of fear and anxiety-based disorders. Benzodiazepines enhance the effect of GABA at the $GABA_A$ receptor and have been shown to have anxiolytic properties. Yet, there is evidence to support the fact that GABA sensitivity is decreased in PTSD patients (Geuze et al., 2008; Trousselard et al., 2016), especially in women (Möller et al., 2016). As highlighted above, allopregnanolone is a positive modulator at $GABA_A$ receptors (reviewed in Wang, (2011)), and levels of allopregnanolone are altered in women with PTSD (Rasmusson et al., 2006), meaning that GABA sensitivity in women may, in part, be modulated by gonadal hormones. These differences may not be a lack of GABA levels *per se*, but they may also reflect changes in GABA receptor signalling. However, high doses of

benzodiazepines have been shown to produce negative side-effects, such as anterograde amnesia and dissociation (Mejo, 1992), which could potentially interfere with the process of extinction learning (i.e. during exposure therapy) if both treatments are concurrent. Therefore, if comparatively higher amounts need to be administered in (female) patients with PTSD due to reduced sensitivity, it may be worth future studies involving both males and females to investigate alternate drugs and therapies to be used in tandem with benzodiazepines to facilitate overall treatment efficacy. This could therefore improve patient response without the need to increase benzodiazepine dose over the course of the treatment regimen to levels where side-effects could interfere with quality of life.

Further to simulating a reduction in inhibition causing the 'switch' from discrimination to generalisation, we also saw the generalisation phenotype emerge from additional excitation in fear neurons within the BLA (Models 2 and 3). As we were able to model excitation of fear neurons from simulated external input from a simplified node representing PL activity, we hypothesised that the resulting generalisation from the excitation and/or disinhibition (i.e. excitatory PL input to S- neurons) of fear neurons may potentially be due to 'over activity' in the PL. Here, we showed that initial levels of PL input to fear and safety neurons had little effect on the discrimination phenotype, yet when we increased PL input we observed the generalisation phenotype as a result. Therefore, it may be that generalisation involves disinhibition of the PL during presentations of the CS-, which then causes a promotion of fear neurons in the BLA, leading to an inappropriate fear response during periods of safety. As a

lack of inhibition of and increased excitation in fear neurons are similar, and both produced the generalisation phenotype, it may be that there is a lack of GABA signalling in the BLA and/or PL of female rats. A lack of GABA in females could potentially cause PL disinhibition, resulting in over-activity and thus additional excitation of fear neurons, leading to the generalisation phenotype. This is supported by research showing that increased PL activity in females, compared to males, is linked to enhanced fear expression as well as failed extinction (Fenton et al., 2014b, 2016).

However, the results of the computational modelling differ from the findings discussed in Chapter 4. Here, we observed increased PL activity during presentations of the CS-, compared to the CS+, as well as discrimination in males, but a lack of PL activity during the safety tone alone, and generalisation, in females. One limitation of our computational models is that we only considered glutamatergic projections from the PL to the BLA (i.e. to F+ and S- neuronal populations), and that we considered output from F and S to represent BLA output from the CEm/l (promoting freezing) and ITC (inhibiting freezing), respectively. It may be that the output of the BLA in females does directly contribute to the generalisation phenotype, but that the differential neuronal populations within the BLA may be mediated by another region (e.g. the hippocampus) rather than the PL directly. It is also important to consider that the models described in Chapter 3 were the first attempt at simulating 'fear' and 'safety' neurons in the BLA, with projections from the PL, to investigate sex differences in fear discrimination and generalisation. Therefore, the results of these simulations provide a foundation on which to build future study, in addition

to reasonable hypotheses, rather than a definitive and complete resolution to the research question proposed by this thesis.

As we based our models on the involvement of the PL and the BLA in modulating fear behaviour directly, in accordance with the supporting literature, we did not take into consideration alternative anatomical connections from the PL to other regions, such as the PAG. From this, one refinement to future models would be to simulate more projections from and between the PL and BLA to other areas to investigate their contributions to fear discrimination and generalisation. Other model refinements are discussed below.

5.2.1 Model Refinements

One potential refinement to the models described in Chapter 3 would be an addition of the IL. Here, we decided to model PL activity due to its apparent role in resistance to fear extinction in females (Fenton et al., 2014, 2016), in addition to its role in fear discrimination (Kim et al., 2013; Piantadosi & Floresco, 2014). It would be interesting to model the IL in future developments of the models described here to see if there is a compensatory or competing effect on the PL influence over the F+ and S- neurons, given that the PL and IL appear to have differential roles in fear extinction and suppression (Sangha et al., 2013). For example, we could see whether the influence of the IL would be able to reverse the 'generalisation' phenotype generated by 'over-activity' of the PL, or whether this additional input would make the original 'discrimination' phenotype more robust and therefore less likely to 'switch' to generalisation. This is supported

by the role of the IL in the inhibition of fear behaviours, wherein ventral mPFC–BLA projections are implicated in the reduction of learned freezing, both at baseline and in stress-induced anxiety (Laurent & Westbrook, 2009; Adhikari et al., 2015).

Further, the BLA is composed of both excitatory pyramidal and inhibitory interneurons (Ciocchi et al., 2010). Although pyramidal neurons account for most neurons in the BLA, they are strongly regulated by several different types of interneurons, which could be beneficial to investigate in future models (Capogna, 2014). This could be achieved by potentially modulating the weight of the inhibitory connections emanating from F- and S- neurons, or having more than one type of interneuron included within future models. For example, including one type of interneuron which acts directly on excitatory neuronal groups, as well as other types of interneurons which act to reduce the global (i.e. perisomatic) activity of the model (Freund & Katona, 2007).

In addition to this, it would also be interesting to develop these models further to illustrate the role of GABA specifically, potentially by looking at biophysical models (e.g. GABA-A receptor mediated Cl$^-$ channel dynamics), on fear and safety neurons within the BLA. Although there are refinements which can be made to the models described here, we have shown that the phenomena dictating discrimination- and generalisation-like behaviours is complex, and is likely to be multi-factorial in nature.

5.3 Sex Differences in *In vivo* Electrophysiology

With the studies described above as our foundation, we also used *in vivo* electrophysiology to investigate the role of the PL and IL sub-regions of the mPFC, in addition to the BLA, on the sex differences observed in behaviour with extended fear discrimination training (Chapter 4). We recorded LFP power and coherence between these regions at both theta (4-12 Hz) and gamma (30-120 Hz) frequencies. Here, we observed a significant increase in PL power in males during presentations of the CS- compared to the CS+ at all frequencies, which was mostly absent in females. We also saw increased IL power during presentations of the CS- compared to the CS+ at both theta and high gamma (64-120 Hz) frequencies in males, but not in females. In contrast, BLA power showed an overall increase during presentations of the CS- vs CS+ at most frequencies in both sexes.

Further to this, we observed an increase in theta coherence between all three areas in females during presentations of the CS+ compared to the CS-, which was absent in males. We also observed an overall increase in PL-BLA coherence to the CS+, compared to the CS-, in females at low and mid gamma frequencies, which was not present in males. In addition, we observed a significant increase in IL-BLA coherence during presentations of the CS+, compared to the CS-, at most gamma frequencies in females, whereas this was mostly absent in males. Finally, we observed that PL-IL coherence showed sex differences at theta and low gamma frequencies. PL-IL coherence in males showed increased coherence during CS+ vs CS- at low gamma but not theta, whereas female PL-IL coherence showed increased coherence during CS+ vs

CS- at theta but not low gamma. However, PL-IL coherence showed a similar pattern in both males and females at mid and high gamma frequencies, with no clear tone-dependent differences.

As we saw the greatest sex differences in PL power, we hypothesised that this region may be the most involved in mediating the sex differences observed in behaviour during retrieval of extended fear discrimination training (i.e. discrimination in males, and generalisation in females). The fact that we saw increased PL power in males during presentations of the CS-, compared to the CS+, was interesting, as it has typically been the IL which has been linked to the inhibition of fear behaviours (reviewed in Do-Monte et al., (2015)). The PL, on the other hand, has previously been linked to the promotion of fear behaviours (Corcoran & Quirk, 2007; Cheriyan et al., 2016). Due to this, we originally hypothesised that we may potentially see increased PL activity during presentations of the CS+ compared to the CS- in males, but that there would be little to no difference in PL activity during presentations of either tone in females.

However, as the PL projects directly to the PAG, which controls freezing (reviewed in Vianna & Brandão, (2003); Kim et al., 2013), the PL could inhibit freezing in response to the CS- via this downstream structure. It would be interesting to see whether the PL and PAG have increased coherence in males throughout presentations of the CS- during retrieval, and whether this coherence differs in females. Similarly, the BNST also receives direct PL input (Radley et al., 2009; Marek et al., 2013), meaning that, in addition to the PAG, the PL in males could potentially be modulating activity within this area to

influence freezing behaviour. This is especially relevant as the BNST is involved in anxiety, hypervigilance and threat monitoring (Somerville et al., 2010). Moreover, the BNST has also been implicated in fear discrimination (reviewed in Radke, (2009)). For example, Duvarci et al. (2009) showed that BNST activity was increased in animals which also showed inappropriate fear behaviour to the CS-. In our study, increased PL activity during the CS-, compared to the CS+, may also be acting to suppress BNST activity and therefore suppress inappropriate fear responding during the safety tone in males. As we did not see comparable increases in PL power during presentations of the CS-, compared to CS+, in females, this process of suppression may not have occurred, leading to generalisation.

Further to this, there is evidence to suggest that PL activity is linked to goal-directed response strategies (i.e. correct choice selection over a more automated or habitual response; Gourley & Taylor, 2016)). In our study, it may be that increased PL activity during presentations of the CS- compared to the CS+ in males results in the males choosing the appropriate response to the CS- (i.e. inhibition of fear behaviours), indicating PL involvement in appropriate response selection rather than promoting fear expression *per se*. It may be that the increased PL activity we observed in males during presentations of the CS- compared to the CS+, is involved in inhibiting inappropriate fear responding during the safety tone (i.e. males choosing to not freeze).

It is also possible that the process of extended discrimination training may have influenced PL activity differentially in males and females. Undergoing repeated sessions of fear discrimination training is a stressful experience, and

prior studies have reported that stress affects fear learning and memory differently in males and females (Dalla et al., 2007; Dalla & Shors, 2009). Recently, there has been evidence to suggest that stress can cause changes in PL activity in the gamma range, and that these changes may be different between males and females (Reincke & Hanganu-Opatz, 2017). However, this study looked at neonatal stress effects in the juvenile period, whereas we used adult rats. It could be that, in our study, prolonged stress from extended training caused differential changes in PL activity in males and females, wherein these changes promoted discrimination in males and generalisation in females.

Although Laviolette et al. (2005) and Fenton et al. (2014a) showed increased mPFC activity during presentations of the CS+ compared to the CS- these studies were conducted under anaesthesia. Therefore, differences between these studies and the results presented here may be due to differences in what PL activity signals under anaesthesia (i.e. learned association between CS+/US and CS-/no US) compared to the role of the PL while conscious (i.e. more associated with behavioural response selection).

We also observed a general increase in BLA power during presentations of the CS-, compared to CS+, in both sexes. The BLA is necessary for associative learning of multiple stimuli, especially in distinguishing neutral, or safe, stimuli in the presence of danger (Holmes et al., 2013). In addition to this, there is also evidence of increased LA activity during CS+ vs CS- in anesthetised and conscious rats (Rosenkranz & Grace, 2002; Collins & Pare 2000). Fenton et al. (2014a) also saw evidence of this in the BLA of anesthetised rats, therefore it is difficult to reconcile our findings with the results

of these previous studies. Recent work suggests a different and somewhat controversial role for BLA. Here, it has been suggested that BLA activity is more involved with the inhibition of behavioural engagement, rather than only the promotion of fear behaviours (reviewed in Pare and Quirk, 2017). It could be that we potentially showed more BLA activity during presentations of the CS-according to this new proposed role of the amygdala, wherein the BLA is more involved in behavioural inhibition than fear behaviour promotion. This may also provide evidence as to why data in conscious animals differs from work by Rosenkranz & Grace, (2002) and Fenton et al. (2014a) in anaesthetised animals. Further, this may partially explain why the data presented in Chapter 4 (where the BLA may be involved with behavioural inhibition) differs from Collins & Pare, 2000 (where the LA is involved with associative learning).

Interestingly, it has been reported that neurons within the BLA can be categorised based on their expression of Protein Kinase C (PKC) sub-types. PKC is a family of enzymes that alter (i.e. switch on or off) the function of other proteins through phosphorylation and can be activated by Ca^{2+} signal cascades. Recently, two sub-populations of neurons have been identified within the CeL of the BLA that have opposing functions related to PKC. One sub-type (CeLOFF cells) is inhibited in response to a CS following fear conditioning and expresses PKCδ(+), whereas another sub-type (CeLON) is excited by CS following fear conditioning and expresses PKCδ(-). Both sub-types of these neurons inhibit one another and project to the CeM. CeLON neurons respond to a fear CS at a shorter latency than CeLOFF cells, suggesting that conditioned fear responses occur following activation of CeLON neurons that inhibit

CeLOFF neurons projecting to CeM output neurons, thereby promoting freezing through disinhibition (Haubensak et al. 2010). If these sub-types were differentially activated in males and females, it could mean that there may be a corresponding activation or inhibition of the PAG and thus an increase or decrease in freezing, depending on which sub-type was active (reviewed in Janak & Tye, (2015)). Therefore, it may be that the general increase in LFP power we saw in the BLA during presentations of the CS- compared to the CS+ in both sexes is reflecting activity from both of these sub-populations, but that each sub-population is differentially activated in males and females during the CS+ and CS-. For example, in females, the CeLON cells could be overactive during the CS-, inhibiting the CeLOFF cells, but that these CeLON cells were not overactive during the CS- in males. This could potentially lead to the promotion of freezing and fear-related behaviours in females, but the inhibition of freezing in males, during the CS-. However, we need further experiments recording from these specific neuronal sub-populations to investigate whether they are differentially activated in males and females. An alternative explanation to this could be that, since males and females both show an overall increase in BLA activity during presentations of the CS- compared to the CS+, the BLA is not directly involved in sex differences found in fear discrimination and generalisation.

We also saw an increase in theta coherence between all three areas, in addition to a general increase in IL-BLA coherence, during presentations of the CS+ compared to the CS- in females, but not males. Further to this, we also observed an overall increase in PL-BLA coherence to the CS+, compared to

the CS-, in females at low and mid gamma frequencies, which was not present in males. Yet we saw preferential freezing to the CS+ compared to the CS- only in males, despite males showing no tone-dependent changes in mPFC-BLA theta coherence. Although it is challenging to hypothesise why increases in mPFC-BLA coherence occur during presentations of the CS+ compared to the CS- in females, yet BLA power is generally increased during presentations of the CS- compared to the CS+ in both sexes, one explanation might be a failed compensatory mechanism of mPFC (PL and IL) to regulate activity in BLA or other downstream areas to suppress fear during the CS-. For example, Fitzgerald et al. (2014b) saw a similar pattern in extinction-deficient mice, where they showed exaggerated single-unit firing in the IL region compared to control mice. In this study, they were also able to facilitate extinction by activating the IL with infusion of a GABA-A antagonist.

Alternatively, the BLA may be receiving additional input from brain regions other than the mPFC to modulate freezing behaviours, which act to promote fear regardless of the type of cue in females. As Likhtik et al. (2014) looked at contributions from the dorsal and ventral hippocampus in fear and safety learning but found no major differences in either region, we did not record from these regions in the present study. However, as only male mice were used by Likhtik et al. (2014), it could be that the hippocampus may contribute differentially in female generalisers (our study) compared to male generalisers (Likhtik et al., 2014). For example, although the VH is known to project to the mPFC and amygdala (Ishikawa & Nakamura, 2006), the balance of projections between the different areas may excite or inhibit differential neurons in males

compared to females. Therefore, in future studies including both males and females, it may be advantageous to include recordings from these hippocampal subregions, especially as hippocampal function also shows sex differences which may be hormone-dependent (Maren et al., 1994; Gupta et al., 2001).

5.3.1 Potential Future Electrophysiological Studies

Although, to our knowledge, this is the first time LFP recordings from all three of these areas have been recorded during retrieval of fear discrimination in both males and females, there is still scope for refinements to be made in future electrophysiological studies. In Chapter 2, we observed the greatest sex difference in behaviour after extended training, wherein males showed increased freezing preferentially to the CS+ compared to the CS- and females showed generalised freezing across both tones. However, we did also see sex differences with limited training, wherein females successfully discriminated after only one day of training, and males did not. Because of this, it would also be interesting to conduct electrophysiological recordings to determine power in, and coherence between, the PL, IL and BLA during retrieval after limited discrimination training. From this, we could then investigate whether activity and synchrony within these regions is comparable when females discriminate versus when males generalise. It may be that, because males are still learning the associations between the CS+, CS- and US with limited training, they show different power and coherence within these regions to females which generalise with extended training, even though they display comparable freezing to both tones.

Further, other studies have shown that phase-amplitude coupling (PAC), wherein the phase of one frequency is coupled to the amplitude of another frequency, is present in a variety of tasks and cortical regions, including fear and safety memory retrieval (Voytek et al., 2010; Bocchio & Capogna, 2014; Stujenske et al., 2014; Zheng et al., 2017). As Stujenske et al. (2014) found strong coupling of BLA gamma to mPFC theta during periods of relative safety, we did investigate coupling of gamma and theta in all three recorded regions during presentations of fear and safety cues, but we have so far not found any evidence of PAC in either sex (analysis ongoing).

There is also the potential caveat of the LFP signals we recorded in this study being volume conducted from other areas. This is especially important for comparing activity from the PL and IL as they are adjacent to one another. To overcome this limitation, future studies investigating these areas should include spike recordings as well as LFPs. From this, the role of LFP-spike interactions, for example theta entrainment of correlated spike firing, could be studied in fear discrimination and generalisation in both males and females.

5.4 Concluding remarks

From the work conducted in this thesis, we have contributed to and expanded upon research describing potential neurobiological phenomena which underpin fear-based mental disorders, such as anxiety and PTSD. Further, by including females in our research, with a focus on the sex differences which may underlie these disorders, we hope to improve on the dearth of animal studies which involve equal contributions from both sexes. To our knowledge, we are the first

to investigate sex differences in behaviour and PL-IL-BLA circuit function, using complementary *in silico* computational modelling and *in vivo* electrophysiology approaches, during cued fear discrimination. We have provided novel evidence highlighting the complex functional interactions between these regions during fear discrimination, in addition to how these interactions may contribute to sex differences in cued fear and safety learning and memory.

6. Appendix

6.1 Professional Internships for PhD Students Reflection Form

Name of Organization

Sense About Science, London.

Details of Placement

To promote a better working relationship between scientists and members of the public, I designed several infographics to debunk detox in partnership with the Wellcome Trust, published news stories for the AllTrials campaign and 'For the Record', and managed the public plant science and energy Q&A forums.

Placement Achievements

Ask for Evidence Workshop, The Royal Society: Helped to plan and teach a workshop to 11-18 year olds as part of my work with SAS on the 'Ask for Evidence' campaign, which encourages the public to question evidence they're given in support of claims seen in digital and print media.

Skill development

- Science Communication

- Photo and Video Editing

- Webpage creation and Maintenance

- Increased knowledge of Science Policy and Law

6.2 MATLAB Code for Models 1, 2 and 3

6.2.1 Code for Model 1

```matlab
function FS_Model1_C = FS_Model1_C()
start=0;
finish=900;
tspan=[0 900];

P.start1=10;
P.start2=710;
P.finish1=600;
P.finish2=finish;
P.on_duration=10;
P.period=40;
P.amplitude=0.5;
P.amplitude2=0.5;

M.start1=30;
M.start2=730;
M.finish1=600;
M.finish2=finish;
M.on_duration=10;
M.period=40;
M.amplitude=0.5;

U.start=19;
U.finish=600;
U.on_duration=1;
U.period=40;
U.amplitude=0.5;

U.TLearn=700;

Fp=1.2;
Ftheta=2.8;

Sp=1.2;
Stheta=2.8;

x0=[0.5;0.5;0.05;0.05];

F.wab=-1;
F.wba=1;

F.alphaA=0.15;
F.alphaB=0.15;
F.rA=0.001;
F.rB=0.001;
F.kA=0.97;
F.kB=0.97;
F.TauA=10;
F.TauB=10;

figure(1);
clf
t=-5:0.1:10;
subplot(2,1,1)
plot(t,SF(t,Fp,Ftheta),'red');
```

```
legend('F Sigmoid');
subplot(2,1,2)
plot(t,SS(t,Sp,Stheta),'green');
legend('S Sigmoid');

figure(2)
clf
[t,x]=ode45(@f,tspan,x0,[],P,M,U,F,Fp,Sp,Ftheta,Stheta);
subplot(3,1,1)
plot(t,x(:,3),'red',t,x(:,4),'green');
axis([start finish -0.1 U.amplitude+0.5])
legend('F','S');
xlabel('Time (t)');ylabel('Neural Activity');
subplot(3,1,2)
plot(t,x(:,1),'red', t,x(:,2),'green');
xlabel('Time (t)');ylabel('Learning Rates');
legend('CS+ and US (F)','CS- (S)');
subplot(3,1,3)
hold on
plot(t,CSPlus(t,P),'r')
plot(t,CSMinus(t,M),'b')
plot(t,US(t,U),'y')
plot(t,CSPlus2(t,P),'r')
plot(t,CSMinus2(t,M),'b')
axis([start finish -0.1 U.amplitude+0.5])
box on
xlabel('Time (t)');ylabel('Input Stimuli');
legend('CS+','CS-','US')
ticks=start:100:finish;
set(gca,'XTick', ticks)

end
function dxdt = f(t,x,P,M,U,F,Fp,Sp,Ftheta,Stheta)
wcf=x(1);
wcs=x(2);
F=x(3);
S=x(4);

if (t < U.TLearn)

dxdt = [F.alphaA*(CSPlus(t,P)+(CSMinus(t,M)+US(t,U)));
        F.alphaB*(CSPlus(t,P)+(CSMinus(t,M)+US(t,U)));
(-F+(F.kF-
F.rF*F)*SF(wcf*(CSPlus(t,P)+(US(t,U))+F.wsf*(S)),Fp,Ftheta))/F.TauF;
(-S+(F.kS-
F.rS*S)*SS(wcs*(CSMinus(t,M)+F.wfs*(F)),Sp,Stheta))/F.TauS];
else
    dxdt = [0;
        0;
(-F+(F.kF-F.rF*F)*SF(wcf*(CSPlus2(t,P)+F.wsf*(B)),Fp,Ftheta))/F.TauF;
(-S+(F.kS-
F.rS*S)*SS(wcs*(CSMinus2(t,M)+F.wfs*(F)),Sp,Stheta))/F.TauS];
end
end
function SF = SF(x,Fp,Ftheta)
SF = 1./(1+exp(-Fp*(x-Ftheta)));
end
function SS = SS(x,Sp,Stheta)
SS = 1./(1+exp(-Sp*(x-Stheta)));
end
function CSPlus = CSPlus(t,P)
CSPlus = (t>P.start1).*(t<P.finish1).*Pluspulse(mod(t-
P.start1,P.period),P);
```

```matlab
end
function CSPlus2 = CSPlus2(t,P)
CSPlus2 = (t>P.start2).*(t<P.finish2).*Pluspulse2(mod(t-
P.start2,P.period),P);
end
function CSMinus = CSMinus(t,M)
CSMinus = (t>M.start1).*(t<M.finish1).*Minuspulse(mod(t-
M.start1,M.period),M);
end
function CSMinus2 = CSMinus2(t,M)
CSMinus2 = (t>M.start2).*(t<M.finish2).*Minuspulse(mod(t-
M.start2,M.period),M);
end
function Pluspulse = Pluspulse(t,P)
Pluspulse = P.amplitude*(t<P.on_duration);
end
function Pluspulse2 = Pluspulse2(t,P)
Pluspulse2 = P.amplitude2*(t<P.on_duration);
end
function Minuspulse = Minuspulse(t,M)
Minuspulse = M.amplitude*(t<M.on_duration);
end
function US = US(t,U)
US = (t>U.start).*(t<U.finish).*USpulse(mod(t-U.start,U.period),U);
end
function USpulse = USpulse(t,U)
USpulse = U.amplitude*(t<U.on_duration);
end
```

6.2.2 Code for Model 2

```matlab
function FPM_SPM_Model2_C = FPM_SPM_Model2_C()

start=0;
finish=900;
tspan= [0 900];

P.start1=10;
P.start2=710;
P.finish1=600;
P.finish2=finish;
P.on_duration=10;
P.period=40;
P.amplitude=0.5;
P.amplitude2=0.5;

M.start1=30;
M.start2=730;
M.finish1=600;
M.finish2=finish;
M.on_duration=10;
M.period=40;
M.amplitude=0.5;
M.amplitude2=0.5;

U.start=19;
U.finish=600;
U.on_duration=1;
U.period=40;
U.amplitude=0.5;
```

```
U.TLearn=700;

S.FpP=1.2;
S.FpT=2.8;
S.FmP=1.2;
S.FmT=2.8;
S.SpP=1.2;
S.SpT=2.8;
S.SmP=1.2;
S.SmT=2.8;

G.kFp=0.97;
G.kFm=0.97;
G.kSp=0.97;
G.kSm=0.97;

G.rFp=0.001;
G.rFm=0.001;
G.rSp=0.001;
G.rSm=0.001;

G.tauFp=10;
G.tauFm=10;
G.tauSp=10;
G.tauSm=10;

Fp0=0.05;
Fm0=0.05;
Sp0=0.05;
Sm0=0.05;

WCpFp0=0;  WCpFm0=0; WCpSp0=0;  WCpSm0=0;
WCmFp=0;   WCmFm=0;  WCmSp0=0; WCmSm0=0;
WCuFp0=0;  WCuFm0=0; WCuSp0=0;  WCuSm0=0;

x0=[Fp0; Fm0; Sp0; Sm0; WCpFp0; WCpFm0; WCmSp0; WCmSm0; WCuFp0;
WCuFm0];

figure(1);
clf
t=-5:0.1:10;
subplot(4,1,1)
plot(t,sigFp(t,S),'red');
legend('F+ Sigmoid');
subplot(4,1,2)
plot(t,sigFm(t,S),'magenta');
legend('F- Sigmoid');
subplot(4,1,3)
plot(t,sigSp(t,S),'green');
legend('S+ Sigmoid');
subplot(4,1,4)
plot(t,sigSm(t,S),'blue');
legend('S- Sigmoid');

figure(2)
clf
[t,x]=ode45(@f,tspan,x0,[],M,P,U,G,S);
subplot(3,1,1)
plot(t,x(:,1),'red',t,x(:,3),'green');
legend('F+','S+');
xlabel('Time (t)');ylabel('Neural Activity');
axis([start finish -0.1 U.amplitude+0.5])
subplot(3,1,2)
```

```
plot(t,x(:,5),'red',t,x(:,9),'yellow',t,x(:,7),'blue');
xlabel('Time (t)');ylabel('CS+ US (F+), CS- (S+)');
legend('wCpFp0','wCuFp0','wCmSp0');
subplot(3,1,3)
hold on
plot(t,CSPlus(t,P),'r')
plot(t,CSMinus(t,M),'b')
plot(t,US(t,U),'y')
plot(t,CSPlus2(t,P),'r')
plot(t,CSMinus2(t,M),'b')
axis([start finish -0.1 U.amplitude+0.2])
box on
xlabel('Time (t)');ylabel('Input Stimuli');
legend('CS+','CS-','US')
ticks=start:100:finish;
set(gca,'XTick', ticks)

figure(3)
clf
[t,x]=ode45(@f,tspan,x0,[],M,P,U,G,S);
subplot(3,1,1)
plot(t,x(:,1),'red',t,x(:,4),'blue');
legend('F+','S-');
xlabel('Time (t)');ylabel('Neural Activity');
axis([start finish -0.1 U.amplitude+0.5])
subplot(3,1,2)
plot(t,x(:,5),'red',t,x(:,9),'yellow',t,x(:,8),'blue');
xlabel('Time (t)');ylabel('CS+ US (F+), CS- (S-)');
legend('wCpFp0','wCuFp0','wCmSm0');
subplot(3,1,3)
hold on
plot(t,CSPlus(t,P),'r')
plot(t,CSMinus(t,M),'b')
plot(t,US(t,U),'y')
plot(t,CSPlus2(t,P),'r')
plot(t,CSMinus2(t,M),'b')
axis([start finish -0.1 U.amplitude+0.2])
box on
xlabel('Time (t)');ylabel('Input Stimuli');
legend('CS+','CS-','US')
ticks=start:100:finish;
set(gca,'XTick', ticks)

figure(4)
clf
[t,x]=ode45(@f,tspan,x0,[],M,P,U,G,S);
subplot(3,1,1)
plot(t,x(:,2),'magenta ',t,x(:,3),'green');
legend('F-','S+');
xlabel('Time (t)');ylabel('Neural Activity');
axis([start finish -0.1 U.amplitude+0.5])
subplot(3,1,2)
plot(t,x(:,6),'red',t,x(:,10),'yellow',t,x(:,7),'blue');
xlabel('Time (t)');ylabel('CS+ US (F-), CS- (S+)');
legend('wCpFm0','wCuFm0','wCmSp0');
subplot(3,1,3)
hold on
plot(t,CSPlus(t,P),'r')
plot(t,CSMinus(t,M),'b')
plot(t,US(t,U),'y')
plot(t,CSPlus2(t,P),'r')
plot(t,CSMinus2(t,M),'b')
axis([start finish -0.1 U.amplitude+0.2])
```

```
box on
xlabel('Time (t)');ylabel('Input Stimuli');
legend('CS+','CS-','US')
ticks=start:100:finish;
set(gca,'XTick', ticks)

figure(5)
clf
[t,x]=ode45(@f,tspan,x0,[],M,P,U,G,S);
subplot(3,1,1)
plot(t,x(:,2),'magenta',t,x(:,4),'blue');
legend('F-','S-');
xlabel('Time (t)');ylabel('Neural Activity');
axis([start finish -0.1 U.amplitude+0.5])
subplot(3,1,2)
plot(t,x(:,6),'red',t,x(:,10),'yellow',t,x(:,8),'blue');
xlabel('Time (t)');ylabel('CS+ US (F-), CS- (S-)');
legend('wCpFm0','wCuFm0','wCmSm0');
subplot(3,1,3)
hold on
plot(t,CSPlus(t,P),'r')
plot(t,CSMinus(t,M),'b')
plot(t,US(t,U),'y')
plot(t,CSPlus2(t,P),'r')
plot(t,CSMinus2(t,M),'b')
axis([start finish -0.1 U.amplitude+0.2])
box on
xlabel('Time (t)');ylabel('Input Stimuli');
legend('CS+','CS-','US')
ticks=start:100:finish;
set(gca,'XTick', ticks)

figure(6)
clf
[t,x]=ode45(@f,tspan,x0,[],M,P,U,G,S);
subplot(2,1,1)
plot(t,x(:,1),'red',t,x(:,2),'magenta',t,x(:,3),'green',t,x(:,4),'blu
e');
legend('F+','F-','S+','S-');
xlabel('Time (t)');ylabel('Neural Activity');
axis([start finish -0.1 U.amplitude+0.5])
subplot(2,1,2)
hold on
plot(t,CSPlus(t,P),'r')
plot(t,CSMinus(t,M),'b')
plot(t,US(t,U),'y')
plot(t,CSPlus2(t,P),'r')
plot(t,CSMinus2(t,M),'b')
axis([start finish -0.1 U.amplitude+0.2])
box on
xlabel('Time (t)');ylabel('Input Stimuli');
legend('CS+','CS-','US')
ticks=start:100:finish;
set(gca,'XTick', ticks)

end

function dxdt = f(t,x,M,P,U,G,S)
Fp0=x(1);
Fm0=x(2);
Sp0=x(3);
Sm0=x(4);
WCpFp0=x(5);
```

```
WCuFp0=x(6);
WCpFm0=x(7);
WCuFm0=x(8);
WCmSp0=x(9);
WCmSm0=x(10);

WFpFp=1; WFpFm=0; WFpSp=0; WFpSm=0;
WFmFp=-1; WFmFm=-1; WFmSp=-1; WFmSm=-1;
WSpFp=0; WSpFm=0; WSpSp=-1; WSpSm=0;
WSmFp=-1; WSmFm=1; WSmSp=-1; WSmSm=-1;

RateCpFp=0.15;
RateCpFm=0.15;
RateCmSp=0.15;
RateCmSm=0.15;
RateCuFp=0.15;
RateCuFm=0.15;

if (t<U.TLearn)

dxdt =
[(-Fp0+(G.kFp-
G.rFp*Fp0)*sigFp(WCpFp0*(CSPlus(t,P)+WCuFp0*(US(t,U))+(WFpFp*Fp0+WFpF
m*Fm0+WFpSp*Sp0+WFpSm*Sm0)),S))/G.tauFp;
        (-Fm0+(G.kFm-
G.rFm*Fm0)*sigFm(WCpFm0*(CSPlus(t,P)+WCuFm0*(US(t,U))+(WFmFm*Fm0+WFmF
p*Fp0+WFmSp*Sp0+WFmSm*Sm0)),S))/G.tauFm;
        (-Sp0+(G.kSp-
G.rSp*Sp0)*sigSp(WCmSp0*(CSMinus(t,M)+(WSpSp*Sp0+WSpFp*Fp0+WSpFm*Fm0+
WSpSm*Sm0)),S))/G.tauSp;
        (-Sm0+(G.kSm-
G.rSm*Sm0)*sigSm(WCmSm0*(CSMinus(t,M)+(WSmSm*Sm0+WSmFp*Fp0+WSmFm*Fm0+
WSmSp*Sp0)),S))/G.tauSm;

         RateCpFp*(CSPlus(t,P)+(CSMinus(t,M)+(US(t,U))));
         RateCpFm*(CSPlus(t,P)+(CSMinus(t,M)+(US(t,U))));
         RateCuFp*(CSPlus(t,P)+(CSMinus(t,M)+(US(t,U))));
         RateCuFm*(CSPlus(t,P)+(CSMinus(t,M)+(US(t,U))));
         RateCmSp*(CSPlus(t,P)+(CSMinus(t,M)+(US(t,U))));
         RateCmSm*(CSPlus(t,P)+(CSMinus(t,M)+(US(t,U))))];

else
dxdt = [(-Fp0+(G.kFp-
G.rFp*Fp0)*sigFp(WCpFp0*(CSPlus2(t,P)+WCuFp0*(US(t,U))+(WFpFp*Fp0+WFp
Fm*Fm0+WFpSp*Sp0+WFpSm*Sm0)),S))/G.tauFp;
        (-Fm0+(G.kFm-
G.rFm*Fm0)*sigFm(WCpFm0*(CSPlus2(t,P)+WCuFm0*(US(t,U))+(WFmFm*Fm0+WFm
Fp*Fp0+WFmSp*Sp0+WFmSm*Sm0)),S))/G.tauFm;
        (-Sp0+(G.kSp-
G.rSp*Sp0)*sigSp(WCmSp0*(CSMinus2(t,M)+(WSpSp*Sp0+WSpFp*Fp0+WSpFm*Fm0
+WSpSm*Sm0)),S))/G.tauSp;
        (-Sm0+(G.kSm-
G.rSm*Sm0)*sigSm(WCmSm0*(CSMinus2(t,M)+(WSmSm*Sm0+WSmFp*Fp0+WSmFm*Fm0
+WSmSp*Sp0)),S))/G.tauSm;
        0;
        0;
        0;
        0;
        0;
        0;];

end
end
```

```matlab
function sigFp = sigFp(x,S)
sigFp=1./(1+exp(-S.FpP*(x-S.FpT)));
end
function sigFm = sigFm(x,S)
sigFm=1./(1+exp(-S.FmP*(x-S.FmT)));
end
function sigSp = sigSp(x,S)
sigSp=1./(1+exp(-S.SpP*(x-S.SpT)));
end
function sigSm = sigSm(x,S)
sigSm=1./(1+exp(-S.SmP*(x-S.SmT)));
end
function CSPlus = CSPlus(t,P)
CSPlus = (t>P.start1).*(t<P.finish1).*Pluspulse(mod(t-
P.start1,P.period),P);
end
function CSPlus2 = CSPlus2(t,P)
CSPlus2 = (t>P.start2).*(t<P.finish2).*Pluspulse2(mod(t-
P.start2,P.period),P);
end
function CSMinus = CSMinus(t,M)
CSMinus = (t>M.start1).*(t<M.finish1).*Minuspulse(mod(t-
M.start1,M.period),M);
end
function CSMinus2 = CSMinus2(t,M)
CSMinus2 = (t>M.start2).*(t<M.finish2).*Minuspulse2(mod(t-
M.start2,M.period),M);
end
function Pluspulse = Pluspulse(t,P)
Pluspulse = P.amplitude*(t<P.on_duration);
end
function Pluspulse2 = Pluspulse2(t,P)
Pluspulse2 = P.amplitude2*(t<P.on_duration);
end
function Minuspulse = Minuspulse(t,M)
Minuspulse = M.amplitude*(t<M.on_duration);
end
function Minuspulse2 = Minuspulse2(t,M)
Minuspulse2 = M.amplitude2*(t<M.on_duration);
end
function US = US(t,U)
US = (t>U.start).*(t<U.finish).*USpulse(mod(t-U.start,U.period),U);
end
function USpulse = USpulse(t,U)
USpulse = U.amplitude*(t<U.on_duration);
end
```

6.2.3 Code for Model 3

```matlab
function Model_3_PL_2 = Model_3_PL_2()
start=0;
finish=900;
tspan= [0 900];
P.start1=10;
P.start2=710;
P.finish1=600;
P.finish2=finish;
P.on_duration=10;
P.period=40;
P.amplitude=0.5;
P.amplitude2=0.5;
```

```
M.start1=30;
M.start2=730;
M.finish1=600;
M.finish2=finish;
M.on_duration=10;
M.period=40;
M.amplitude=0.5;
M.amplitude2=0.5;
U.start=19;
U.finish=600;
U.on_duration=1;
U.period=40;
U.amplitude=0.5;

U.TLearn=700;
S.FpP=1.2;
S.FpT=2.8;
S.FmP=1.2;
S.FmT=2.8;
S.SpP=1.2;
S.SpT=2.8;
S.SmP=1.2;
S.SmT=2.8;
G.kFp=0.97;
G.kFm=0.97;
G.kSp=0.97;
G.kSm=0.97;
G.rFp=0.001;
G.rFm=0.001;
G.rSp=0.001;
G.rSm=0.001;
G.tauFp=10;
G.tauFm=10;
G.tauSp=10;
G.tauSm=10;
Fp0=0.05;
Fm0=0.05;
Sp0=0.05;
Sm0=0.05;

WCpFp0=0;   WCpFm0=0; WCpSp=0;   WCpSm=0;
WCmFp=0;    WCmFm=0;  WCmSp0=0; WCmSm0=0;
WCuFp0=0;   WCuFm0=0; WCuSp=0;   WCuSm=0;
WPLFp0=0;   WPLFm0=0; WPLSp0=0; WPLSm0=0;

x0=[Fp0; Fm0; Sp0; Sm0; WCpFp0; WCpFm0; WCmSp0; WCmSm0; WCuFp0;
WCuFm0; WPLFp0; WPLFm0; WPLSp0; WPLSm0;];

figure(1);
clf
t=-5:0.1:10;
subplot(4,1,1)
plot(t,sigFp(t,S),'red');
legend('F+ Sigmoid');
subplot(4,1,2)
plot(t,sigFm(t,S),'magenta');
legend('F- Sigmoid');
subplot(4,1,3)
plot(t,sigSp(t,S),'green');
legend('S+ Sigmoid');
subplot(4,1,4)
plot(t,sigSm(t,S),'blue');
legend('S- Sigmoid');
```

266

```
figure(2)
clf
[t,x]=ode45(@f,tspan,x0,[],M,P,U,G,S);
subplot(3,1,1)
plot(t,x(:,1),'red',t,x(:,3),'green');
legend('F+','S+');
xlabel('Time (t)');ylabel('Neural Activity');
axis([start finish -0.1 U.amplitude+0.5])
subplot(3,1,2)
plot(t,x(:,5),'red',t,x(:,9),'yellow',t,x(:,7),'blue');
xlabel('Time (t)');ylabel('CS+ US (F+), CS- (S+)');
legend('wCpFp0','wCuFp0','wCmSp0');
subplot(3,1,3)
hold on
plot(t,CSPlus(t,P),'r')
plot(t,CSMinus(t,M),'b')
plot(t,US(t,U),'y')
plot(t,CSPlus2(t,P),'r')
plot(t,CSMinus2(t,M),'b')
axis([start finish -0.1 U.amplitude+0.2])
box on
xlabel('Time (t)');ylabel('Input Stimuli');
legend('CS+','CS-','US')
ticks=start:100:finish;
set(gca,'XTick', ticks)

figure(3)
clf
[t,x]=ode45(@f,tspan,x0,[],M,P,U,G,S);
subplot(3,1,1)
plot(t,x(:,1),'red',t,x(:,4),'blue');
legend('F+','S-');
xlabel('Time (t)');ylabel('Neural Activity');
axis([start finish -0.1 U.amplitude+0.5])
subplot(3,1,2)
plot(t,x(:,5),'red',t,x(:,9),'yellow',t,x(:,8),'blue');
xlabel('Time (t)');ylabel('CS+ US (F+), CS- (S-)');
legend('wCpFp0','wCuFp0','wCmSm0');
subplot(3,1,3)
hold on
plot(t,CSPlus(t,P),'r')
plot(t,CSMinus(t,M),'b')
plot(t,US(t,U),'y')
plot(t,CSPlus2(t,P),'r')
plot(t,CSMinus2(t,M),'b')
axis([start finish -0.1 U.amplitude+0.2])
box on
xlabel('Time (t)');ylabel('Input Stimuli');
legend('CS+','CS-','US')
ticks=start:100:finish;
set(gca,'XTick', ticks)

figure(4)
clf
[t,x]=ode45(@f,tspan,x0,[],M,P,U,G,S);
subplot(3,1,1)
plot(t,x(:,2),'magenta ',t,x(:,3),'green');
legend('F-','S+');
xlabel('Time (t)');ylabel('Neural Activity');
axis([start finish -0.1 U.amplitude+0.5])
subplot(3,1,2)
plot(t,x(:,6),'red',t,x(:,10),'yellow',t,x(:,7),'blue');
```

```
xlabel('Time (t)');ylabel('CS+ US (F-), CS- (S+)');
legend('wCpFm0','wCuFm0','wCmSp0');
subplot(3,1,3)
hold on
plot(t,CSPlus(t,P),'r')
plot(t,CSMinus(t,M),'b')
plot(t,US(t,U),'y')
plot(t,CSPlus2(t,P),'r')
plot(t,CSMinus2(t,M),'b')
axis([start finish -0.1 U.amplitude+0.2])
box on
xlabel('Time (t)');ylabel('Input Stimuli');
legend('CS+','CS-','US')
ticks=start:100:finish;
set(gca,'XTick', ticks)
figure(5)
clf
[t,x]=ode45(@f,tspan,x0,[],M,P,U,G,S);
subplot(3,1,1)
plot(t,x(:,2),'magenta',t,x(:,4),'blue');
legend('F-','S-');
xlabel('Time (t)');ylabel('Neural Activity');
axis([start finish -0.1 U.amplitude+0.5])
subplot(3,1,2)
plot(t,x(:,6),'red',t,x(:,10),'yellow',t,x(:,8),'blue');
xlabel('Time (t)');ylabel('CS+ US (F-), CS- (S-)');
legend('wCpFm0','wCuFm0','wCmSm0');
subplot(3,1,3)
hold on
plot(t,CSPlus(t,P),'r')
plot(t,CSMinus(t,M),'b')
plot(t,US(t,U),'y')
plot(t,CSPlus2(t,P),'r')
plot(t,CSMinus2(t,M),'b')
axis([start finish -0.1 U.amplitude+0.2])
box on
xlabel('Time (t)');ylabel('Input Stimuli');
legend('CS+','CS-','US')
ticks=start:100:finish;
set(gca,'XTick', ticks)
figure(6)
clf
[t,x]=ode45(@f,tspan,x0,[],M,P,U,G,S);
subplot(2,1,1)
plot(t,x(:,1),'red',t,x(:,2),'magenta',t,x(:,3),'green',t,x(:,4),'blu
e');
legend('F+','F-','S+','S-');
xlabel('Time (t)');ylabel('Neural Activity');
axis([start finish -0.1 U.amplitude+0.5])
subplot(2,1,2)
hold on
plot(t,CSPlus(t,P),'r')
plot(t,CSMinus(t,M),'b')
plot(t,US(t,U),'y')
plot(t,CSPlus2(t,P),'r')
plot(t,CSMinus2(t,M),'b')
axis([start finish -0.1 U.amplitude+0.2])
box on
xlabel('Time (t)');ylabel('Input Stimuli');
legend('CS+','CS-','US')
ticks=start:100:finish;
set(gca,'XTick', ticks)
end
```

```
function dxdt = f(t,x,M,P,U,G,S)
Fp0=x(1);
Fm0=x(2);
Sp0=x(3);
Sm0=x(4);
WCpFp0=x(5);
WCuFp0=x(6);
WCpFm0=x(7);
WCuFm0=x(8);
WCmSp0=x(9);
WCmSm0=x(10);
WPLFp0=x(11);
WPLFm0=x(12);
WPLSp0=x(13);
WPLSm0=x(14);
WFpFp=-1; WFpFm=1; WFpSp=0; WFpSm=0;
WFmFp=-1; WFmFm=-1; WFmSp=-1; WFmSm=-1;
WSpFp=0; WSpFm=0; WSpSp=-1; WSpSm=1;
WSmFp=-1; WSmFm=0; WSmSp=-1; WSmSm=-1;
WPLFp=1; WPLFm=0; WPLSp=0; WPLSm=1;
RateCpFp=0.15;
RateCpFm=0.15;
RateCmSp=0.15;
RateCmSm=0.15;
RateCuFp=0.15;
RateCuFm=0.15;
RatePLFp=0.15;
RatePLFm=0.15;
RatePLSp=0.15;
RatePLSm=0.15;
if (t<U.TLearn
dxdt = [(-Fp0+(G.kFp-
G.rFp*Fp0)*sigFp(WCpFp0*(CSPlus(t,P)+WCuFp0*(US(t,U))+(WFpFp*Fp0+WFpF
m*Fm0+WFpSp*Sp0+WFpSm*Sm0+WPLFp*Fp0)),S))/G.tauFp;
        (-Fm0+(G.kFm-
G.rFm*Fm0)*sigFm(WCpFm0*(CSPlus(t,P)+WCuFm0*(US(t,U))+(WFmFm*Fm0+WFmF
p*Fp0+WFmSp*Sp0+WFmSm*Sm0+WPLFm*Fm0)),S))/G.tauFm;
        (-Sp0+(G.kSp-
G.rSp*Sp0)*sigSp(WCmSp0*(CSMinus(t,M)+(WSpSp*Sp0+WSpFp*Fp0+WSpFm*Fm0+
WSpSm*Sm0+WPLSp*Sp0)),S))/G.tauSp;
        (-Sm0+(G.kSm-
G.rSm*Sm0)*sigSm(WCmSm0*(CSMinus(t,M)+(WSmSm*Sm0+WSmFp*Fp0+WSmFm*Fm0+
WSmSp*Sp0+WPLSm*Sm0)),S))/G.tauSm;
        RateCpFp*(CSPlus(t,P)+(CSMinus(t,M)+(US(t,U)))));
        RateCpFm*(CSPlus(t,P)+(CSMinus(t,M)+(US(t,U)))));
        RateCuFp*(CSPlus(t,P)+(CSMinus(t,M)+(US(t,U)))));
        RateCuFm*(CSPlus(t,P)+(CSMinus(t,M)+(US(t,U)))));
        RateCmSp*(CSPlus(t,P)+(CSMinus(t,M)+(US(t,U)))));
        RateCmSm*(CSPlus(t,P)+(CSMinus(t,M)+(US(t,U)))));
        RatePLFp;
        RatePLFm;
        RatePLSp;
        RatePLSm;];
else
dxdt = [(-Fp0+(G.kFp-
G.rFp*Fp0)*sigFp(WCpFp0*(CSPlus2(t,P)+WCuFp0*(US(t,U))+(WFpFp*Fp0+WFp
Fm*Fm0+WFpSp*Sp0+WFpSm*Sm0+WPLFp*Fp0)),S))/G.tauFp;
        (-Fm0+(G.kFm-
G.rFm*Fm0)*sigFm(WCpFm0*(CSPlus2(t,P)+WCuFm0*(US(t,U))+(WFmFm*Fm0+WFm
Fp*Fp0+WFmSp*Sp0+WFmSm*Sm0+WPLFm*Fm0)),S))/G.tauFm;
        (-Sp0+(G.kSp-
G.rSp*Sp0)*sigSp(WCmSp0*(CSMinus2(t,M)+(WSpSp*Sp0+WSpFp*Fp0+WSpFm*Fm0
+WSpSm*Sm0+WPLSp*Sp0)),S))/G.tauSp;
```

```matlab
        (-Sm0+(G.kSm-
G.rSm*Sm0)*sigSm(WCmSm0*(CSMinus2(t,M)+(WSmSm*Sm0+WSmFp*Fp0+WSmFm*Fm0
+WSmSp*Sp0+WPLSm*Sm0)),S))/G.tauSm;
        0;
        0;
        0;
        0;
        0;
        0;
        0;
        0;
        0;
        0;];
    end
end
function sigFp = sigFp(x,S)
sigFp=1./(1+exp(-S.FpP*(x-S.FpT)));
end
function sigFm = sigFm(x,S)
sigFm=1./(1+exp(-S.FmP*(x-S.FmT)));
end
function sigSp = sigSp(x,S)
sigSp=1./(1+exp(-S.SpP*(x-S.SpT)));
end
function sigSm = sigSm(x,S)
sigSm=1./(1+exp(-S.SmP*(x-S.SmT)));
end
function CSPlus = CSPlus(t,P)
CSPlus = (t>P.start1).*(t<P.finish1).*Pluspulse(mod(t-
P.start1,P.period),P);
end
function CSPlus2 = CSPlus2(t,P)
CSPlus2 = (t>P.start2).*(t<P.finish2).*Pluspulse2(mod(t-
P.start2,P.period),P);
end
function CSMinus = CSMinus(t,M)
CSMinus = (t>M.start1).*(t<M.finish1).*Minuspulse(mod(t-
M.start1,M.period),M);
end
function CSMinus2 = CSMinus2(t,M)
CSMinus2 = (t>M.start2).*(t<M.finish2).*Minuspulse2(mod(t-
M.start2,M.period),M);
end
function Pluspulse = Pluspulse(t,P)
Pluspulse = P.amplitude*(t<P.on_duration);
end
function Pluspulse2 = Pluspulse2(t,P)
Pluspulse2 = P.amplitude2*(t<P.on_duration);
end
function Minuspulse = Minuspulse(t,M)
Minuspulse = M.amplitude*(t<M.on_duration);
end
function Minuspulse2 = Minuspulse2(t,M)
Minuspulse2 = M.amplitude2*(t<M.on_duration);
end
function US = US(t,U)
US = (t>U.start).*(t<U.finish).*USpulse(mod(t-U.start,U.period),U);
end
function USpulse = USpulse(t,U)
USpulse = U.amplitude*(t<U.on_duration);
end
```

References

Abbott, L. F., DePasquale, B., & Memmesheimer, R.-M. (2016). Building functional networks of spiking model neurons. *Nature Neuroscience*, *19*(3), 350–355.

Adhikari, A., Lerner, T. N., Finkelstein, J., Pak, S., Jennings, J. H., Davidson, T. J., Deisseroth, K. (2015). Basomedial amygdala mediates top-down control of anxiety and fear. *Nature*, *527*.

Adhikari, A., Topiwala, M. A., & Gordon, J. A. (2010). Synchronized Activity between the Ventral Hippocampus and the Medial Prefrontal Cortex during Anxiety. *Neuron*, *65*(2), 257–269.

Adhikari, A., Topiwala, M. A., & Gordon, J. A. (2011). Single units in the medial prefrontal cortex with anxiety-related firing patterns are preferentially influenced by ventral hippocampal activity. *Neuron*, *71*(5), 898–910.

Aghdaee, S. M., Battelli, L., & Assad, J. A. (2014). Relative timing: from behaviour to neurons. *Philosophical Transactions of the Royal Society of London. Series B, Biological Sciences*, *369*(1637), 20120472.

Aguilar, R., Gil, L., Gray, J. A., Driscoll, P., Flint, J., Dawson, G. R., … Tobeña, A. (2003). Fearfulness and sex in F2 Roman rats: males display more fear though both sexes share the same fearfulness traits. *Physiology & Behavior*, *78*(4–5), 723–732.

Akam, T., & Kullmann, D. M. (2014). Oscillatory multiplexing of population codes for selective communication in the mammalian brain. *Nature Reviews. Neuroscience*, *15*(2), 111–22.

Amjad, A. M., Halliday, D. M., Rosenberg, J. R., & Conway, B. A. (1997). An extended difference of coherence test for comparing and combining several independent coherence estimates: theory and application to the study of motor units and physiological tremor. *Journal of Neuroscience Methods*, *73*(1), 69–79.

Anagnostaras, S. G., Gale, G. D., & Fanselow, M. S. (2001). Hippocampus and contextual fear conditioning: recent controversies and advances. *Hippocampus*, *11*(1), 8–17.

Anagnostaras, S. G., Maren, S., & Fanselow, M. S. (1999). Temporally graded retrograde amnesia of contextual fear after hippocampal damage in rats: within-subjects examination. *The Journal of Neuroscience : The Official Journal of the Society for Neuroscience*, *19*(3), 1106–14.

Andrews, J. S., Jansen, J. H., Linders, S., Princen, A., & Broekkamp, C. L. (1995). Performance of four different rat strains in the autoshaping, two-object discrimination, and swim maze tests of learning and memory. *Physiology & Behavior*, *57*(4), 785–90.

Antoniadis, E. A., & McDonald, R. J. (2006). Fornix, medial prefrontal cortex, nucleus accumbens, and mediodorsal thalamic nucleus: Roles in a fear-based context discrimination task. *Neurobiology of Learning and Memory*, *85*(1), 71–85.

Antunes, R., & Moita, M. A. (2010). Discriminative Auditory Fear Learning Requires Both Tuned and Nontuned Auditory Pathways to the Amygdala. *Journal of Neuroscience*, *30*(29), 9782–9787.

Armony, J., Servan-Schreiber, D., Cohen, J. D., & LeDoux, J. E. (1995). An anatomically constrained neural network model of fear conditioning. *Behavioral Neuroscience*, *109*(2), 246–57.

Armony, J., Servanschreiber, S., Cohen, J., & LeDoux, j. (1997). Computational modeling of emotion: explorations through the anatomy and physiology of fear conditioning. *Trends in Cognitive Sciences*, *1*(1), 28–34.

Arve Flaten Donald A. Powell, M., & Powell, D. A. (1998). Conditioned-Reflex Facilitation in Young and Older Adults. *Experimental Aging Research*, *24*(4), 387–410.

Ashwell, R., & Ito, R. (2014). Excitotoxic lesions of the infralimbic, but not prelimbic cortex facilitate reversal of appetitive discriminative context conditioning: the role of the infralimbic cortex in context generalization. *Frontiers in Behavioral Neuroscience*, *8*.

Ashwin, P., Coombes, S., & Nicks, R. (2015). Mathematical frameworks for oscillatory network dynamics in neuroscience.

Ayers, E. D., & Powell, D. A. (2002). Multiple response measures during classical conditioning. *Journal of Neuroscience Methods*, *114*(1), 33–8.

Baeg, E. H., Kim, Y. B., Jang, J., Kim, H. T., Mook-Jung, I., & Jung, M. W. (2001). Fast Spiking and Regular Spiking Neural Correlates of Fear Conditioning in the Medial Prefrontal Cortex of the Rat. *Cerebral Cortex*, *11*(5), 441–451.

Baker-Andresen, D., Flavell, C. R., Li, X., & Bredy, T. W. (2013). Activation of BDNF signaling prevents the return of fear in female mice. *Learning & Memory*, *20*(5), 237–240.

Baker, T. I., & Cowan, J. D. (2009). Spontaneous pattern formation and pinning in the primary visual cortex. *Journal of Physiology-Paris*, *103*(1–2), 52–68.

Balkenius, C., & Morén, J. (1999). Dynamics of a Classical Conditioning Model. *Autonomous Robots*, *7*(1), 41–56.

Balleine, B. W., Killcross, A. S., & Dickinson, A. (2003). The effect of lesions of the basolateral amygdala on instrumental conditioning. *The Journal of Neuroscience : The Official Journal of the Society for Neuroscience*, *23*(2), 666–75.

Bandettini, P. A. (2009). What's New in Neuroimaging Methods? *Annals of the New York Academy of Sciences*, *1156*(1), 260–293.

Baran, S. E., Armstrong, C. E., Niren, D. C., & Conrad, C. D. (2010). Prefrontal cortex lesions and sex differences in fear extinction and perseveration. *Learning & Memory*, *17*(5), 267–78.

Baran, S. E., Armstrong, C. E., Niren, D. C., Hanna, J. J., & Conrad, C. D. (2009). Chronic stress and sex differences on the recall of fear conditioning and extinction. *Neurobiology of Learning and Memory*, *91*(3), 323–332.

Barot, S. K., Chung, A., Kim, J. J., Bernstein, I. L., Rudy, J., Brown, R., Josselyn, S. (2009). Functional Imaging of Stimulus Convergence in Amygdalar Neurons during Pavlovian Fear Conditioning. *PLoS ONE*, *4*(7), e6156.

Bartos, M., Vida, I., & Jonas, P. (2007). Synaptic mechanisms of synchronized gamma oscillations in inhibitory interneuron networks. *Nature Reviews Neuroscience, 8*(1), 45-56.

Beatty, W. W., & Fessler, R. G. (1977). Sex differences in sensitivity to electric shock in rats and hamsters. *Bulletin of the Psychonomic Society*, *10*(3), 189–190.

Bechara, A., Tranel, D., & Damasio, H. (2000). Characterization of the decision-making deficit of patients with ventromedial prefrontal cortex lesions. *Brain : A Journal of Neurology*, *123 (Pt 11)*, 2189–202.

Belluscio, M. A., Mizuseki, K., Schmidt, R., Kempter, R., & Buzsáki, G. (2012). Cross-frequency phase-phase coupling between θ and γ oscillations in the hippocampus. *The Journal of Neuroscience*, *32*(2), 423–35.

Bergado-Acosta, J. R., Sangha, S., Narayanan, R. T., Obata, K., Pape, H.-C., & Stork, O. (2008). Critical role of the 65-kDa isoform of glutamic acid decarboxylase in consolidation and generalization of Pavlovian fear memory. *Learning & Memory*, *15*(3), 163–171.

Blain, L. M., Galovski, T. E., & Robinson, T. (2010). Gender differences in recovery from posttraumatic stress disorder: A critical review. *Aggression and Violent Behavior*, *15*(6), 463–474.

Blair, H. T., Schafe, G. E., Bauer, E. P., Rodrigues, S. M., & LeDoux, J. E. Synaptic plasticity in the lateral amygdala: a cellular hypothesis of fear conditioning. *Learning & Memory*, *8*(5), 229–42.

Blair, R. J. R. (2008). The amygdala and ventromedial prefrontal cortex: functional contributions and dysfunction in psychopathy. *Philosophical Transactions of the Royal Society of London. Series B, Biological Sciences*, *363*(1503), 2557–65.

Bloodgood, D. W., Sugam, J. A., Holmes, A., & Kash, T. L. (2017). Fear extinction requires infralimbic cortex projections to the basolateral amygdala. *Doi.org*, 172791.

Bocchio, M., & Capogna, M. (2014). Oscillatory Substrates of Fear and Safety. *Neuron*, *83*(4).

Bouton, M. E. (2004). Context and Behavioral Processes in Extinction. *Learning & Memory*, *11*(5), 485–494.

Bouton, M. E., & Bolles, R. C. (1980). Conditioned fear assessed by freezing and by the suppression of three different baselines. *Animal Learning & Behavior*, *8*(3), 429–434.

Bouton, M. E., & Peck, C. A. (1989). Context effects on conditioning, extinction, and reinstatement in an appetitive conditioning preparation. *Animal Learning & Behavior*, *17*(2), 188–198.

Bremner, J. D., Innis, R. B., Southwick, S. M., Staib, L., Zoghbi, S., & Charney, D. S. (2000). Decreased Benzodiazepine Receptor Binding in Prefrontal Cortex in Combat-Related Posttraumatic Stress Disorder. *American Journal of Psychiatry*, *157*(7), 1120–1126.

Breslau, N. Gender differences in trauma and posttraumatic stress disorder. *The Journal of Gender-Specific Medicine : JGSM : The Official Journal of the Partnership for Women's Health at Columbia*, *5*(1), 34–40.

Brette, R., Rudolph, M., Carnevale, T., Hines, M., Beeman, D., Bower, J. M., … Destexhe, A. (2007). Simulation of networks of spiking neurons: a review of tools and strategies. *Journal of Computational Neuroscience*, *23*(3), 349–98.

Broadwater, M., & Spear, L. P. (2013). Age differences in fear retention and extinction in male Sprague-Dawley rats: effects of ethanol challenge during conditioning. *Behavioural Brain Research*, *252*, 377–87.

Brodland, G. W. (2015). How computational models can help unlock biological systems. *Seminars in Cell & Developmental Biology*, *47–48*, 62–73.

Brown, T. H., Kairiss, E. W., & Keenan, C. L. (1990). Hebbian Synapses: Biophysical Mechanisms and Algorithms. *Annual Review of Neuroscience*, *13*(1), 475–511.

Bruchey, A. K., Jones, C. E., & Monfils, M.-H. (2010). Fear conditioning by-proxy: Social transmission of fear during memory retrieval. *Behavioural Brain Research*, *214*(1), 80–84.

Bukalo, O., Pinard, C. R., & Holmes, A. (2014). Mechanisms to medicines: elucidating neural and molecular substrates of fear extinction to identify novel treatments for anxiety disorders. *British Journal of Pharmacology*, *171*(20), 4690–718.

Burgos-Robles, A., Vidal-Gonzalez, I., & Quirk, G. J. (2009). Sustained Conditioned Responses in Prelimbic Prefrontal Neurons Are Correlated with Fear Expression and Extinction Failure. *Journal of Neuroscience*, *29*(26), 8474–8482.

Burman, M. A., & Gewirtz, J. C. (2004). Timing of Fear Expression in Trace and Delay Conditioning Measured by Fear-Potentiated Startle in Rats. *Learning & Memory*, *11*(2), 205–212.

Burnovicz, A., & Hermitte, G. (2010). Conditioning of an autonomic response in Crustacea. *Physiology & Behavior*, *101*(1), 168–175.

Buzsáki, G. (2002). Theta Oscillations in the Hippocampus. *Neuron*, *33*(3), 325–340.

Buzsáki, G., Anastassiou, C. A., & Koch, C. (2012). The origin of extracellular fields and currents - EEG, ECoG, LFP and spikes. *Nature Reviews Neuroscience*, *13*(6), 407–420.

Buzsaki, G., & Draguhn, A. (2004). Neuronal Oscillations in Cortical Networks. *Science*, *304*(5679), 1926–1929.

Buzsáki, G., & Watson, B. O. (2012). Brain rhythms and neural syntax: implications for efficient coding of cognitive content and neuropsychiatric disease. *Dialogues in Clinical Neuroscience*, *14*(4), 345–67.

Cabral, J., Kringelbach, M. L., & Deco, G. (2014). Exploring the network dynamics underlying brain activity during rest. *Progress in Neurobiology*, *114*, 102–131.

Camp, M. C., Macpherson, K. P., Lederle, L., Graybeal, C., Gaburro, S., Debrouse, L. M., Holmes, A. (2012). Genetic strain differences in learned fear inhibition associated with variation in neuroendocrine, autonomic, and amygdala dendritic phenotypes. *Neuropsychopharmacology*, *37*(6), 1534–47.

Campbell, S., & DeLiang Wang, D. (1996). Synchronization and desynchronization in a network of locally coupled Wilson-Cowan oscillators. *IEEE Transactions on Neural Networks*, *7*(3), 541–554.

Capogna, M. (2014). GABAergic cell type diversity in the basolateral amygdala. *Current Opinion in Neurobiology*. https://doi.org/10.1016/j.conb.2014.01.006

Carlson, D. E., Borg, J. S., Dzirasa, K., & Carin, L. (2014). On the relationship between LFP & spiking data. *Proceedings of the 27th International Conference on Neural Information Processing Systems*. MIT Press.

Cassaday, H. J., Shilliam, C. S., & Marsden, C. A. (2001). Serotonergic depletion increases conditioned suppression to background stimuli in the rat. *Journal of Psychopharmacology*, *15*(2), 83–92.

Catuzzi, J. E., & Beck, K. D. (2014). Anxiety vulnerability in women: A two-hit hypothesis. *Experimental Neurology*, *259*, 75–80.

Chauret, M., La Buissonnière-Ariza, V., Lamoureux-Tremblay, V., Suffren, S., Servonnet, A., Pine, D. S., & Maheu, F. S. (2014). The conditioning and extinction of fear in youths: what's sex got to do with it? *Biological Psychology*, *100*, 97–105.

Cheriyan, J., Kaushik, M. K., Ferreira, A. N., & Sheets, P. L. (2016). Specific targeting of the basolateral amygdala to projectionally defined pyramidal neurons in prelimbic and infralimbic cortex. *eNeuro*, *3*(2).

Choi, D. C., Maguschak, K. A., Ye, K., Jang, S.-W., Myers, K. M., & Ressler, K. J. (2010). Prelimbic cortical BDNF is required for memory of learned fear but not extinction or innate fear. *Proceedings of the National Academy of Sciences*, *107*(6), 2675–2680.

Cholanian, M., Lobzova, A., Das, B., Yelleswarapu, C., & Donaldson, S. T. (2014). Digital holographic microscopy discriminates sex differences in medial prefrontal cortex GABA neurons following amphetamine sensitization. *Pharmacology Biochemistry and Behavior*, *124*, 326–332.

Christianson, J. P., Fernando, A. B. P., Kazama, A. M., Jovanovic, T., Ostroff, L. E., & Sangha, S. (2012). Inhibition of Fear by Learned Safety Signals: A Mini-Symposium Review. *Journal of Neuroscience*, *32*(41).

Chudasama, Y., Passetti, F., Rhodes, S. E. V, Lopian, D., Desai, A., & Robbins, T. W. (2003). Dissociable aspects of performance on the 5-choice serial reaction time task following lesions of the dorsal anterior cingulate, infralimbic and orbitofrontal cortex in the rat: differential effects on selectivity, impulsivity and compulsivity. *Behavioural Brain Research*, *146*(1–2), 105–19.

Ciocchi, S., Herry, C., Grenier, F., Wolff, S. B. E., Letzkus, J. J., Vlachos, I., … Lüthi, A. (2010). Encoding of conditioned fear in central amygdala inhibitory circuits. *Nature*, *468*(7321), 277–282.

Cooke, S. F., & Bliss, T. V. P. (2006). Plasticity in the human central nervous system. *Brain*, *129*(7), 1659–1673.

Coombes, S. (2005). Waves, bumps, and patterns in neural field theories. *Biological Cybernetics*, *93*(2), 91–108.

Coplan, J. D., & Lydiard, R. B. (1998). Brain circuits in panic disorder. *Biological Psychiatry*, *44*(12), 1264–1276.

Corcoran, K. A., & Quirk, G. J. (2007). Activity in prelimbic cortex is necessary for the expression of learned, but not innate, fears. *The Journal of Neuroscience*, *27*(4), 840–4.

Courbage, M., Nekorkin, V. I., & Vdovin, L. V. (2007). Chaotic oscillations in a map-based model of neural activity. *Chaos: An Interdisciplinary Journal of Nonlinear Science*, *17*(4), 43109.

Courtin, J., Bienvenu, T. C. M., Einarsson, E. Ö., & Herry, C. (2013). Medial prefrontal cortex neuronal circuits in fear behavior. *Neuroscience*, *240*, 219–242.

Courtin, J., Chaudun, F., Rozeske, R. R., Karalis, N., Gonzalez-Campo, C., Wurtz, H., … Herry, C. (2014). Prefrontal parvalbumin interneurons shape neuronal activity to drive fear expression. *Nature*, *505*(7481). https://doi.org/10.1038/nature12755

Courtin, J., Karalis, N., Gonzalez-Campo, C., Wurtz, H., & Herry, C. (2014). Persistence of amygdala gamma oscillations during extinction learning predicts spontaneous fear recovery. *Neurobiology of Learning and Memory*, *113*, 82–89.

Cowan, J. D., Neuman, J., & van Drongelen, W. (2016). Wilson-Cowan Equations for Neocortical Dynamics. *Journal of Mathematical Neuroscience*, *6*(1), 1.

Cox, D. D. (1996). Spectral Analysis for Physical Applications: Multitaper and Conventional Univariate Techniques. *Technometrics*, *38*(3), 294–294.

Craske, M. G., Treanor, M., Conway, C. C., Zbozinek, T., & Vervliet, B. (2014). Maximizing exposure therapy: an inhibitory learning approach. *Behaviour Research and Therapy*, *58*, 10–23.

Daldrup, T., Remmes, J., Lesting, J., Gaburro, S., Fendt, M., Meuth, P., … Seidenbecher, T. (2015). Expression of freezing and fear-potentiated startle during sustained fear in mice. *Genes, Brain and Behavior*, *14*, 281–291.

Dalla, C., Edgecomb, C., Whetstone, A. S., & Shors, T. J. (2007). Females do not Express Learned Helplessness like Males do. *Neuropsychopharmacology*, *33*(7), 1559–1569.

Dalla, C., & Shors, T. J. (2009). Sex differences in learning processes of classical and operant conditioning. *Physiology & Behavior*, *97*(2), 229–38.

David, O., & Friston, K. J. (2003). A neural mass model for MEG/EEG: coupling and neuronal dynamics. *NeuroImage*, *20*(3), 1743–55.

Davis, M. (2001). Fear-Potentiated Startle in Rats. In *Current Protocols in Neuroscience* (Vol. Chapter 8, p. Unit 8.11A). Hoboken, NJ, USA: John Wiley & Sons, Inc.

Desiderato, O., & Newman, A. (1971). Conditioned suppression produced in rats by tones paired with escapable or inescapable shock. *Journal of Comparative and Physiological Psychology*, *77*(3), 427–431.

Destexhe, A., & Paré, D. (1999). Impact of network activity on the integrative properties of neocortical pyramidal neurons in vivo. *Journal of Neurophysiology*, *81*(4), 1531–47.

Destexhe, A., & Sejnowski, T. J. (2009). The Wilson-Cowan model, 36 years later. *Biological Cybernetics*, *101*(1), 1–2.

Dielenberg, R. A., Hunt, G. E., & McGregor, I. S. (2001). "When a rat smells a cat": the distribution of Fos immunoreactivity in rat brain following exposure to a predatory odor. *Neuroscience*, *104*(4), 1085–97.

Diggle, P. (1990). *Time series : a biostatistical introduction*. Clarendon Press.

Ditlevsen, D. N., & Elklit, A. (2010). The combined effect of gender and age on post traumatic stress disorder: do men and women show differences in the lifespan distribution of the disorder? *Annals of General Psychiatry*, *9*, 32.

Do-Monte, F. H., Manzano-Nieves, G., Quiñones-Laracuente, K., Ramos-Medina, L., & Quirk, G. J. (2015). Revisiting the role of infralimbic cortex in fear extinction with optogenetics. *The Journal of Neuroscience : The Official Journal of the Society for Neuroscience*, *35*(8).

Donner, N. C., & Lowry, C. A. (2013). Sex differences in anxiety and emotional behavior. *Pflugers Archiv : European Journal of Physiology*, *465*(5), 601–26.

Dunsmoor, J. E., & Paz, R. (2015). Fear Generalization and Anxiety: Behavioral and Neural Mechanisms. *Biological Psychiatry*, *78*(5), 336–343.

Dunsmoor, J. E., Prince, S. E., Murty, V. P., Kragel, P. A., & LaBar, K. S. (2011). Neurobehavioral mechanisms of human fear generalization. *NeuroImage*, *55*(4), 1878-88

Dupret, D., Pleydell-Bouverie, B., & Csicsvari, J. (2008). Inhibitory interneurons and network oscillations. *Proceedings of the National Academy of Sciences of the United States of America*, *105*(47), 18079–80.

Duvarci, S., Bauer, E. P., & Pare, D. (2009). The Bed Nucleus of the Stria Terminalis Mediates Inter-individual Variations in Anxiety and Fear. *Journal of Neuroscience*, *29*(33), 10357–10361.

Ehrlich, I., Humeau, Y., Grenier, F., Ciocchi, S., Herry, C., & Lüthi, A. (2009). Amygdala inhibitory circuits and the control of fear memory. *Neuron*, *62*(6), 757–71.

Einevoll, G. T., Kayser, C., Logothetis, N. K., & Panzeri, S. (2013). Modelling and analysis of local field potentials for studying the function of cortical circuits. *Nature Reviews Neuroscience*, *14*(11), 770–785.

Ermentrout, G. B., & Chow, C. C. (2002). Modeling neural oscillations. *Physiology & Behavior*, *77*, 629–633.

Esfahani ZG, Gollo LL, Valizadeh A. Stimulus-dependent synchronization in delayed-coupled neuronal networks. *Scientific reports*. 2016; 6.

Fanselow, M. S. (1990). Factors governing one-trial contextual conditioning. *Animal Learning & Behavior*, *18*(3), 264–270.

Fanselow, M. S. (2010). From contextual fear to a dynamic view of memory systems. *Trends in Cognitive Sciences*, *14*(1), 7–15.

Fanselow, M. S., LeDoux, J. (1999). Why we think plasticity underlying Pavlovian fear conditioning occurs in the basolateral amygdala. *Neuron*, *23*(2), 229–32.

Farrell, M. R., Gruene, T. M., & Shansky, R. M. (2015). The influence of stress and gonadal hormones on neuronal structure and function. *Hormones and Behavior*, *76*, 118–124.

Fell, J., & Axmacher, N. (2011). The role of phase synchronization in memory processes. *Nature Reviews Neuroscience*, *12*(2), 105–118.

Fenalti, G., Law, R. H. P., Buckle, A. M., Langendorf, C., Tuck, K., Rosado, C. J., Whisstock, J. C. (2007). GABA production by glutamic acid decarboxylase is regulated by a dynamic catalytic loop. *Nature Structural & Molecular Biology*, *14*(4), 280–286.

Fenton, G. E., Halliday, D. M., Mason, R., Bredy, T. W., & Stevenson, C. W. (2016). Sex differences in learned fear expression and extinction involve altered gamma oscillations in medial prefrontal cortex. *Neurobiology of Learning and Memory*, *135*, 66–72.

Fenton, G. E., Halliday, D. M., Mason, R., & Stevenson, C. W. (2014a). Medial prefrontal cortex circuit function during retrieval and extinction of associative learning under anesthesia. *Neuroscience*, *265*, 204–216.

Fenton, G. E., Pollard, A. K., Halliday, D. M., Mason, R., Bredy, T. W., & Stevenson, C. W. (2014b). Persistent prelimbic cortex activity contributes to enhanced learned fear expression in females. *Learning & Memory (Cold Spring Harbor, N.Y.)*, *21*(2), 55–60.

Fenton, G. E., Spicer, C. H., Halliday, D. M., Mason, R., & Stevenson, C. W. (2013). Basolateral amygdala activity during the retrieval of associative learning under anesthesia. *Neuroscience*, *233*, 146–56.

Fischer, H. P. (2008). Mathematical modeling of complex biological systems: from parts lists to understanding systems behavior. *Alcohol Research & Health : The Journal of the National Institute on Alcohol Abuse and Alcoholism*, *31*(1), 49–59.

Fitzgerald, P. J., Whittle, N., Flynn, S. M., Graybeal, C., Pinard, C. R., Gunduz-Cinar, O., Holmes, A. (2014). Prefrontal single-unit firing associated with deficient extinction in mice. *Neurobiology of Learning and Memory*, *113*, 69–81.

Foa, E. B. (2010). Cognitive behavioral therapy of obsessive-compulsive disorder. *Dialogues in Clinical Neuroscience*, *12*(2), 199–207.

Foilb, A. R., & Christianson, J. P. (2016). Serotonin 2C receptor antagonist improves fear discrimination and subsequent safety signal recall. *Progress in NeuroPsychopharmacology and Biological Psychiatry*, *65*, 78–84.

Foster, B. L., Bojak, I., & Liley, D. T. J. (2008). Population based models of cortical drug response: insights from anaesthesia. *Cognitive Neurodynamics*, *2*(4), 283–96.

Fransén, E., & Lansner, A. (1998). A model of cortical associative memory based on a horizontal network of connected columns. *Network (Bristol, England)*, *9*(2), 235–64.

Freund, T. F., & Katona, I. (2007). Perisomatic Inhibition. *Neuron*, *56*(1), 33–42.

Fries, P. (2009). Neuronal Gamma-Band Synchronization as a Fundamental Process in Cortical Computation. *Annual Review of Neuroscience*, *32*(1), 209–224.

Frijling, J. L. (2017). Preventing PTSD with oxytocin: effects of oxytocin administration on fear neurocircuitry and PTSD symptom development in recently trauma-exposed individuals. *European Journal of Psychotraumatology*, *8*(1), 1302652.

Friston, K. J., & Dolan, R. J. (2010). Computational and dynamic models in neuroimaging. *NeuroImage*, *52*(3), 752–765.

Gabbott, P. L. A., Warner, T. A., & Busby, S. J. (2006). Amygdala input monosynaptically innervates parvalbumin immunoreactive local circuit neurons in rat medial prefrontal cortex. *Neuroscience*, *139*(3), 1039–1048.

Galovski, T. E., Blain, L. M., Chappuis, C., & Fletcher, T. (2013). Sex differences in recovery from PTSD in male and female interpersonal assault survivors. *Behaviour Research and Therapy*, *51*(6), 247–55.

Gamwell, K., Nylocks, M., Cross, D., Bradley, B., Norrholm, S. D., & Jovanovic, T. (2015). Fear conditioned responses and PTSD symptoms in children: Sex differences in fear-related symptoms. *Developmental Psychobiology*, *57*(7), 799–808.

Ganguly, K., & Kleinfeld, D. (2004). Goal-directed whisking increases phase-locking between vibrissa movement and electrical activity in primary sensory cortex in rat. *Proceedings of the National Academy of Sciences*, *101*(33), 12348–12353.

Garelick, M. G., & Storm, D. R. (2005). The relationship between memory retrieval and memory extinction. *Proceedings of the National Academy of Sciences of the United States of America*, *102*(26), 9091–2.

Gelperin, A. (1975). Rapid food-aversion learning by a terrestrial mollusk. *Science*, *189*(4202).

Geracitano, R., Kaufmann, W. A., Szabo, G., Ferraguti, F., & Capogna, M. (2007). Synaptic heterogeneity between mouse paracapsular intercalated neurons of the amygdala. *The Journal of Physiology*, *585*(1), 117–134.

Geuze, E., van Berckel, B. N. M., Lammertsma, A. A., Boellaard, R., de Kloet, C. S., Vermetten, E., & Westenberg, H. G. M. (2008). Reduced GABAA benzodiazepine receptor binding in veterans with PTSD. *Molecular Psychiatry*, *13*(1), 74–83.

Gewirtz, J. C., McNish, K. A., & Davis, M. (2000). Is the hippocampus necessary for contextual fear conditioning? *Behavioural Brain Research*, *110*(1–2), 83–95.

Giustino, T. F., & Maren, S. (2015). The Role of the Medial Prefrontal Cortex in the Conditioning and Extinction of Fear. *Frontiers in Behavioral Neuroscience*, *9*(11).

Glover, E. M., Jovanovic, T., Mercer, K. B., Kerley, K., Bradley, B., Ressler, K. J., & Norrholm, S. D. (2012). Estrogen Levels Are Associated with Extinction Deficits in Women with Posttraumatic Stress Disorder. *Biological Psychiatry*, *72*(1), 19–24.

Glover, G. H. (2011). Overview of functional magnetic resonance imaging. *Neurosurgery Clinics of North America*, *22*(2), 133–139.

Goldental, A., Vardi, R., Sardi, S., Sabo, P., & Kanter, I. (2015). Broadband macroscopic cortical oscillations emerge from intrinsic neuronal response failures. *Frontiers in Neural Circuits*, *9*, 65.

Goldstein, J. M., Seidman, L. J., Horton, N. J., Makris, N., Kennedy, D. N., Caviness, V. S., Tsuang, M. T. (2001). Normal sexual dimorphism of the adult human brain assessed by in vivo magnetic resonance imaging. *Cerebral Cortex*, *11*(6), 490–7.

Gonzalez Andino, S. L., Herrera-Rincon, C., Panetsos, F., & Grave de Peralta, R. (2011). Combining BMI Stimulation and Mathematical Modeling for Acute Stroke Recovery and Neural Repair. *Frontiers in Neuroscience*, *5*, 87.

Good, M., & Honey, R. C. (1991). Conditioning and contextual retrieval in hippocampal rats. *Behavioral Neuroscience*, *105*(4), 499–509.

Goode, T. D., & Maren, S. (2014). Animal models of fear relapse. *ILAR Journal*, *55*(2), 246–58.

Gourley, S. L., & Taylor, J. R. (2016). Going and stopping: dichotomies in behavioral control by the prefrontal cortex. *Nature Neuroscience*, *19*(6), 656–664.

Graham, B. M., & Milad, M. R. (2011). The study of fear extinction: implications for anxiety disorders. *The American Journal of Psychiatry*, *168*(12), 1255–65.

Graham, B. M., & Milad, M. R. (2013). Blockade of Estrogen by Hormonal Contraceptives Impairs Fear Extinction in Female Rats and Women. *Biological Psychiatry*, *73*(4), 371–378.

Gray, J. A., & Lalljee, B. (1974). Sex differences in emotional behaviour in the rat: Correlation between open-field defecation and active avoidance. *Animal Behaviour*, *22*, 856–861.

Gresack, J. E., Schafe, G. E., Orr, P. T., & Frick, K. M. (2009). Sex differences in contextual fear conditioning are associated with differential ventral hippocampal extracellular signal-regulated kinase activation. *Neuroscience*, *159*(2), 451–467.

Gross, C. T., & Canteras, N. S. (2012). The many paths to fear. *Nature Reviews Neuroscience*, *13*(9), 651–658.

Grossberg, S., Cytawa, J., Teitelbaum, P., West, D. C., Schroder, J., & Carpenter, W. T. (2000). The imbalanced brain: from normal behavior to schizophrenia. *Biological Psychiatry*, *48*(2), 81–98.

Grossberg, S., & Schmajuk, N. A. (1987). Neural dynamics of attentionally modulated Pavlovian conditioning: Conditioned reinforcement, inhibition, and opponent processing. *Psychobiology*, *15*(3), 195–240.

Gruene, T. M., Flick, K., Stefano, A., Shea, S. D., & Shansky, R. M. (2015a). Sexually divergent expression of active and passive conditioned fear responses in rats. *eLife*, *4*.

Gruene, T. M., Roberts, E., Thomas, V., Ronzio, A., & Shansky, R. M. (2015b). Sex-Specific Neuroanatomical Correlates of Fear Expression in Prefrontal-Amygdala Circuits. *Biological Psychiatry*, *78*(3), 186–193.

Gupta, R. R., Sen, S., Diepenhorst, L. L., Rudick, C. N., & Maren, S. (2001). Estrogen modulates sexually dimorphic contextual fear conditioning and hippocampal long-term potentiation (LTP) in rats(1). *Brain Research*, *888*(2), 356–365.

Gurvits, T. V, Shenton, M. E., Hokama, H., Ohta, H., Lasko, N. B., Gilbertson, M. W., Pitman, R. K. (1996). Magnetic resonance imaging study of hippocampal volume in chronic, combat-related posttraumatic stress disorder. *Biological Psychiatry*, *40*(11), 1091–9.

Gutkin, B., Gutkin, B., Pinto, D., & Ermentrout, B. (2003). Mathematical Neuroscience: From Neurons to Circuits to Systems. *Journal of physiology Paris*, *97*, 209--219.

Halliday, D. (1995). A framework for the analysis of mixed time series/point process data-Theory and application to the study of physiological tremor, single motor unit discharges and electromyograms. *Progress in Biophysics and Molecular Biology*, *64*(2–3), 237-278.

Halliday, D. M. (2015). Nonparametric directionality measures for time series and point process data. *Journal of Integrative Neuroscience*, *14*(2), 253–277.

Halliday, D. M., Senik, M. H., Stevenson, C. W., & Mason, R. (2016). Non-parametric directionality analysis - Extension for removal of a single common predictor and application to time series, *268*, 87–97.

Hankins, M. J., Nagy, T., & Kiss, I. Z. (2013). Methodology for a nullcline-based model from direct experiments: Applications to electrochemical reaction models. *Computers & Mathematics with Applications*, *65*(10), 1633–1644.

Harris, A. Z., & Gordon, J. A. (2015). Long-range neural synchrony in behavior. *Annual Review of Neuroscience*, *38*, 171–94.

Harris, J. A., Jones, M. L., Bailey, G. K., & Westbrook, R. F. (2000). Contextual control over conditioned responding in an extinction paradigm. *Journal of Experimental Psychology. Animal Behavior Processes*, *26*(2), 174–85.

Haubensak, P.S. Kunwar, H. Cai, S. Ciocchi, N.R. Wall, R. Ponnusamy, J. Biag, H.W. Dong, K. Deisseroth, E.M. Callaway (2010) Genetic dissection of an amygdala microcircuit that gates conditioned fear. *Nature*, 468 (2010), pp. 270-276

Heath, F. C., Jurkus, R., Bast, T., Pezze, M. A., Lee, J. L. C., Voigt, J. P., & Stevenson, C. W. (2015). Dopamine D1-like receptor signalling in the hippocampus and amygdala modulates the acquisition of contextual fear conditioning. *Psychopharmacology*.

Heldt, S. A., Mou, L., & Ressler, K. J. (2012). In vivo knockdown of GAD67 in the amygdala disrupts fear extinction and the anxiolytic-like effect of diazepam in mice. *Translational Psychiatry*, *2*(11), e181.

Herry, C., Ciocchi, S., Senn, V., Demmou, L., Müller, C., & Lüthi, A. (2008). Switching on and off fear by distinct neuronal circuits. *Nature*, *454*(7204), 600–606.

Hobin, J. A., Goosens, K. A., & Maren, S. (2003). Context-dependent neuronal activity in the lateral amygdala represents fear memories after extinction. *The Journal of Neuroscience*, *23*(23), 8410–6.

Hodgkin, A. L., & Huxley, A. F. (1952). A quantitative description of membrane current and its application to conduction and excitation in nerve. *The Journal of Physiology*, *117*(4), 500–44.

Hok, V., Save, E., Lenck-Santini, P. P., & Poucet, B. (2005). Coding for spatial goals in the prelimbic/infralimbic area of the rat frontal cortex. *PNAS*, *102*(12), 4602–7.

Holland, P. C., Petrovich, G. D., & Gallagher, M. (2002). The effects of amygdala lesions on conditioned stimulus-potentiated eating in rats. *Physiology & Behavior*, *76*(1), 117–129.

Holmes, N. M., Parkes, S. L., Killcross, A. S., & Westbrook, R. F. (2013). The Basolateral Amygdala Is Critical for Learning about Neutral Stimuli in the Presence of Danger, and the Perirhinal Cortex Is Critical in the Absence of Danger. *Journal of Neuroscience*, *33*(32), 13112–13125.

Huang, Y. Y., & Kandel, E. R. (1998). Postsynaptic induction and PKA-dependent expression of LTP in the lateral amygdala. *Neuron*, *21*(1), 169–78.

Huff, N. C., Hernandez, J. A., Fecteau, M. E., Zielinski, D. J., Brady, R., & Labar, K. S. (2011). Revealing context-specific conditioned fear memories with full immersion virtual reality. *Frontiers in Behavioral Neuroscience*, *5*, 75.

Hughes, J. R., Sleigh, J. W., Kirk, I. J., Williams, M. L., Jonkman, E. J., Stam, C. J., & Szucs, A. (2008). Gamma, fast, and ultrafast waves of the brain: their relationships with epilepsy and behavior. *Epilepsy & Behavior : E&B*, *13*(1), 25–31.

Hyman, J. M., Ma, L., Balaguer-Ballester, E., Durstewitz, D., & Seamans, J. K. (2012). Contextual encoding by ensembles of medial prefrontal cortex neurons. *Proceedings of the National Academy of Sciences of the United States of America*, *109*(13), 5086–91.

Iordanova, M. D., Killcross, A. S., & Honey, R. C. (2007). Role of the medial prefrontal cortex in acquired distinctiveness and equivalence of cues. *Behavioral Neuroscience*, *121*(6), 1431–1436.

Ishikawa, A., & Nakamura, S. (2006). Ventral Hippocampal Neurons Project Axons Simultaneously to the Medial Prefrontal Cortex and Amygdala in the Rat. *Journal of Neurophysiology*, *96*(4), 2134–2138.

Ito, W., Pan, B.-X., Yang, C., Thakur, S., & Morozov, A. (2009). Enhanced generalization of auditory conditioned fear in juvenile mice. *Learning & Memory (Cold Spring Harbor, N.Y.)*, *16*(3), 187–92.

Izhikevich, E. M. (2004). Which Model to Use for Cortical Spiking Neurons? *IEEE Transactions on neural networks*, *15*(5).

Janak, P. H., & Tye, K. M. (2015). From circuits to behaviour in the amygdala. *Nature*, *517*(7534), 284–92.

Ji, G., & Neugebauer, V. (2012). Modulation of medial prefrontal cortical activity using in vivo recordings and optogenetics. *Molecular Brain*, *5*, 36.

Jones, C. E., Riha, P. D., Gore, A. C., & Monfils, M.-H. (2014). Social transmission of Pavlovian fear: fear-conditioning by-proxy in related female rats. *Animal Cognition*, *17*(3), 827–834.

Jones, N. (2009). Electrodes spark neuron growth. *Nature*.

Joseph, M. H., Peters, S. L., Moran, P. M., Grigoryan, G. A., Young, A. M. J., & Gray, J. A. (2000). Modulation of latent inhibition in the rat by altered dopamine transmission in the nucleus accumbens at the time of conditioning. *Neuroscience*, *101*(4), 921–930.

Jovanovic, T., Kazama, A., Bachevalier, J., & Davis, M. (2012). Impaired safety signal learning may be a biomarker of PTSD. *Neuropharmacology*.

Jovanovic, T., & Norrholm, S. D. (2011). Neural mechanisms of impaired fear inhibition in posttraumatic stress disorder. *Frontiers in Behavioral Neuroscience*, *5*(44).

Kaplan, O., & Lubow, R. E. (2011). Ignoring irrelevant stimuli in latent inhibition and Stroop paradigms: The effects of schizotypy and gender. *Psychiatry Research*, *186*(1), 40–45.

Kazarinoff, N. D. (1990). Elements of Differentiable Dynamics and Bifurcation Theory (David Ruelle). *SIAM Review*, *32*(4), 698–698.

Keeley, R. J., Bye, C., Trow, J., & McDonald, R. J. (2015). Strain and sex differences in brain and behaviour of adult rats: Learning and memory, anxiety and volumetric estimates. *Behavioural Brain Research*, *288*, 118–31.

Keller, S. M., Schreiber, W. B., Stanfield, B. R., & Knox, D. (2015). *Inhibiting corticosterone synthesis during fear memory formation exacerbates cued fear extinction memory deficits within the single prolonged stress model. Behavioural Brain Research* (Vol. 287).

Kerr, R., Lev-Ram, V., Baird, G., Vincent, P., Tsien, R. Y., & Schafer, W. R. (2000). Optical imaging of calcium transients in neurons and pharyngeal muscle of C. elegans. *Neuron*, *26*(3), 583–94.

Kessler, R. C., Berglund, P., Demler, O., Jin, R., Merikangas, K. R., Walters, E. E., S, C. (2005). Lifetime Prevalence and Age-of-Onset Distributions of DSM-IV Disorders in the National Comorbidity Survey Replication. *Archives of General Psychiatry*, *62*(6), 593.

Kilkenny, C., Browne, W. J., Cuthill, I. C., Emerson, M., & Altman, D. G. (2010). Improving Bioscience Research Reporting: The ARRIVE Guidelines for Reporting Animal Research. *PLoS Biology*, *8*(6), e1000412.

Killcross, S., & Coutureau, E. (2003). Coordination of actions and habits in the medial prefrontal cortex of rats. *Cerebral Cortex (New York, N.Y. : 1991)*, *13*(4), 400–8.

Killcross, S., Robbins, T. W., & Everitt, B. J. (1997). Different types of fear-conditioned behaviour mediated by separate nuclei within amygdala. *Nature*, *388*(6640), 377–380.

Kilpatrick, D. G., Resnick, H. S., Milanak, M. E., Miller, M. W., Keyes, K. M., & Friedman, M. J. (2013). National estimates of exposure to traumatic events and PTSD prevalence using DSM-IV and DSM-5 criteria. *Journal of Traumatic Stress*, *26*(5), 537–47.

Kim, E. J., Horovitz, O., Pellman, B. A., Tan, L. M., Li, Q., Richter-Levin, G., & Kim, J. J. (2013). Dorsal periaqueductal gray-amygdala pathway conveys both innate and learned fear responses in rats. *PNAS, 110*(36), 14795–800.

Kim, E. J., Kim, N., Kim, H. T., & Choi, J.-S. (2013). The prelimbic cortex is critical for context-dependent fear expression. *Frontiers in Behavioral Neuroscience*, *7*, 73.

Kim, J. J., & Jung, M. W. (2006). Neural circuits and mechanisms involved in Pavlovian fear conditioning: a critical review. *Neuroscience and Biobehavioral Reviews*, *30*(2), 188–202.

Kishi, T., Tsumori, T., Yokota, S., & Yasui, Y. (2006). Topographical projection from the hippocampal formation to the amygdala: A combined anterograde and retrograde tracing study in the rat. *The Journal of Comparative Neurology*, *496*(3), 349–368.

Klavir, O., Genud-Gabai, R., & Paz, R. (2012). Low-Frequency Stimulation Depresses the Primate Anterior-Cingulate-Cortex and Prevents Spontaneous Recovery of Aversive Memories. *Journal of Neuroscience*, *32*(25), 8589–8597.

Knapska, E., & Maren, S. (2009). Reciprocal patterns of c-Fos expression in the medial prefrontal cortex and amygdala after extinction and renewal of conditioned fear. *Learning & Memory, 16*(8), 486–93.

Koenen, K. C., & Widom, C. S. (2009). A prospective study of sex differences in the lifetime risk of posttraumatic stress disorder among abused and neglected children grown up. *Journal of Traumatic Stress*, *22*(6), 566–74.

Kong, E., Monje, F. J., Hirsch, J., & Pollak, D. D. (2014). Learning not to fear: neural correlates of learned safety. *Neuropsychopharmacology*, *39*(3), 515–27.

Kozai, T. D. Y., Jaquins-Gerstl, A. S., Vazquez, A. L., Michael, A. C., & Cui, X. T. (2015). Brain tissue responses to neural implants impact signal sensitivity and intervention strategies. *ACS Chemical Neuroscience*, *6*(1), 48–67.

Kurayama, T., Matsuzawa, D., Komiya, Z., Nakazawa, K., Yoshida, S., & Shimizu, E. (2012). P50 suppression in human discrimination fear conditioning paradigm using danger and safety signals. *International Journal of Psychophysiology*, *84*(1), 26–32.

LaBar, K. S., LeDoux, J. E., Spencer, D. D., & Phelps, E. A. (1995). Impaired fear conditioning following unilateral temporal lobectomy in humans. *The Journal of Neuroscience : The Official Journal of the Society for Neuroscience*, *15*(10), 6846–55.

Lange, M. D., Jüngling, K., Paulukat, L., Vieler, M., Gaburro, S., Sosulina, L., … Pape, H.-C. (2014). Glutamic Acid Decarboxylase 65: A Link Between GABAergic Synaptic Plasticity in the Lateral Amygdala and Conditioned Fear Generalization. *Neuropsychopharmacology*, *39*(9), 2211–2220.

Laurent, V., & Westbrook, R. F. (2009). Inactivation of the infralimbic but not the prelimbic cortex impairs consolidation and retrieval of fear extinction. *Learning & Memory*, *16*(9), 520–529.

Laviolette, S. R., Lipski, W. J., & Grace, A. A. (2005). A Subpopulation of Neurons in the Medial Prefrontal Cortex Encodes Emotional Learning with Burst and Frequency Codes through a Dopamine D4 Receptor-Dependent Basolateral Amygdala Input. *Journal of Neuroscience*, *25*(26), 6066–6075.

Laxmi, T. R., Stork, O., & Pape, H.-C. (2003). Generalisation of conditioned fear and its behavioural expression in mice. *Behavioural Brain Research*, *145*(1–2), 89–98.

Le Van Quyen, M., & Bragin, A. (2007). Analysis of dynamic brain oscillations: methodological advances. *Trends in Neurosciences*, *30*(7), 365–373.

Lebron-Milad, K., & Milad, M. R. (2012). Sex differences, gonadal hormones and the fear extinction network: implications for anxiety disorders. *Biology of Mood & Anxiety Disorders*, *2*(1), 3.

LeDoux, J. (2003). The emotional brain, fear, and the amygdala. *Cellular and Molecular Neurobiology*, *23*(4–5), 727–38.

LeDoux, J. (2012). Rethinking the emotional brain. *Neuron*, *73*(4), 653–76.

LeDoux, J. (2000). Emotion circuits in the brain. *Annual Review of Neuroscience*, *23*, 155–84.

LeDoux, J. (2014). Coming to terms with fear. *PNAS*, *111*(8), 2871–8.

Lee, I., & Solivan, F. (2008). The roles of the medial prefrontal cortex and hippocampus in a spatial paired-association task. *Learning & Memory*, *15*(5), 357–367.

Lee, Y. K., & Choi, J.-S. (2012). Inactivation of the medial prefrontal cortex interferes with the expression but not the acquisition of differential fear conditioning in rats. *Experimental Neurobiology*, *21*(1), 23–9.

Lehmann, J., Pryce, C. ., Bettschen, D., & Feldon, J. (1999). The Maternal Separation Paradigm and Adult Emotionality and Cognition in Male and Female Wistar Rats. *Pharmacology Biochemistry and Behavior*, *64*(4), 705–715.

Leranth, C., Petnehazy, O., & MacLusky, N. J. (2003). Gonadal hormones affect spine synaptic density in the CA1 hippocampal subfield of male rats. *The Journal of Neuroscience : The Official Journal of the Society for Neuroscience*, *23*(5), 1588–92.

Lesting, J., Daldrup, T., Narayanan, V., Himpe, C., Seidenbecher, T., Pape, H.-C., … Mulert, C. (2013). Directional Theta Coherence in Prefrontal Cortical to Amygdalo-Hippocampal Pathways Signals Fear Extinction. *PLoS ONE*, *8*(10), e77707.

Lesting, J., Narayanan, R. T., Kluge, C., Sangha, S., Seidenbecher, T., & Pape, H.-C. (2011). Patterns of coupled theta activity in amygdala-hippocampal-prefrontal cortical circuits during fear extinction. *PloS One*, *6*(6), e21714.

Li, G. (2017). Computational Models of the Amygdala in Acquisition and Extinction of Conditioned Fear. In *The Amygdala - Where Emotions Shape Perception, Learning and Memories*. InTech. https://doi.org/10.5772/67834

Li, G., Amano, T., Pare, D., & Nair, S. S. (2011). Impact of infralimbic inputs on intercalated amygdala neurons: a biophysical modeling study. *Learning & Memory (Cold Spring Harbor, N.Y.)*, *18*(4), 226–40.

Li, G., Nair, S. S., & Quirk, G. J. (2009). A Biologically Realistic Network Model of Acquisition and Extinction of Conditioned Fear Associations in Lateral Amygdala Neurons. *Journal of Neurophysiology*, *101*(3), 1629–1646.

Li, Y., Nakae, K., Ishii, S., Naoki, H., Niv, Y., & Nair, S. (2016). Uncertainty-Dependent Extinction of Fear Memory in an Amygdala-mPFC Neural Circuit Model. *PLOS Computational Biology*, *12*(9), e1005099.

Likhtik, E., & Gordon, J. A. (2014). Circuits in sync: decoding theta communication in fear and safety. *Neuropsychopharmacology*, *39*(1), 235–6.

Likhtik, E., Stujenske, J. M., Topiwala, M. A., Harris, A. Z., & Gordon, J. A. (2014). Prefrontal entrainment of amygdala activity signals safety in learned fear and innate anxiety. *Nature Neuroscience*, *17*(1), 106–13.

Lindquist, K. A., Wager, T. D., Kober, H., Bliss-Moreau, E., & Barrett, L. F. (2012). The brain basis of emotion: a meta-analytic review. *The Behavioral and Brain Sciences*, *35*(3), 121–43.

Lisman, J. E., & Jensen, O. (2013). The θ-γ neural code. *Neuron*, *77*(6), 1002–16.

Lissek, S., Kaczkurkin, A. N., Rabin, S., Geraci, M., Pine, D. S., & Grillon, C. (2014). Generalized anxiety disorder is associated with overgeneralization of classically conditioned fear. *Biological Psychiatry*, *75*(11), 909–15.

Lissek, S., Powers, A. S., McClure, E. B., Phelps, E. A., Woldehawariat, G., Grillon, C., & Pine, D. S. (2005). Classical fear conditioning in the anxiety disorders: a meta-analysis. *Behaviour Research and Therapy*, *43*(11), 1391–424.

Liu, Z., Xu, C., Xu, Y., Wang, Y., Zhao, B., Lv, Y., … Du, C. (2010). Decreased regional homogeneity in insula and cerebellum: A resting-state fMRI study in patients with major depression and subjects at high risk for major depression. *Psychiatry Research: Neuroimaging*, *182*(3), 211–215.

Lonsdorf, T. B., Haaker, J., Schümann, D., Sommer, T., Bayer, J., Brassen, S., Kalisc, R. (2015). Sex differences in conditioned stimulus discrimination during context-dependent fear learning and its retrieval in humans: the role of biological sex, contraceptives and menstrual cycle phases. *Journal of Psychiatry & Neuroscience*, *40*(6), 368–375.

Lopes da Silva, F. (2013). EEG and MEG: Relevance to Neuroscience. *Neuron*, *80*(5), 1112-1128.

Lowet, E., Roberts, M. J., Bonizzi, P., Karel, J., & De Weerd, P. (2016). Quantifying Neural Oscillatory Synchronization: A Comparison between Spectral Coherence and Phase-Locking Value Approaches. *PloS One*, *11*(1), e0146443.

Lynch, J., Cullen, P. K., Jasnow, A. M., & Riccio, D. C. (2013). Sex differences in the generalization of fear as a function of retention intervals. *Learning & Memory*, *20*(11), 628–32.

Lynch, J. F., Vanderhoof, T., Winiecki, P., Latsko, M. S., Riccio, D. C., & Jasnow, A. M. (2016). Aromatized testosterone attenuates contextual generalization of fear in male rats. *Hormones and Behavior*, *84*, 127–135.

Maass, W. (1997). Networks of spiking neurons: The third generation of neural network models. *Neural Networks*, *10*(9), 1659–1671.

Malkki, H. A. I., Donga, L. A. B., de Groot, S. E., Battaglia, F. P., NeuroBSIK Mouse Phenomics Consortium, N. M. P., & Pennartz, C. M. A. (2010). Appetitive operant conditioning in mice: heritability and dissociability of training stages. *Frontiers in Behavioral Neuroscience*, *4*, 171.

Marek, R., Strobel, C., Bredy, T. W., & Sah, P. (2013). The amygdala and medial prefrontal cortex: partners in the fear circuit. *J Physiol*, *59110*.

Maren, S. (2001). Neurobiology of Pavlovian fear conditioning. *Annual Review of Neuroscience*, *24*, 897–931.

Maren, S., De Oca, B., & Fanselow, M. S. (1994). Sex differences in hippocampal LTP and Pavlovian fear conditioning in rats: positive correlation between LTP and contextual learning. *Brain Research*, *661*(1–2), 25–34.

Maren, S., & Fanselow, M. S. (1997). Electrolytic lesions of the fimbria/fornix, dorsal hippocampus, or entorhinal cortex produce anterograde deficits in contextual fear conditioning in rats. *Neurobiology of Learning and Memory*, *67*(2), 142–9.

Maren, S., & Holt, W. (2000). The hippocampus and contextual memory retrieval in Pavlovian conditioning. *Behavioural Brain Research*, *110*(1–2), 97–108.

Maren, S., Phan, K. L., & Liberzon, I. (2013). The contextual brain: implications for fear conditioning, extinction and psychopathology. *Nature Reviews Neuroscience*, *14*(June).

Marron Fernandez de Velasco, E., Hearing, M., Xia, Z., Victoria, N. C., Luján, R., & Wickman, K. (2015). Sex differences in GABABR-GIRK signaling in layer 5/6 pyramidal neurons of the mouse prelimbic cortex. *Neuropharmacology*, *95*, 353–360.

Martin, P. (2003). The epidemiology of anxiety disorders: a review. *Dialogues in Clinical Neuroscience*, *5*(3), 281–98.

Masuda, Y., Odashima, J., Murai, S., Saito, H., Itoh, M., & Itoh, T. (1994). Radial arm maze behavior in mice when a return to the home cage serves as the reinforcer. *Physiology & Behavior*, *56*(4), 785–8.

Matsuda, S., Matsuzawa, D., Ishii, D., Tomizawa, H., Sutoh, C., & Shimizu, E. (2015). Sex differences in fear extinction and involvements of extracellular signal-regulated kinase (ERK). *Neurobiology of Learning and Memory*, *123*, 117–24.

McLean, C. P., & Anderson, E. R. (2009). Brave men and timid women? A review of the gender differences in fear and anxiety. *Clinical Psychology Review*, *29*(6), 496–505.

McLean, C. P., Asnaani, A., Litz, B. T., & Hofmann, S. G. (2011). Gender differences in anxiety disorders: prevalence, course of illness, comorbidity and burden of illness. *Journal of Psychiatric Research*, *45*(8), 1027–35.

McNish, K. A., Gewirtz, J. C., & Davis, M. (1997). Evidence of contextual fear after lesions of the hippocampus: a disruption of freezing but not fear-potentiated startle. *The Journal of Neuroscience, 17*(23), 9353–60.

Mejo, S. L. (1992). Anterograde amnesia linked to benzodiazepines. *The Nurse Practitioner*, *17*(10), 44, 49–50.

Meuret, A. E., Wolitzky-Taylor, K. B., Twohig, M. P., & Craske, M. G. (2012). Coping skills and exposure therapy in panic disorder and agoraphobia: latest advances and future directions. *Behavior Therapy*, *43*(2), 271–84.

Mikosz, M., Nowak, A., Werka, T., & Knapska, E. (2015). Sex differences in social modulation of learning in rats. *Scientific Reports*, *5*, 18114.

Milad, M. R., Goldstein, J. M., Orr, S. P., Wedig, M. M., Klibanski, A., Pitman, R. K., & Rauch, S. L. (2006). Fear conditioning and extinction: Influence of sex and menstrual cycle in healthy humans. *Behavioral Neuroscience*, *120*(6), 1196–1203.

Milad, M. R., Igoe, S. A., Lebron-Milad, K., & Novales, J. E. (2009). Estrous cycle phase and gonadal hormones influence conditioned fear extinction. *Neuroscience*, *164*(3), 887-895.

Milad, M. R., Pitman, R. K., Ellis, C. B., Gold, A. L., Shin, L. M., Lasko, N. B., … Rauch, S. L. (2009). Neurobiological basis of failure to recall extinction memory in posttraumatic stress disorder. *Biological Psychiatry*, *66*(12), 1075–82.

Milad, M. R., & Quirk, G. J. (2002). Neurons in medial prefrontal cortex signal memory for fear extinction. *Nature*, *420*(6911), 70–74.

Milad, M. R., & Quirk, G. J. (2012). Fear extinction as a model for translational neuroscience: ten years of progress. *Annual Review of Psychology*, *63*, 129–51.

Milad, M. R., Zeidan, M. A., Contero, A., Pitman, R. K., Klibanski, A., Rauch, S. L., & Goldstein, J. M. (2010). The influence of gonadal hormones on conditioned fear extinction in healthy humans. *Neuroscience*, *168*(3), 652–658.

Möller, A. T., Bäckström, T., Nyberg, S., Söndergaard, H. P., & Helström, L. (2016). Women with PTSD have a changed sensitivity to GABA-A receptor active substances. *Psychopharmacology*, *233*(11), 2025–2033.

Morén, J. (2002). *Emotion and learning : a computational model of the amygdala. Lund University Cognitive Studies; 93 (2002)* (Vol. 93).

Morriss, J., Christakou, A., & van Reekum, C. M. (2015). Intolerance of uncertainty predicts fear extinction in amygdala-ventromedial prefrontal cortical circuitry. *Biology of Mood & Anxiety Disorders*, *5*(1), 4.

Motzkin, J. C., Philippi, C. L., Wolf, R. C., Baskaya, M. K., Koenigs, M., Sirigu, A., & al., et. (2015). Ventromedial prefrontal cortex is critical for the regulation of amygdala activity in humans. *Biological Psychiatry*, *77*(3), 276–84.

Mueller, E. M., Panitz, C., Hermann, C., & Pizzagalli, D. A. (2014). Prefrontal oscillations during recall of conditioned and extinguished fear in humans. *The Journal of Neuroscience 34*(21), 7059–66.

Muller, J. F., Mascagni, F., & McDonald, A. J. (2006). Pyramidal cells of the rat basolateral amygdala: synaptology and innervation by parvalbumin-immunoreactive interneurons. *The Journal of Comparative Neurology*, *494*(4), 635–50.

Myers, K. M., & Davis, M. (2007). Mechanisms of fear extinction. *Molecular Psychiatry*, *12*(2), 120–50.

Myers, K. M., Ressler, K. J., & Davis, M. (2006). Different mechanisms of fear extinction dependent on length of time since fear acquisition. *Learning & Memory*, *13*(2), 216–223.

Nair, S. S., Paré, D., & Vicentic, A. (2016). Biologically based neural circuit modelling for the study of fear learning and extinction, *1*, 16015.

Neufang, S., Specht, K., Hausmann, M., Güntürkün, O., Herpertz-Dahlmann, B., Fink, G. R., & Konrad, K. (2009). Sex differences and the impact of steroid hormones on the developing human brain. *Cerebral Cortex (New York, N.Y. : 1991)*, *19*(2), 464–73.

Neves, L. L., & Monteiro, L. H. A. (2016). A Linear Analysis of Coupled Wilson-Cowan Neuronal Populations. *Computational Intelligence and Neuroscience*, *2016*, 1–6.

Nyhus, E., & Curran, T. (2010). Functional role of gamma and theta oscillations in episodic memory. *Neuroscience and Biobehavioral Reviews*, *34*(7), 1023–35.

Olff, M. (2017). Sex and gender differences in post-traumatic stress disorder: an update. *European Journal of Psychotraumatology ISSNOnline) Journal*, *homepage*, 2000–8198.

Onishi, B. K. A., & Xavier, G. F. (2010). Contextual, but not auditory, fear conditioning is disrupted by neurotoxic selective lesion of the basal nucleus of amygdala in rats. *Neurobiology of Learning and Memory*, *93*(2), 165–174.

Onslow, A. C. E., Jones, M. W., Bogacz, R., Glowinski, J., & Fuchs, E. (2014). A Canonical Circuit for Generating Phase-Amplitude Coupling. *PLoS ONE*, *9*(8), e102591.

Oren, I., Mann, E. O., Paulsen, O., & Hajos, N. (2006). Synaptic Currents in Anatomically Identified CA3 Neurons during Hippocampal Gamma Oscillations In Vitro. *Journal of Neuroscience*, *26*(39), 9923–9934.

Orr, S. P., Metzger, L. J., Lasko, N. B., Macklin, M. L., Peri, T., & Pitman, R. K. (2000). De novo conditioning in trauma-exposed individuals with and without posttraumatic stress disorder. *Journal of Abnormal Psychology*, *109*(2), 290–8.

Orsini, C. A., Kim, J. H., Knapska, E., & Maren, S. (2011). Hippocampal and prefrontal projections to the basal amygdala mediate contextual regulation of fear after extinction. *The Journal of Neuroscience*, *31*(47), 17269–77.

Orsini, C. A., Yan, C., & Maren, S. (2013). Ensemble coding of context-dependent fear memory in the amygdala. *Frontiers in Behavioral Neuroscience*, *7*, 199.

Pape, H.-C., & Pare, D. (2010). Plastic synaptic networks of the amygdala for the acquisition, expression, and extinction of conditioned fear. *Physiological Reviews*, *90*(2), 419–63.

Pape, H. C., & Driesang, R. B. (1998). Ionic mechanisms of intrinsic oscillations in neurons of the basolateral amygdaloid complex. *Journal of Neurophysiology*, *79*(1), 217–26.

Pare, D., Quirk, G. J., & Ledoux, J. E. (2004). New Vistas on Amygdala Networks in Conditioned Fear. *Journal of Neurophysiology*, *92*(1), 1–9.

Paré, D., Quirk, G. J., & Ledoux, J. E. (2004). New vistas on amygdala networks in conditioned fear. *Journal of Neurophysiology*, *92*(1), 1–9.

Pavlov, & P., I. (1927). Conditioned reflexes: an investigation of the physiological activity of the cerebral cortex. Oxford Univ. Press.

Payne, J. D., & Nadel, L. (2004). Sleep, dreams, and memory consolidation: the role of the stress hormone cortisol. *Learning & Memory*, *11*(6), 671–8.

Paz, R., Bauer, E. P., & Paré, D. (2008). Theta synchronizes the activity of medial prefrontal neurons during learning. *Learning & Memory, 15*(7), 524–31.

Pendyam, S., Bravo-Rivera, C., Burgos-Robles, A., Sotres-Bayon, F., Quirk, G. J., & Nair, S. S. (2013). Fear signaling in the prelimbic-amygdala circuit: a computational modeling and recording study. *Journal of Neurophysiology*, *110*(4), 844–61.

Percival, D. B., & Walden, A. T. (1993). *Spectral Analysis for Physical Applications*. Cambridge: Cambridge University Press.

Perel, P., Roberts, I., Sena, E., Wheble, P., Briscoe, C., Sandercock, P., Khan, K. S. (2007). Comparison of treatment effects between animal experiments and clinical trials: systematic review. *BMJ (Clinical Research Ed.)*, *334*(7586), 197.

Pevzner, A., Izadi, A., Lee, D. J., Shahlaie, K., & Gurkoff, G. G. (2016). Making Waves in the Brain: What Are Oscillations, and Why Modulating Them Makes Sense for Brain Injury. *Frontiers in Systems Neuroscience*, *10*, 30.

Phelps, E. A., Delgado, M. R., Nearing, K. I., & LeDoux, J. E. (2004). Extinction learning in humans: role of the amygdala and vmPFC. *Neuron*, *43*(6), 897–905.

Phelps, E. A., O'Connor, K. J., Gatenby, J. C., Gore, J. C., Grillon, C., & Davis, M. (2001). Activation of the left amygdala to a cognitive representation of fear. *Nature Neuroscience*, *4*(4), 437–441.

Phillips, R. G., & LeDoux, J. E. (1992). Differential contribution of amygdala and hippocampus to cued and contextual fear conditioning. *Behavioral Neuroscience*, *106*(2), 274–85.

Piantadosi, P. T., & Floresco, S. B. (2014). Prefrontal Cortical GABA Transmission Modulates Discrimination and Latent Inhibition of Conditioned Fear: Relevance for Schizophrenia. *Neuropsychopharmacology*, *39*(10), 2473–2484.

Pine, J. (1980). Recording action potentials from cultured neurons with extracellular microcircuit electrodes. *Journal of Neuroscience Methods*, *2*(1), 19–31.

Pitman, R. K., Rasmusson, A. M., Koenen, K. C., Shin, L. M., Orr, S. P., Gilbertson, M. W., … Liberzon, I. (2012). Biological studies of post-traumatic stress disorder. *Nature Reviews Neuroscience*, *13*(11), 769–787.

Platkiewicz, J., & Brette, R. (2010). A threshold equation for action potential initiation. *PLoS Computational Biology*, *6*(7), e1000850.

Popa, D., Duvarci, S., Popescu, A. T., Léna, C., & Paré, D. (2010). Coherent amygdalocortical theta promotes fear memory consolidation during paradoxical sleep. *PNAS*, *107*(14), 6516-9.

Poulos, A. M., Li, V., Sterlace, S. S., Tokushige, F., Ponnusamy, R., & Fanselow, M. S. (2009). Persistence of fear memory across time requires the basolateral amygdala complex. *Proceedings of the National Academy of Sciences, 106*(28), 11737–11741.

Prut, L., & Belzung, C. (2003). The open field as a paradigm to measure the effects of drugs on anxiety-like behaviors: a review. *European Journal of Pharmacology*, *463*(1-3), 3-33.

Puig, M. V., Ushimaru, M., & Kawaguchi, Y. (2008). Two distinct activity patterns of fast-spiking interneurons during neocortical UP states. *Proceedings of the National Academy of Sciences of the United States of America*, *105*(24), 8428-33.

Quinlan, M. G., Duncan, A., Loiselle, C., Graffe, N., & Brake, W. G. (2010). Latent inhibition is affected by phase of estrous cycle in female rats. *Brain and Cognition*, *74*(3), 244-248.

Quinn, J. J., Ma, Q. D., Tinsley, M. R., Koch, C., & Fanselow, M. S. (2008). Inverse temporal contributions of the dorsal hippocampus and mPFC to the expression of long-term fear memories. *Learning & Memory, 15*(5), 368-72.

Quirk, G. J., Likhtik, E., Pelletier, J. G., & Paré, D. (2003). Stimulation of mPFC decreases the responsiveness of central amygdala output neurons. *The Journal of Neuroscience : The Official Journal of the Society for Neuroscience*, *23*(25), 8800-7.

Quirk, G. J., Paré, D., Richardson, R., Herry, C., Monfils, M. H., Schiller, D., & Vicentic, A. (2010). Erasing fear memories with extinction training. *Journal of Neuroscience, 30*(45), 14993-7.

Quirk, G. J., Russo, G. K., Barron, J. L., & Lebron, K. (2000). The Role of Ventromedial Prefrontal Cortex in the Recovery of Extinguished Fear. *J. Neurosci.*, *20*(16), 6225–6231.

Radke, A. K. (2009). The role of the bed nucleus of the stria terminalis in learning to fear. *The Journal of Neuroscience : The Official Journal of the Society for Neuroscience*, *29*(49), 15351–2.

Radley, J. J., Gosselink, K. L., & Sawchenko, P. E. (2009). A Discrete GABAergic Relay Mediates Medial Prefrontal Cortical Inhibition of the Neuroendocrine Stress Response. *Journal of Neuroscience*, *29*(22), 7330–7340.

Rasch, M., Logothetis, N. K., & Kreiman, G. (2009). From neurons to circuits: linear estimation of local field potentials. *The Journal of Neuroscience*, *29*(44), 13785–96.

Rasmusson, A. M., Pinna, G., Paliwal, P., Weisman, D., Gottschalk, C., Charney, D., … Guidotti, A. (2006). Decreased Cerebrospinal Fluid Allopregnanolone Levels in Women with Posttraumatic Stress Disorder. *Biological Psychiatry*, *60*(7), 704–713.

Raymond, J. G., Steele, J. D., & Seriès, P. (2017). Modeling Trait Anxiety: From Computational Processes to Personality. *Frontiers in Psychiatry*, *8*, 1.

Reincke, S. A. J., & Hanganu-Opatz, I. L. (2017). Early-life stress impairs recognition memory and perturbs the functional maturation of prefrontal-hippocampal-perirhinal networks. *Scientific Reports*, *7*, 42042.

Reisenzein, R., Hudlicka, E., Dastani, M., Gratch, J., Hindriks, K., Lorini, E., & Meyer, J.-J. C. (2013). Computational Modeling of Emotion: Toward Improving the Inter- and Intradisciplinary Exchange. *IEEE Transactions on Affective Computing*, *4*(3), 246–266.

Reppucci, C. J., Kuthyar, M., & Petrovich, G. D. (2013). Contextual fear cues inhibit eating in food-deprived male and female rats. *Appetite*, *69*, 186–195.

Rescorla, R. A. (1969). Pavlovian Conditioned Inhibition. *Psychological Bulletin*, *72*(2).

Rescorla, R. A., & Heth, C. D. (1975). Reinstatement of fear to an extinguished conditioned stimulus. *Journal of Experimental Psychology. Animal Behavior Processes*, *1*(1), 88–96.

Rey, C. D., Lipps, J., & Shansky, R. M. (2014). Dopamine D1 receptor activation rescues extinction impairments in low-estrogen female rats and induces cortical layer-specific activation changes in prefrontal-amygdala circuits. *Neuropsychopharmacology*, *39*(5),

Rhodes, S. E. V., & Killcross, A. S. (2007). Lesions of rat infralimbic cortex enhance renewal of extinguished appetitive Pavlovian responding. *European Journal of Neuroscience*, *25*(8), 2498–2503.

Rich, E. L., & Shapiro, M. L. (2007). Prelimbic/Infralimbic Inactivation Impairs Memory for Multiple Task Switches, But Not Flexible Selection of Familiar Tasks. *Journal of Neuroscience*, *27*(17), 4747–4755.

Roenneberg, T., Chua, E. J., Bernardo, R., & Mendoza, E. (2008). Modelling Biological Rhythms. *Current Biology*, *18*(17), R826–R835.

Rogan, M. T., Leon, K. S., Perez, D. L., & Kandel, E. R. (2005). Distinct Neural Signatures for Safety and Danger in the Amygdala and Striatum of the Mouse. *Neuron, 46*(2), 309-320.

Rogan, M. T., Stäubli, U. V., & LeDoux, J. E. (1997). Fear conditioning induces associative long-term potentiation in the amygdala. *Nature, 390*(6660), 604–607.

Rosenberg, J. R., Halliday, D. M., Breeze, P., & Conway, B. A. (1998). Identification of patterns of neuronal connectivity—partial spectra, partial coherence, and neuronal interactions. *Journal of Neuroscience Methods*, *83*(1), 57–72.

Rosenkranz, J. A., & Grace, A. A. (2002). Dopamine-mediated modulation of odour-evoked amygdala potentials during pavlovian conditioning. *Nature, 417*(6886), 282–287.

Rosenkranz, J. A., Moore, H., & Grace, A. A. (2003). The Prefrontal Cortex Regulates Lateral Amygdala Neuronal Plasticity and Responses to Previously Conditioned Stimuli. *Journal of Neuroscience*, *23*(35).

Rothbaum, B. O., Hodges, L. F., Ready, D., Graap, K., & Alarcon, R. D. (2001). Virtual reality exposure therapy for Vietnam veterans with posttraumatic stress disorder. *The Journal of Clinical Psychiatry*, *62*(8), 617–22.

Rovó, Z., Ulbert, I., & Acsády, L. (2012). Drivers of the primate thalamus. *The Journal of Neuroscience : The Official Journal of the Society for Neuroscience*, *32*(49), 17894–908.

Roxin, A., Brunel, N., & Hansel, D. (2005). Role of Delays in Shaping Spatiotemporal Dynamics of Neuronal Activity in Large Networks. *Physical Review Letters*, *94*(23).

Royer, S., Martina, M., & Paré, D. (1999). An inhibitory interface gates impulse traffic between the input and output stations of the amygdala. *The Journal of Neuroscience : The Official Journal of the Society for Neuroscience*, *19*(23), 10575–83.

Rudy, J. W., Barrientos, R. M., & O'Reilly, R. C. (2002). Hippocampal formation supports conditioning to memory of a context. *Behavioral Neuroscience*, *116*(4), 530–8.

Rutishauser, U., Ross, I. B., Mamelak, A. N., & Schuman, E. M. (2010). Human memory strength is predicted by theta-frequency phase-locking of single neurons. *Nature*, *464*(7290), 903–907.

Sah, P., Faber, E. S. L., Lopez De Armentia, M., & Power, J. (2003). The amygdaloid complex: anatomy and physiology. *Physiological Reviews*, *83*(3), 803–34.

Samanez-Larkin, G. R., & Knutson, B. (2015). Decision making in the ageing brain: changes in affective and motivational circuits. *Nature Reviews Neuroscience*, *16*(5), 278–289.

Sangha, S., Chadick, J. Z., & Janak, P. H. (2013). Safety Encoding in the Basal Amygdala. *Journal of Neuroscience*, *33*(9), 3744–3751.

Sangha, S., Narayanan, R. T., Bergado-Acosta, J. R., Stork, O., Seidenbecher, T., & Pape, H.-C. (2009). Deficiency of the 65 kDa Isoform of Glutamic Acid Decarboxylase Impairs Extinction of Cued But Not Contextual Fear Memory. *Journal of Neuroscience*, *29*(50), 15713–15720.

Sangha, S., Robinson, P. D., Greba, Q., Davies, D. A., & Howland, J. G. (2014). Alterations in reward, fear and safety cue discrimination after inactivation of the rat prelimbic and infralimbic cortices. *Neuropsychopharmacology*, *39*(10), 2405–13.

Sars, D., & van Minnen, A. (2015). On the use of exposure therapy in the treatment of anxiety disorders: a survey among cognitive behavioural therapists in the Netherlands. *BMC Psychology*, *3*(1), 26.

Sase, T., Katori, Y., Komuro, M., & Aihara, K. (2017). Bifurcation Analysis on Phase-Amplitude Cross-Frequency Coupling in Neural Networks with Dynamic Synapses. *Frontiers in Computational Neuroscience*, *11*, 18.

Scanziani, M., & Häusser, M. (2009). Electrophysiology in the age of light. *Nature*, *461*(7266), 930–939.

Schafe, G. E., & LeDoux, J. E. (2000). Memory consolidation of auditory pavlovian fear conditioning requires protein synthesis and protein kinase A in the amygdala. *The Journal of Neuroscience, 20*(18), RC96.

Schellenberger Costa, M., Weigenand, A., Ngo, H.-V. V., Marshall, L., Born, J., Martinetz, T., & Claussen, J. C. (2016). A Thalamocortical Neural Mass Model of the EEG during NREM Sleep and Its Response to Auditory Stimulation. *PLOS Computational Biology*, *12*(9), e1005022.

Schmidt, M., Bakker, R., Shen, K., Bezgin, G., Hilgetag, C.-C., Diesmann, M., & van Albada, S. J. (2015). Full-density multi-scale account of structure and dynamics of macaque visual cortex.

Schnitzler, A., & Gross, J. (2005). Normal and pathological oscillatory communication in the brain. *Nature Reviews Neuroscience*, *6*(4), 285–296.

Scott, K. M., Du, J., Lester, H. A., & Masmanidis, S. C. (2012). Variability of acute extracellular action potential measurements with multisite silicon probes. *Journal of Neuroscience Methods, 211*(1), 22–30.

Seedat, S., Stein, D. J., & Carey, P. D. (2005a). Post-Traumatic Stress Disorder in Women. *CNS Drugs*, *19*(5), 411–427.

Seidenbecher, T., Laxmi, T. R., Stork, O., & Pape, H.-C. (2003). Amygdalar and Hippocampal Theta Rhythm Synchronization During Fear Memory Retrieval. *Science*, *301*(5634), 846–850.

Seliger, D. L. (1977). Effects of Age, Sex, and Brightness of Field on Open-Field Behaviors of Rats. *Perceptual and Motor Skills*, *45*(3), 1059–1067.

Senkowski, D., Schneider, T. R., Foxe, J. J., & Engel, A. K. (2008). Crossmodal binding through neural coherence: implications for multisensory processing. *Trends in Neurosciences*, *31*(8), 401–409.

Servedio, M. R., Brandvain, Y., Dhole, S., Fitzpatrick, C. L., Goldberg, E. E., Stern, C. A., … Yeh, D. J. (2014). Not Just a Theory—The Utility of Mathematical Models in Evolutionary Biology. *PLoS Biology*, *12*(12), e1002017.

Shaban, H., Humeau, Y., Herry, C., Cassasus, G., Shigemoto, R., Ciocchi, S., Lüthi, A. (2006). Generalization of amygdala LTP and conditioned fear in the absence of presynaptic inhibition. *Nature Neuroscience*, *9*(8), 1028–1035.

Shadlen, M. N., Newsome, W. T., Olshen, R., Bair, W., Barberini, C., Cumming, B., … Nichols, J. (1998). The Variable Discharge of Cortical Neurons: Implications for Connectivity, Computation, and Information Coding. *The Journal of Neuroscience*, *18*(10), 3870–3896.

Shansky, R. M. (2015). Sex differences in PTSD resilience and susceptibility: Challenges for animal models of fear learning. *Neurobiology of Stress*, *1*, 60–65.

Shansky, R. M., Hamo, C., Hof, P. R., Lou, W., McEwen, B. S., & Morrison, J. H. (2010). Estrogen Promotes Stress Sensitivity in a Prefrontal Cortex-Amygdala Pathway. *Cerebral Cortex*, *20*(11), 2560–2567.

Sharpe, M. J., & Killcross, S. (2015). The prelimbic cortex directs attention toward predictive cues during fear learning. *Learning & Memory*, *22*(6), 289–93.

Shvil, E., Sullivan, G. M., Schafer, S., Markowitz, J. C., Campeas, M., Wager, T. D., … Neria, Y. (2014a). Sex differences in extinction recall in posttraumatic stress disorder: A pilot fMRI study. *Neurobiology of Learning and Memory, 113*, 101–108.

Sierra-Mercado, D., Corcoran, K. A., Lebrón-Milad, K., & Quirk, G. J. (2006). Inactivation of the ventromedial prefrontal cortex reduces expression of conditioned fear and impairs subsequent recall of extinction. *The European Journal of Neuroscience*, *24*(6), 1751–8.

Sierra-Mercado, D., Padilla-Coreano, N., & Quirk, G. J. (2011). Dissociable roles of PL and IL cortices, ventral hippocampus, and basolateral amygdala in the expression and extinction of conditioned fear. *Neuropsychopharmacology*, *36*(2), 529-38.

Siettos, C., & Starke, J. (2016). Multiscale modeling of brain dynamics: from single neurons and networks to mathematical tools. *Wiley Interdisciplinary Reviews: Systems Biology and Medicine*, *8*(5), 438–458.

Sigmundi, R. A., & Bolles, R. C. (1983). CS modality, context conditioning, and conditioned freezing. *Animal Learning & Behavior*,11, 205–212.

Simpson, E. R., & Davis, S. R. (2001). Minireview: Aromatase and the Regulation of Estrogen Biosynthesis—Some New Perspectives. *Endocrinology*, *142*(11), 4589–4594.

Softky, W. R., & Koch, C. (1993). The highly irregular firing of cortical cells is inconsistent with temporal integration of random EPSPs. *The Journal of Neuroscience : The Official Journal of the Society for Neuroscience*, *13*(1), 334–50.

Soler-Cedeño, O., Cruz, E., Criado-Marrero, M., & Porter, J. T. (2016). Contextual fear conditioning depresses infralimbic excitability. *Neurobiology of Learning and Memory*, *130*, 77–82.

Somerville, L. H., Whalen, P. J., & Kelley, W. M. (2010). Human bed nucleus of the stria terminalis indexes hypervigilant threat monitoring. *Biological Psychiatry*, *68*(5), 416–24.

Sompolinsky, H. (2014). Computational neuroscience: beyond the local circuit. *Current Opinion in Neurobiology*, *25*, xiii–xviii.

Sotres-Bayon, F., Bush, D. E. A., & LeDoux, J. E. (2004). Emotional Perseveration: An Update on Prefrontal-Amygdala Interactions in Fear Extinction. *Learning & Memory*, *11*(5), 525–535.

Sotres-Bayon, F., Bush, D. E. A., & LeDoux, J. E. (2007). Acquisition of Fear Extinction Requires Activation of NR2B-Containing NMDA Receptors in the Lateral Amygdala. *Neuropsychopharmacology*, *32*(9), 1929–1940.

Sotres-Bayon, F., Cain, C. K., & LeDoux, J. E. (2006). Brain Mechanisms of Fear Extinction: Historical Perspectives on the Contribution of Prefrontal Cortex. *Biological Psychiatry*, *60*(4), 329–336.

Sotres-Bayon, F., & Quirk, G. J. (2010). Prefrontal control of fear: more than just extinction. *Current Opinion in Neurobiology*, *20*(2), 231–5.

Sotres-Bayon, F., Sierra-Mercado, D., Pardilla-Delgado, E., & Quirk, G. J. (2012). Gating of fear in prelimbic cortex by hippocampal and amygdala inputs. *Neuron*, *76*(4), 804–12.

Standage, D., Wang, D.-H., & Blohm, G. (2014). Neural dynamics implement a flexible decision bound with a fixed firing rate for choice: a model-based hypothesis. *Frontiers in Neuroscience*, *8*, 318.

Steimer, T. (2002). The biology of fear- and anxiety-related behaviors. *Dialogues in Clinical Neuroscience*, *4*(3), 231–49.

Stevenson, C. W. (2011). Role of amygdala-prefrontal cortex circuitry in regulating the expression of contextual fear memory. *Neurobiology of Learning and Memory*, *96*(2), 315–323.

Stevenson, C. W., Halliday, D. M., Marsden, C. A., & Mason, R. (2007). Systemic administration of the benzodiazepine receptor partial inverse agonist FG-7142 disrupts corticolimbic network interactions. *Synapse*, *61*(8), 646–663.

Stevenson, C. W., Spicer, C. H., Mason, R., & Marsden, C. A. (2009). Early life programming of fear conditioning and extinction in adult male rats. *Behavioural Brain Research*, *205*(2), 505–510.

Stratton, P., Cheung, A., Wiles, J., Kiyatkin, E., Sah, P., & Windels, F. (2012). Action Potential Waveform Variability Limits Multi-Unit Separation in Freely Behaving Rats. *PLoS ONE*, *7*(6), e38482.

Stujenske, J. M., Likhtik, E., Topiwala, M. A., & Gordon, J. A. (2014). Fear and safety engage competing patterns of theta-gamma coupling in the basolateral amygdala. *Neuron*, *83*(4), 919–33.

Szinyei, C., Narayanan, R. T., & Pape, H.-C. (2007). Plasticity of inhibitory synaptic network interactions in the lateral amygdala upon fear conditioning in mice. *European Journal of Neuroscience*, *25*(4), 1205–1211.

Tallon-Baudry, W., Bertrand, R., Tallon-Baudry, C., Bertrand, O., Tallon-Baudry, C., & Bertrand, O. (1999). Oscillatory gamma activity in humans and its role in object representation. *Trends in Cognitive Sciences*, *3*(4), 151–162.

Tejeda, H. A., & O'Donnell, P. (2014). Amygdala inputs to the prefrontal cortex elicit heterosynaptic suppression of hippocampal inputs. *The Journal of Neuroscience : The Official Journal of the Society for Neuroscience*, *34*(43), 14365–74.

Terada, S., Takahashi, S., & Sakurai, Y. (2013). Oscillatory interaction between amygdala and hippocampus coordinates behavioral modulation based on reward expectation. *Frontiers in Behavioral Neuroscience*, *7*, 177.

Terman, D., Rubin, J. E., Yew, A. C., & Wilson, C. J. (2002). Activity Patterns in a Model for the Subthalamopallidal Network of the Basal Ganglia. *Journal of Neuroscience*, *22*(7).

Thompson, R. S., Strong, P. V, & Fleshner, M. (2012). Physiological consequences of repeated exposures to conditioned fear. *Behavioral Sciences (Basel, Switzerland)*, *2*(2), 57–78.

Tierney, P. L., Degenetais, E., Thierry, A.-M., Glowinski, J., & Gioanni, Y. (2004). Influence of the hippocampus on interneurons of the rat prefrontal cortex. *European Journal of Neuroscience*, *20*(2), 514–524.

Toufexis, D. J., Myers, K. M., Bowser, M. E., & Davis, M. (2007). Estrogen disrupts the inhibition of fear in female rats, possibly through the antagonistic effects of estrogen receptor alpha (ERalpha) and ERbeta. *The Journal of Neuroscience*, *27*(36), 9729–35.

Trousselard, M., Lefebvre, B., Caillet, L., Andruetan, Y., de Montleau, F., Denis, J., & Canini, F. (2016). Is plasma GABA level a biomarker of Post-Traumatic Stress Disorder (PTSD) severity? A preliminary study. *Psychiatry Research*, *241*, 273–279.

Tsujimoto, T., Shimazu, H., Isomura, Y., & Sasaki, K. (2003). Prefrontal theta oscillations associated with hand movements triggered by warning and imperative stimuli in the monkey. *Neuroscience Letters*, *351*(2), 103–6.

Ueta, T., & Chen, G. (2003). On synchronization and control of coupled wilson–cowan neural oscillators. *International Journal of Bifurcation and Chaos*, *13*(1), 163–175.

Urcelay, G. P., & Miller, R. R. (2014). The functions of contexts in associative learning. *Behavioural Processes*, *104*, 2–12.

van Aerde, K. I., Heistek, T. S., & Mansvelder, H. D. (2008). Prelimbic and Infralimbic Prefrontal Cortex Interact during Fast Network Oscillations. *PLoS ONE*, *3*(7), e2725.

van Haaren, F., van Hest, A., & Heinsbroek, R. P. W. (1990). Behavioral differences between male and female rats: Effects of gonadal hormones on learning and memory. *Neuroscience & Biobehavioral Reviews*, *14*(1), 23–33.

van Vreeswijk, C., & Sompolinsky, H. (1996). Chaos in neuronal networks with balanced excitatory and inhibitory activity. *Science (New York, N.Y.)*, *274*(5293), 1724–6.

Vanderschuren, L. J. M. J., & Everitt, B. J. (2004). Drug Seeking Becomes Compulsive After Prolonged Cocaine Self-Administration. *Science*, *305*(5686).

Vanderwolf, C. H. (2000). Are neocortical gamma waves related to consciousness? *Brain Research*, *855*(2), 217–224.

VanElzakker, M. B., Kathryn Dahlgren, M., Caroline Davis, F., Dubois, S., & Shin, L. M. (2014). From Pavlov to PTSD: The extinction of conditioned fear in rodents, humans, and anxiety disorders. *Neurobiology of Learning and Memory*, *113*, 3–18.

Vanvinckenroye, A., Vandewalle, G., Phillips, C., & Chellappa, S. L. (2016). Eyes Open on Sleep and Wake: In Vivo to In Silico Neural Networks. *Neural Plasticity*, *2016*, 1–13.

Vertes, R. P. (2004). Differential projections of the infralimbic and prelimbic cortex in the rat. *Synapse (New York, N.Y.)*, *51*(1), 32–58.

Vianna, D. M. L., & Brandão, M. L. (2003). Anatomical connections of the periaqueductal gray: specific neural substrates for different kinds of fear. *Brazilian Journal of Medical and Biological Research*, *36*(5), 557–566.

Vidal-Gonzalez, I., Vidal-Gonzalez, B., Rauch, S. L., & Quirk, G. J. (2006). Microstimulation reveals opposing influences of prelimbic and infralimbic cortex on the expression of conditioned fear. *Learning & Memory*, *13*(6), 728–33.

Vlachos, I., Herry, C., Lüthi, A., Aertsen, A., & Kumar, A. (2011). Context-Dependent Encoding of Fear and Extinction Memories in a Large-Scale Network Model of the Basal Amygdala. *PLoS Computational Biology*, *7*(3), e1001104.

Voglis, G., & Tavernarakis, N. (2006). The role of synaptic ion channels in synaptic plasticity. *EMBO Reports*, *7*(11), 1104–10.

Voytek, B., Canolty, R. T., Shestyuk, A., Crone, N. E., Parvizi, J., & Knight, R. T. (2010). Shifts in gamma phase-amplitude coupling frequency from theta to alpha over posterior cortex during visual tasks. *Frontiers in Human Neuroscience*, *4*, 191.

Wang, J., Korczykowski, M., Rao, H., Fan, Y., Pluta, J., Gur, R. C., Detre, J. A. (2007). Gender difference in neural response to psychological stress. *Social Cognitive and Affective Neuroscience*, *2*(3), 227–239.

Wang, M. (2011). Neurosteroids and GABA-A Receptor Function. *Frontiers in Endocrinology*, *2*, 44.

Watson, T. C., Cerminara, N. L., Lumb, B. M., & Apps, R. (2016). Neural Correlates of Fear in the Periaqueductal Gray. *Journal of Neuroscience*, *36*(50).

Weinhardt, J. M., & Vancouver, J. B. (2012). Computational models and organizational psychology: Opportunities abound. *Organizational Psychology Review*, *2*(4), 267–292.

Wessa, M., & Flor, H. (2007). Failure of Extinction of Fear Responses in Posttraumatic Stress Disorder: Evidence From Second-Order Conditioning. *American Journal of Psychiatry*, *164*(11), 1684–1692.

Wilson, H. R., & Cowan, J. D. (1972). Excitatory and inhibitory interactions in localized populations of model neurons. *Biophysical Journal*, *12*(1), 1–24.

Winkelmann, T., Grimm, O., Pohlack, S. T., Nees, F., Cacciaglia, R., Dinu-Biringer, R., Flor, H. (2016). Brain morphology correlates of interindividual differences in conditioned fear acquisition and extinction learning. *Brain Structure and Function*, *221*(4), 1927-1937.

Wolff, S. B. E., Gründemann, J., Tovote, P., Krabbe, S., Jacobson, G. A., Müller, C., … Lüthi, A. (2014). Amygdala interneuron subtypes control fear learning through disinhibition. *Nature*, *509*(7501).

Wood, G. E., & Shors, T. J. (1998). Stress facilitates classical conditioning in males, but impairs classical conditioning in females through activational effects of ovarian hormones. *PNAS*, *95*(7), 4066–71.

Xu, W., Südhof, T. C., Schairer, W., Janak, P., Shigemoto, R., Ciocchi, S., Lüthi, A. (2013). A neural circuit for memory specificity and generalization. *Science*, *339*(6125), 1290–5.

Yeragani, V. K., Cashmere, D., Miewald, J., Tancer, M., Keshavan, M. S., & Daia, G. (2006). Decreased coherence in higher frequency ranges (beta and gamma) between central and frontal EEG in patients with schizophrenia: A preliminary report. *Psychiatry Research*, *141*(1), 53–60.

Yoder, M., Tuerk, P. W., Price, M., Grubaugh, A. L., Strachan, M., Myrick, H., & Acierno, R. (2012). Prolonged exposure therapy for combat-related PTSD: comparing outcomes for veterans of different wars. *Psychological Services*, *9*(1), 16–25.

Young, A. M. J., Moran, P. M., & Joseph, M. H. (2005). The role of dopamine in conditioning and latent inhibition: What, when, where and how? *Neuroscience & Biobehavioral Reviews*, *29*(6), 963–976.

Zavala, B., Tan, H., Ashkan, K., Foltynie, T., Limousin, P., Zrinzo, L., … Brown, P. (2016). Human subthalamic nucleus-medial frontal cortex theta phase coherence is involved in conflict and error related cortical monitoring. *NeuroImage*, *137*, 178–187.

Zeeb, F. D., Baarendse, P. J. J., Vanderschuren, L. J. M. J., & Winstanley, C. A. (2015). Inactivation of the prelimbic or infralimbic cortex impairs decision-making in the rat gambling task. *Psychopharmacology*, *232*(24), 4481–4491.

Zeidan, M. A., Igoe, S. A., Linnman, C., Vitalo, A., Levine, J. B., Klibanski, A., … Milad, M. R. (2011). Estradiol Modulates Medial Prefrontal Cortex and Amygdala Activity During Fear Extinction in Women and Female Rats. *Biological Psychiatry*, *70*(10), 920–927.

Zheng, J., Anderson, K. L., Leal, S. L., Shestyuk, A., Gulsen, G., Mnatsakanyan, L., … Lin, J. J. (2017). Amygdala-hippocampal dynamics during salient information processing. *Nature Communications*, *8*, 14413.

Zhu, S., Wang, J., Zhang, Y., Li, V., Kong, J., He, J., & Li, X.-M. (2014). Unpredictable chronic mild stress induces anxiety and depression-like behaviors and inactivates AMP-activated protein kinase in mice. *Brain Research*, *1576*, 81–90.

Zlomuzica, A., Dere, D., Machulska, A., Adolph, D., Dere, E., & Margraf, J. (2014). Episodic memories in anxiety disorders: clinical implications. *Frontiers in Behavioral Neuroscience*, *8*, 131.

Zovkic, I. B., Guzman-Karlsson, M. C., & Sweatt, J. D. (2013). Epigenetic regulation of memory formation and maintenance. *Learning & Memory*, *20*(2), 61–74.